Departamento de Estratigrafía y Paleontología

UNIVERSIDAD DE GRANADA

2012

PALEOECOLOGICAL AND PALEOCEANOGRAPHICAL STUDY OF MESSINIAN DEPOSITS FROM THE LOWER GUADALQUIVIR BASIN (SW SPAIN)

José Noel Pérez Asensio

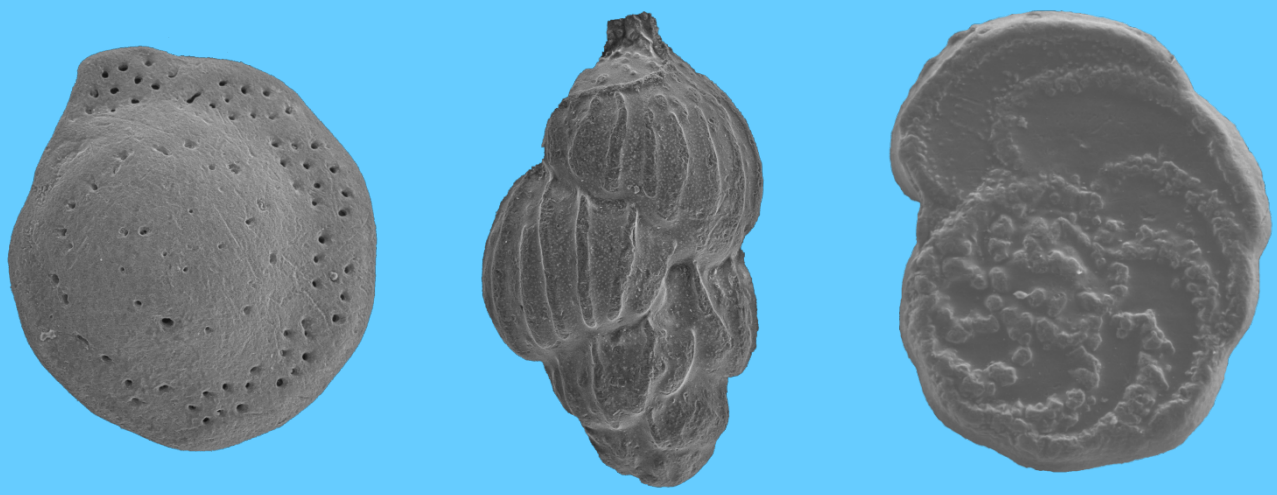

Posgrado Ciencias de la Tierra

Departamento de Estratigrafía y Paleontología

UNIVERSIDAD DE GRANADA

PALEOECOLOGICAL AND PALEOCEANOGRAPHICAL STUDY OF MESSINIAN DEPOSITS FROM THE LOWER GUADALQUIVIR BASIN (SW SPAIN)

Tesis Doctoral

Memoria de la Tesis Doctoral presentada por el Licenciado en Geología D. José Noel Pérez Asensio para optar al Grado de Doctor por la Universidad de Granada

Granada 21 de septiembre de 2012

VºBº del Director

Fdo. José Noel Pérez Asensio

Fdo. Julio Aguirre Rodríguez

UNIVERSIDAD DE GRANADA 2012

Editor: Editorial de la Universidad de Granada
Autor: José Noel Pérez Asensio
D.L.: GR 725-2013
ISBN: 978-84-9028-441-4

Departamento de Estratigrafía y Paleontología

UNIVERSIDAD DE GRANADA

Paleoecological and paleoceanographical study of Messinian deposits from the lower Guadalquivir Basin (SW Spain)

PhD THESIS

José Noel Pérez Asensio

Director: Julio Aguirre Rodríguez

UNIVERSIDAD DE GRANADA 2012

“Hermoso es lo que vemos. Más hermoso es lo que sabemos.

Pero mucho más hermoso es lo que no conocemos”

(Niels Steensen).

ABSTRACT

This PhD thesis deals with the study of Messinian marine deposits from the Montemayor-1 core that is located closed to Huelva (SW Spain) at the northwestern margin of the lower Guadalquivir Basin. The core ranges from the latest Tortonian to the early Zanclean (early Pliocene), thus including marine sediments coetaneous to the interval before, during and after the Mediterranean Messinian salinity crisis (MSC). The magnetobiostratigraphic age model proposed for the core has been accurately improved using oxygen stable isotopes that have allowed to identify the Messinian glacial-interglacial cycles (TG's cycles) based on astronomical tuning. In this thesis, the paleoenvironmental evolution of these Messinian sediments, as well as changes in paleoceanographic circulation and paleoproductivity in the NE Atlantic have been studied using benthic foraminiferal assemblages and oxygen and carbon stable isotopes.

Changes in the benthic foraminiferal assemblages along the Montemayor-1 core show a transgressive-regressive trend. A sharp sea-level rise from the inner-middle shelf to the middle slope took place during the latest Tortonian-earliest Messinian. Then, sea level dropped from the middle slope to the inner-middle shelf during the early Messinian-early Pliocene.

Other key factors controlling the distribution of the benthic foraminifera, further to sea-level variations, were the quantity and the quality of the organic matter that reached the sea floor. The inner-middle shelf was an eutrophic setting with very low oxygenation and high input of continental degraded organic matter derived from river run-off. The outer shelf and the shelf edge were oligotrophic environments with high oxygenation. In the outer shelf, organic matter supply was mostly due to riverine discharges. Finally, mesotrophic conditions with moderate oxygenation prevailed in the upper and middle slope settings, where upwelling currents supplied marine fresh organic matter to the sea floor.

The paleogeographic position of the Montemayor-1 core close to the last Betic seaway to be closed, the Guadalhorce Corridor, is crucial to study the impact of the Mediterranean outflow water (MOW) on the eastern Atlantic oceanography. The improved age model suggests that the closure of the Guadalhorce Corridor occurred at 6.18 Ma. Oxygen stable isotopes indicate that the study area was bathed by the MOW up to the closure of the Guadalhorce Corridor. When the MOW was interrupted, only

Atlantic upwelled waters (AUW) reached the study area. The cessation of the MOW reduced the formation of North Atlantic deep waters (NADW) and, consequently, weaken the Atlantic meridional overturning circulation (AMOC) and promoted cooling in the northern hemisphere. Furthermore, the AMOC was week during glacial periods but strong during interglacials. In the earliest Pliocene, the opening of the Strait of Gibraltar increased the NADW promoting a stronger AMOC.

Stable isotopic records and high-productivity target taxa have revealed that glacioeustatic fluctuations exerted a significant control on the paleoproductivity in the lower Guadalquivir Basin during the Messinian. Under glacial conditions, there was high productivity related to the supply of fresh organic matter from upwelling currents induced by strong winds. In contrast, interglacial periods are characterised by the presence of marine degraded organic matter in the upper slope after upwelling events, and supply of continental degraded organic matter in the outer shelf derived from riverine discharge.

The detailed study of the paleoenvironmental and paleoceanographic changes throughout the core provides new clues for proposing a new model for the onset and end of the MSC. This model suggests that a glacioeustatic sea-level drop with only a minor contribution of tectonic uplift provoked the initiation of the MSC. The marine reflooding of the Mediterranean, which marks the end of the MSC occurred in two-steps: 1) a glacioeustatic sea-level rise during the interglacial stage TG 11 (5.52 Ma) allowed relatively warm Atlantic waters to enter, at least, into the western-central Mediterranean; and 2) the opening of the Strait of Gibraltar at the lowermost Pliocene caused the final refilling of the entire Mediterranean Sea.

RESUMEN

Esta tesis doctoral se ocupa del estudio de los depósitos marinos del Messiniense del testigo de Montemayor-1 el cual se localiza cerca de Huelva (SO de España) en el margen noroccidental de la Cuenca del bajo Guadalquivir. El testigo abarca sedimentos de edades comprendidas entre la última parte del Tortoniense tardío y el Zancliense temprano (Plioceno temprano), por lo tanto incluye sedimentos marinos coetáneos al intervalo anterior, durante y posterior a la crisis de salinidad del Messiniense en el Mediterráneo (CSM). El modelo de edad magnetobioestratigráfico propuesto para el testigo ha sido mejorado con precisión usando isótopos estables de oxígeno que han permitido identificar los ciclos glaciales-interglaciales (ciclos TG) basados en métodos astrocronológicos. En esta tesis, la evolución paleoambiental de estos sedimentos messinienses, además de los cambios en la circulación paleoceanográfica y paleoproductividad en el Atlántico nororiental han sido estudiados a partir de las asociaciones de foraminíferos bentónicos y los isótopos estables de oxígeno y carbono.

Cambios en las asociaciones de foraminíferos bentónicos a lo largo del testigo de Montemayor-1 muestran una tendentica transgresiva-regresiva. Una subida del nivel del mar abrupta desde la plataforma interna-media hasta el talud medio tuvo lugar durante el la última parte del Tortoniense tardío y la primera parte del Messiniense temprano. A continuación, el nivel del mar bajó desde el talud medio hasta la plataforma interna-media durante el Messiniense temprano-Plioceno temprano.

Otros factores clave que controlaron la distribución de los foraminíferos bentónicos, además de las variaciones del nivel del mar, fueron la cantidad y calidad de la materia orgánica que llegó al fondo del mar. La plataforma interna-media era un medio eutrófico con muy baja oxigenación y alto aporte de materia orgánica degradada de origen continental aportada por la descarga fluvial. La plataforma externa y el borde de plataforma eran medios oligotróficos con alta oxigenación. En la plataforma externa, el aporte de materia orgánica en su mayor parte se debía a descarga fluvial. Por último, condiciones mesotróficas con oxigenación moderada prevalecieron en el talud medio y superior, donde corrientes de afloramiento proporcionaban materia orgánica poco degradada al fondo marino.

La posición paleogeográfica del testigo de Montemayor-1 cerca del último estrecho Bético que se cerró, el Corredor del Guadalhorce, es crucial para estudiar el

impacto de la corriente de salida del Mediterráneo (MOW) en la oceanografía del Atlántico oriental. El modelo de edad mejorado sugiere que el cierre del Corredor del Guadalhorce ocurrió hace 6,18 millones de años. Los isótopos estables de oxígeno indican que el área de estudio estuvo bañada por la MOW hasta el cierre del Corredor del Guadalhorce. Cuando la MOW fue interrumpida, sólo las aguas atlánticas relacionadas con corrientes de afloramiento (AUW) alcanzaron la zona de estudio. El cese final de la MOW redujo la formación de agua profunda del Atlántico Norte (NADW) y, por consiguiente, debilitó la circulación termohalina meridional del Atlántico (AMOC) y fomentó el enfriamiento del hemisferio norte. Además, la AMOC era débil durante periodos glaciales pero fuerte durante periodos interglaciales. Al comienzo del Plioceno, la apertura del Estrecho de Gibraltar incrementó la NADW que a su vez fomentó una AMOC más fuerte.

Los registros de los isótopos estables y los taxones asociados a alta productividad han revelado que las fluctuaciones glacioeustáticas ejercieron un control significativo de la paleoproductividad en la Cuenca del bajo Guadalquivir durante el Messiniense. Durante las condiciones glaciales, hubo una alta productividad relacionada con el aporte de materia orgánica poco degradada proporcionada por corrientes de afloramiento inducidas por fuertes vientos. Por el contrario, los periodos interglaciales se caracterizaban por la presencia de materia orgánica degradada de origen marino en el talud superior después de eventos de afloramiento y aporte de materia orgánica degradada continental en la plataforma externa derivada de descarga fluvial.

El estudio detallado de los cambios paleoambientales y paleoceanográficos a lo largo del testigo proporciona nuevas pistas para proponer un modelo nuevo para el comienzo y final de la CSM. Este modelo sugiere que una caída del nivel de mar glacioeustática con sólo una contribución menor del levantamiento tectónico provocó el inicio de la CSM. La reinundación marina del Mediterráneo, la cual marca el final de la CSM ocurrió en 2 pasos: 1) una subida del nivel del mar glacioeustática durante el estadío interglacial TG 11 (5,52 millones de años) permitió que aguas atlánticas relativamente cálidas entraran, al menos, en el Mediterráneo occidental-central; y 2) la apertura del Estrecho de Gibraltar en la base del Plioceno causó la reinundación final del todo el Mar Mediterráneo.

Agradecimientos/Acknowledgments

En primer lugar, quiero dar mi más sincero agradecimiento a mi director de tesis Julio Aguirre. Por su excelente trabajo en la dirección de esta tesis que ha hecho posible la realización de la misma. Por darme libertad para trabajar pero también presionarme en los momentos adecuados. Muchas gracias por dedicarme gran parte de tu tiempo en nuestras múltiples reuniones diarias y por aportarme la necesaria visión positiva de los problemas a los que me he enfrentado. Además, gracias por formarme como investigador y por las interesantísimas conversaciones que hemos tenido sobre ciencia y otros temas. En definitiva, enhorabuena por tu gran trabajo y muchas gracias por todo Julio.

A todos los compañeros del Departamento de Estratigrafía y Paleontología. A nuestra magnífica secretaria Socorro por hacerme la vida más fácil y resolver con gran eficacia todos los problemas administrativos que han surgido. A Pepe Martín por iniciarme en la investigación y por su gran interés y apoyo durante la realización de esta tesis. A Juan Carlos Braga por todo su apoyo, ayuda e interés durante el desarrollo de esta tesis. A Ángel Puga Bernabéu por ayudarme a resolver los múltiples problemas informáticos que he tenido y por enseñarme a levigar muestras durante mi beca de colaboración. Además, muchas gracias Pepe, Juan Carlos y Ángel por todas las anécdotas y los buenos ratos que hemos pasado durante el café de la mañana. A Gonzalo Jiménez Moreno por su colaboración en el trabajo presentado en el capítulo 6 de esta tesis y por su gran interés sobre el desarrollo de la tesis. Muchas gracias por compartir conmigo la docencia de micropaleontología y por los proyectos de investigación que tenemos en curso o por empezar. Espero que los estudios combinando foraminíferos y polen sigan dando excelentes resultados. Gracias también a los compañeros del departamento que se han interesado por mi tesis (Francis Rodríguez Tovar, José Sandoval, Miguel Company, Antonio Checa, Antonio Jiménez, Pascual Rivas, Marcos Lamolda, Elvira Martín, Agustín…). A Isa Sánchez Almazo por su gran ayuda durante las sesiones de SEM y en la preparación de muestras para análisis de isótopos estables.

A Jorge Civis por su aportación como colaborador en los 4 trabajos presentados en esta tesis, por su apoyo y por su gran acogida durante mi estancia en Salamanca. I also thank to Robert Riding for the revision of this thesis and the interesting talks we had when we met in Granada. I am also very grateful to Nils Andersen for his excellent work with the stable isotope analyses.

To my colleagues from Hamburg: my special thanks goes to Gerhard Schmiedl for his excellent work as co-author of the 4 works presented in this thesis. For his support and help with the taxonomy and statistical analyses. Thanks for the interesting discussions about science and for sharing your knowledge and experience with me. Vielen Dank Gerhard!. Muchas gracias también a Christian Betzler por su gran acogida y ayuda durante mis estancias en Hamburgo. Asimismo, quisiera agradecerle la revisión de esta tesis. Furthermore, I would like to thank Annemarie Gerhard for her kindness and for helping me to find a flat in Hamburg. I am also very grateful to Yvonne Milker for her support and for helping me with the statistical software. In addition, thank you very much Yvonne and Thomas for the nice dinners at 17:00 h! at Geo restaurant and for advising me about the Edelcurry restaurant where I tried the best currywurst of

the world. I also want to thank Marc Theodor and Alex for their support, the excellent recommendation of the Die Kartoffelstube restaurant and your visit to Carboneras. Furthermore, thank you very much Lars for the wonderful boat trip at Alster river and for your tasty homemade pizza. My thanks also goes to the rest of my colleagues at the Geologisch-Paläontologisches Institut (Ulrich Kotthoff, Sebastian Lindhorst, Wolfgang Weitschat, Juliane, Kathleen, Nadine...). Muchísimas gracias también a mis amigos hispano-hablantes de Hamburgo. A Julio y Sasha por los buenos momentos que hemos pasado juntos y por hacer mi estancia en Hamburgo más llevadera. A Julio y Viktor por las noches de fútbol y el inolvidable fiestón de cumpleaños de Julio. A Iria muchas gracias por tu ayuda, apoyo y por acompañarme a la Mensa casi todos los días.

A mis antiguos y actuales compañeros de nuestro despacho internacional mucha gracias por acompañarme durante estos cuatro años de tesis (Anja, Vedrana, Rute, Antonio, Elena, Carmina, Simone, Amalia). A Anja, Vedrana, Elena y Simone por los momentos de relax durante los almuerzos (alguna vez peligrosos) en los bares de Gonzalo Gallas y por todo lo bueno que hemos vivido juntos. A Rute gracias por darme ánimos y por ayudarme con los programas de diseño gráfico. A Carmina por ser tan buena compañera y persona y compartir conmigo las English lessons con Diana. A Antonio por salvar mi portátil con el superantispyware, su interesantísimo libro sobre un pavo y las conversaciones que hemos mantenido sobre temas variados. Al resto de mis compañeros becarios del departamento de Estratigrafía y Paleontología (Pili, Sila, Saturn, Io). A Pili por animarme con el final de la tesis y facilitarme la vida con sus consejos sobre los papeleos del doctorado. A los compañeros becarios del departamento de Mineralogía y Petrología (Aitor, Juan Antonio, Anna, Sandra), de geodinámica (Pedro, Silvia) y del IACT (Marta, Nieves).

A mis compis de piso por ayudarme a desconectar del trabajo todos los días y por todas las experiencias vividas (Roca, Cid, Turu, Pedro, Rubén, Javi, Pedro Sola, Esther, Idaira…). A mis amigos de Olula de Río (Almería) porque a pesar de que nos vemos poco siempre estáis ahí (Juanmi, Javi, Loren…). A mis amigos de Granada (Pedro, Fernando, Migue, Sonia…). A mis compañeros de promoción (Bea, Isa, Juanmi y Guille) por todos los buenos momentos que hemos pasado durante la carrera especialmente en las salidas de campo.

A toda mi familia. En especial a mis padres y mi hermano David por todo su apoyo y cariño. Por educarme, enseñarme a valorar la vida y por apoyarme siempre en todas las decisiones importantes que he tomado. A mis abuelos, tíos y primos muchas gracias por todo.

Y especialmente a Gloria por aguantarme todos estos años juntos y apoyarme ciegamente durante esta etapa de mi vida. Por animarme en todos mis malos momentos y no quejarse durante mis fines de semana de trabajo. Muchas gracias por compartir estos años conmigo y por ser como eres. Gracias Gloria.

TABLE OF CONTENTS

CHAPTER 1

CHAPTER 1

INTRODUCTION

The Messinian was a significant time interval in the evolution of the Betic-Rifian mountain belt since significant tectonic and paleogeographic changes took place in the region. Emersion of new relieves with subsequent modifications of the Mediterranean paleogeography led to the most dramatic episode of the recent history of the Mediterranean Sea. The progressive restriction of the different Betic and Rifian Corridors connecting the Atlantic and the Mediterranean ended with the isolation of the Mediterranean from the world's oceans (Benson et al., 1991; Esteban et al., 1996; Krijgsman et al., 1999a; Soria et al., 1999; Barbieri and Ori, 2000; Martín et al., 2001; Betzler et al., 2006). This, in turn, forced the deposition of extensive evaporites in the Mediterranean during the so-called Messinian salinity crisis (MSC) (Hsü et al., 1973, 1977). The beginning of this event has been dated at 5.96 ± 0.02 Ma (Krijgsman et al., 1999b).

Ever since the publication of the pioneering works of Hsü et al. (1973, 1977), when the Mediterranean evaporite deposits and the MSC were presented to the scientific community, Messinian sediments in the central Mediterranean and its satellite basins have been intensively studied (e.g. Ryan and Cita, 1978; Borsetti et al., 1990; Riding et al., 1991; Martín and Braga, 1994; Braga and Martín, 1996; Clauzon et al., 1996; Riding et al., 1998, 1999, 2000; Iaccarino and Bossio, 1999; Krijgsman et al., 1999b; Fortuin and Krijgsman, 2003; Sánchez-Almazo et al., 2001, 2007; Aguirre and Sánchez-Almazo, 2004; Braga et al., 2006; Cosentino et al., 2006, 2012; Rouchy and Caruso, 2006; Roveri and Manzi, 2006; Di Stefano et al., 2010; García et al., 2011). However, little is known about what happened during the Messinian in the Atlantic Ocean close to the Strait of Gibraltar. Some works dealing with the Messinian paleoenvironmental evolution in the Atlantic side of the Rifian Corridors have been carried out (Hodell et al., 1989; Gebhardt, 1993; Hodell et al., 1994; Barbieri, 1998; Barbieri and Ori, 2000). However, no detailed studies in the vicinity of the Betic Corridors in the Atlantic-linked Guadalquivir Basin have been done. Previous studies analysed the general stratigraphic and biostratigraphic frameworks of the basin (Perconig, 1973; Perconig and Granados,

1973; Viguier, 1974; Civis et al., 1987; Sierro, 1985a, 1985b, 1987, 1993; Flores, 1987; Aguirre et al., 1995; Sierro et al., 1996; Riaza and Martínez del Olmo, 1996), with local magnetostratigraphic data (Larrasoaña et al., 2008). The paleoenviromental evolution in the western part of the basin, the so-called the lower Guadalquivir Basin, has also been studied based on different groups of microfossils, specially foraminifera, nannoplankton and ostracods (Berggren and Haq, 1976; Flores, 1987; Sierro, 1987; Sierro et al., 1993; González-Regalado and Ruiz, 1990; González-Regalado et al., 2005). These works show a transgression with glauconitic deposition in middle-upper slope settings (Galán and González, 1993; Baceta and Pendón, 1999; González-Regalado et al., 2005) followed by a shallowing upward trend up to sands and calcarenites deposited in the inner shelf. These shallow sediments have been associated with the sea level drop leading to the onset of the MSC (Berggren and Haq, 1976; Flores, 1987; Sierro, 1987; González-Regalado and Ruiz, 1990). In addition, a decrease in the paleotemperature of Atlantic waters when the Messinian started has been suggested based on planktonic foraminifera and nannoplankton assemblages (Sierro, 1985a; Flores, 1987; Sierro et al., 1993). Similar sea level fall around the onset of the MSC and general Messinian cooling have been proposed for the sediments in the Atlantic side of the Rifian Corridors (Hodell et al., 1989; Gebhardt, 1993; Hodell et al., 1994; Barbieri, 1998; Barbieri and Ori, 2000).

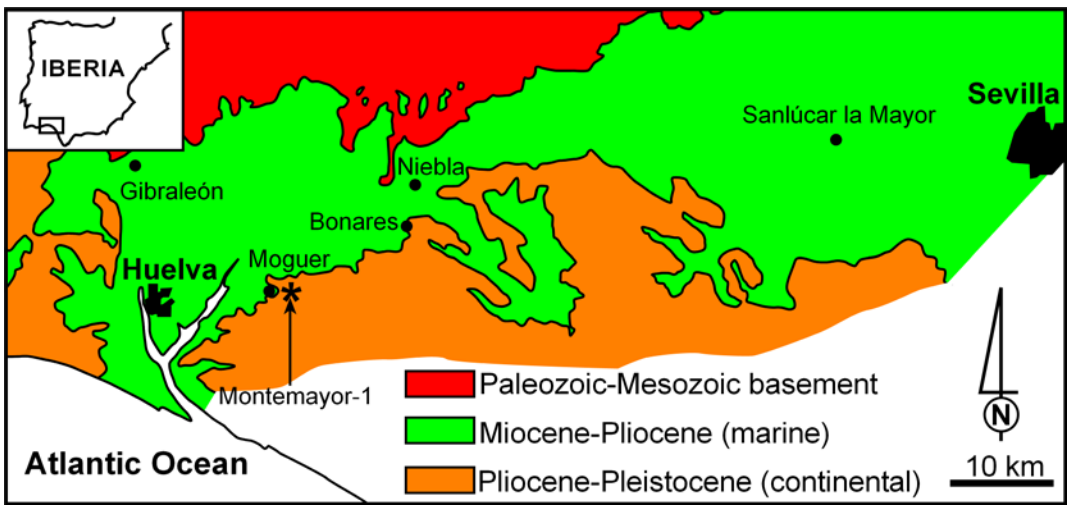

Figure 1.1. Geology of the lower Guadalquivir Basin and location of the Montemayor-1 core (modified from Civis et al., 1987).

In this PhD thesis, the Messinian paleoenvironmental evolution of the lower Guadalquivir Basin is analysed through the study of the continuous Montemayor-1 core located close to Huelva (SW Spain) (Fig. 1.1).This study is based on the analysis of benthic foraminifera and oxygen and carbon stable isotopes measured on foraminiferal shells. These widely distributed and abundant organisms depend on the substrate and their distribution is controlled by several physical, chemical and biological factors (e.g. Boltovskoy and Wright, 1976; Murray, 1991, 2006; Sen Gupta 1999). Furthermore, they are excellent indicators of paleobathymetry, type of substrate, oxygen content and organic matter flux to the sea floor (Jorissen et al., 2007). Additionally, foraminiferal O and C stable isotopes are good proxies of density, temperature, salinity, ventilation and nutrient content of water masses (e.g. Rohling and Cooke, 1999; Armstrong and Brasier, 2005; Ravelo and Hillaire-Marcel., 2007; James and Austin, 2008; Mackensen, 2008). Therefore, a comprehensive analysis of benthic foraminiferal assemblages and stable isotope geochemistry from the lower Guadalquivir Basin is fundamental to reconstruct the paleoenvironmental evolution of the basin during the Messinian.

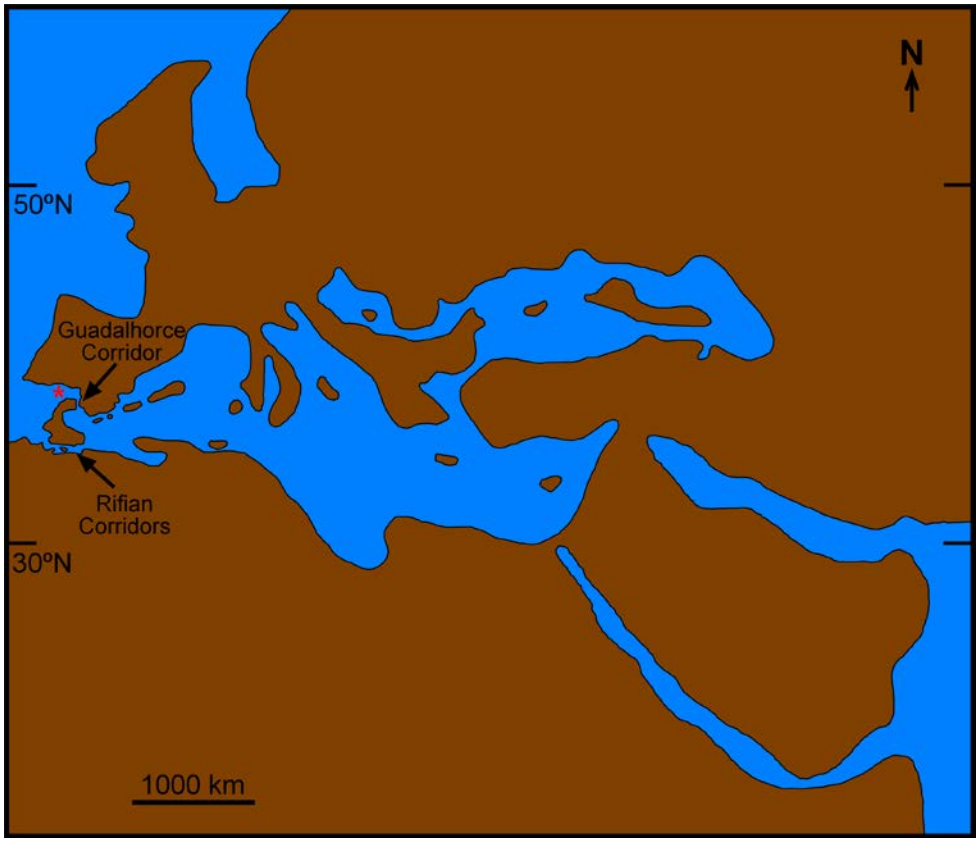

Figure 1.2. Paleogeography of the Mediterranean region during the early Messinian (after Martín et al., 2009; Braga et al. 2009). The location of the Montemayor-1 core is indicated by a red asterisk.

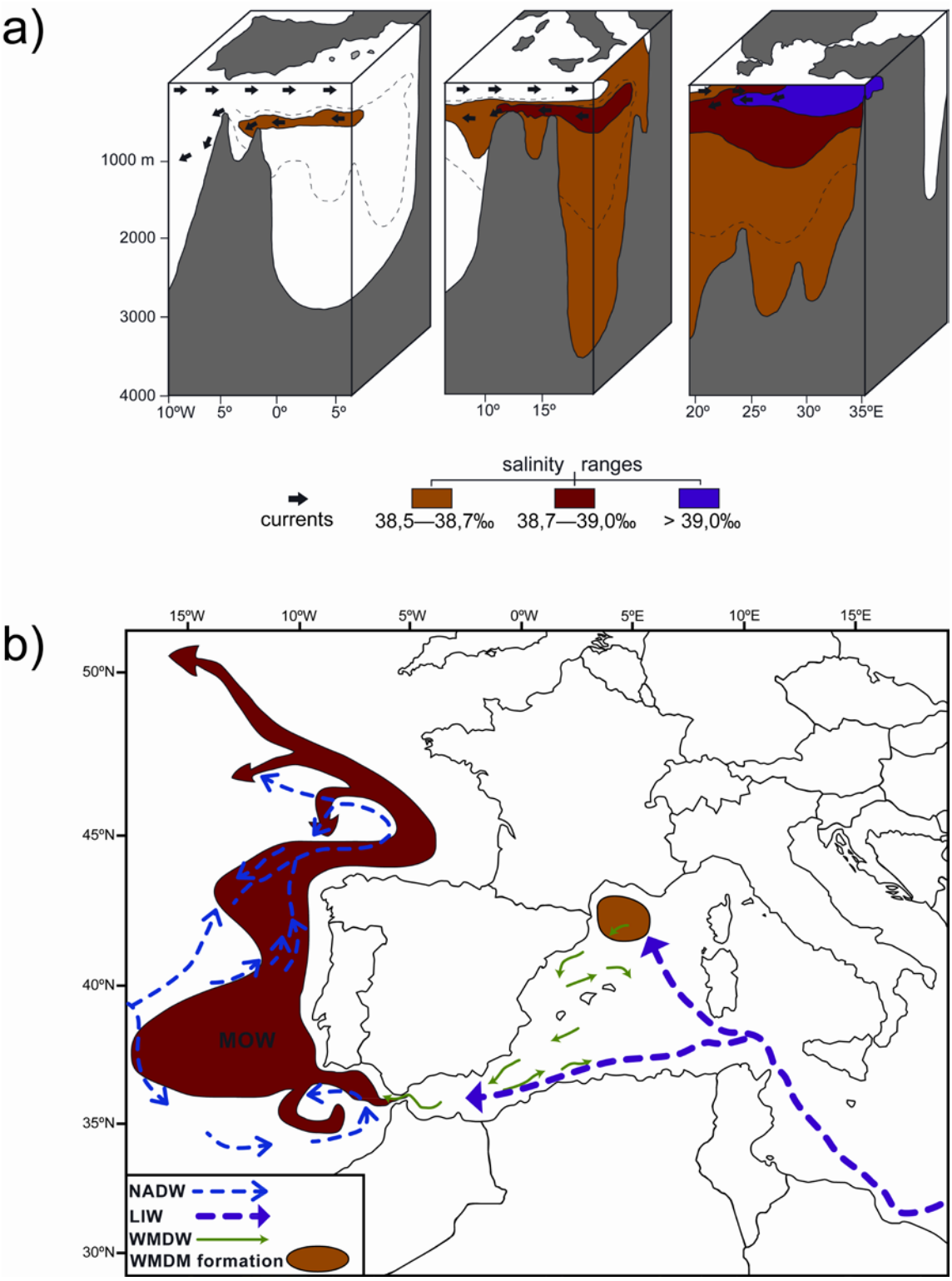

Figure 1.3. (a) Present-day salinity and circulation patterns at the Strait of Gibraltar and in the Mediterranean (based on Wüst, 1961). (b) Present-day general circulation pattern at the eastern North Atlantic and Mediterranean Sea (based on Hernández-Molina et al., 2011; Pinardi and Masetti, 2000). Mediterranean Outflow Water (MOW), North Atlantic Deep Water (NADW), Levantine Intermediate Water (LIW), Western Mediterranean Deep Water (WMDW) and WMDW formation are shown.

This PhD thesis focuses on the study of the Montemayor-1 core since it is located close to the last active Atlantic-Mediterranean Betic seaway, the Guadalhorce Corridor (Martín et al., 2001, 2009) (Fig. 1.2). Hence, the information recorded in this core is essential to report changes in the water mass exchanges between the Atlantic and the Mediterranean whereas the Guadalhorce Corridor was open and it also provides key information on paleoceanographic as well as paleoclimatic changes occurring when it became closed.

At the present day, the Atlantic-Mediterranean water mass exchange is through the Strait of Gibraltar and follows an anti-estuarine circulation pattern (Wüst, 1961) (Fig. 1.3). Atlantic waters with low salinity and density superficially enters the Mediterranean flowing eastwards. Conversely, dense and saline Mediterranean intermediate and deep waters produced in the eastern Mediterranean form a bottom current called Mediterranean Outflow Water (MOW) that flow westward through the Strait of Gibraltar. This current principally consists of Levantine Intermediate Water (LIW), which contributes to 2/3 of the MOW and is produced by convection in the Eastern Mediterranean (Bryden and Stommel, 1984, Marshall and Schott, 1999; Millot, 1999; Hernández-Molina et al., 2011). The remaining 1/3 of the MOW is the contribution of the Western Mediterranean Deep Water (WMDW) that is produced in the Gulf of Lion during cold and windy winters (MEDOC Group, 1970; Bryden and Stommel, 1984; Lacombe et al., 1985; Millot, 1999). The MOW through the Strait of Gibraltar travels in the Atlantic Ocean flowing along the Iberian margin and penetrating towards the north reaching up to the Rockall Channel at around 50º20'N and possibly the sill of the Wyville-Thomson Ridge close to the North Pole (Iorga and Lozier, 1999).

The MOW current has a significant impact on the upper-ocean circulation in the subtropical North Atlantic Ocean and could play a critical role in the establishment of the Azores Current (Özgökmen et al., 2001). Furthermore, it contributes to the Atlantic meridional overturning circulation (AMOC), which is the driving force for the entire Atlantic Ocean circulation and the global thermohaline circulation (Reid, 1979; Rahmstorf, 1998; Bethoux et al., 1999; Bigg and Wadley, 2001; Bigg et al., 2003). Major climate change can be induced by alterations of the global thermohaline circulation that modifies the global radiation budget and global carbon cycling (Brown et al., 1989; Bigg et al., 2003; Murphy et al., 2009). Therefore, fluctuations in the MOW flow might have a strong impact on the AMOC, global oceanic circulation and climate. For example, a steady AMOC in the North Atlantic needs the contribution of the MOW

(Rahmstorf, 1998; Bethoux et al., 1999). In addition, changes in the MOW affecting the global circulation and climate might influence the primary productivity in the northeastern Atlantic. In the southeastern Atlantic, a reduction of the AMOC provoked by the decrease or interruption of the MOW and a biogenic bloom are recorded during the Messinian (Rommerskirchen et al., 2011). The MOW is also fundamental to restart the AMOC after its collapse (Rogerson et al., 2006, 2012; Voelker et al., 2006). Glacial-interglacial variability exerts an influence on the intensity and depth settling of the MOW. Under glacial conditions the MOW presents an enhanced current activity in deeper areas due to a higher density. In contrast, a less dense MOW flows at shallower depths during interglacial periods (Schönfeld and Zahn, 2000; Rogerson et al., 2005; Llave et al., 2006).

Comprehensive studies about the impact of the MOW on the circulation of the Atlantic Ocean during the Pliocene, Pleistocene and Holocene have been carried out in the last decades (e.g. Loubere, 1987; Nelson et al., 1993; Schönfeld, 1997; Maldonado and Nelson, 1999; Schönfeld and Zahn, 2000; Rogerson et al., 2005; Hernández-Molina et al., 2006, 2011; Llave et al., 2006, 2011; Toucanne et al., 2007; Khélifi et al., 2009; Rogerson et al., 2010, 2011, 2012; Stumpf et al., 2010; van Rooij et al., 2010; Estrada et al., 2011). These studies analyse the evolution of the MOW and its impact on the Atlantic oceanic circulation after the opening of the Strait of Gibraltar. Nevertheless, there are very few studies on the impact of the MOW during the Messinian when the current flowed through the Betic and Rifian Corridors reaching at least 50ºN in the northeastern Atlantic Ocean or in the period between the closure of these corridors and the opening of the Strait of Gibraltar (Benson et al., 1991; Zhang and Scott, 1996; Abouchami et al., 1999; van der Laan et al., 2012). During the earliest Messinian, when both the Betic and the Rifian corridors were active, Atlantic waters entered the Mediterranean through the southern Moroccan gateways and the MOW flowed through the Betic Corridors according to the siphon model of Benson et al. (1991). When the last Betic Corridor, the Guadalhorce Corridor (Martín et al., 2001, 2009), was closed the MOW flowed out through the Rifian Corridors until their closure at around 6 Ma (Krijgsman et al., 1999a; van der Laan et al., 2012). However, contrary to these studies, the impact of the MOW on the deep circulation in the north Atlantic has been questioned (Keigwin et al., 1987). Further, the impact on the NE Atlantic circulation of the blockage of the siphon circulation has not been yet studied.

Glacioeustatic fluctuations related to changes in global climate control the primary productivity due to variations in the wind systems and humidity. Paleoproductivity changes induced by glacioeustacy have been recorded in the northeastern Atlantic during the Pliocene, Pleistocene and Holocene (Diester-Haass and Schrader, 1979; Abrantes, 1991, 2000; Lebreiro et al., 1997; Eberwein and Mackensen, 2008; Martinez et al., 1999; van der Laan et al., 2006, Naafs et al., 2010; Salgueiro et al., 2010: Zarriess and Mackensen, 2010). These works show how global climate can control humidity and wind systems affecting the intensity and seasonality of primary productivity. For example, under glacial conditions, winds are stronger inducing upwelling in the northeastern Atlantic. As occurs during the Plio-Pleistocene and Holocene, the paleoproductivity in the northeastern Atlantic during the Messinian was higher due to enhanced upwelling induced by stronger winds during glacial periods (van der Laan et al., 2006, 2012). During interglacial periods, productivity associated to upwelling current is lower and river run-off related to precipitation is higher due to warm and wet conditions (van der Laan et al., 2012).

The knowledge of the paleoenvironmental evolution of the Atlantic-linked lower Guadalquivir Basin where there were neither desiccation nor evaporite deposition allow to obtain a more precise idea of the global geological processes that affected the Mediterranean before, during and after the MSC. Glacioeustatic sea level lowering, regional tectonic uplift in the Arc of Gibraltar or a combination of both has been considered as the trigger mechanisms for the onset of the MSC (Weijermars, 1988; Kastens, 1992; Hodell et al., 1994, 2001; Clauzon et al., 1996; Krijgsman et al., 1999a, 1999b, 2004; Duggen et al., 2003; Hilgen et al., 2007). Moreover, the timing and causes of the refilling of the Mediterranean that marks the end of the MSC are still controversially discussed (Martín and Braga, 1994; Riding et al., 1998; Krijgsman et al., 1999b; Aguirre and Sánchez-Almazo, 2004; Braga et al., 2006; van der Laan et al., 2006; Hilgen et al., 2007; Rouchy et al., 2007). In the Mediterranean, the complex Messinian paleogeography related to different local tectono-sedimentary regimes, as well as problems of precise correlation between central Mediterranean basins and marginal basins, hampers the study of the triggering mechanisms for the onset and the end of the MSC (e.g. Roveri and Manzi, 2006). Therefore, the analysis of complete continuous Messinan sedimentary records of the Montemayor-1 core in the lower Guadalquivir Basin located in the undisturbed Atlantic Ocean will help to decipher the contribution of global and regional processes to the initiation and end of the MSC.

1.1. Open questions and importance of the thesis

There are few studies dealing with the paleoenvironmental evolution of the lower Guadalquivir Basin during the Messinian (Berggren and Haq, 1976; Civis and Sierro, 1987; Flores, 1987; Sierro, 1987; González-Regalado and Ruiz, 1990; Gläser and Betzler, 2002). This basin constituted the Atlantic side of the Betic Corridors: the North Betic Strait, the Dehesas de Guadix Corridor, the Granada Basin and the Guadalhorce Corridor (Esteban et al., 1996; Braga et al., 2003; Betzler et al., 2006; Martín et al., 2001, 2009). Furthermore, Messinian marine sediments of the basin cover the interval before, during and after the MSC. In addition, the general biostratigraphic and magnetostratigraphic frameworks of the lower Guadalquivir Basin have been researched comprehensively (Perconig, 1973; Perconig and Granados, 1973; Viguier, 1974; Sierro, 1985a, 1985b, 1987, 1993; Flores, 1987; Aguirre et al., 1995; Sierro et al., 1996; Larrasoaña et al., 2008). However, a precise age model for these Messinian sediments has not been established yet. The use of a precise age model is critical to correlate Atlantic events that reflect global changes with regional Mediterranean events at the time of the MSC.

Since the lower Guadalquivir Basin was close to the Guadalhorce Corridor, which connected the Atlantic with the Mediterranean Sea during the early Messinian (Martín et al., 2001), Messinian marine sediments close to the Atlantic side of the seaway might have recorded the impact of the MOW on the oceanic circulation in the Guadalquivir Basin and the northeastern Atlantic Ocean during this time interval. Furthermore, the closure of the Guadalhorce Corridor could be dated using the age of interruption of the MOW in the lower Guadalquivir Basin before the MSC. In addition, the different proposed models for the exchange of water masses through the Atlantic and Mediterranean, including the antiestuarine, the estuarine and the siphon models, can be tested. As mentioned before, there are few works on the impact of the MOW on the Atlantic circulation during the Messinian (Zhang and Scott, 1996; Abouchami et al., 1999; van der Laan et al., 2012). Further, the effect of restriction of the Atlantic-Mediterranean connections on the MOW and eastearn Atlantic circulation during the Messinian has not been analysed yet. It is especially interesting to assess the changes in the Atlantic circulation and global climate produced by the interruption or reduction of the MOW when the Betic and the Rifian Corridors became definitely closed.

Variations in the temperatures, humidity and intensity of winds produced by global climate changes can control the supply of both marine and continental organic matter to the ocean. Upwelling currents and river run-off could be the major sources of organic matter as occur at the present day. So far, few studies on the Messinian paleoproductivity in the northeastern Atlantic have been carried out (van der Laan et al., 2006, 2012). In this period, changes in the oceanic circulation in the northeastern Atlantic as a result of the cessation or reduction of the MOW due to the restriction of the Atlantic-Mediterranean gateways might have affected the productivity in the region.

As explained above, the controlling factors for the isolation and reflooding of the Mediterranean leading to the onset and end of the MSC are not clear yet. Research performed in the Mediterranean basins has proved to be uncapable to unravel this conundrum because of the complex Messinian paleogeography of the Mediterranean. This problem can be solve studying complete, continuous Messinian marine records of the Atlantic Ocean, where there was neither desiccation nor evaporite deposition, near the Atlantic-Mediterranean gateways. All these requirements are satisfied by the Gualdalquivir Basin. Furthermore, the Guadalquivir Basin was an open embayment during the Messinian (Martín et al., 2009), so it is an exceptional area to link global events to regional Mediterranean events. Therefore, research on Messinian sedimentary records of this basin might be crucial to disentangle the controlling mechanisms both for the onset and the end of the MSC.

1.2. Objectives

All the aforementioned open questions constitute the main objectives of this PhD thesis:

1) To analyse the paleoevironmental evolution of the lower Guadalquivir Basin during the Messinian.

2) To establish an accurate and reliable age model for the Messinian deposits of the lower Guadalquivir Basin.

3) To assess the impact of the restriction of the Atlantic-Mediterranean Betic gateways on the MOW and the Atlantic oceanic circulation during the Messinian.

4) To test the proposed models for the Atlantic-Mediterranean water mass exchange.

5) To study paleoproductivity changes and organic carbon cycling in the northeastern Atlantic during the Messinian.

6) To assess the impact of the MOW on the productivity.

7) To establish the effect of the global oceanography and climate on the Messinian productivity.

8) To decipher the contribution of glacieustacy and tectonic activity for the onset and end of the MSC.

9) To define a comprehensive model for the desiccation and refilling of the Mediterranean Sea during the Messinian.

1.3. Structure of the thesis

This PhD thesis is organised in nine chapters. Chapter 1 presents the state-of-the-art and the background knowledge about the paleoenvironmental and paleoceanographic evolution of the lower Guadalquivir Basin and the nearby Atlantic during the Messinian, as well as the triggering mechanisms for the initiation and end of the MSC, are described. The open questions, aims and importance of the thesis are also presented in this chapter. The chapter 2 includes the age and stratigraphy of the studied material and the methodological procedures. The main results are presented in chapters 3, 4, 5 and 6. Chapter 3 analyses the Messinian paleoenvironmental evolution of the lower Guadalquivir Basin using benthic foraminifera (Pérez-Asensio et al., 2012a). Chapter 4 assesses the impact of the MOW on the eastern Atlantic circulation and global climate in relation with the restriction of the Atlantic-Mediterranean seaways (Pérez-Asensio et al., 2012b). In chapter 5, paleoproductivity changes and organic carbon cycling in the northeastern Atlantic during the Messinian are analysed (Pérez-Asensio et al. in prep. 1). Chapter 6 describes a novel model for the MSC with emphasis on the causes and timing of the onset of the evaporite deposition and the marine refilling of the Mediterranean (Pérez-Asensio et al., in prep. 2). In chapter 7, all the results of this thesis are integrated to improve our knowledge on the Messinian history of the lower Guadalquivir Basin and to show their implications to solve the MSC problem in the Mediterranean. Chapter 8 enumerates the main conclusions of this thesis. Finally, chapter 9 deals with the future perspectives of the research on the Messinian paleoclimate and paleoceanography by means of the analyses of marine sedimentary records from the Atlantic Ocean.

CHAPTER 2

CHAPTER 2

MATERIAL AND METHODS

2.1. Material

In this PhD thesis, the Montemayor-1 core has been analysed. This core was stored at the Universidad de Salamanca (Spain). A total of 475 samples were collected with a sampling resolution of 0.5 m. This core is 260 m long and ranges from the latest Tortonian to the Zanclean (Larrasoaña et al., 2008), and its age framework was established by magnetobiostratigraphic methods. First of all, the magnetostratigraphic dating was carried out using the revised astronomically-tuned geomagnetic polarity timescale of Lourens et al. (2004) (ATNTS2004). According to this scale, the core ranges from the upper part of the C3Br.2r (ca. 7.4 Ma) to the C3n/C2Ar boundary (ca. 4.3–4.2 Ma) (Larrasoaña et al., 2008) (see below). Regarding the biostratigraphic dating, the planktonic foraminiferal (PF) events 3, 4 and 6 of Sierro et al. (1993), and the first occurrence of *Globorotalia puncticulata* were used. The PF event 3 is the replacement of the *Globorotalia menardii* group II by the *Globorotalia miotumida* group and it is correlated with the Tortonian/Messinian boundary; the PF event 4 is the first abundant occurrence of dextral specimens of the *Neogloboquadrina acostaensis* group; and the PF event 6 is first abundant occurrence of *Globorotalia margaritae* s.s.

The Montemayor-1 core consists of the uppermost part of the basement and marine sediments of four formations that crop-out in the onland Neogene of Huelva and surrounding areas. The Niebla Formation is the lowermost unit (Civis et al., 1987; Baceta and Pendón, 1999). This unit consists of carbonate– siliciclastic mixed deposits of the late Tortonian that unconformably onlap the Paleozoic–Mesozoic basement of the Iberian Massif (Baceta and Pendón, 1999). The second unit is the Arcillas de Gibraleón Formation (Civis et al., 1987) which is latest Tortonian–Messinian according to planktonic foraminifera and calcareous nannoplankton (Sierro, 1985, 1987; Flores, 1987; Sierro et al., 1993). This unit presents 2–4 m of glauconitic silts at the base (Baceta and Pendón, 1999) and consists mostly of greenish-bluish clays. The third unit is the Arenas de Huelva Formation (Civis et al., 1987) that begins with a glauconitic

layer and includes silts and highly fossiliferous sands of the early Pliocene. The uppermost unit is the Arenas de Bonares Formation. This unit unconformably overlays the Arenas de Huelva Formation, and it is late Pliocene in age with no biostratigraphic precision (Mayoral and Pendón, 1987).

The Montemayor-1 core starts with 1.5 m of reddish clays from the Paleozoic-Mesozoic basement. Unconformably overlaying the basement, there is a well-cemented 0.5 m-thick sandy calcarenite layer of the Niebla Formation. This layer is overlaid by 198 m of silts and clays from the Arcillas de Gibraleón Formation. At the base of the formation a 3 m-thick glauconitic layer is present. The boundary between the Niebla and Arcillas de Gibraleón formations located at 258 m is a discontinuity that outcrops onland (Baceta and Pendón, 1999). The Arcillas de Gibraleón Formation is overlaid by 42 m of sands and silts from the Arenas de Huelva Formation. At the base of this formation, there is a 3 m-thick glauconitic layer. The magnetostratigraphy of the core indicate that there is a discontinuity located at the base of the Arenas de Huelva formation (60 m) (Larrasoaña et al., 2008). The core finishes with 14.5 m of highly fossiliferous brownish sands of the Arenas de Bonares Formation that has a discontinuity at the base (18 m), and 3.5 m of a recent soil.

2.2. Faunal analyses

For faunal analysis, a total of 288 samples of 50 g have been studied. The sampling interval was 0.5 m from 240 to 100 m, and 2.5 m from 256.5 to 240 m and from 100 to 36.5 m. Every sample was wet-sieved through a 63 μm sieve and dried in an oven at 40°C. Then, samples were split into equal portions with a microsplitter to get sub-samples with at least 300 benthic foraminifera. These sub-samples were dry-sieved through a 125 μm sieve, and benthic foraminifera were identified at species level and counted. Finally, census data were transformed into relative abundances in percentage.

To assess diversity changes in the benthic foraminiferal assemblages several metrics were calculated:

1) Number of taxa (species richness): calculated summing all the taxa of each sample.

2) The Shannon index (H)**:**

$$H = -\Sigma p_i \ln p_i$$

where p_i is the proportion of the *i*th species and ln is the natural logarithm.

3) evenness (E) sensu Hayek and Buzas (1997):

$$E = e^H/S$$

where e is the base of the natural logarithms, H is the Shannon index, and S is the number of species.

4) The dominance (D) is the percentage of the species with the highest abundance (Levin and Cage, 1998).

Furthermore, the total number of benthic foraminifera per gram of dry sediment (N/g) was calculated.

For paleoecological purposes, benthic foraminiferal species were divided into five different microhabitats following Lutze and Thiel (1989) and Schmiedl et al. (2000): epifaunal (elevated epibenthic species), epifaunal-shallow infaunal (0–0.7 cm below the water–sediment interface; BWSI), shallow infaunal (0.7–1.5 cm BWSI), intermediate infaunal (1.5–3 cm BWSI), and deep infaunal (>3 cm BWSI).

2.3. Stable isotope analyses

For $\delta^{18}O$ and $\delta^{13}C$ stable isotopes a total of 185 samples were analysed. About ten individuals of *Cibicidoides pachyderma* for benthic foraminifera and twenty individuals of *Globigerina bulloides* for planktonic foraminifera were picked from the size fraction >125 μm. Before the analyses, foraminiferal shells were cleaned with an ultrasonic cleaner, and washed with demineralised water. Next, samples were analysed in the Leibniz-Laboratory for Radiometric Dating and Isotope Research in Kiel (Germany) where the isotopic analyses were performed. The stable isotope analyses were performed on a Finnigan MAT 251 mass spectrometer connected to a Kiel I (prototype) preparation device for carbonates. Results are presented in δ-notation (‰), and standardised to the Vienna Pee Dee belemnite (VPDB) scale. This scale is defined by a certain value of the National Bureau of Standards (NBS) carbonate standard NBS-19. The international and lab-internal standard material indicate that the analytical reproducibility is < ±0.05 ‰ for $\delta^{13}C$, and < ±0.07 ‰ for $\delta^{18}O$.

2.4. Age model of the Montemayor-1 core

To establish the age model of the Montemayor-1 core a combination of paleomagnetism, biostratigraphy, and stable oxygen isotope stratigraphy was used. In the lower part of the core, the tie points are eight magnetic reversal boundaries ranging from chron C3Br.2r to chron C3An.1n. Magnetostratigraphic reversal boundaries in the upper part of the core cannot be confidently used as tie points because there is a discontinuity on top of chron C3r, between chrons C3r and C3n (Larrasoaña et al., 2008; Pérez-Asensio et al., 2012). For this reason, the long reversal magnetic chron C3r was dated by means of oxygen isotope stratigraphy. This technique allows to identify several glacial-interglacial TG stages (*sensu* Shackleton et al., 1995 and van der Laan et al., 2006) such as the glacial stages TG 22, TG 20, TG 12 and TG 4, as well as the interglacial stages TG 11 and TG 7, to constraint the time frame.

Stages TG22 and TG 20 are two distinctive maxima at the end of an increasing trend in the $\delta^{18}O$ benthic foraminiferal record (Shackleton et al., 1995). The cycle TG 12-TG 11 represents an important $\delta^{18}O$ decrease that correlates with the major global warming and sea-level rise during the late Messinian (Vidal et al., 2002). Both the TG 22-TG 20 couple and the TG 12-TG 11 isotopic shift have been globally observed, including the Pacific Ocean (Shackleton et al., 1995) and the Atlantic Ocean (Hodell et al., 2001; Vidal et al., 2002). Finally, TG 7 and TG 4 can be confidently recognized by counting glacial-interglacial stages from TG 12 onwards when comparing the TG stages, as named in the Rifian corridor by van der Laan et al. (2005, 2006) and the La2004 orbital solution curve.

Taking into consideration the accurate identification of the aforementioned TG stages in the Montemayor-1 core, we have used the astronomically estimated ages of the TG 22, TG 12 and TG 7 to tighten the age model for the studied core: TG 20 and TG 12 have been dated at 5.79 Ma and 5.55 Ma, respectively (Krijgsman et al., 2004), and TG 7 at 5.359 Ma (van der Laan et al., 2006).

2.5. Sedimentation rate and sand content

Sedimentation rate in cm/kyr was estimated using the tie points of the age model. An estimation of the sedimentation rate is given between consecutive tie points. It is not possible to estimate the sedimentation rates in the lowermost and uppermost

parts of the core due to the discontinuities located at 258, 60 and 18 m. In addition, the sand content was calculated using the percentage of the fraction >63 μm.

2.6. Spectral analyses

In order to identify periodic changes in the benthic $\delta^{18}O$ record, spectral analysis was performed in the time domain using the software PAST (Hammer et al., 2001) and the REDFIT procedure of Schulz and Mudelsee (2002). Using this procedure is possible to perfom the spectral analysis with unevenly spaced samples. Only spectral peaks over the 95% confidence interval (CI) were considered significant.

2.7. Statistical analyses

Benthic foraminifera assemblages were established based on Q and R-mode principal component analyses (PCA) using the software package SYSTAT 12. This technique reduces the number of variables of the data matrix by means of extraction of uncorrelated axes, the principal components. In the Q-mode PCA, dominant species are grouped into assemblages. The R-mode PCA assembles species with similar distribution patterns independently from their relative abundance. Only species representing ≥1% of the total assemblage at least in 3 samples were considered for the analysis. Furthermore, Pearson correlation coefficients were calculated to quantify the relationships between several metrics used in this PhD thesis. Only correlations with a *p*-value<0.01 were considered significant.

2.8. Qualitative and quantitative sea-level reconstructions

Qualitative sea-level reconstructions were made using the planktonic/benthic ratio (P/B ratio henceforward) and benthic foraminiferal target taxa with a narrow and well-defined depth distribution range (depth markers) as a proxies for relative sea-level change. Nonetheless, depth markers distribution might be controlled by different environmental conditions other than of water depth, mainly oxygen and organic matter supply (van Hinsbergen et al., 2005). The selected depth markers for this work are: *Ammonia beccarii* and *Ammonia* sp. (inner-middle shelf); *Cibicidoides floridanus* (outer shelf); *Planulina ariminensis* (predominantly upper slope); *Anomalinoides flinti* (middle

and lower slope); and *Oridorsalis umbonatus* and *Siphonina reticulata* (predominantly middle and lower slope). Moreover, the dinocyst/pollen ratio [d/p ratio = (d-p)/(d+p)] (Jiménez-Moreno et al., submitted) was used to infer relative sea-level changes since this ratio increases with the distance to coast and deepening (Warny et al., 2003; Jiménez-Moreno et al., 2006; Iaccarino et al., 2008).

Quantitative sea-level reconstructions were estimated using the tranfer function developed by Hohenegger (2005) based on depth ranges of benthic foraminiferal taxa, later modified by Báldi and Hohenegger (2008) and Hohenegger et al. (2008) to include the relative abundances of species:

$$\text{paleodepth (m)} = \Sigma\ (n_j l_j d_j^{-1}) / \Sigma\ (n_j d_j^{-1})$$

where n_j is the relative abundance of the *j*th species, l_j is the geometric average of the distribution borders, and d_j is the dispersion. Only species that represent ≥1% of the total assemblage at least in 3 samples were considered for the transfer function. Following the methodology of Hohenegger (2005), global data of water-depth distribution of benthic foraminifera were used. This way, local or geographical biases in their bathymetric ranges are avoided. The 95% confidence intervals were calculated to express the accuracy of the water depth estimates. In addition, transported shallow-water taxa were removed before applying the transfer function.

2.9. Orbital target curves

The orbital obliquity and eccentricity curves were constructed using the Laskar orbital solutions La2004 and La2010 respectively (Laskar et al., 2004, 2011) following the recommendations of Laskar et al. (2011). To generate the ETP (eccentricity, obliquity, precession) curve the normalised eccentricity La2010 orbital solution, the normalised obliquity La2004 orbital solution and the negative normalised precession La2004 orbital solution were summed.

2.10. Backstripping analysis

Backstripping analysis was carried out following the methodology proposed by van Hinsbergen et al. (2005). This method is used to reconstruct the vertical movement

of the basin floor by correcting the paleobathymetric changes of the basin due to sedimentation, compaction and eustatic sea-level fluctuations. First of all, the thickness (in meters) of accumulated sediment is added to the estimated paleodepth (in meters). Secondly, the amount of compaction (in meters) has to be added. The Montemayor-1 core consists of mostly bluish-greenish clays from the Arcillas de Gibraleón Formation. Therefore, the compaction of clays was estimated using the formula of Einsele (1992) to calculate the decompacted thickness:

$$h_{sl} = [(1-n_p)/(1-n_l)] \times (h_{sp})$$

where h_{sl} is the original thickness before compaction, h_{sp} is the compacted thickness, n_l is the original mean porosity, and n_p is the final mean porosity after compaction. An average n_l of 80%, and n_p of 20% for clays was used (Leeder, 1982; Velde, 1996; Boggs, 2009). Using this formula, the compaction of the Montemayor-1 core is 75%. Finally, the correction for eustatic sea-level variation is performed using the average values of global sea-level curve of Miller et al., (2005).

CHAPTER 3

CHAPTER 3

MESSINIAN PALEOENVIRONMENTAL EVOLUTION IN THE LOWER GUADALQUIVIR BASIN (SW SPAIN) BASED ON BENTHIC FORAMINIFERA

José N. Pérez-Asensio, Julio Aguirre, Gerhard Schmiedl, Jorge Civis

Published in Palaeogeography, Palaeoclimatology, Palaeoecology 326-328, 135−151 (1 April 2012).

Abstract

Benthic foraminiferal assemblages of a drill core from the lower Guadalquivir Basin (northern Gulf of Cádiz, SW Spain) have been analyzed in order to reconstruct the paleoenvironmental evolution in the vicinity of the Betic seaways during the Messinian. The core consists of marine sediments ranging from the latest Tortonian to the early Pliocene. Changes in the abundance of certain marker species, planktonic/benthic ratio (P/B ratio), paleodepth estimated with a transfer function, content of sand grains and presence of glauconitic layers indicate a complete transgressive-regressive sea-level cycle from the bottom to the top of the section. An abrupt sea-level rise, from inner-middle shelf to middle slope, is recorded at the lowermost part of the core (latest Tortonian–earliest Messinian), followed by a relatively rapid shallowing from middle slope to outer shelf. Magnetobiostratigraphic data show that this sea-level fall postdates the onset of the Messinian salinity crisis (MSC) in the Mediterranean. Finally, the early Pliocene deposits are interpreted as inner-middle shelf.

Changes in the benthic foraminiferal assemblages through the core are mainly controlled by the trophic conditions, specifically by the quantity and quality of the organic matter reaching the sea floor. The upper slope and part of the outer shelf assemblages are highly diverse and dominated by shallow infaunal species, indicating a generally mesotrophic environment with moderate oxygenation. These environments

have likely been affected by repeated upwelling events, documented by increased abundance of *Uvigerina peregrina* s.l., an opportunistic species thriving in environments with enhanced labile organic matter supply. The assemblages of the transitional interval between upper slope to outer shelf, and of the outer shelf are generally characterized by a relatively low diversity and epifaunal-shallow infaunal taxa, indicating oligotrophic and well-oxygenated conditions. The inner middle shelf assemblages are characterized by very low diversity and dominance of intermediate to deep infaunal taxa, suggesting an eutrophic environment with low oxygen content. These assemblages are dominated by *Nonion fabum* and *Bulimina elongata*, two taxa that are able to feed from continental low-quality organic matter, most likely derived from river run-off. The paleoenviromental evolution on the Atlantic side of Betic and Rifian seaways is similar during the Messinian, with a Messinian continuous sea-level lowering driven by regional tectonic uplift and upwelling-related waters reaching the upper slope. This study will further contribute to understand the role of tectonics on the sea-level changes as well as on the closure of the Atlantic-Mediterranean gateways that led to the MSC, and on the paleoceanography on the Atlantic sides of these corridors.

3.1. Introduction

The Messinian was a time of drastic paleoenvironmental and paleogeographic changes in the Mediterranean (Hsü et al., 1973, 1977). During this time interval, tectonic processes together with glacioeustatic sea-level oscillations led to the isolation of the Mediterranean triggering the formation of thick evaporite deposits during the so-called Messinian salinity crisis (MSC) (Benson, 1986; Benson et al., 1991; Martín and Braga, 1994; Esteban et al., 1996; Riding et al., 1998; Martín et al., 2010). This event took place at around 6 Ma (Gautier et al., 1994; Krijgsman et al., 1999b) as a consequence of the closure of the different gateways connecting the Atlantic and the Mediterranean in the Betic Cordillera in southern Spain (Esteban et al., 1996; Soria et al., 1999; Martín et al., 2001; Betzler et al., 2006; Aguirre et al., 2007; Martín et al., 2009) and the Rifian counterparts in northern Morocco (Benson et al., 1991; Esteban et al., 1996; Krijgsman et al., 1999a; Barbieri and Ori, 2000).

The paleoenvironmental changes that occurred before, during and after the MSC in the Mediterranean and its satellite basins have been intensively studied. Nonetheless, the detailed paleogeographic evolution and the precise timing of the different processes

leading to the MSC and the later Mediterranean reflooding are still discussed controversially (Riding et al., 1998; Krijgsman et al., 1999b; Aguirre and Sánchez-Almazo, 2004; Braga et al., 2006; Roveri and Manzi, 2006). Various studies addressed the Messinian paleoenvironmental evolution on the Atlantic side of the Rifian corridors (Hodell et al., 1989; Benson et al., 1991; Gebhardt, 1993; Hodell et al., 1994; Barbieri, 1998; Barbieri and Ori, 2000). The results of these studies show a significant sea-level fall (about 300 m) indicating the onset of the MSC, a reversal water flux through the Rifian corridors and cooling during the Messinian.

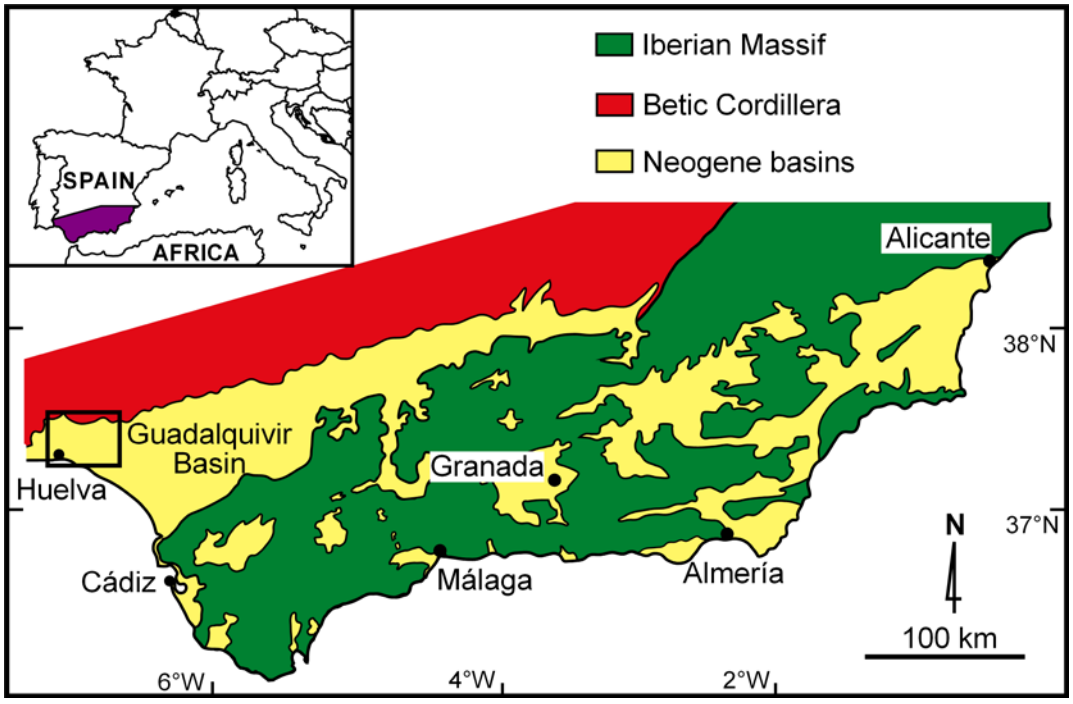

Figure 3.1. Geological map of the Betic Cordillera showing the Guadalquivir foreland basin (modified from Martín et al., 2010). The inset is shown in Fig. 3.2.

The Betic marine passages connected the western Mediterranean with the Atlantic Ocean throughout the Guadalquivir Basin. There are papers dealing with the biochronology of the late Neogene deposits filling the Guadalquivir Basin (Perconig, 1973; Perconig and Granados, 1973; Viguier, 1974; Sierro, 1985; Aguirre et al., 1995; Sierro et al., 1996) and with the tectonostratigraphic framework (Riaza and Martínez del Olmo, 1996; Sierro et al., 1996). However, the available studies on the Messinian paleoenvironmental evolution of the basin are scarce (Berggren and Haq, 1976; Gläser

and Betzler, 2002). According to these studies a sea-level drop from middle slope to inner shelf related to the MSC took place during the Messinian.

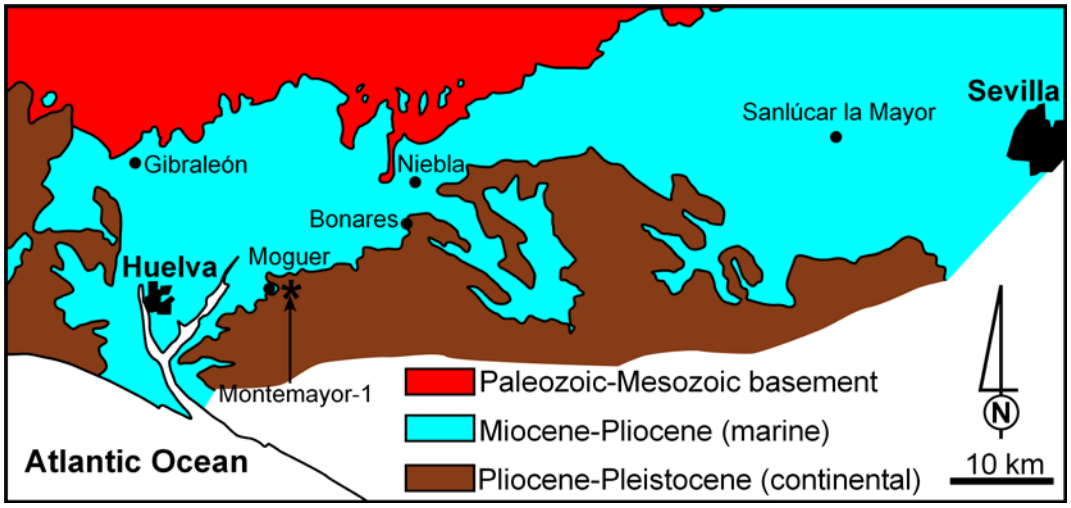

Figure 3.2. Geological map of the lower Guadalquivir Basin including Montemayor-1 core location (modified from Civis et al., 1987).

In this paper, we study the Montemayor-1 core, located in the westernmost part of the northern margin of the Guadalquivir Basin (SW Spain) (Figs. 3.1 and 3.2). It covers a complete Messinian sedimentary record (Larrasoaña et al., 2008). The location of the core is exceptional to investigate the paleoenviromental evolution in an area close to the last Betic gateway to be closed, the Guadalhorce corridor (Martín et al., 2001), during the Messinian.

Among the most abundant organisms in the studied sediments are benthic foraminifera. It is largely proved that these organisms are very useful to reconstruct the paleoenviromental conditions in marine settings, as their distribution depends on several physical, chemical and biological factors (Murray, 1991, 2006). They can be used as proxies of oceanographic parameters such as water depth, substrate, oxygen content and organic matter supply (Jorissen et al., 2007). Thus, the analysis of the variations in the benthic foraminiferal assemblages allows us to infer the key paleoenvironmental factors controlling their distribution, composition, diversity and microhabitat preferences during the Messinian in an Atlantic-linked basin close to the Guadalhorce corridor. The main objectives of this study are to characterize the benthic foraminiferal assemblages along the core and to assess the changes in the main components of the assemblages in relation with variations in paleoenvironmental parameters, such as sea-level

fluctuations, source of organic matter (whether continental or primarily produced in marine contexts), and oxygen content around to the seafloor-substrate interface.

This study aims to improve our understanding of the paleoenvironmental and tectonic evolution of the Atlantic-Mediterranean gateways during the MSC, with particular emphasis on the Betic corridor.

3.2. Study area

The Montemayor-1 core, a continuous core located very close to Moguer (Huelva, SW Spain) (Fig. 3.2) has been studied. The core was drilled in the northwestern margin of the lower Guadalquivir Basin, an ENE-WSW elongated Atlantic-linked foreland basin of the Betic Cordillera (Sanz de Galdeano and Vera, 1992; Braga et al., 2002). It is limited to the N by the Iberian Massif and to the S by the Subbetic nappes of the Betic Cordillera, and is opened to the Atlantic Ocean to the W (Fig. 3.1). The Guadalquivir Basin was originated in the earliest Tortonian (late Miocene) as a consequence of the uplifting of the Subbetic Zone of the Betic Cordillera that closed the so-called North Betic Strait (Aguirre et al., 2007; Martín et al., 2009; Braga et al., 2010).

After the closure of the North-Betic Strait, the Guadalquivir Basin was established as a wide, open marine embayment opened to the Atlantic Ocean (Martín et al., 2009). This basin was filled with marine and continental sediments ranging from the early Tortonian to the late Pliocene (Aguirre et al., 1995; Roldán, 1995; Sierro et al., 1996; González-Delgado et al., 2004). The sedimentary infilling produced a migration of the depocentre approximately along the longitudinal axis of the basin, from the ENE to the WSW. This sedimentary succession has been divided into five depositional sequences (A-E) that have been correlated with third-order cycles of the Haq et al. (1987) global sea-level curve (Sierro et al., 1996).

In Huelva and neighbouring areas, the Neogene deposits have been divided into four lithostratigraphic units formally described as formations. The lowermost unit is the Niebla Formation (Civis et al., 1987; Baceta and Pendón, 1999). It consists of late Tortonian carbonate-siliciclastic mixed deposits that unconformably onlap the Paleozoic-Mesozoic basement of the Iberian Massif (Baceta and Pendón, 1999). The second unit, latest Tortonian-Messinian according to planktonic foraminifera and calcareous nannoplankton (Sierro, 1985, 1987; Flores, 1987; Sierro et al., 1993), is the

Arcillas de Gibraleón Formation (Civis et al., 1987). This unit, which begins with 2-4 m of glauconitic silts (Baceta and Pendón, 1999), consists mostly of greenish-bluish clays. The third unit is the Arenas de Huelva Formation (Civis et al., 1987) that includes early Pliocene silts and highly fossiliferous sands. A glauconite-rich layer is found at the lowermost part of the formation. Finally, this unit is unconformably overlain by sand of the uppermost unit, the Arenas de Bonares Formation, which is attributed to the late Pliocene with no biostratigraphic precision (Mayoral and Pendón, 1987).

3.3. Stratigraphy of the Montemayor-1 core

The Montemayor-1 core ranges from the latest Tortonian to the Zanclean (Larrasoaña et al., 2008) (Fig. 3.3). The age of the core is well constrained based on magnetobiostratigraphic methods. The magnetostratigraphic dating was performed with the revised astronomically-tuned geomagnetic polarity timescale of Lourens et al. (2004) (ATNTS2004). The paleomagnetic record of the core comprises from the upper part of the C3Br.2r (ca. 7.4 Ma) to the C3n/C2Ar boundary (ca. 4.3-4.2 Ma) (Larrasoaña et al., 2008) (Fig. 3.3). The biostratigraphic framework is based on planktonic foraminiferal (PF) events 3, 4 and 6 of Sierro et al. (1993), and the first occurrence of *Globorotalia puncticulata*. According to these authors, the PF event 3, which is correlated with the Tortonian/Messinian boundary, is the replacement of the *Globorotalia menardii* group II by the *Globorotalia miotumida* group; the PF event 4 is the first abundant occurrence of dextral specimens in the *Neogloboquadrina acostaensis* group; and the PF event 6 is first abundant occurrence of *Globorotalia margaritae* s.s.

The Montemayor-1 core is 260 m long including the uppermost part of the basement and the marine sediments of the four aforementioned formations (Fig. 3.3). The core begins with 1.5 m of reddish clays from the Paleozoic–Mesozoic substrate. A well-cemented sandy calcarenite layer 0.5 m thick, corresponding to the Niebla Forma tion, unconformably overlays the basement. Silt and clay belonging to the Arcillas de Gibraleón Formation, 198 min thickness, overlay the sandy calcarenites. A glauconitic layer, 3 m in thickness, is present at the base of the formation. The sharp boundary between the Niebla and Arcillas de Gibraleón formations, located at 258 m, could be correlated with the unconformity observed in coeval deposits cropping out onland (Baceta and Pendón, 1999). Sands and silts from the Arenas de Huelva Formation, 42 m thick, overlay the underlying formation. A 3 m-thick glauconitic layer is found at the

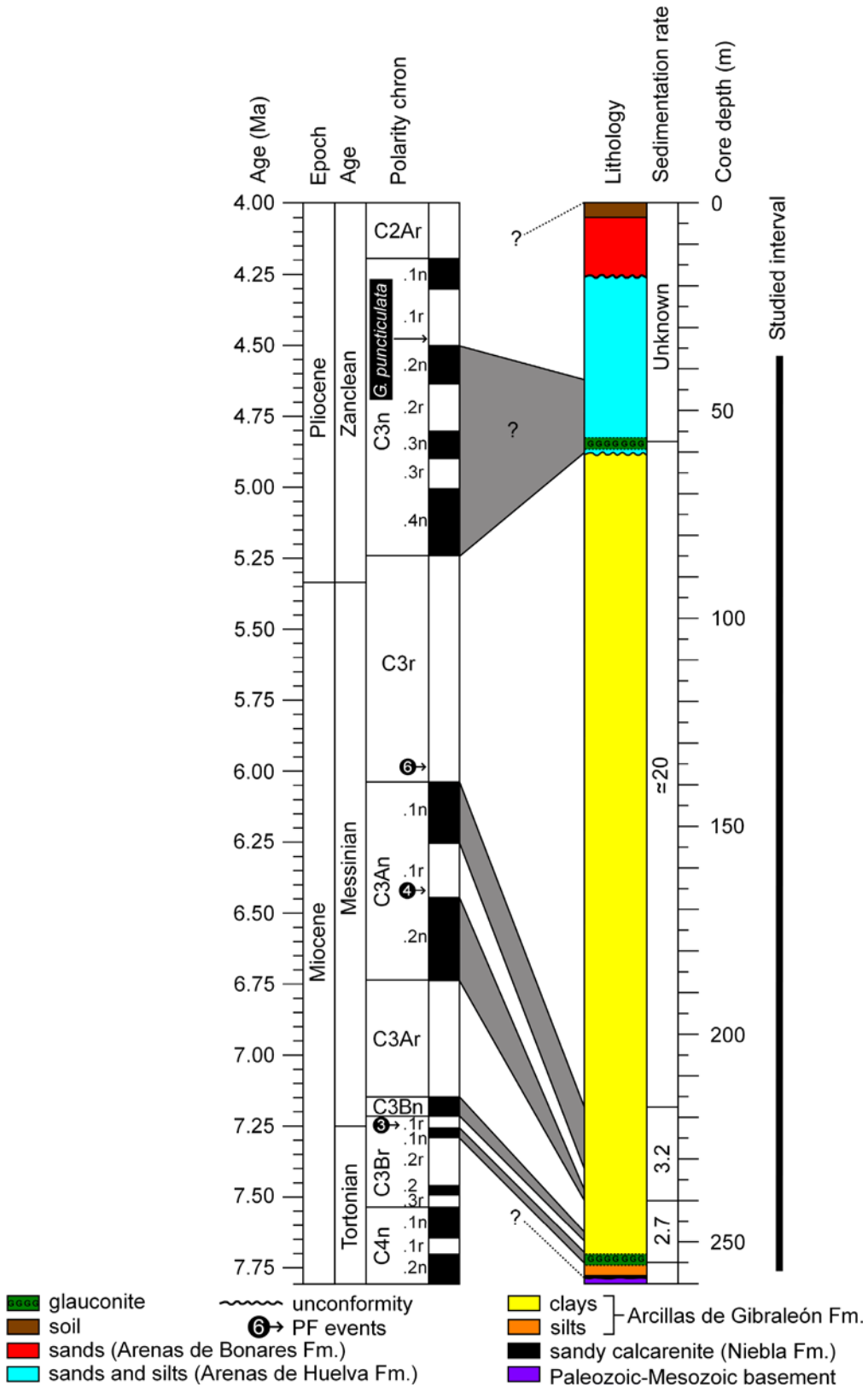

Figure 3.3. Log of theMontemayor-1 core and magneto biostratigraphic framework. Magnetostratigraphy follows the ATNTS2004 (Lourens et al., 2004). Biostratigraphy is based on the planktonic foraminiferal events (PF events) of Sierro et al. (1993) and first occurrence of *Globorotalia puncticulata*. Numbers in the right-hand side column are sedimentation rates (cm/kyr) estimated for the Montemayor-1 core.

base of the unit. According to the paleomagnatic data, a discontinuity, located at 60 m, separates these deposits from the Arcillas de Gibraleón (Larrasoaña et al., 2008). The Montemayor-1 core endswith 14.5 m of brownish sands with marine fossils, the Arenas de Bonares Formation which presents a discontinuity at the bottom (18 m), and 3.5 m of recent soil.

Sedimentation rate was estimated in cm/kyr using thickness of paleomagnetic chrons and the calibrated time scale in Fig. 3.3. Sedimentation rate was calculated in 3 intervals: 1) from the bottom of the chron C3Br.1n to the top of the chron C3Ar; 2) from the bottom of the chron C3An to the top of the chron C3An; and 3) from the bottom of the chron C3r to the top of the chron C3r (Fig. 3.3). Concerning the three discontinuities of the core, the lower and upper discontinuities, located at 258 and 18 m respectively, prevent us from estimating the sedimentation rate for the lowermost and uppermost parts of the core (Fig. 3.3). The sedimentation rate for the chron C3r is also uncertain because of the discontinuity located at 60 m (Fig. 3.3).

3.4. Methods

In this paper, an interval of 220 m, from 256.5 m to 36.5 m in the core, has been studied. This interval encompasses the Arcillas de Gibraleón, and the lower part of the Arenas de Huelva. According to the magnetobiostratigraphy, the sedimentary record of the studied interval is continuous except for a discontinuity close to the Miocene-Pliocene boundary, located at 60m (Fig. 3.3). A total of 89 samples each 2.5 m have been analyzed. All samples were washed over a 63 μm sieve and oven dried at 40 °C.

For faunal analysis, samples were divided into equal aliquots with a microsplitter to obtain sub-samples containing at least 300 benthic foraminifera. These sub-samples were dry-sieved over a 125 μm sieve, and benthic foraminifera were identified and counted. Census data were transformed into relative abundances. Several metrics were calculated: 1) number of taxa (species richness), 2) the Shannon index (H):

$$H = -\Sigma p_i \ln p_i$$

where pi is the proportion of the ith species and ln is the natural logarithm; 3) evenness (E) *sensu* Hayek and Buzas (1997):

$E = e^H/S$

where *e* is the base of the natural logarithms, H is the Shannon index, and S is the number of species; and 4) the dominance (D), defined as the percentage of the most abundant species (Levin and Cage, 1998), has also been quantified.

The sand content was determined as percentage of the >63 μm fraction. The total number of benthic foraminifera per gram of dry sediment (N/g) was also calculated.

Changes in paleowater depth have been inferred applying various proxies, including the planktonic/benthic ratio (P/B ratio hereafter), specific marker taxa with a narrow and well-defined depth distribution range (depth markers), and a quantitative transfer function based on benthic foraminiferal depth ranges. The P/B ratio, scored as [P/(P+B)], was used as an approximation to infer sea-level changes. The use of P/B ratio to represent sea-level changes exhibits many drawbacks. For instance, dissolution affects preferentially to planktic foraminifera (Kucera, 2007), and the planktic foraminifera abundance decreases in brackish waters (Arnold and Parker, 1999; Retailleau et al., 2009). Furthermore, benthic foraminiferal abundance interferes with oxygen and food levels at the sea floor affecting the P/B ratio (van Hinsbergen et al., 2005; Milker, 2010). In spite of these limitations, the P/B ratio can be used to infer general sea-level trends. Depth markers can be used for a qualitative estimation of water depth, notwithstanding their occurrence can be related to environmental conditions instead of water depth, such as oxygen and organic matter supply (van Hinsbergen et al., 2005). In order to define depth markers, we discarded species with a wide bathyme tric range such as bolivinids, buliminids and uvigerinids. Depth markers used in this study are: 1) *Ammonia beccarii* and *Ammonia* sp. (inner-middle shelf); 2) *Cibicidoides floridanus* (outer shelf); 3) *Planulina ariminensis* (predominantly upper slope); 4) *Anomalinoides flinti* (middle and lower slope); 5) Oridorsalis umbonatus and *Siphonina reticulata* (predominantly middle and lower slope). Finally, the transfer function developed by Hohenegger (2005) based on depth ranges of benthic foraminiferal taxa, later modified by Báldi and Hohenegger (2008) and Hohenegger et al. (2008) to include the species relative abundances, was applied to quantitatively estimate sea-level fluctuations:

$$\text{paleodepth (m)} = \Sigma (n_j l_j d_j^{-1}) / \Sigma (n_j d_j^{-1})$$

Species	Minimum depth	Maximum depth	Average depth	SD
Ammonia beccarii	0	100	50	50.00
Ammonia inflata	20	30	25	5.00
Ammonia sp.	0	100	50	50.00
Amphicoryna sp.	9	2860	1434.5	1425.50
Anomalinoides flinti	600	2000	1300	700.00
Bolivina punctata	50	2000	1025	975.00
Brizalina dilatata	15	3000	1507.5	1492.50
Brizalina spathulata	30	3547	1788.5	1758.50
Brizalina sp.	15	3547	1781	1766.00
Bulimina aculeata	5	4000	2002.5	1997.50
Bulimina costata	50	3241	1645.5	1595.50
Bulimina elongata	16	200	108	92.00
Bulimina mexicana	100	2000	1050	950.00
Bulimina sp.	5	4000	2002.5	1997.50
Cassidulina laevigata	30	2500	1265	1235.00
Cassidulina sp.	30	3588	1809	1779.00
Cibicides sp.	0	2000	1000	1000.00
Cibicidoides dutemplei	100	600	350	250.00
Cibicidoides floridanus	100	200	150	50.00
Cibicidoides pachyderma	30	4000	2015	1985.00
Cibicidoides ungerianus	50	4000	2025	1975.00
Cibicidoides sp.	30	4000	2015	1985.00
Fursenkoina schreibersiana	20	200	110	90.00
Globocassidulina subglobosa	50	4000	2025	1975.00
Gyroidinoides soldanii	100	5000	2550	2450.00
Gyroidinoides umbonatus	16	2000	1008	992.00
Hanzawaia boueana	30	200	115	85.00
Hoeglundina elegans	30	4330	2180	2150.00
Lagena sp.	16	3500	1758	1742.00
Lenticulina sp.	19	4500	2259.5	2240.50
Marginulina costata	50	310	180	130.00
Martinottiella communis	200	3000	1600	1400.00
Melonis barleeanum	13	3974	1993.5	1980.50
Melonis soldanii	90	1000	545	455.00
Melonis sp.	13	4800	2406.5	2393.50
Nonion fabum	12	200	106	94.00
Oridorsalis umbonatus	65	4000	2032.5	1967.50
Orthomorphina tenuicostata	50	1000	525	475.00
Planulina ariminensis	70	1300	685	615.00
Planulina sp.	70	4700	2385	2315.00
Pullenia bulloides	60	4000	2030	1970.00
Siphonina reticulata	55	1500	777.5	722.50
Siphotextularia concava	50	631	340.5	290.50
Sphaeroidina bulloides	25	4500	2262.5	2237.50
Stilostomella monilis	100	2500	1300	1200.00
Textularia sp.	0	2000	1000	1000.00
Trifarina bradyi	0	600	300	300.00
Uvigerina canariensis	150	1097	623.5	473.50
Uvigerina peregrina s.l.	100	4400	2250	2150.00
Uvigerina striatissima	200	2000	1100	900.00
Valvulineria complanata	30	100	65	35.00

Table 3.1. Depth ranges of the benthic foraminifera from the Montemayor-1 core. Minimum, maximum, average depth and standard deviation (SD) are indicated. Bathymetric ranges are based on Berggren and Haq (1976), Berggren et al. (1976), Lutze (1980), van Morkhoven et al. (1986), van Marle (1988), González-Regalado (1989), Sgarrella and Moncharmont Zei (1993), Schönfeld (1997), González-Regalado et al. (2001), Murray (2006), Schönfeld (2006), Spezzaferri and Tamburini (2007), Pascual et al. (2008), Villanueva-Guimerans and Canudo (2008), González-Regalado et al. (2009), and Corbí (2010).

where n_j is the relative abundance of the jth species, l_j is the geometric average of the distribution borders, and d_j is the dispersion. For the transfer function, very rare species were not used, only species with ≥1% of the total assemblage at least in 3 samples were considered (Table 3.1). Following the recommendations made by Hohenegger (2005), we use global data of water-depth distribution of benthic foraminiferal species, thus, avoiding local or geographical biases in their bathymetric ranges. Thus, we consider the largest depth range possible for each species (Table 3.1). The accuracy of the water depth estimates was expressed with the 95% confidence intervals (Table 3.2).

Q and R-mode principal component analyses (PCA) were performed to determine the benthic foraminiferal assemblages using the software package SYSTAT 12. The Q-mode PCA groups the dominant species into assemblages. In the R-mode PCA, species with similar distribution patterns independent from their relative abundance are grouped together. To remove the effect of very rare species, only those representing ≥1% of the total assemblage at least in 3 samples were considered. Pearson correlation coefficients were calculated to quantify the relationships between all the metrics used in this study. Correlations with a *p*-value<0.01 were considered significant.

Benthic foraminifera were classified according to their microhabitat preferences (Table 3.3). Five different microhabitats have been recognized, following Lutze and Thiel (1989) and Schmiedl et al. (2000): a) epifaunal, elevated epibenthic species, b) epifaunal-shallow infaunal (0-0.7 cm below the water-sediment interface; BWSI), c) shallow infaunal (0.7-1.5 cm BWSI), d) intermediate infaunal (1.5-3 cm BWSI), and e) deep infaunal (>3 cm BWSI).

Depth (m)	Paleodepth (m)	Lower CL	Upper CL
256.50	31.88	-25.32	89.08
254.00	449.67	301.18	598.16
251.50	394.53	239.99	549.08
249.00	383.67	244.64	522.69
246.50	321.86	210.09	433.63
244.00	447.91	313.78	582.05
241.50	443.72	295.62	591.81
239.00	383.02	251.29	514.75
236.50	440.75	283.07	598.43
234.00	458.48	317.39	599.57
231.50	401.62	298.15	505.10
229.00	370.43	231.37	509.48
227.00	439.12	298.50	579.75
224.00	342.36	222.61	462.11
221.50	372.87	234.63	511.10
219.00	405.48	275.03	535.93
216.50	405.27	230.55	580.00
214.00	383.92	218.85	548.98
211.50	156.63	48.45	264.81
209.00	247.46	121.20	373.71
206.50	303.18	186.51	419.85
204.00	339.13	192.95	485.31
201.50	341.18	230.76	451.60
199.50	375.50	248.36	502.64
196.50	333.72	216.86	450.58
194.00	334.10	224.06	444.13
191.50	326.20	175.12	477.27
189.00	307.78	180.57	434.99
186.50	269.44	166.35	372.54
184.00	301.41	171.45	431.36
181.50	287.80	162.02	413.58
179.00	282.82	165.26	400.39
176.50	113.74	25.65	201.83
174.00	182.35	123.74	240.96
171.50	166.25	72.89	259.61
169.00	197.67	117.59	277.74
166.50	166.83	105.78	227.88
164.00	167.09	106.56	227.63
161.50	161.61	99.03	224.19
159.00	189.16	109.18	269.14
157.00	161.68	102.72	220.65
154.00	164.57	100.07	229.07
151.50	155.43	92.55	218.30
149.00	155.08	105.60	204.55
146.50	171.87	111.02	232.72
144.00	162.91	106.42	219.40
141.50	214.61	140.83	288.39
139.00	162.52	102.45	222.58
136.50	179.19	117.94	240.44
134.00	173.87	112.11	235.63
131.50	168.71	106.75	230.67
129.00	190.47	128.67	252.27
126.50	179.28	119.27	239.29
124.00	230.78	160.65	300.90
121.50	175.32	119.02	231.62
119.00	176.16	120.81	231.51
116.50	166.96	111.89	222.03
114.00	194.59	127.54	261.65
112.50	181.35	124.82	237.87
109.00	168.79	107.86	229.72
106.50	186.27	118.63	253.90
104.00	183.70	123.02	244.38
101.50	170.59	113.55	227.64
99.00	167.50	105.51	229.50
96.50	151.64	95.13	208.15
94.00	175.42	114.56	236.27
91.50	165.42	102.85	227.99
88.50	180.08	120.27	239.89
86.50	145.96	90.01	201.91
84.00	170.39	97.52	243.25
81.50	142.10	86.03	198.17
79.00	149.95	102.74	197.17
76.50	155.04	96.88	213.21
74.50	160.35	101.69	219.02
71.50	149.16	92.25	206.07
69.00	148.26	92.60	203.93
66.50	134.91	81.70	188.12
64.50	37.94	-14.25	90.13
61.50	46.80	15.50	78.09
59.00	47.83	20.87	74.78
56.50	52.97	0.84	105.11
54.00	44.27	2.30	86.25
51.50	48.18	0.29	96.06
49.00	40.04	-1.01	81.09
46.50	49.58	4.65	94.51
44.00	40.99	4.73	77.25
41.50	52.68	23.16	82.19
39.00	12.37	-27.85	52.60
36.50	13.26	-11.84	38.36

Table 3.2. Paleodepth estimates in meters, and lower and upper confidence limits (CL).

Microhabitat				
Epifauna	**Epifauna-shallow infauna**	**Shallow infauna**	**Intermediate infauna**	**Deep infauna**
Asterigerinata mamilla	*Ammonia beccarii*	*Amphicoryna scalaris*	*Melonis barleeanum*	*Cassidulinoides bradyi*
Asterigerinata sp.	*Ammonia inflata*	*Amphicoryna semicostata*	*Melonis soldanii*	*Fursenkoina schreibersiana*
Cibicides refulgens	*Ammonia tepida*	*Amphicoryna sublineata*	*Melonis* sp.	*Globobulimina affinis*
Cibicides lobatulus	*Ammonia* sp.	*Amphicoryna* sp.	*Nonion boueanum*	*Globobulimina ovula*
Cibicides wuellerstorfi	*Anomalinoides flinti*	*Bigenerina nodosaria*	*Nonionella turgida*	*Globobulimina* sp.
Cibicides sp.	*Anomalinoides helicinus*	*Bolivina punctata*	*Nonionella* sp.	*Pleurostomella* sp.
Cymbaloporetta squammosa	*Anomalinoides* sp.	*Bolivina reticulata*	*Rectuvigerina* sp.	*Praeglobobulimina ovata*
Discorbis sp.	*Burseolina calabra*	*Bolivina* sp.		
Elphidium advenum	*Cassidulina crassa*	*Brizalina arta*		
Elphidium complanatum	*Cassidulina* sp. 1	*Brizalina dilatata*		
Elphidium macellum	*Cassidulina* sp.	*Brizalina spathulata*		
Hanzawaia boueana	*Cibicidoides dutemplei*	*Brizalina* sp.		
Hanzawaia sp.	*Cibicidoides floridanus*	*Bulimina aculeata*		
Planulina ariminensis	*Cibicidoides incrassatus*	*Bulimina alazanensis*		
Planulina sp.	*Cibicidoides kullenbergi*	*Bulimina costata*		
Rosalina sp.	*Cibicidoides pachyderma*	*Bulimina elongata*		
	Cibicidoides ungerianus	*Bulimina mexicana*		
	Cibicidoides sp.	*Bulimina subulata*		
	Elphidium sp.	*Bulimina* sp.		
	Eponides sp.	*Cancris auriculus*		
	Fissurina sp.	*Cancris* sp.		
	Globocassidulina subglobosa	*Cassidulina carinata*		
	Gyroidinoides laevigatus	*Cassidulina laevigata*		
	Gyroidinoides soldanii s.l.	*Chrysalogonium* sp.		
	Gyroidinoides umbonatus	*Dentalina leguminiformis*		
	Gyroidinoides sp.	*Dentalina* sp.		
	Heterolepa bellincionii	*Dorothia gibbosa*		
	Hoeglundina elegans	*Eggerella bradyi*		
	Lagena striata	*Florilus* sp.		
	Lagena sp.	*Glandulina* sp.		
	Lenticulina calcar	*Globulina* sp.		
	Lenticulina cultrata	*Martinottiella communis*		
	Lenticulina curvisepta	*Nodosarella* sp.		
	Lenticulina inornata	*Nodosaria pentecostata*		
	Lenticulina rotulata	*Nodosaria* sp.		
	Lenticulina vortex	*Nonion* sp.		
	Lenticulina sp.	*Orthomorphina tenuicostata*		
	Marginulina costata	*Orthomorphina* sp.		
	Marginulina glabra	*Pandaglandulina dinapolii*		
	Marginulina hirsuta	*Pullenia bulloides*		
	Marginulina sp.	*Pullenia quinqueloba*		
	Neoeponides sp. 1	*Pullenia salisburyi*		
	Oridorsalis umbonatus	*Reussella spinulosa*		
	Planularia sp.	*Stilostomella monilis*		
	Quinqueloculina sp.	*Stilostomella vertebralis*		
	Siphonina reticulata	*Stilostomella* sp. 1		
	Siphotextularia concava	*Stilostomella* sp.		
	Sphaeroidina bulloides	*Trifarina angulosa*		
	Spiroplectinella sagittula	*Trifarina bradyi*		
	Textularia agglutinans	*Uvigerina canariensis*		
	Textularia calva	*Uvigerina peregrina*		
	Textularia pala	*Uvigerina rutila*		
	Textularia pseudorugosa	*Uvigerina striatissima*		
	Textularia sp.	*Valvulineria complanata*		
	Vaginulina sp.	*Valvulineria* sp.		

Table 3.3. Microhabitat preferences of benthic foraminifera from the Montemayor-1 core.

3.5. Results

Results of the measured parameters allow the division of the studied section into three intervals: a) The lower interval is from 256.5 m, the base of the core, to 180 m. This ranges the latest Tortonian and lower part of the Messinian. b) The middle interval is from 180 to 60 m. This includes the upper part of the Messinian up to the unconformity detected close to the Miocene–Pliocene boundary. c) The upper interval is from 60 m to the end of the section, 36.5 m, that corresponds with the lower part of the Pliocene deposits. For practical reasons, in the description and discussion following below, we will refer to these three parts or intervals.

3.5.1. Numerical faunal parameters, sand content, and sedimentation rate

The P/B ratio shows a very sharp increase in the lowermost part, with maximum values around 0.6, followed by a gradual decrease to values between approximately 0.1 and 0.3 in the middle and uppermost part of the section. The lowest P/B ratios (<0.1) appear in the upper part of the section (Fig. 3.4). The sand content is lower than 5% throughout most of the core, except in the two first samples, at 256.5 and 254 m (nearly 50%), and in the upper part of the section (fluctuating values with up to 38%). The total number of benthic foraminifera per gram of dry sediment (N/g) shows high values in the lower part (>50 N/g as an average) of the core. The middle part of the section starts with values below 50 N/g and ends with values above 50 N/g. Fluctuating values (mostly higher than 50 N/g) are recorded in the upper part of the section.

In the lowermost part of the core (256.5–240 m), the estimated sedimentation rate shows the lowest values throughout the section, with 2.7 cm/kyr (Fig. 3.3).The estimated sedimentation rate exhibits an abrupt increase at 217.5 m, corresponding to the base of chron C3r, changing from 3.2 cm/kyr to 20 cm/kyr (Fig. 3.3). This significant change in sedimentation rate is also detected by a sharp decrease in natural remanent magnetization intensities (Larrasoaña et al., 2008).

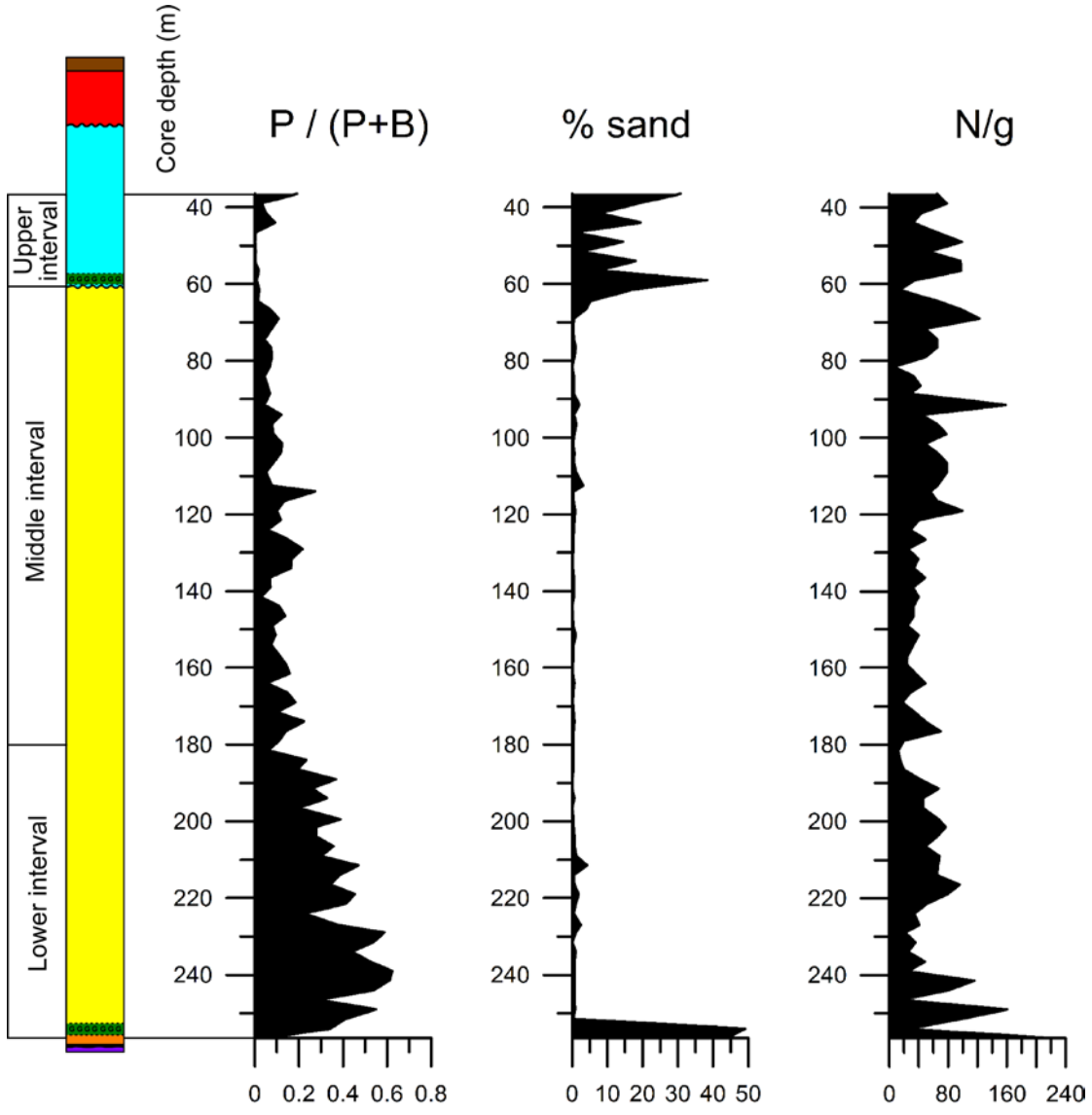

Figure 3.4. Curves showing the planktonic–benthonic ratio (P/B ratio), sand content, and number of benthic foraminiferal per gram of sediment (N/g) along the Montemayor-1 core.

3.5.2. Species richness, diversity and dominance

In the lower part of the section, the number of taxa ranges between 40 and 50, followed by a decrease with values ranging between 30 and 40. In the middle part, the values fluctuate around 40. In the upper part, the number of taxa first decreases sharply, reaching the lowest values (<30) between approximately 60 and 45 m, followed by increased values>30 (Fig. 3.5).

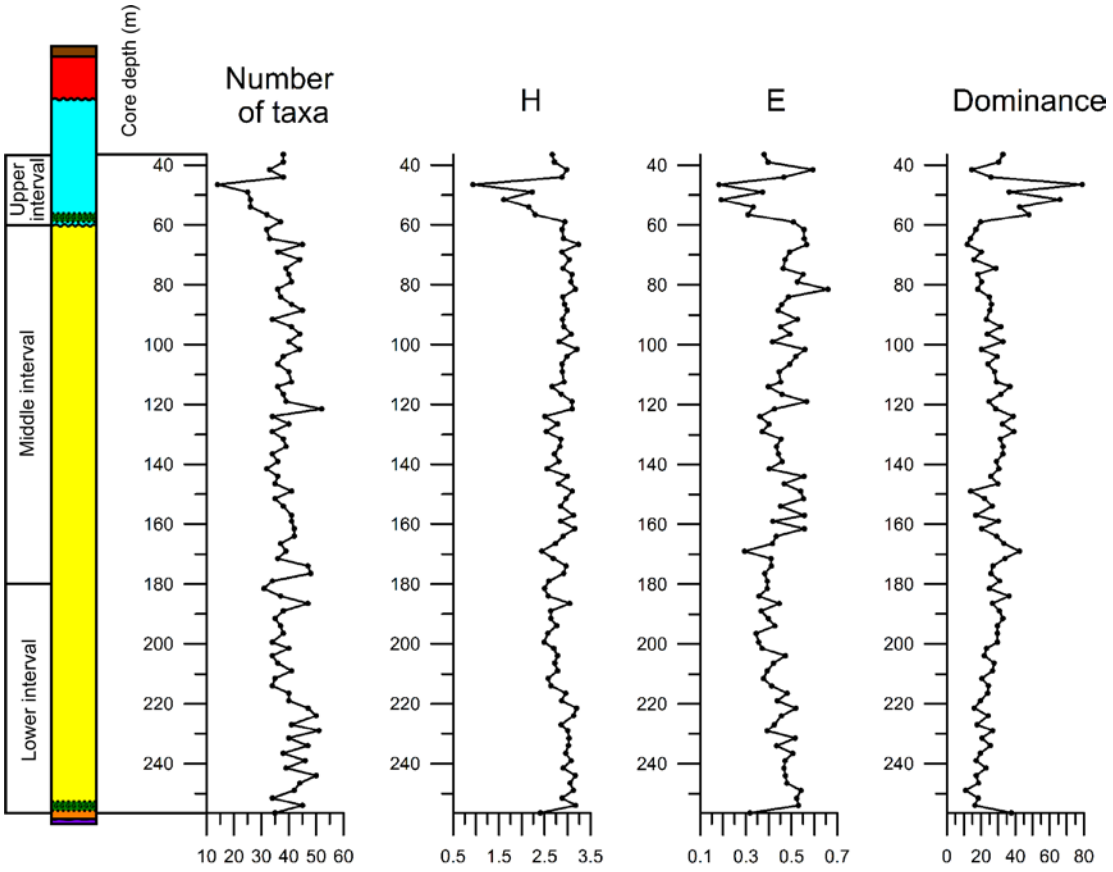

Figure 3.5. Number of taxa, diversity metrics (Shannon index H, evenness E) and dominance.

The Shannon index (H) and the evenness (E) have very similar trends as they show a positive high Pearson correlation coefficient (Table 3.4), but fluctuations in the evenness are more expressed (Fig. 3.5). Both H and E decrease progressively through the lower part of the core. In the middle part, both metrics alternate between relatively higher, then lower and finally higher values. In the upper part, H and E sharply decrease reaching the lowest values (H=0.93, E=0.18). Above this low diversified interval, both parameters abruptly increase. The dominance shows an opposite trend as those shown by H and E. This is consistent with the negative high Pearson correlation coefficients (Table 3.4).

3.5.3. Benthic foraminiferal assemblages

The Q-mode PCA yields 3 assemblages that explain 81.8% of the total variance (Table 3.5). The *Cibicidoides pachyderma* assemblage (PC1), with *Cibicidoides* sp.,

	QPC1	QPC2	QPC3	RPC1	RPC2	RPC3	P/B ratio	% sand	N/g	G/g	Number of taxa	H	E	D
QPC1	1.000													
QPC2	-0.674	1.000												
QPC3		-0.643	1.000											
RPC1		0.318	-0.753	1.000										
RPC2		-0.492	0.472		1.000									
RPC3	0.848	-0.575				1.000								
P/B ratio		-0.483	0.655		0.816		1.000							
% sand	-0.529	0.552	-0.428	0.372		0.488		1.000						
N/g	-0.283	0.311							1.000					
G/g								0.641		1.000				
Number of taxa	0.392	-0.571	0.294		0.317	0.415	0.374				1.000			
H	0.481	-0.567				0.553					0.787	1.000		
E	0.356	-0.314				0.498					0.358	0.828	1.000	
D		0.458			-0.324	-0.316	-0.313				-0.567	-0.880	-0.822	1.000

Table 3.4. Pearson correlation coefficients at *p*-valueb0.01 of the Q-mode and R-mode PCA assemblages and the other measured parameters.

Cibicidoides floridanus and *Brizalina spathulata* as accompanying species (Fig. 3.6A-D, Table 3.5), shows a fluctuating pattern in the lower part and becomes dominant in the middle part of the core (Fig. 3.7). The *Nonion fabum* assemblage (PC2) includes *Ammonia beccarii*, *Spiroplectinella* sp., *Ammonia* sp., *Bulimina elongata* and *Brizalina spathulata* as associated taxa (Fig. 3.6D-H, Table 3.5). This assemblage is important in the lowermost sample and in the upper part of the section (Fig. 3.7). The *Uvigerina peregrina* s.l. assemblage (PC3) dominates the lower part and shows significant values in the middle part, between 160 and 140 m (Fig. 3.7). *Bulimina subulata, Cibicidoides pachyderma, Planulina ariminensis* and *Cibicidoides* sp. are the associated taxa (Fig. 3.6A-B, 3.6I-K, Table 3.5).

The relative abundances of dominant and associated taxa from Q-mode assemblages are shown in Fig. 3.8. Three distinctive patterns of relative abundance can be distinguished. The first group of species dominates in the lower part of the core, comprising *Uvigerina peregrina* s.l. (*Uvigerina peregrina*+*Uvigerina pygmaea*), *Bulimina subulata* and *Planulina ariminensis*. The latter species is exclusively limited to this part of the core (Fig. 3.8). The second group of species is important throughout the section, except in the upper part, comprising *Cibicidoides pachyderma, Cibicidoides* sp., and in lesser abundance *Cibicidoides floridanus*. The third group of species dominates in the upper part of the section, comprising *Ammonia beccarii*, *Ammonia* sp., *Spiroplectinella* sp., *Bulimina elongata*, *Nonion fabum* and *Brizalina spathulata*.

Among them, *Nonion fabum* reaches the highest values when the others show low percentages (Fig. 3.8). These species show also a peak of abundance in the first sample of the core.

PC assemblage	Variance (%)	Species	Score
1	49.6	***Cibicidoides pachyderma***	6.86
		Cibicidoides sp.	1.98
		Cibicidoides floridanus	1.22
		Brizalina spathulata	1.03
2	8.5	***Nonion fabum***	7.2
		Ammonia beccarii	2.01
		Spiroplectinella sp.	1.31
		Ammonia sp.	1.19
		Bulimina elongata	1.13
		Brizalina spathulata	1.05
3	23.7	***Uvigerina peregrina* s.l.**	6.01
		Bulimina subulata	2.65
		Cibicidoides pachyderma	2.46
		Planulina ariminensis	1.77
		Cibicidoides sp.	1.22

Table 3.5. Results of the Q-mode principal component analysis with indication of the more representative benthic foraminiferal species.

The R-mode PCA explains 31.2% of the total variance and differentiates 3 assemblages (Fig. 3.9, Table 3.6). The *Anomalinoides flinti* assemblage (PC2) is only important in the lower, part between 254 and 211.5 m (Fig. 3.9). Some of the associated taxa of this assemblage are *Siphonina reticulata*, *Oridorsalis umbonatus*, *Uvigerina striatissima* and *Planulina ariminensis* (Fig. 3.6K, 3.6O-R, Table 3.6). In the middle part, the *Cibicidoides pachyderma* assemblage (PC3) becomes significant (Fig. 3.9). *Cibicidoides floridanus* and *Hanzawaia boueana* are other important taxa of this assemblage (Fig. 3.6A-C, 3.6S, Table 3.6). In the upper part, from 44m to the top, the *Spiroplectinella* sp. assemblage dominates (PC1) (Fig. 3.9). This assemblage includes V*alvulineria complanata*, *Textularia* sp., *Melonis barleeanum*, *Textularia agglutinans*, *Cassidulina laevigata* and *Ammonia beccarii* as secondary species (Fig. 3.6G, 3.6L-N, Table 3.6).

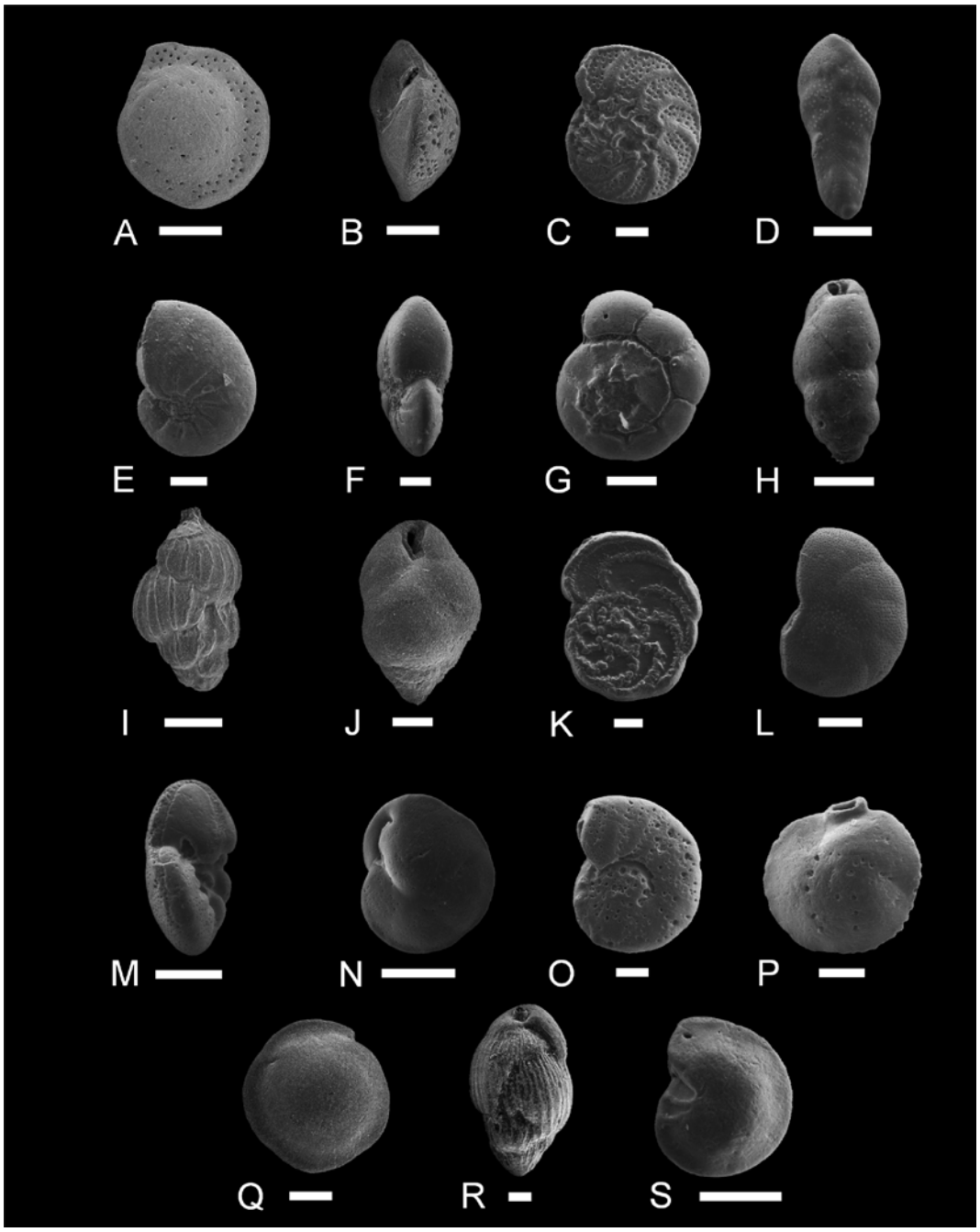

Figure 3.6. Some of the most abundant and representative benthic foraminiferal species in the Montemayor-1 core. A) *Cibicidoides pachyderma*, spiral side; B) *Cibicidoides pachyderma*, peripheral view; C) *Cibicidoides floridanus*, spiral side; D) *Brizalina spathulata*, side view; E) *Nonion fabum*, side view; F) *Nonion fabum*, peripheral view; G) *Ammonia beccarii*, spiral side; H) *Bulimina elongata*, side view; I) *Uvigerina peregrina* s.l., side view; J) *Bulimina subulata*, side view; K) *Planulina ariminensis*, spiral side; L) *Valvulineria complanata*, spiral side; M) *Valvulineria complanata*, peripheral view; N) *Cassidulina laevigata*, apertural side; O) *Anomalinoides flinti*, spiral side; P) *Siphonina reticulata*, side view; Q) *Oridorsalis umbonatus*, spiral side; R) *Uvigerina striatissima*, side view; S) *Hanzawaia boueana*, umbilical side. Scale bars=100 μm.

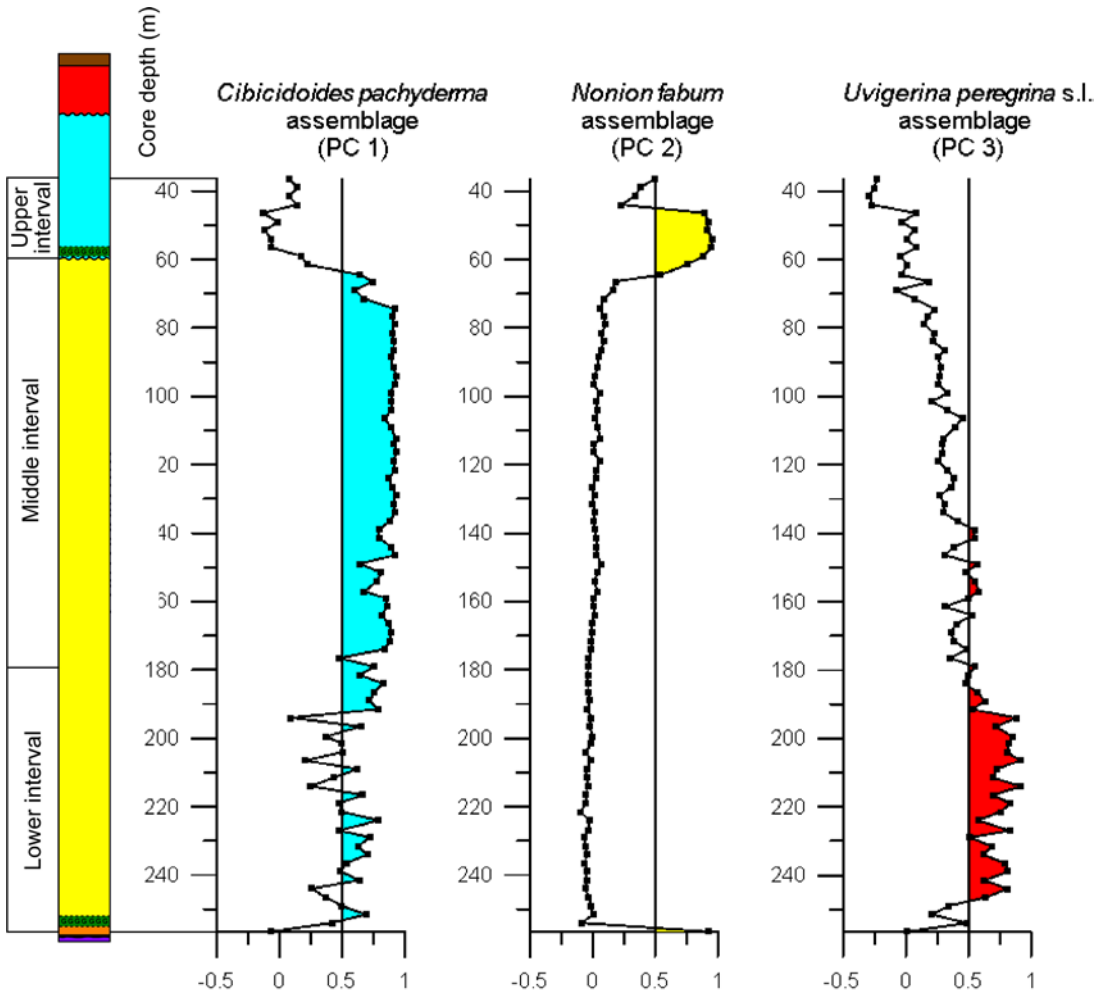

Figure 3.7. Benthic foraminiferal assemblages as derived from Q-mode principal component analyses (PCA). Principal component loadings higher than 0.5 are considered significant following the suggestions of Malmgren and Haq (1982) and indicated by colour shading.

3.5.4. Estimated paleodepth

A water depth of 31.88 m is estimated for the lowermost sample (Fig. 3.10, Table 3.2). Then, paleodepth sharply increases reaching 449.67 m, and decreases to 282.82 m at the end of the lower part. An important sea-level lowering is detected at 211.5 m, in the middle part of the lower interval, followed by a rapid increment up to 375.50 m. Paleodepth suddenly diminishes at the beginning of the middle part, then slightly decreases and finally abruptly drops to 37.94 m. In the upper part, paleodepth remains stable with values between 40 and 50 m, except for the last two samples that has values around 12 m (Table 3.2).

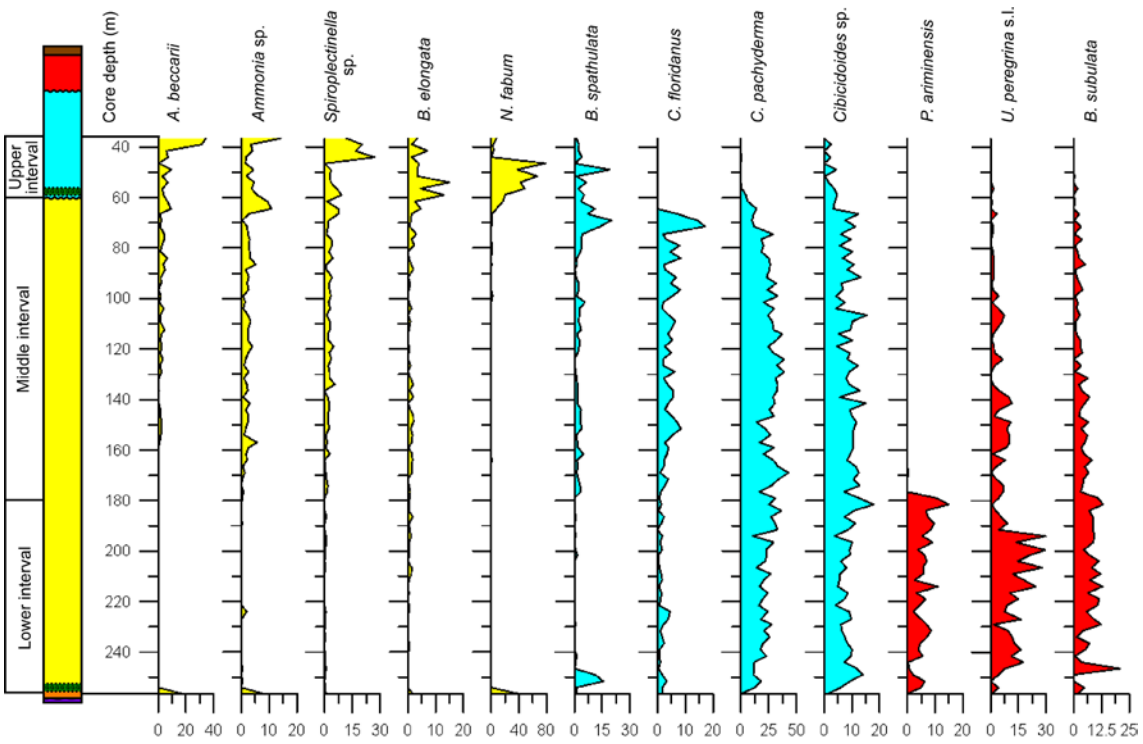

Figura 3.8. Relative abundance (in percentage) of dominant taxa as extracted from the Q-mode benthic foraminiferal assemblages.

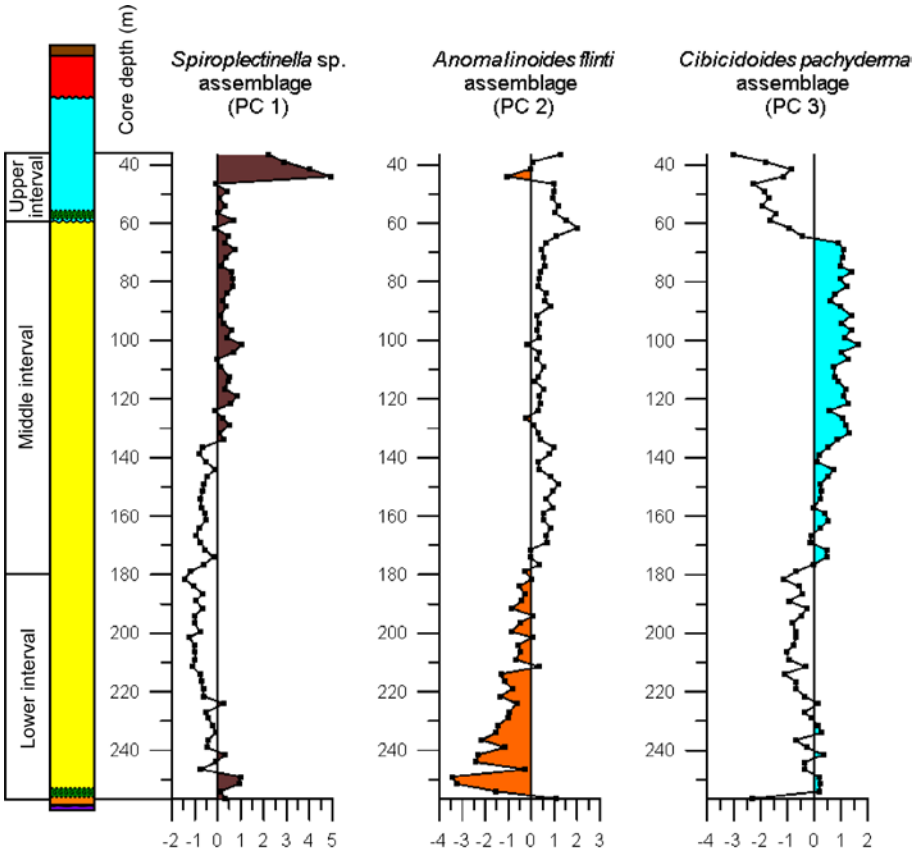

Figure 3.9. Benthic foraminiferal assemblages as derived from R-mode principal component analyses (PCA). Significant principal component scores are indicated in colour.

PC assemblage	Variance (%)	Species	Loading
1	11.5	***Spiroplectinella* sp.**	0.85
		Valvulineria complanata	0.76
		Textularia sp.	0.7
		Orthomorphina tenuicostata	0.68
		Melonis barleeanum	0.68
		Textularia agglutinans	0.67
		Cassidulina laevigata	0.66
		Ammonia beccarii	0.56
2	9.9	***Anomalinoides flinti***	-0.7
		Cibicidoides incrassatus	-0.67
		Uvigerina canariensis	-0.65
		Globocassidulina subglobosa	-0.6
		Planulina sp.	-0.59
		Siphonina reticulata	-0.58
		Oridorsalis umbonatus	-0.57
		Uvigerina striatissima	-0.56
		Planulina ariminensis	-0.55
		Gyroidinoides sp.	-0.54
		Anomalinoides sp.	-0.53
3	9.7	***Cibicidoides pachyderma***	0.61
		Cibicidoides floridanus	0.6
		Pullenia bulloides	0.59
		Sphaeroidina bulloides	0.55
		Lenticulina sp.	0.55
		Hanzawaia boueana	0.53
		Melonis soldanii	0.53
		Gyroidinoides soldanii	0.51

Table 3.6. Results of the R-mode principal component assemblages with indication of the more representative benthic foraminiferal species.

3.5.5. Distribution of benthic foraminiferal microhabitats

The lowermost sample has a high percentage of intermediate infaunal species (Fig. 3.11). In the lower part of the core, between 254 and 194 m, shallow infaunal taxa show high percentages and epifauna only amounts to 10% on average. Between 194 and 180 m, the epifauna and epifauna-shallow infauna increase, and the shallow infauna decreases. In the middle part of the core, between 165 and 130 m, the shallow infauna has relatively high values. Up in the section, epifaunal-shallow infaunal species become significant but then gradually diminish, being replaced by shallow infauna towards the

top of the middle part (around 60 m). In the upper part, between 64.5 and 46.5 m, intermediate infaunal species are significantly abundant, reaching up to 80%. In this interval, deep infauna also reaches the highest values. From 56.5 to the top of the core, the fauna is dominated by shallow infaunal and epifaunal shallow infaunal taxa (Fig. 3.11).

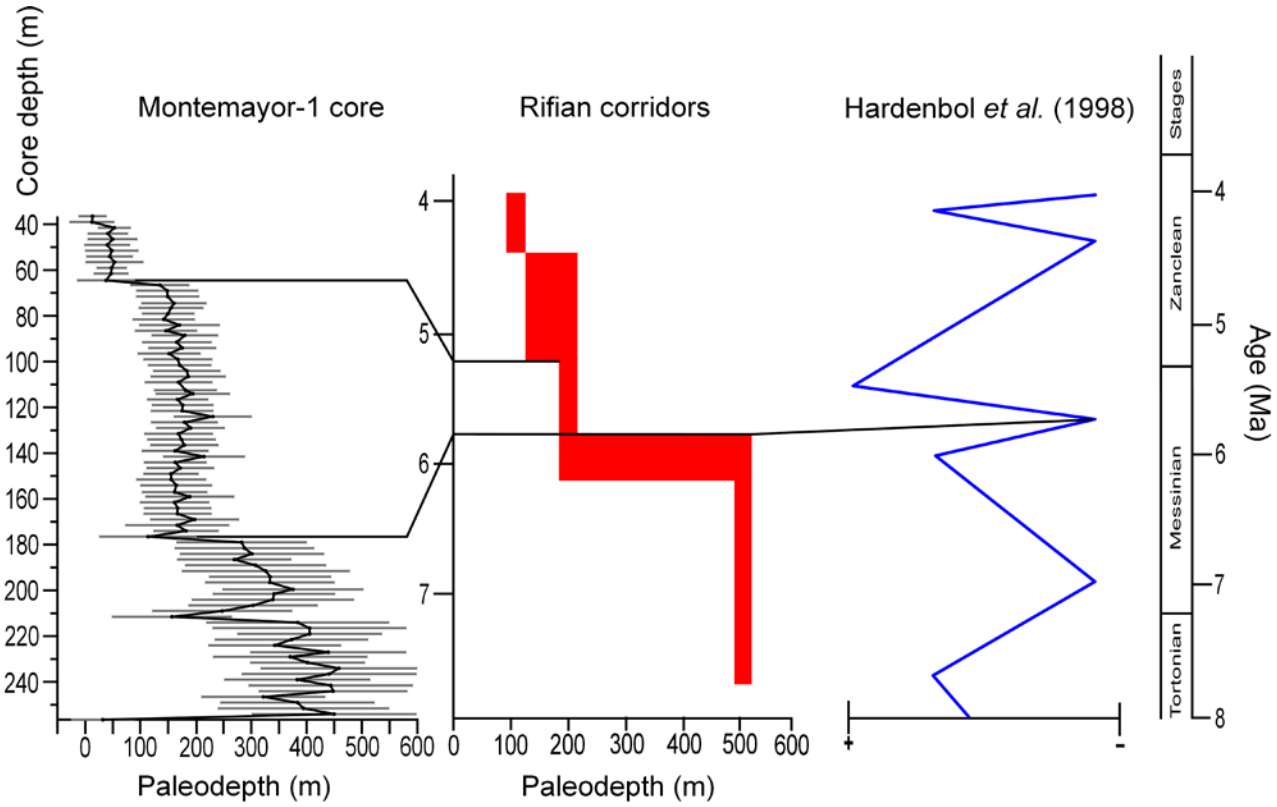

Figure 3.10. Estimated paleodepth changes for theMontmayor-1 core. Horizontal bars represent the 95% confidence intervals. Three important sea-level drops are shown at 211.5, 176.5, and 61.5 m. This sea-level trend is correlated with that inferred in the Rifian corridors by Barbieri and Ori (2000) and with the global sea-level curve of Hardenbol et al. (1998). The two last shallowing events correlates precisely with similar lowering inferred in the Rifian corridors. The sea-level fall at about 211.5 m can be linked with the onset of the MSC.

3.6. Discussion

3.6.1. Relative sea-level fluctuations

According to the paleobathymetric indicators used in this study, a very abrupt sea-level rise is inferred at the lowermost part of the core. The Q-mode PCA *Nonion*

fabum assemblage, which includes species inhabiting inner-middle shelf such as *Ammonia beccarii* and *Ammonia* sp. (Murray, 1991, 2006), occurs in the lowermost sample of the section (Fig. 3.7, Table 3.5). A peak in sand content in this sample (Fig. 3.4) is consistent with a shallow inner-middle shelf paleoenvironment. Further, this is supported by a paleodepth of 31.88m estimated with the transfer function (Fig. 3.10, Table 3.2). Coincidently, a very low value of the P/B ratio is also shown (Fig. 3.4).

The next three samples show a significant increase in the *Cibicidoides pachyderma* assemblage that includes *Cibicidoides floridanus*, a species living on the outer shelf (van Morkhoven et al., 1986; Barbieri and Ori, 2000), as associated species (Fig. 3.7, Table 3.5). Coinciding with the increased importance of this assemblage, the P/B ratio and paleodepth rise concomitantly (Figs. 3.4 and 3.10), responding to the rapid sea-level rise. Sand-sized particles virtually disappear, which is consistent with the inferred deepening (Fig. 3.4).

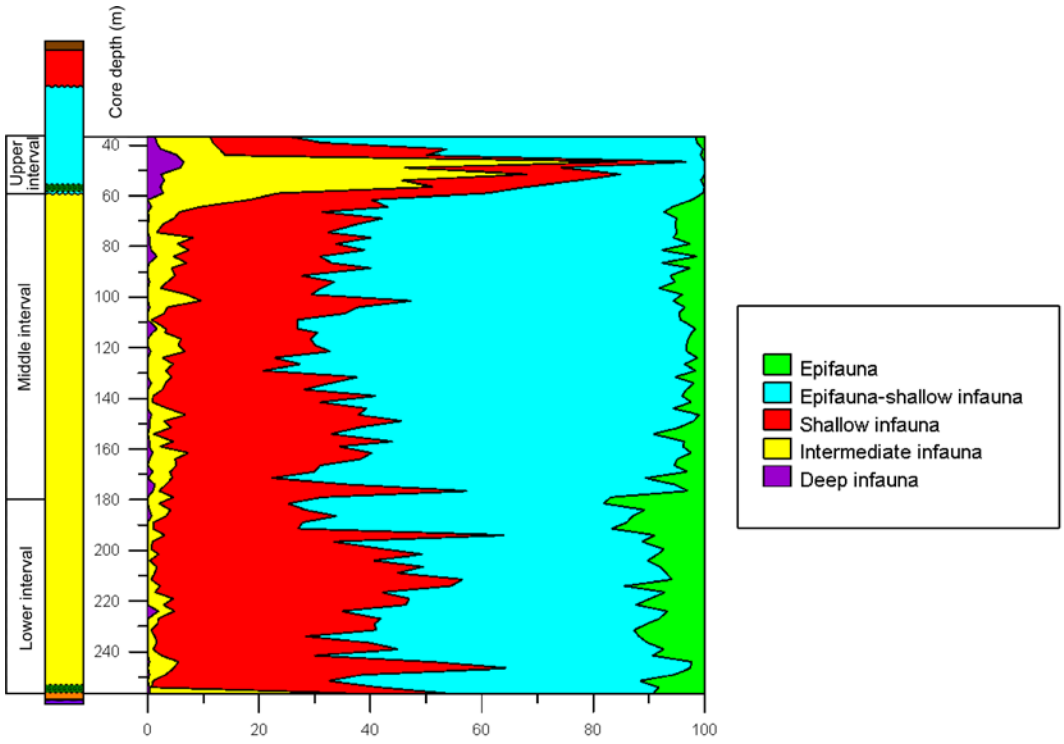

Figure 3.11. Distribution of microhabitat preferences of benthic foraminifera (in percentage of the total taxa) along the studied section.

Enhanced glauconite concentration is recorded in the second sample of the section. Glauconite is commonly formed along the shelf to continental slope during transgressions and under very low sedimentation rates (Odin and Matter, 1981; Galán et

al., 1989; Harris and Whiting, 2000). The rapid transgression produced a sharp onshore shift of the depositional systems, trapping the coarse-grained sediment in shallower areas of the platform. Sedimentation rate dropped and sand grains virtually disappeared in this interval (Figs. 3.3 and 3.4), thus promoting the deposition of glauconite. As a recent analogue, glauconite is formed on the present-day outer shelf off Guadiana River (SW Spain), close to the study area (Gonzalez et al., 2004).

Magnetobiostratigraphic data indicate that the rapid sea-level rise occurred during the latest Tortonian-earliest Messinian. The same sea-level rise has been also inferred from the investigation of onland sections along the northern margin of the lower Guadalquivir Basin (Baceta and Pendón, 1999; González-Regalado et al., 2005).

The maximum flooding is reached between 254 and 236.50m core depth as indicated by the dominance of the R-mode PCA *Anomalinoides flinti* assemblage (Fig. 3.9), and the highest paleodepth values (Fig. 3.10, Table 3.2). *Anomalinoides flinti* is common in middle and lower slope settings (Berggren and Haq, 1976). Some additional taxa of this assemblage (Table 3.6), such as *Siphonina reticulata* and *Oridorsalis umbonatus*, also inhabit the middle and lower slope (Berggren and Haq, 1976; Berggren et al., 1976; Hayward et al., 2003). This assemblage shows a positive Pearson correlation coefficient with P/B ratio (Table 3.4) and dominates at highest P/B ratios (Fig. 3.4). Consequently, maximum flooding detected in this part of the core reached at least the middle talus slope.

Following the maximum flooding, the P/B ratio and paleodepth decrease progressively up to the end of the lower core interval, suggesting a sea-level lowering (Figs. 3.4 and 3.10). This interpretation is supported by a decrease of the *Anomalinoides flinti* assemblage scores (Fig. 3.9). The dominance of the *Uvigerina peregrina* s.l. assemblage in this part of the section (Fig. 3.7) suggests an upper slope depositional environment. Similarly, *Planulina ariminensis* (Table 3.5), an associated species of the *U. peregrina* s.l. assemblage, predominantly inhabits the upper slope, with maximum abundances commonly between 300 and 500 m (Berggren and Haq, 1976; Schönfeld, 1997). The same bathymetric preference of *P. ariminensis* was also inferred for occurrences in Miocene-early Pliocene deposits off Morocco (Gebhardt, 1993). This species also inhabits the upper slope in the continental margins off NW Africa, off southern Portugal, and in the Gulf of Cádiz (Lutze, 1980; Schönfeld, 1997, 2002). Quantitative transfer function also suggests an upper slope water depth between 400 and

250 m (Fig. 3.10, Table 3.2). Coincidently, *U. peregrina* is below 300 m depth in the Gulf of Mexico (Parker, 1954; Schönfeld, 2006).

In the last 10 m of the lower interval, 190–180 m, the P/B ratio, estimated paleodepth, and the *Uvigerina peregrina* s.l. assemblage decrease rapidly (Figs. 3.4, 3.7 and 3.10, Table 3.2). All these changes are interpreted as a sea-level fall. Concurrently, the *Cibicidoides pachyderma* assemblage dominates, as documented by the Q-mode assemblage (Fig. 3.7). Above this benthic foraminifera faunal turnover, at 179 m, *Planulina ariminensis* disappears (Fig. 3.8), thus indicating the transition to the outer shelf, and corroborating the sea-level decrease. At the north of Cape Blanc in the continental margin of NW Africa the shallowest occurrence of *P. ariminensis* also indicates the transition to the outer shelf (Lutze and Coulbourn, 1984).

This sea-level drop occurred in chron C3r (Fig. 3.10, Table 3.2). Therefore the age uncertainty for this event is from 6.033 to 5.235 Ma. However, it can be correlated with the global sea-level fall that took place during the mid Messinian (Haq et al., 1987; Hardenbol et al., 1998) (Fig. 3.10). At the northwestern margin of Morocco, Barbieri and Ori (2000) also detected a sea-level fall during the middle part of the Messinian that can be correlated with the sea-level drop observed in the Montemayor-1 core (Fig. 3.10). These authors associated the mid-Messinian shallowing with the onset of the MSC on the Atlantic side of the Rifian corridors and correlated it with the glacial stages TG22 and TG20 of Shackleton et al. (1995), two of the most pronounced glacial events occurring during the Messinian. Nonetheless, these glacial stages have been dated at 5.79 and 5.75 Ma, respectively (Krijgsman et al., 2004), well after the onset of the MSC that took place at 5.96±0.02 Ma according to Krijgsman et al. (1999b). Hence, the major sea-level fall observed both in the Montemayor-1 core and in the Rifian corridors would most likely postdate the start of the MSC. The detailed record along the core of the estimated paleodepth trend based on the transfer function allows us to identify a major sea-level fall at 211.5 m, before the aforementioned major sea-level drop (Fig. 3.10, Table 3.2). This sea-level fall could be related to the onset of the MSC.

In spite of the constant dominance of the outer shelf *Cibicidoides pachyderma* assemblage throughout the middle core interval, the continuous upward decrease in P/B ratios and paleodepth (Figs. 3.4 and 3.10) suggests a slight and progressive lowering in sea level. The middle core interval ends with a sharp sea-level fall reaching the middle shelf. This shallowing is also recorded in the Rifian corridors (Fig. 3.10).

The continuous Messinian record is interrupted by a discontinuity around the Miocene-Pliocene boundary (Fig. 3.3). After this unconformity, an inner-middle shelf setting established during the deposition of the upper part of the section. This setting is indicated by the dominance of the *Nonion fabum* assemblage (Fig. 3.7), and paleodepth values between 40 and 50m (Fig. 3.10, Table 3.2).

The glauconitic layer at the base of the upper part of the core caps the unconformity (Fig. 3.3). This bed is also present in onland sections and has been interpreted as the transgressive deposits formed during the early Pliocene (Sierro and Flores, 1992; Sierro et al., 1996). Nonetheless, this deepening did not exceed the early Messinian inundation since only shelf deposits were formed during the early Pliocene at the studied site.

The global sea-level curve of Hardenbol et al. (1998) shows three transgressive-regressive 3rd-order cycles during the late Tortonian- early Pliocene (Fig. 3.10). This global trend is not recorded in the Montemayor-1 core. As previously discussed, sea-level at the Montemayor-1 core site shows a very rapid rise close to the Tortonian-Messinian boundary, when the global sea-level curve shows a progressive shallowing (Fig. 3.10). After the sudden deepening in the Montemayor-1 core, sea-level followed a continuous fall until the end of the Messinian (Fig. 3.10). The Hardenbol et al. (1998) eustatic curve shows, however, a fluctuating sea level. Gebhardt (1993) and Barbieri and Ori (2000) noticed a similar Messinan sea-level trend in the Atlantic side of the Rifean corridors as that observed in Montemayor-1 core, thus differing from the global one. According to these authors, a regional tectonic uplifting might account for the continuous sea-level drop through the Messinian in a context of global fluctuating sea level. Tectonic uplifting also led to the closure of the Guadalhorce corridor during the Messinian, most likely just before the main gypsum deposition in the Mediterranean (Martín et al., 2001). The N-S compressional regime established during the Messinian in the Betic-Rifean domain (Sanz de Galdeano, 1990; Maldonado et al., 1999) supports this interpretation. Thus, our data sustain that the tectonic uplift could played an important role in the relative sea-level changes observed in the Atlantic side of the Atlantic-Mediterranean gateways in both the Rifian corridors and the Betic ones. This might explain the age disagreement between the major sea-level fall observed during the mid Messinian and that leading to the onset of the MSC.

3.6.2. Paleoenvironmental key factors: continental versus marine organic matter supply and seafloor oxygen content

It is well known that organic matter supply and dissolved oxygen content in the sea bottom and pore waters are among the key environmental factors affecting benthic foraminifera distribution (e.g., Jorissen et al., 1995; Fariduddin and Loubere, 1997; De Rijk et al., 2000; Jorissen et al., 2007). The impact of these factors on benthic foraminifera cannot be analyzed separately. The oxygen content of the sea floor and in the pore waters is controlled by the quantity of organic matter. In environments with high organic input, the remineralisation of organic matter decreases the oxygen concentration on the sea floor as well as the depth of oxygen penetration below the water-sediment interface (Jorissen et al., 1995; Mojtahid et al., 2009, 2010a). Consequently, eutrophic environments are commonly characterized by a low oxygen concentration and shallow oxygen penetration, while oligotrophic environments exhibit a high oxygen concentration and deep oxygen penetration. Furthermore, changes in the trophic conditions can produce variations in the diversity and microhabitat preferences. Oligotrophic environments are dominated by epifaunal taxa and have rather low diversity; mesotrophic environments show the highest diversity and all microhabitats are represented; and finally, eutrophic environments are characterized by low diversity and dominance of (deep) infaunal taxa (Jorissen et al., 1995).

Based on this concept, it appears likely that the benthic foraminiferal fauna at the study site was also influenced by changes in trophic conditions, particularly in quantity and quality of the available food source. In general, continental organic matter is more refractory than organic matter primarily produced in marine settings since terrestrial-derived organic matter is degraded before reaching the marine environment (Zonneveld et al., 2010). High input of this terrestrial organic matter can provoke eutrophication and led to oxygen depletion at the bottom and pore waters (Van der Zwaan and Jorissen, 1991; Jorissen et al., 1992; Donnici and Serandrei Barbero, 2002)

The inner-middle shelf *Nonion fabum* assemblage at the base of the section (Fig. 3.7) indicates the most eutrophic conditions, suggesting organic matter run-off from the continent. This assemblage is characterized by low diversity and dominance of intermediate infaunal taxa (Figs. 3.5 and 3.11). *Nonion fabum* is usually associated with eutrophic environments with high organic matter of low quality and significant oxygen depletion (Fontanier et al., 2002; Duchemin et al., 2008; Mojtahid et al., 2010a, 2010b).

In the prodelta of the Rhône River, high proportions of *N. fabum* occur under the influence of the river plume reflecting low-quality continental organic matter supply from river discharge and low oxygen penetration (Mojtahid et al., 2010b; Goineau et al., 2011). Similarly, *Bulimina elongata*, an associated species of the *N. fabum* assemblage, can also feed from low quality organic matter and tolerates low oxygen concentrations (Diz and Francés, 2008; Mojtahid et al., 2009). Coincidently, *B. elongata* also occurs in the Rhône prodelta close to the river mouth (Mojtahid et al., 2009).

Above the *Nonion fabum* assemblage, the *Uvigerina peregrina* s.l. and the *Cibicidoides pachyderma* assemblages alternate (Fig. 3.7). *Uvigerina peregrina* s.l. is an opportunistic taxon commonly present in fine grained sediments deposited in environments with significant fluxes of labile organic matter and moderate oxygen depletion (Schmiedl et al., 1997, 2000; 2010; Fontanier et al., 2002; Koho et al., 2008). The presence of *Uvigerina peregrina* s.l. indicates a productivity between 4.0 and 17.0 g C m^{-2} yr^{-1} in NW-Africa and Gulf of Guinea and from 4.0 to 5.1 g C m^{-2} yr^{-1} in the northeastern Atlantic (Schönfeld and Altenbach, 2005). Furthermore, this species is common in upper slope and outer shelf environments under the influence of seasonal upwelling events, for example off Southwest Africa (Schmiedl et al., 1997), off the Ría de Vigo, NW Spain (Martins et al., 2006), off Congo (Mojtahid et al., 2006), and off the Guadiana platform, SW Spain (Mendes et al., 2004), close to the study area.

Accordingly, the presence of upwelling above the upper slope may account for the dominance of *Uvigerina peregrina* s.l. assemblage in the lower part of the section. This assemblage indicates mesotrophic conditions, characterized by a relatively high benthic foraminiferal diversity and low dominance (Fig. 3.5), as well as the highest percentages of shallow infaunal taxa (Fig. 3.11). The high abundance of shallow infaunal taxa in mesotrophic settings is attributed to a diversification of infaunal niches (Milker et al., 2009). The present-day current system in the northern Gulf of Cádiz can be used as a possible analogue for the paleoceanographic setting in the study area during the Messinian. In the present Gulf of Cádiz, major upwelling is located near Cape St. Vicent (S Portugal), and during westerly conditions, upwelled waters extend eastwards along the shelf margin reaching our study area (Vargas et al., 2003; Criado-Aldeanueva et al., 2006).

On the other hand, the C. pachyderma assemblage shows a high abundance of epifaunal-shallow infaunal taxa and relatively low diversity indicating more oligotrophic conditions (Figs. 3.5 and 3.11). *Cibicidoides pachyderma* is a suspension

feeder that inhabits oligo- to mesotrophic environments with high oxygenation contents (Gebhardt, 1999; Schmiedl et al., 2000, 2003). This species feeds from episodic inputs of labile organic matter (Fontanier et al., 2002; Melki et al., 2009). The presence of *Cibicidoides* sp. is also consistent with a well-oxygenated and relatively oligotrophic setting (Kaiho, 1994, 1999; Takata, et al., 2010).

To summarize, the alternation of *Uvigerina peregrina* s.l. and *Cibicidoides pachyderma* assemblages in the lower part of the section suggests episodic influence of upwelling currents and related food pulses at the core site.

At the end of deposition of the lower core interval (194–180 m), the influence of upwelling currents diminished, indicated by the disappearance of the *Uvigerina peregrina* s.l. assemblage and the consistent establishment of the *Cibicidoides pachyderma* assemblage. This faunal turnover coincides with a maximum proportion of epifaunal taxa in the interval between 194 and 180m, attributable to the high abundance of the epifaunal species *Planulina ariminensis* (Figs. 3.7, 3.8 and 3.11). This transition interval likely represents particularly oligotrophic conditions.

The outer shelf *Cibicidoides pachyderma* assemblage dominates throughout the middle part of the section (180–60 m), although some short-term occurrences of the *Uvigerina peregrina* s.l. assemblage are observed between 160 and 140 m.

Similarly, the sporadical influence of upwelling currents likely also fostered high diversity and increase of shallow infaunal species, such as *B. spathulata*, at the end of deposition of the middle core interval (120–60 m) (Figs. 3.5, 3.8 and 3.11). *Brizalina spathulata* can tolerate low oxygen concentrations (Barmawidjaja et al., 1992; Stefanelli, 2004) and shows an opportunistic life style, rapidly responding to pulses of fresh organic matter in high oxygen environments (Fontanier et al., 2003; Diz et al., 2006; Diz and Francés, 2008). In the Ría de Vigo (NW Spain), this species reproduces immediately after phytoplankton blooms related to upwelling conditions (Diz et al., 2006; Diz and Francés, 2008). It is also related to upwelling events off Guadiana River in SW Iberia (Mendes et al., 2004). However, the increased abundance of *B. spathulata* could also be related to nutrient influx derived fromthe continent as has been observed by other authors (i.e. Duchemin et al., 2008; Schmiedl et al., 2010).

During deposition of the upper part of the section (60–36.5 m), the inner-middle shelf was inhabited by the *N. fabum* assemblage indicating eutrophic conditions. Here, species dominance and percentages of deep and intermediate infauna reach maximum values (Figs. 3.5 and 3.11). *Nonion fabum* is found in the finer-grained interval,

between 56.5 and 39 m (Figs. 3.4 and 3.8), consistent with its preference to muddy sediments (Haunold et al., 1997; Rezqi et al., 2000; Duchemin et al., 2008). In the present-day northern and northeastern Gulf of Cádiz, extensive mud deposits accumulate on the middle shelf, related to the Guadiana run-off (Gonzalez et al., 2004) and to the Guadalquivir prodelta (Gutiérrez-Mas et al., 1996; Nelson et al., 1999). Recent *N. fabum* populations proliferate in the prodelta muddy sediments of the Guadalquivir River (Villanueva-Guimerans and Canudo, 2008). In late Pliocene deposits from the Almería-Níjar basin (SE Spain), *N. fabum* is a major component in silts and fine-grained sands of middle fan-delta deposits and in varve-like laminated deposits that indicate low-oxygen conditions and high organic input derived from terrestrial run-off (Pérez-Asensio and Aguirre, 2010). Hence, the dominance of this species in the upper part of the studied section points to periods of high river run-off supplying fine-grained sediment and low quality continental organic matter.

The interpretation of river-derived continental matter input is corroborated by appearance of *Bulimina elongata* that has been observed in comparable environments of the Mediterranean Sea (Jorissen, 1988; Mojtahid et al., 2009). Enhanced river run-off influence is also suggested by the low P/B ratio values in the muddy interval (Fig. 3.4), because planktic foraminifera do not tolerate brackish waters (Arnold and Parker, 1999; Retailleau, et al., 2009).

The upper limit of the muddy interval is dominated by the R-mode *Spiroplectinella* assemblage, coinciding with a sandy substrate and high diversity (Figs. 3.4, 3.5 and 3.9). *Valvulineria complanata* and *Textularia* sp. (Table 3.6) are also abundant in this assemblage. In the prodelta of the Rhône River, *V. complanata* and some arenaceous taxa, such as *Textularia agglutinans* and *Textularia porrecta*, occur close to the end of the freshwater layer entering the marine waters. Food supply in this environment is mainly of marine origin although there is still influence of organic matter provided from the continent (Mojtahid et al., 2009; Goineau et al., 2011). Thus, the *Spiroplectinella* sp. Assemblage is indicative of shallow freshwater-marine transitional conditions with a greater influence of marine organic matter in a sandy inner shelf environment.

Benthic foraminiferal assemblages of the Montemayor-1 core show a mesotrophic upper slope setting influenced by seasonal upwelling, an oligotrophic outer shelf less affected by upwelling, and inner-middle shelf settings with high continental run-off influence. Upwelling conditions also prevailed on the upper slope of the Atlantic

side of the Rifian corridors during the Messinian (Gebhardt, 1993). The coastal upwellings have persisted off NW Africa up to the present day (Sarnthein et al., 1982). In our study case, however, it seems that the position of the area of major influence of upwelling nuclei has changed westwards from the Messinian to the recent. This paleoceanographic reconfiguration in the northern Gulf of Cádiz can be due to the observed Messinan progressive shallowing. This is consistent with the change in organic matter supply from marine labile to continental refractory inferred along the Montemayor-1 core.

3.7. Conclusions

1) A detailed paleoenvironmental evolution of the lower Guadalquivir Basin during the Messinian has been proposed using benthic foraminifera from the Montemayor-1 core.

2) Relative sea-level fluctuations during the late Miocene-early Pliocene have been reconstructed using P/B ratio, depth marker species and a quantitative transfer function. A very sharp transgressive episode, changing from inner-middle shelf to middle slope settings, took place at the beginning of the studied deposits (latest Tortonian-earliest Messinian). After this maximum flooding, sea-level dropped, passing from the middle slope to the outer shelf. This sea-level fall appears to postdate the onset of the Messinian salinity crisis in the Mediterranean. Next, a progressive but slow sea level lowering occurred. Sea-level abruptly dropped close to the end of the Messinian. After a discontinuity close to the Miocene-Pliocene boundary, inner middle shelf established during the early Pliocene. This transgressive-regressive sea-level trend is similar to that observed on the Atlantic side of the Rifian corridors. In the context of global fluctuating sea level, the continuous Messinian shallowing trend on the Betic and Rifian corridors is likely caused by regional tectonic uplift.

3) The distribution, composition, diversity and microhabitat preferences of the benthic foraminiferal assemblages of the late Miocene-early Pliocene in the lower Guadalquivir Basin are predominantly controlled by trophic conditions in terms of quantity and quality of the organic matter reaching the sea floor.

4) During the Messinian, the outer shelf fauna is characterized by relatively low diverse foraminiferal assemblages and dominance of epifaunal-shallow infaunal taxa. Similarly, the assemblages of the transitional interval between the upper slope and the

outer shelf are low diverse and dominated by epifaunal-shallow infaunal taxa although epifaunal taxa are more important than on the outer shelf. Both the outer shelf and the transitional interval between the upper slope and the outer shelf faunas are consistent with a low organic matter input and high oxygen contents. The upper slope faunas are highly diverse and mainly dominated by shallow infaunal taxa indicating mesotrophic conditions with moderate oxygenation. The inner-middle shelf environments are characterized by a very low diverse fauna, dominated by intermediate infaunal and various deep infaunal taxa. Eutrophic conditions with very high organic matter supply and low oxygen concentrations are in agreement with this fauna.

5) Upwelling currents and river run-off are considered to be the major sources of organic matter at the study area. The sediments deposited in the upper slope are dominated by species from the *Uvigerina peregrina* s.l. assemblage that profit from pulses of labile marine organic matter related to upwelling events. The outer shelf has likely also been influenced by upwelling events indicated by the presence of *U. peregrina* s.l. and *Brizalina spathulat*a. The middle shelf muddy sediments may have been influenced by continental organic matter derived from river run-off. These environments have been inhabited by *Nonion fabum* and *Bulimina elongata* that can tolerate continental low quality organic matter.

Acknowledgements

We are very grateful to two anonymous reviewers for their constructive suggestions on an early version of the manuscript. This paper is part of the Research Projects CGL2010-20857 and CGL2009-11539/BTE of the Ministerio de Ciencia e Innovación of Spain, and the Research Group RNM-190 of the Junta de Andalucía. JNPA has been funded by a research scholarship provided by the Ministerio de Educación of Spain (F.P.U. scholarship).

CHAPTER 4

CHAPTER 4

IMPACT OF RESTRICTION OF THE ATLANTIC-MEDITERRANEAN GATEWAY ON THE MEDITERRANEAN OUTFLOW WATER AND EASTERN ATLANTIC CIRCULATION DURING THE MESSINIAN

José N. Pérez-Asensio, Julio Aguirre, Gerhard Schmiedl, Jorge Civis

Published in Paleoceanography 27, PA3222, 14 pp (28 August 2012).

Abstract

Messinian foraminiferal stable oxygen and carbon isotopes of the Montemayor-1 core (Guadalquivir Basin, SW Spain) have been investigated. This record is exceptional to study the Mediterranean Outflow Water (MOW) impact on the Atlantic meridional overturning circulation (AMOC) and global climate during the Messinian because the core is near the Guadalhorce Corridor, the last Betic gateway to be closed during the early Messinian. Our results allow dating accurately its closure at 6.18 Ma. Constant benthic $\delta^{18}O$ values, high difference between benthic and planktonic $\delta^{18}O$, and low sedimentation rates before 6.18 Ma indicate the presence of a two-layer water column, with bottom winnowing due to an enhanced Mediterranean outflow current. The enhanced contribution of dense MOW to the North Atlantic Ocean likely fostered the formation of North Atlantic Deep Water (NADW). After 6.18 Ma, benthic $\delta^{18}O$ values parallel that of the global glacioeustatic curve, the difference between benthic and planktonic $\delta^{18}O$ is low, and sedimentation rates considerably increased. This indicates a good vertical mixing of the water column, interruption of the MOW, and a dominant glacioeustatic control on the isotopic signatures. According to the role of MOW in the modern Atlantic thermohaline circulation, the reduction of the MOW after the closure of the Guadalhorce Corridor might have resulted in a decreased NADW formation rate between 6.0 and 5.5 Ma weakening the AMOC and promoting northern hemisphere cooling. After the Gibraltar Strait opening, the restoration of the MOW and related salt export from the Mediterranean could have promoted an enhanced NADW formation.

4.1. Introduction

At present, the Mediterranean connects with the Atlantic by the Strait of Gibraltar. The water mass exchange throughout the Strait of Gibraltar is characterized by an anti-estuarine circulation pattern (Fig. 4.1a) (Wüst, 1961). This anti-estuarine circulation pattern was definitively established after the opening of the Strait of Gibraltar (Nelson, 1990), although it has been suggested that the movements of water masses reversed to estuarine-type circulation during the early Pleistocene (Huang and Stanley, 1972). Lower salinity surface waters from the North Atlantic flow superficially eastwards into the Mediterranean (Fig. 4.1a). On the other hand, strong evaporation and production of dense, saline intermediate and deep-water in the eastern Mediterranean forces a high-velocity density driven bottom current westwards as MOW through the Strait of Gibraltar. This mass of water is mainly fed by the Levantine Intermediate Water (LIW) (Bryden and Stommel, 1984), formed by convection in the Eastern Mediterranean (Marshall and Schott, 1999; Hernández-Molina et al., 2011), and in lesser extent by the Western Mediterranean Deep Water (WMDW), which is formed in the Gulf of Lion during cold and windy winters (MEDOC Group, 1970; Bryden and Stommel, 1984; Lacombe et al., 1985). Today, the LIW contributes to 2/3 of the MOW while WMDW only represents 1/3 of the MOW (Millot, 1999). Therefore, the LIW might be more important in controlling the MOW than WMDW. The MOW is characterized by higher $\delta^{13}C$ and $\delta^{18}O$ than the Atlantic waters (Vergnaud-Grazzini, 1983; Sierro et al., 2005).

The outflow of the MOW into the Eastern Atlantic has a significant effect on the Atlantic oceanic circulation as well as on the global climate. The dense MOW mixes with the North Atlantic intermediate waters forming a high salinity tongue (Fig. 4.1b) that contributes to the momentum of the Atlantic meridional overturning circulation (AMOC) (Reid, 1979; Rahmstorf, 1998; Bigg and Wadley, 2001; Bigg et al., 2003). In turn, the AMOC is the driving force for the Atlantic Ocean circulation, and even the global thermohaline circulation (Bethoux et al., 1999). Global thermohaline circulation affects the global radiation budget and global carbon cycling and can thus produce major climate changes (Brown et al., 1989; Bigg et al., 2003; Murphy et al., 2009). Therefore, a reduction or interruption of the MOW could have a critical impact both on the AMOC and on the global circulation, as well as on the global climate. Without the contribution of the saline MOW, the formation of dense water, which triggers the

AMOC, would have most likely not taken place steadily in the North Atlantic (Rahmstorf, 1998; Bethoux et al., 1999).

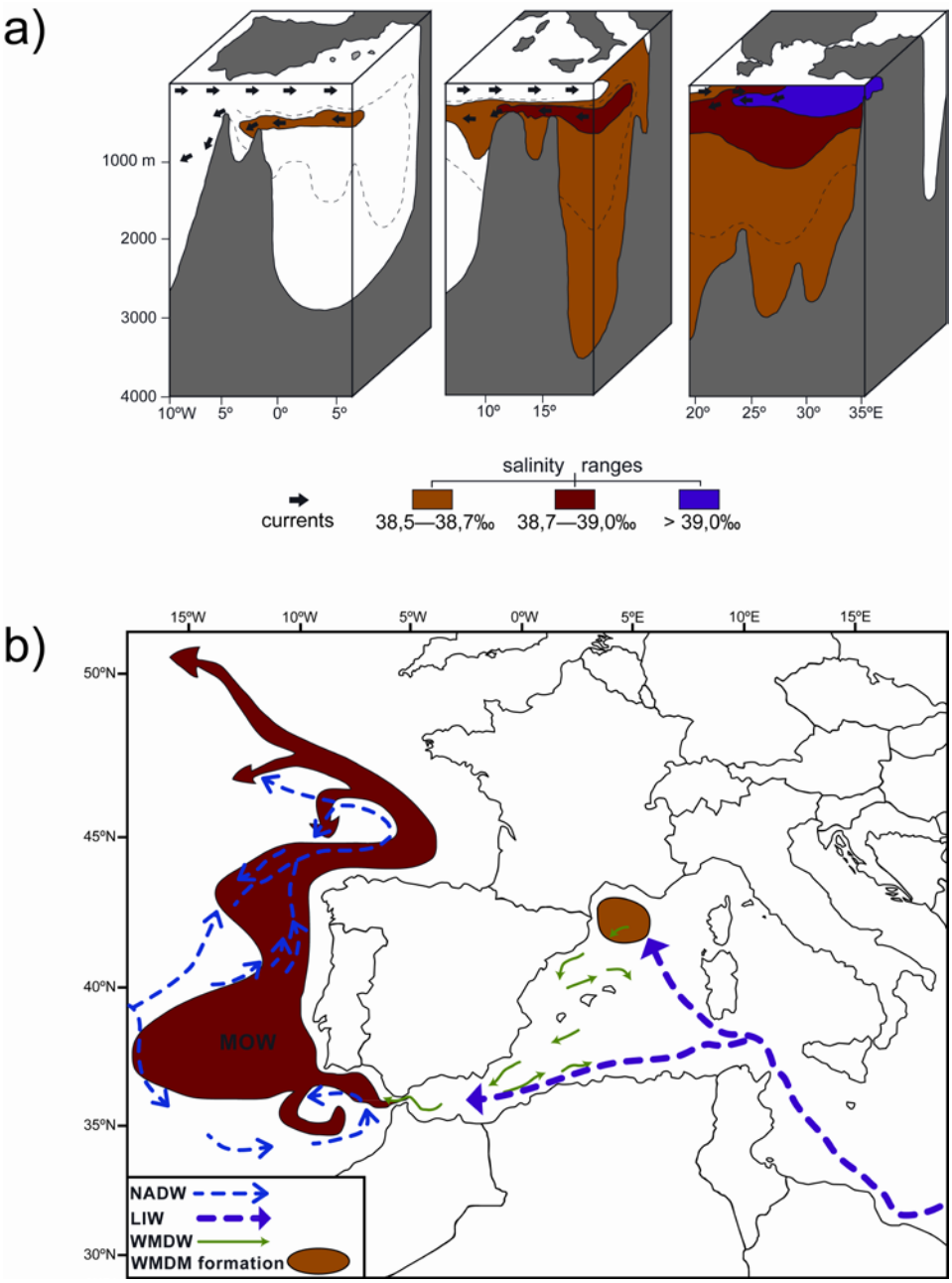

Figure 4.1. (a) Present salinity and circulation patterns at the Strait of Gibraltar and in the Mediterranean (based on Wüst, 1961). The dense and saline Mediterranean intermediate and deep waters form a bottom ouflow, while lower salinity surface waters from the Atlantic enters the Mediterranean representing an anti-estuarine circulation pattern. (b) Present-day general circulation pattern at the eastern North Atlantic and Mediterranean Sea (based on Hernández-Molina et al., 2011; Pinardi and Masetti, 2000). Mediterranean Outflow Water (MOW), North Atlantic Deep Water (NADW), Levantine Intermediate Water (LIW), Western Mediterranean Deep Water (WMDW) and WMDW formation are indicated.

The impact of the MOW on the Atlantic Ocean circulation during the Pliocene, Pleistocene, and Holocene, has been comprehensively studied (Loubere, 1987; Nelson et al., 1993; Schönfeld, 1997; Maldonado and Nelson, 1999; Schönfeld and Zahn, 2000; Rogerson et al., 2005; Hernández-Molina et al., 2006, 2011; Llave et al., 2006, 2011; Toucanne et al., 2007; Khélifi et al., 2009; Rogerson et al., 2010, 2011, 2012; Stumpf et al., 2010; van Rooij et al., 2010; Estrada et al., 2011). These studies show an Upper North Atlantic Deep Water (UNADW) formation produced by an enhanced MOW flow related to an increased Mediterranean deep-water formation and enhanced aridity in the Mediterranean region. Furthermore, the supply of salt by the MOW into the intermediate North Atlantic waters favors the resumption of the AMOC during interglacials (Rogerson et al., 2006, 2012; Voelker et al., 2006).

All these studies have analyzed the history and impact of the MOW on the Atlantic circulation after the end of Messinian salinity crisis (MSC), when the Atlantic-Mediterranean connections were reestablished through the Strait of Gibraltar. However, little is known about the impact of the MOW during the Messinian, when the connections were through the Betic and Rifian Corridors (van der Laan et al., 2012) or after the cessation of the MOW due to the closure of these corridors. Keigwin et al. (1987) questioned that the MSC had any effect on the deep circulation in the North Atlantic. On the contrary, Zhang and Scott (1996) reported the presence of the MOW at the northeastern Atlantic Ocean, at least reaching 50ºN of latitude, during the Messinian. Moreover, Pb and Nd isotopic studies also pointed out to the influence of the MOW in the NE Atlantic during the Messinian (Abouchami et al., 1999). Apart from these works deciphering the influence of the MOW in the distant Atlantic, no study has focused on the areas close to the Atlantic-Mediterranean connections in the Betics.

It has been largely substantiated that the restriction of the Atlantic-Mediterranean connections played a major role in the onset of the MSC (e.g. Esteban et al., 1996; Riding et al., 1998; Krijgsman et al., 1999a, 1999b; Martín et al., 2001; Braga et al., 2006). The Betic Corridors together with their southern counterparts, the Rifian Corridors (NW Morocco), were the main gateways connecting the Atlantic and Mediterranean until their closure (Benson et al., 1991; Esteban et al., 1996; Martín et al., 2001, 2009; Betzler et al., 2006).

The Guadalquivir Basin, located in the south of the Iberian Peninsula, represents the Atlantic side of the Betic Corridors that extended through southern Spain during the early late Miocene (Benson et al., 1991; Martín et al., 2001, 2009; Braga et al., 2002).

The last active Betic gateway was the Guadalhorce Corridor, which controlled the Messinian pre-evaporitic circulation in the western Mediterranean, and allowed the MOW to enter the Atlantic Ocean (Martín et al., 2001). The Guadalhorce Corridor was a NW-SE trending strait with an estimated maximum width of 5 km and maximum water depth of 120 m (Martín et al., 2001). The corridor was filled by sediment displaying huge unidirectional sedimentary structures indicating Mediterranean waters flowing out into the Atlantic at estimated current velocities of about 1.0-1.5 m/s (Martín et al., 2001). This water mass circulation is consistent with the siphon model of Benson et al. (1991) stating that prior to the closure of the Betic Corridors, the water exchange between the Mediterranean and the Atlantic during the Messinian was characterized by Atlantic inflow through the Rifian Corridors and MOW through the Guadalhorce Corridor (Benson et al., 1991; Martín et al., 2001). After the closure of the Guadalhorce Corridor in the early Messinian (Martín et al., 2001), MOW was interrupted and circulation was restricted to the Rifian Corridors (Esteban et al., 1996). Later the closure of the Rifian Corridors in the late Messinian (Krijgsman et al., 1999a) caused the isolation of the Mediterranean Sea and, consequently, a hydrographical deficit that triggered the onset of the MSC with deposition of extensive evaporites in the central and deeper parts of the Mediterranean (Hsü et al., 1973, 1977).

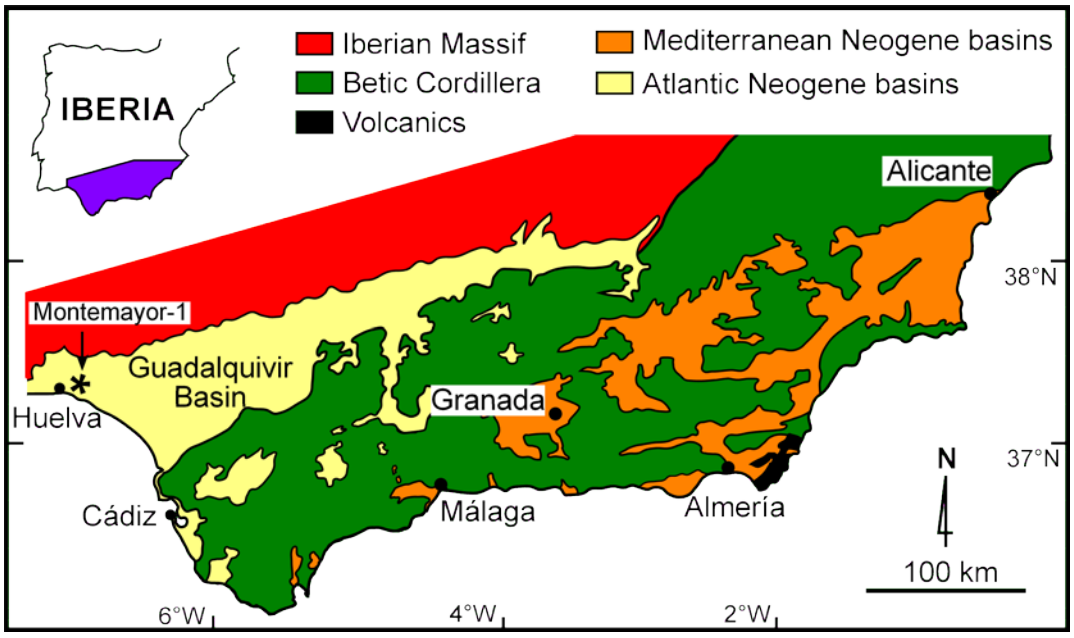

Figure 4.2. Geological setting of the lower Guadalquivir Basin. Asterisk indicates the location of the Montemayor-1 core.

In this study, we examine the impact of the MOW during the Messinian close to the Betic corridors. We analyze foraminiferal stable O and C isotope composition in the Montemayor-1 core (SW Spain) (Fig. 4.2). The core site is located close to the Guadalhorce Corridor, the last Betic corridor to be closed (Martín et al., 2001, 2009), and shows a continuous Messinian record accurately dated by magnetobiostratigraphic methods (Larrasoaña et al., 2008). The Guadalquivir Basin was well connected with the Atlantic Ocean during the MSC, so there was neither desiccation nor evaporite deposition. Furthermore, according to the siphon model of Benson et al. (1991), Mediterranean outflow took place only throughout the Betic Corridors. Therefore, the location of the core is exceptional to study the effect of the MOW on the eastern Atlantic Ocean circulation during the Messinian, as well as its possible impact on global climate changes.

The main aims of this study are: 1) to assess the impact of the MOW on the AMOC during the Messinian; and 2) to precisely date the closure of the Guadalhorce Corridor.

4.2. Geological Setting

The study area is located in the westernmost part of the northwestern edge of the lower Guadalquivir Basin (SW Spain) (Fig. 4.2). This is an ENE-WSW elongated Atlantic Neogene foreland basin (Sanz de Galdeano and Vera, 1992; Vera, 2000; Braga et al., 2002) with a sedimentary infilling consisting of marine and continental sediments ranging from the early Tortonian to the late Pliocene (Aguirre, 1992, 1995; Aguirre et al., 1993, 1995; Riaza and Martínez del Olmo, 1996; Sierro et al., 1996; Braga et al., 2002; González-Delgado et al., 2004; Martín et al., 2009).

The Guadalquivir foreland basin was formed as a consequence of the Betic Cordillera compressional overthrusting during the early-middle Miocene (Sanz de Galdeano and Vera, 1992; Riaza and Martínez del Olmo, 1996; Sanz de Galdeano and Rodríguez-Fernández, 1996; Martín et al., 2009; Braga et al., 2010). During the Serravallian, the Atlantic-Mediterranean connection started to be restricted in the northeastern edge of the Guadalquivir Basin, in the Prebetic Domain of the Betic Cordillera (Aguirre et al., 2007; Martín et al., 2009; Braga et al., 2010). The progressive tectonic uplifting of the Betic mountain chain led to a progressive closure of this seaway, originating the so-called North Betic Strait during the latest middle Miocene-

earliest late Miocene (topmost Serravallian-earliest Tortonian) (Aguirre et al., 2007; Martín et al., 2009; Braga et al., 2010). The final closure of the North Betic Strait took place during the early Tortonian (Sierro et al., 1996; Martín et al., 2009; Braga et al., 2010) and the Guadalquivir Basin was established as a wide, marine embayment only opened to the Atlantic Ocean (Martín et al., 2009).

After the cessation of the North Betic Strait, other Betic gateways connected the Atlantic and the Mediterranean through the Guadalquivir Basin. They were progressively closed during the late Miocene. In the late Tortonian, the Dehesas de Guadix Corridor and the Granada Basin were the main Atlantic-Mediterranean connections (Esteban et al., 1996; Braga et al., 2003; Betzler et al., 2006; Martín et al., 2009). After their closure, the Guadalhorce Corridor was the only connection during the earliest Messinian (Martín et al., 2001). This last Betic Corridor became closed in the early Messinian (Martín et al., 2001). Since its closure, the Rifian Corridors were the unique Atlantic-Mediterranean gateways (Esteban et al., 1996).

4.3. Material and Methods

4.3.1. Montemayor-1 Core

The studied material is the Montemayor-1 core, a 260 m long core that has been drilled in the northwestern margin of the lower Guadalquivir Basin close to Moguer (SW Spain) (Figs. 4.2 and 4.3). This core includes marine sediments that can be divided into four lithostratigraphic units (see a detail description in Pérez-Asensio et al., 2012) (Fig. 4.3): the Niebla Formation (Tortonian), the Arcillas de Gibraleón Formation (latest Tortonian-Messinian), the Arenas de Huelva Formation (early Pliocene), and the Arenas de Bonares Formation (late Pliocene-Pleistocene).

In this study, we analyzed an interval of 70 m, from 240 to 170 m (from 6.67 Ma to 5.7 Ma according to the age model. See below), including Messinian sediments from the Arcillas de Gibraleón Formation (Fig. 4.3). In this interval, a total of 132 samples were collected with a sampling interval of 0.5 m. Samples were wet sieved over a 63 µm mesh and dried out in an oven at 40 ºC. A representative split was dry-sieved over a 125 µm mesh to estimate the planktonic/benthic ratio (P/B ratio henceforth), calculated as [P/(P+B)] as a proxy for relative sea-level change.

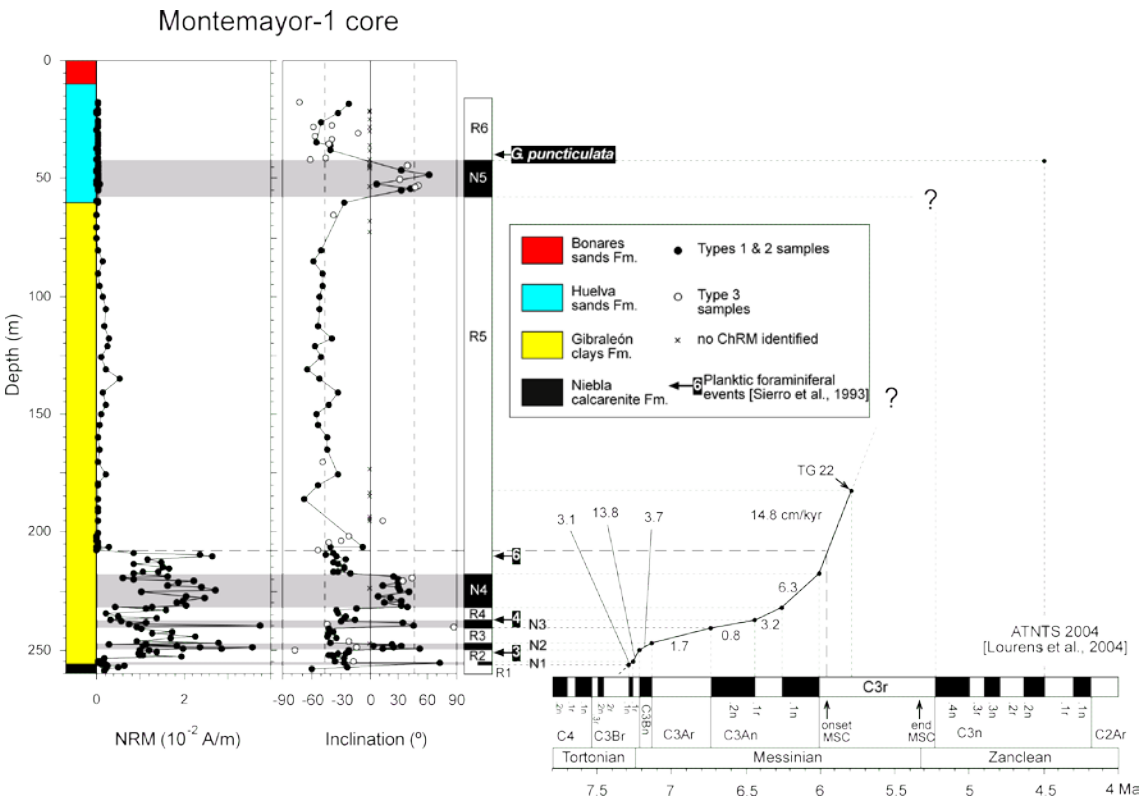

Figure 4.3. Age model, estimation of the sedimentation rate (estimated in cm/kyr) and magnetobiostratigraphic framework for the Montemayor-1 core. Magnetostratigraphy is based on the ATNTS2004 (Lourens et al., 2004). Type 1 samples have higher quality than types 2 & 3 samples. CrRM is the characteristic remanent magnetization. Biostratigraphy has been established using the planktonic foraminiferal events (PF events) of *Sierro et al*. (1993) and first occurrence of *Globorotalia puncticulata*. Position of glacial stage TG 22 is indicated. Question marks show uncertainties in the chronology and sedimentation rate.

4.3.2. Stable Isotope Analyses

Stable isotope analyses ($\delta^{18}O$ and $\delta^{13}C$) were performed on 10 individuals of *Cibicidoides pachyderma* for benthic foraminifera and 20 individuals of *Globigerina bulloides* for planktonic foraminifera separated from the size fraction >125 µm. Foraminiferal shells were ultrasonically cleaned, and washed with distilled water prior to the analyses. The isotopic analyses were performed on a Finnigan MAT 251 mass spectrometer connected to a Kiel I (prototype) preparation device for carbonates at the Leibniz-Laboratory for Radiometric Dating and Isotope Research, Kiel, Germany. Results are given in δ-notation in per mil, and are reported on the Vienna Pee Dee belemnite (VPDB) scale. The VPDB scale is defined by a certain value of the National

Bureau of Standards (NBS) carbonate standard NBS-19. On the basis of the international and lab-internal standard material, the analytical reproducibility is < ± 0.05 ‰ for $\delta^{13}C$, and < ± 0.07 ‰ for $\delta^{18}O$.

4.3.3. Spectral Analyses

Spectral analysis was performed in order to identify the nature and significance of periodic changes in the benthic $\delta^{18}O$ record. The analysis was carried out in the time domain using the software PAST (Hammer et al., 2001) and the REDFIT procedure of Schulz and Mudelsee (2002). This procedure allows assessing the spectral analysis with unevenly spaced samples. Spectral peaks over the 95% confidence interval (CI) were considered significant.

4.4. Age Model

The age model of the Montemayor-1 core was established using a combination of paleomagnetism, biostratigraphy, and stable oxygen isotope stratigraphy (Fig. 4.3). The reversed chron C3r is almost continuously recorded since a discontinuity is detected close to the boundary between chrons C3r and C3n, which prevent us from using this magnetostratigraphic reversal boundary as a chronological datum in the upper part of the core (Pérez-Asensio et al., 2012).

To complete the age model above the normal magnetic chron C3An.1n, we have used the glacial stage TG 22 as a tie point, which was astronomically calibrated at 5.79 Ma (Krijgsman et al., 2004). We identified this glacial stage by means of stable oxygen isotope stratigraphy (Fig. 4.4). The benthic oxygen isotope record shows two distinctly pronounced “paired” glacial peak stages that we identify as the glacial stages TG 20 and TG 22 (Fig. 4.4) according to the nomenclature established by Shackleton et al. (1995). These two stages are easily identifiable because they are the most pronounced “paired” glacial peaks at the end of a progressively increasing trend in the $\delta^{18}O$ record along the chron C3r (Fig. 4.4). Both the isotopic trend and the two “paired” glacial maxima are evident and have been observed in other cores at global scale including the Pacific Ocean (Shackleton et al., 1995), the Atlantic Ocean (Hodell et al., 2001; Vidal et al., 2002), as well as in sediments from the Rifian Corridors (Hodell et al., 1994).

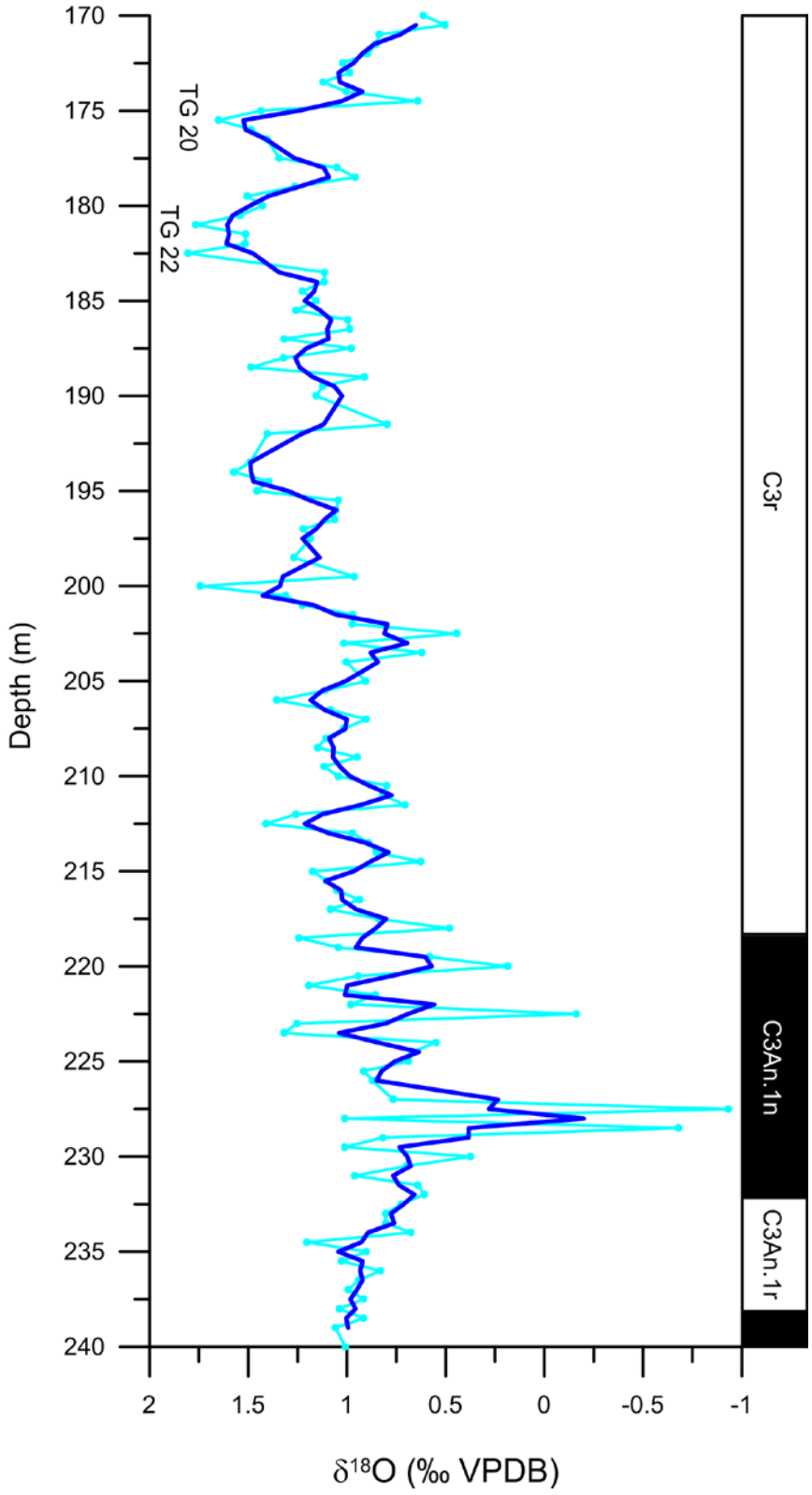

Figure 4.4. Benthic (*Cibicidoides pachyderma*) stable oxygen isotope record *versus* core depth (light blue line) and three-point running average of the benthic oxygen isotope record (dark blue line) of the Montemayor-1 core. Glacial stages TG 20 and TG 22 defined by Shackleton et al. (1995) in benthic oxygen isotope record of the ODP site 846 are indicated.

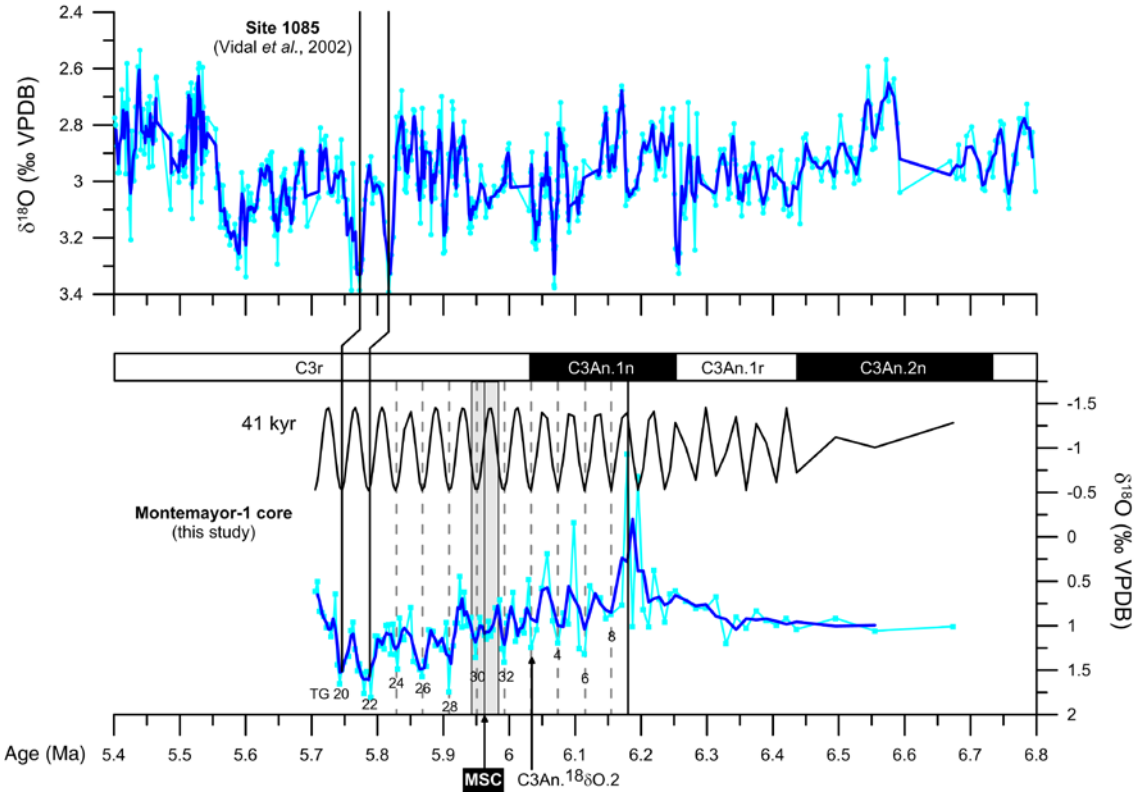

Figure 4.5. Benthic (*Cibicidoides pachyderma*) stable oxygen isotope record *versus* time (light blue lines) and three-point running average of the benthic oxygen isotope record (dark blue lines) from the Site 1085 (*Vidal et al.*, 2002) and Montemayor-1 core. The obliquity component of the benthic isotope record is extracted by sinusoidal curve fitting with a period of 41 kyr. The onset of the Messinian salinity crisis (MSC) is indicated (vertical gray bar in the lower diagram). The vertical black line at 6.18 Ma marks the end of the Atlantic-Mediterranean connection through the Guadalhorce Corridor. Glacial stages from TG 20 to TG 32 defined by *Shackleton et al.* (1995) and from C3An.δ^{18}O.2 to C3An.δ^{18}O.8 according to the nomenclature used in *Hodell et al.* (1994) are indicated. The two vertical black solid lines mark glacial stages TG 20 and 22 from the Montemayor-1 core and Site 1085. Vertical gray dashed lines mark glacial stages and the obliquity component of the benthic oxygen isotope record of the Montemayor-1 core.

Using the TG 22 as a tie point in the chronological framework, the estimated age for the TG 20 based on the reconstructed sedimentation rate (14.8 cm/kyr) is 5.75 Ma (Figs. 4.3 and 4.5). This age estimation is coincident with the age estimated by Krijgsman et al. (2004) using astronomical tuning.

Further to the TG 20 and TG 22, we have identified the rest of the glacial stages following the nomenclature of Shackleton et al. (1995). These authors found that the benthic O isotope record was controlled by 41-kyr cycles related to orbital obliquity. Hodell et al. (1994) also showed that the benthic isotope record from the Salé

Briqueterie core at the Rifian Corridors reflects obliquity induced changes. The benthic oxygen isotope record from the Montemayor-1 core is also mainly controlled by 41-kyr cycles related to orbital obliquity (Fig. 4.6).

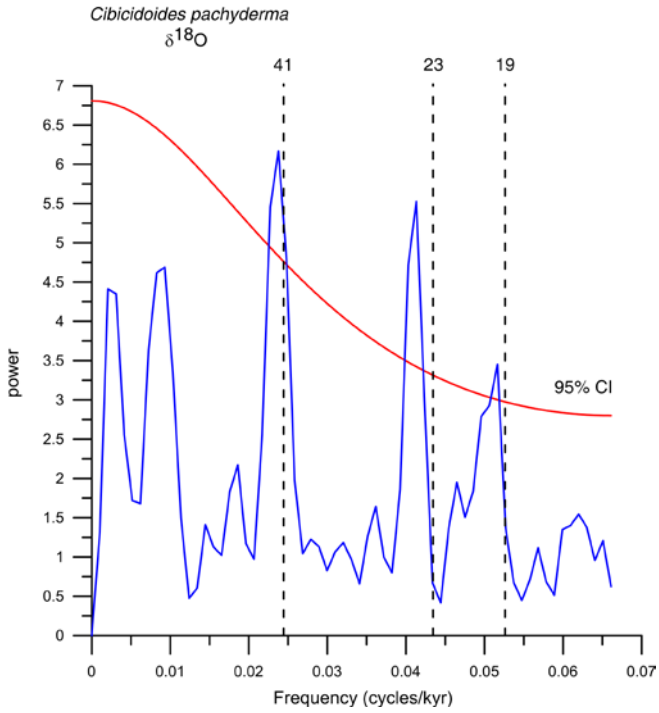

Figure 4.6. Power spectrum of the benthic (*Cibicidoides pachyderma*) stable oxygen isotope record of the Montemayor-1 core with main orbital periodicities indicated in kiloyears. The 95% confidence interval (CI) is indicated.

Since the TG glacial stages of Shackleton et al. (1995) were related to obliquity, we use the same methodology to identify the rest of the TG stages in the chron C3r. Further, in order to confirm the reliability of the identification of TG 20 and TG 22 in the Montemayor-1 core, we plotted the benthic isotope record versus age (Ma), including the TG 22 datum (5.79 Ma), and counted obliquity cycles backwards (Fig. 4.5). Comparing the benthic oxygen isotope record from the Montemayor-1 core with its obliquity component (Fig. 4.5) we identified up to stage TG 32 for chron C3r. However, Hodell et al. (1994) and van der Laan et al. (2005) recognized one extra obliquity cycle, up to TG 34 stage. The discrepancy in just one obliquity cycle (1 glacial stage and 1 interglacial stage) can be due to the fact that Hodell et al. (1994) identified glacial stages versus depth instead of time. This could result in counting cycles of different periodicities. On the other hand, van der Laan et al. (2005), considered the

glacial stage TG 30, which is a precession-related signal, at the same level of the rest of the obliquity-related cycles.

4.5. Results

The benthic oxygen isotope record shows stable values around 1‰ before 6.35 Ma, and then it decreases reaching a minimum of -0.93‰ at 6.18 Ma (Fig. 4.7). After 6.18 Ma, it exhibits fluctuations with a trend towards heavier values reaching the maximum values at 5.79 Ma (TG 22), and then it decreases towards lighter values (Fig. 4.7). The benthic stable O isotope curves of the Montemayor-1 core and site 1085 (Vidal et al., 2002) reveal different trends for the time interval before 6.18 Ma (Fig. 4.5). On the contrary, both curves show a parallel trend with similar fluctuations after 6.18 Ma. In this interval, heavy values of $\delta^{18}O$ from the Montemayor-1 core can be easily matched with glacial peaks from site 1085 (Fig. 4.5).

The planktonic oxygen isotope record exhibits a fluctuating trend with values ≤ 0‰ before 6.18 Ma and values > 0‰ after this age (Fig. 4.7). Both the benthic and planktonic O isotopic curves follow different trends before 6.18 Ma. After 6.18 Ma, the planktonic O isotopic curve parallels that of the benthic one except for some low values around 5.79 Ma (Fig. 4.7). The similar trend of both records is confirmed by a statistically significant positive correlation ($\rho = 0.415$). The $\Delta\delta^{18}O_{benthic\text{-}planktonic}$ ($\Delta\delta^{18}O_{b\text{-}p}$) curve reflects these differences before and after 6.18 Ma between the benthic and planktonic O isotope values, being higher before 6.18 Ma (Fig. 4.7). The difference reaches average values close to 0 at around 6.2 Ma (Fig.4.7).

The planktonic carbon isotope record exhibits significant fluctuations with average values around -0.8‰ before 6.18 Ma (Fig. 4.7). After 6.18 Ma, the $\delta^{13}C$ decreases reaching its lowest values from 6.05 to 5.85 Ma. Then, it drastically increases from average values of -1‰ to 0‰ at 5.85 Ma, and remains with relatively high average values around 0 until 5.77 Ma. At this age, another carbon shift took place recovering average values of -1‰ (Fig. 4.7). The benthic carbon isotope record shows fluctuations with average values around 0.4‰ before 6.18 Ma. After 6.18 Ma, the $\delta^{13}C$ decreases reaching its lowest values from 6 to 5.9 Ma. Finally, it increases and remains with relatively high values around 0.4‰ from 5.9 to 5.7 Ma (Fig. 4.7).

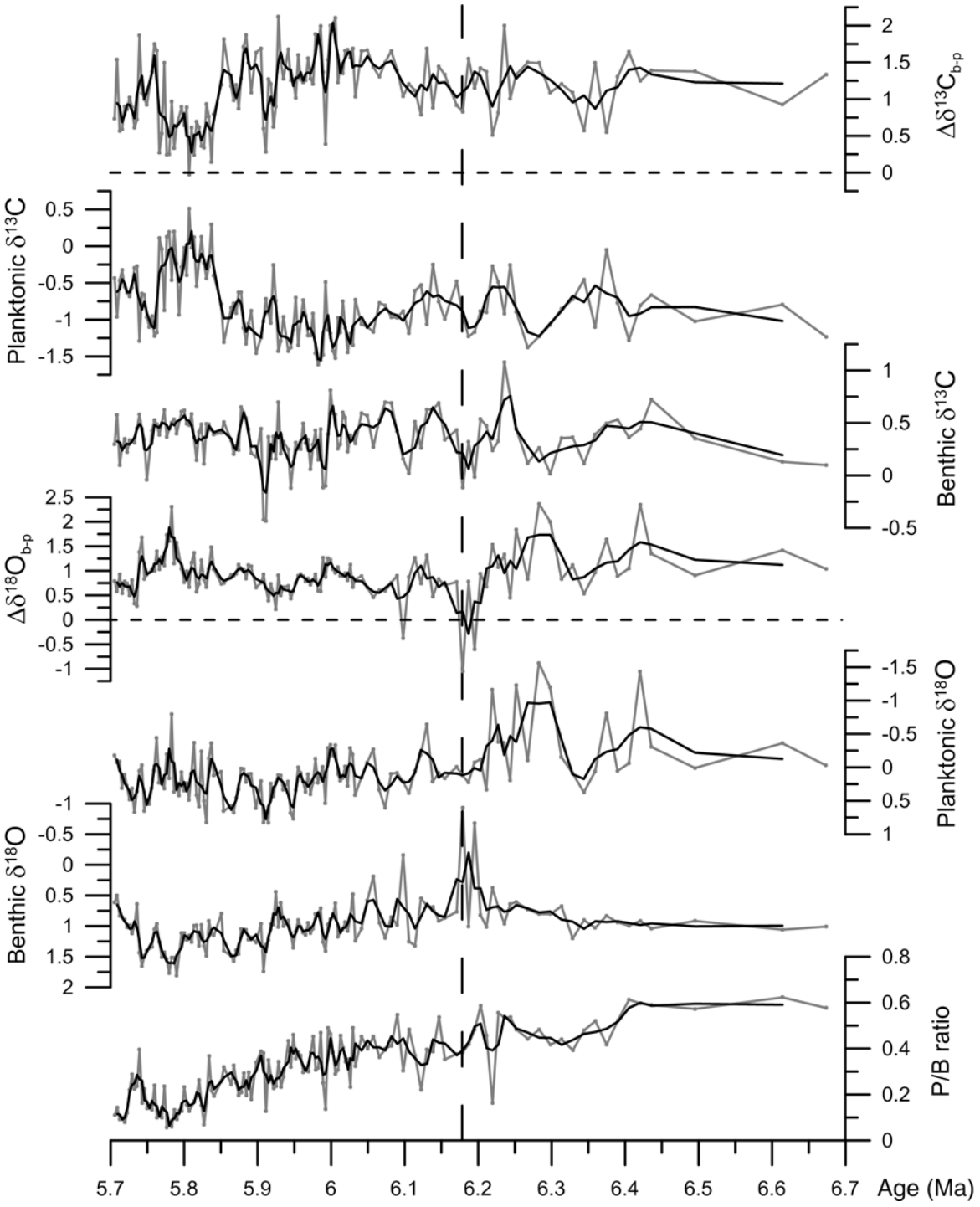

Figure 4.7. Benthic (*Cibicidoides pachyderma*) and planktonic (*Globigerina bulloides*) $\delta^{18}O$ and $\delta^{13}C$ records in ‰ VPDB, difference between $\delta^{18}O$ and $\delta^{13}C$ values of benthic and planktonic foraminifera ($\Delta\delta^{18}O_{b\text{-}p}$ and $\Delta\delta^{13}C_{b\text{-}p}$), as well as the planktonic-benthic ratio (P/B ratio) *versus* time (gray lines) and three-point running average (black lines) of the Montemayor-1 core. The vertical dashed line at 6.18 Ma marks the end of the Atlantic-Mediterranean connection through the Guadalhorce Corridor.

4.6. Discussion

4.6.1. Identification of the MOW in the northeastern Atlantic and age of the closure of the Guadalhorce Corridor

4.6.1.1. MOW presence before 6.18 Ma

The benthic O isotopic values from the Montemayor-1 core depart from the fluctuating global trend, based on Vidal et al. (2002), from the base of the studied interval to 6.18 Ma (Fig. 4.5). The presence of a dense, i.e. highly saline, bottom water mass affecting the study area might account for the observed deviation towards heavier values in the O isotope record.

The Montemayor-1 core site is located adjacent to the Guadalhorce Corridor, the last Atlantic-Mediterranean gateway providing a connection between the Mediterranean and Atlantic oceans through the Betic Cordillera prior to the onset of the MSC (Fig. 4.8a). Based on the vicinity of the core site to this gateway it appears most likely that the benthic habitats of the study area were bathed by the highly saline MOW prior to 6.18 Ma (Fig. 4.8a).

In the Montemayor-1 core, benthic O values remain approximately constant at around 1‰ before 6.35 Ma. This suggests a more or less constant MOW flux as indicated by the scarcity of reactivation surfaces in the sedimentary structures of the Guadalhorce Corridor (Martín et al., 2001). The benthic stable O isotope values of 1‰ reflect the density of the MOW that is the product of mixing between the exported Mediterranean water and the ambient Atlantic water. This value is in the range of recent benthic stable O isotope values of the upper core of the MOW, which ranges between 1 and 2‰ (Rogerson et al., 2011). Before 6.35 Ma the exchange through the Guadalhorce Corridor is expected to be maximal because of the increased density between the MOW and Atlantic surface waters ($\Delta\delta^{18}O_{b\text{-}p}$) and the high sea-level indicated by the P/B ratios (Fig. 4.7). The benthic C isotope record could partially reflect MOW activity. Using the modern analogue, high values of benthic $\delta^{13}C$ are associated to MOW because of the low residence time of this water mass (Vergnaud-Grazzini, 1983; Schönfeld and Zahn, 2000; Raddatz et al., 2011; Rogerson et al., 2011). Thus, relatively high benthic C isotopic values around 6.4-6.5 Ma might be the result of increased MOW presence (Fig. 4.7).

The presence of the MOW before 6.18 Ma is also supported by the paleobathymetry of the study area during this period. At the present day, the MOW entering the Atlantic flows along the western Iberian continental slope between 400 and 1,500 m water depth (Schönfeld and Zahn, 2000; Llave et al., 2006). In the study area, the presence of R-mode *Anomalinoides flinti* assemblage and *Planulina ariminensis* before 6.18 Ma (below 227.5 m core depth in Pérez-Asensio et al., 2012) indicates that the current flowed along the middle and upper slope (Pérez-Asensio et al., 2012). This is within the depth range of MOW flow at the present day.

A comparison between benthic and planktonic O isotopic records from the Montemayor-1 core offers another indication of the MOW presence before 6.18 Ma. The decoupling and high difference between the benthic and planktonic O isotopic signals before 6.18 Ma (Fig. 4.7) are indicative of a two-layer water column with the presence of MOW at the sea floor. Moreover, the lowest sedimentation rates are estimated before 6.18 Ma (Fig. 4.3). Thus, winnowing by the MOW might most likely account for this result.

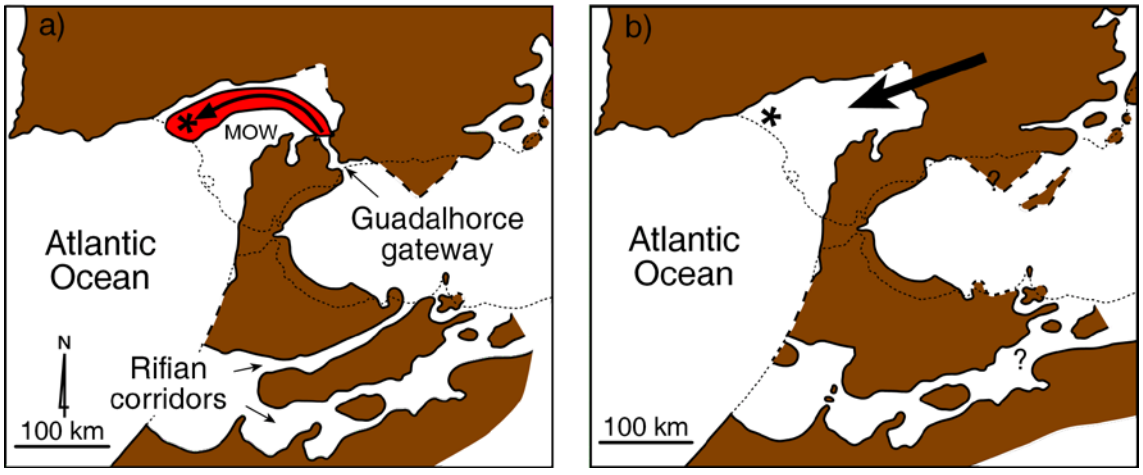

Figure 4.8. Paleogeographic and paleoceanographic evolution of the lower Guadalquivir Basin during the Messinian (based on Martín et al., 2009): a) situation before 6.18 Ma, when the Mediterranean Outflow Water (MOW) reaches the studied core (asterisk); and b) situation after 6.18 Ma, when the MOW was interrupted. The black thick arrow marks the progradation of the main depositional systems along the axis of the Guadalquivir Basin.

4.6.1.2. Response of the MOW plume to the restriction of the Guadalhorce Corridor (6.35 to 6.18 Ma)

Between 6.35 and 6.18 Ma, the benthic O isotopic record underwent a significant negative excursion of about 2‰, from 1‰ to a minimum of -0.93‰ (Figs. 4.5 and 4.7). This noteworthy isotopic shift suggests a MOW product with a lighter O isotopic signature. The ambient Atlantic water has a lower density than the MOW (Price and O'Neil-Baringer, 1994). Hence, the local minimum in the benthic $\delta^{18}O$ from 6.35 to 6.18 Ma could be explained by a higher proportion of the lighter ambient Atlantic water in the final MOW product as occurs at present day outside the upper core of the MOW plume (Rogerson et al., 2011). In addition, this fact could reflect a gradual reduction in the exchange through the Guadalhorce Corridor as it is indicated by the reduction of density between the MOW and the Atlantic surface waters ($\Delta\delta^{18}O_{b\text{-}p}$) and relatively low sea-level (Fig. 4.7). The reduced exchange from 6.35 to 6.18 Ma is also reflected by the decrease in the benthic C isotopes (Fig. 4.7). Similarly, the diminished outflow of Mediterranean waters in the Rifian Corridors is indicated by a negative excursion in the planktonic C isotopes at 6.0 Ma (van der Laan et al., 2012).

Alternatively, the local minimum in the benthic $\delta^{18}O$ might reflect the isotopic signature of less dense Atlantic waters. Increased salinity of Mediterranean source waters due to the restriction of the Guadalhorce Corridor could produce a denser MOW that mixes faster with ambient Atlantic waters reducing its density and consequently shoaling on the slope (Rogerson et al., 2012). Therefore, the location of the Montemayor-1 core would be beneath the MOW between 6.35 and 6.18 Ma. Our data from the Montemayor-1 core do not allow us to rule out any of these two alternative explanations.

4.6.1.3. Cessation of the MOW at 6.18 Ma

After 6.18 Ma, the benthic $\delta^{18}O$ parallels that of the global benthic O record, with main glacial stages easily distinguishable in both records (Fig. 4.5). Therefore, benthic O isotopic values at the study area were primarily controlled by global glacioeustatic fluctuations. Most likely, the striking change in the $\delta^{18}O$ record at 6.18

Ma can be linked with the cessation of the dense MOW influence in the study area (Fig. 4.8b).

A comparison between benthic and planktonic O isotopic records from the Montemayor-1 core also supports the interruption of the MOW after 6.18 Ma. Benthic and planktonic O isotopic values covary after 6.18 Ma indicating enhanced vertical mixing and absence of MOW. This is also supported by low $\Delta\delta^{18}O_{b\text{-}p}$ and positive statistical correlation between benthic and planktonic O isotopic values (ρ = 0.415) (Fig. 4.7). The covariation and the decreasing difference between planktonic and benthic O isotopes might have also been favored by the shallowing-upward trend that reduces the difference between benthic and planktonic isotopic values.

Moreover, sedimentation rate could be affected by the interruption of the MOW at 6.18 Ma. After this date, sedimentation rates drastically increases from 6.3 to 14.8 cm/kyr (Fig. 4.3) likely due to the interruption of the MOW and the resulting progradation of depositional systems along the axis of the Guadalquivir Basin (Sierro et al., 1996) (Figure 8b).

The closure of this corridor at 6.18 Ma caused the final interruption of MOW. The observed age for the end of this Betic gateway is consistent with planktonic foraminifera recorded in the sediments filling the Guadalhorce Corridor that indicate that the strait was open at least from 7.2 to 6.3 Ma (Martín et al., 2001). Further, it is also coincident with the first land mammal exchange between Africa and the Iberian Peninsula prior to the MSC taking place at 6.1 Ma (Garcés et al., 1998). Therefore, according to our data, the closure of the Guadalhorce Corridor (6.18 Ma) predates by about 220-kyr the onset of the MSC, dated at 5.96 ± 0.02 Ma by Krijgsman et al. (1999b).

4.6.2. Impact of the MOW on the eastern North Atlantic Ocean circulation

The MOW is essential to maintain the meridional overturning circulation (AMOC) because it increases the North Atlantic density gradient and can restart the AMOC after its collapse (Rogerson et al., 2012). It appears likely that any fluctuation of the MOW can alter the AMOC. During the Messinian period, the increase of the NADW presence in the South Atlantic Ocean between 6.6 and 6.0 Ma (Billups, 2002) suggests an enhanced NADW formation due to the suspected salinity increase of the MOW before the closure of the Atlantic-Mediterranean gateways. During this interval,

MOW affected our study area before the closure of the Guadalhorce Corridor at 6.18 Ma (Figs. 4.5 and 4.7). It has to be mentioned however, that the increase in NADW flow in the South Atlantic Ocean could have also been caused by the shoaling of the Central American Seaway (Panamanian Seaway) during the middle-late Miocene (Billups, 2002; Nisancioglu et al., 2003; Butzin et al., 2011).

The MOW is predominantly fed by the LIW (Bryden and Stommel, 1984). During the Quaternary, cold stadials have been associated with production of a denser LIW (Cacho et al., 2000) that enhanced the current activity and depth of settling of the MOW (Schönfeld and Zahn, 2000; Rogerson et al., 2005). Similarly, during the late Miocene global cooling (Zachos et al., 2001; Murphy et al., 2009) a denser LIW could have enhanced the MOW via increasing its buoyancy loss, which is consistent with the observed increase of the NADW formation and AMOC intensification during this time interval.

The final closure of the Guadalhorce Corridor might have produced a dramatic reduction of the MOW, which then could only flow through the Rifian Corridors until their final closure at around 6.0 Ma (Krijgsman et al., 1999a). This led to a diminished NADW production as is recorded between 6.0 and 5.5 Ma in the South Atlantic (Billups, 2002). Concomitantly, the cessation of the MOW increased the freshwater input in the North Atlantic reducing or interrupting the NADW formation (Rahmstorf, 1998). This might have had a critical impact on the AMOC, global thermohaline circulation and global climate (Bethoux et al., 1999). Specifically, the reduction or interruption of the NADW by MOW cessation would reduce the AMOC leading to northern hemisphere cooling (Clark et al., 2002). This is supported by development of northern hemisphere ice sheets in Greenland margin (Fronval and Jansen, 1996; Thiede et al., 1998).

Finally, with the restoration of the Atlantic-Mediterranean connections through the Strait of Gibraltar, the MOW enhanced the NADW formation as it is indicated by the rise in NADW flow around the Miocene-Pliocene boundary in the South Atlantic and the western equatorial Atlantic Ocean (King et al., 1997; Billups, 2002).

4.7. Conclusions

The Messinian stable isotope records from the Montemayor-1 core located in the lower Guadalquivir Basin (SW Spain) allow the accurate dating of the closure of the

Guadalhorce Corridor, the last Betic Corridor connecting the Atlantic and the Mediterranean before the MSC, at 6.18 Ma.

Before the closure of the Guadalhorce Corridor, the export of highly saline intermediate waters as MOW contributed to increased NADW formation in the North Atlantic Ocean. During this period, constant benthic $\delta^{18}O$ values that depart from the global glacioeustatic trend, high $\Delta\delta^{18}O_{b\text{-}p}$, and low sedimentation rates indicate a strong water stratification and bottom water winnowing due to the MOW flow. After the closure of the corridor, benthic $\delta^{18}O$ values, which parallel that of the global glacioeustatic curve, low $\Delta\delta^{18}O_{b\text{-}p}$, and high sedimentation rates suggest an improved vertical mixing of the water column and interruption of MOW. Changes in the stable O isotope composition of the subsurface North Atlantic water masses during this time interval are primarily controlled by glacioeustatic processes. The cessation of the MOW might have resulted in decreased NADW formation between 6.0 and 5.5 Ma weakening the AMOC and promoting northern hemisphere cooling. Then, the restoration of the MOW due to the opening of the Strait of Gibraltar around the Miocene-Pliocene boundary would have favored an enhanced NADW formation.

Acknowledgments

We acknowledge the comments provided by reviewers Michael Rogerson and Marit-Solveig Seidenkrantz which substantially improved the quality of an earlier version of the manuscript. This paper is part of the Research Projects CGL2010-20857 and CGL2009-11539/BTE of the Ministerio de Ciencia e Innovación of Spain, and the Research Group RNM-190 of the Junta de Andalucía. JNPA has been funded by a research F.P.U. scholarship (ref. AP2007-00345) provided by the Ministerio de Educación of Spain. We are grateful to N. Andersen (Leibniz-Laboratory, Kiel, Germany) for stable isotope analysis. We also thank L. Vidal who provided the stable isotope data of benthic foraminifera from the ODP Site 1085 (SE Atlantic).

CHAPTER 5

CHAPTER 5

MESSINIAN PALEOPRODUCTIVITY CHANGES AND ORGANIC CARBON CYCLING IN THE NORTHEASTERN ATLANTIC

José N. Pérez-Asensio, Julio Aguirre, Gerhard Schmiedl, Jorge Civis

In preparation for submission

Abstract

Stable O and C records and benthic foraminifera of the continuous Montemayor-1 core (SW Spain) have been studied in order to analyse the productivity changes and organic carbon cycling in the northeastern Atlantic during the Messinian. Our results show that glacioeustatic fluctuations controlled the productivity in the region. Glacial periods are characterized by high planktic and benthic $\delta^{18}O$, low planktic and benthic $\delta^{13}C$, low sea-level and high abundance of *Uvigerina peregrina* s.l. (*U. peregrina* + *U. pygmaea*) suggesting high productivity related to upwelling currents. In contrast, interglacial periods have low planktic and benthic $\delta^{18}O$, high sea-level and high abundance of *Bulimina subulata* in the upper slope, and *Brizalina spathulata* and *Bulimina aculeata* in the outer shelf. These indicators suggest presence of degraded organic matter after upwelling events in the upper slope and high input of degraded terrestrial organic matter derived from riverine discharge in the outer shelf. Before the closure of the adjacent Guadalhorce Corridor at 6.18 Ma, the study area was alternatively influence by the well-ventilated Mediterranean Outflow Water (MOW) and the poor-ventilated Atlantic Upwelled Waters (AUW). After the closure of this corridor, the cessation of the MOW, which reduce the Atlantic meridional overturning circulation (AMOC) and promotes glacial conditions in the northern hemisphere, led to high productivity. Furthermore, the variability of the AMOC was recorded by fluctuations in the benthic $\delta^{13}C$ with high values indicating well-ventilated bottom waters due to strong AMOC during interglacial periods and low values reflecting poor ventilation as a result of weak AMOC during glacial periods.

5.1. Introduction

Continental shelves and slopes play a fundamental role in the biogeochemical cycles of C and N (Walsh, 1991). These areas present high productivity due to the supply of both continental and marine organic matter. At present-day, regions under upwelling influence represent areas with the highest primary productivity in the world's ocean (Bakun et al., 2010). The main upwelling areas are located in the eastern South and North Atlantic, and the eastern South and North Pacific (Schmiedl et al., 1997; Martinez et al., 1999; Bakun et al., 2010; Iles et al., 2012). Upwelling currents are produced by Ekman pumping induced by strong winds (Lebreiro et al., 1997; Martinez et al., 1999; Salgueiro et al., 2010), which might be affected by glacioeustasy. Paleoproductivity proxies including benthic foraminifera, diatoms, radiolarians, fish debris, phosphorite grains, and stable C isotopes are consistent with more intense upwelling during glacial periods (Diester-Haass and Schrader, 1979; Martinez et al., 1999; Abrantes, 1991, 2000; Eberwein and Mackensen, 2008). Furthermore, the variability of the Atlantic meridional overturning circulation (AMOC) can also influence productivity related to upwelling in the Atlantic region. A weak AMOC induces northern hemisphere cooling leading to stronger winds that promote upwelling (Zahn et al., 1997; Clark et al., 2002).

Close to the coast, high input of terrestrial organic matter via river run-off along with a shallow water depth result in high organic matter content on the sea floor (McKee et al., 2004). High supply of continental organic matter can cause eutrophication and oxygen depletion at the bottom and pore waters (Van der Zwaan and Jorissen, 1991; Jorissen et al., 1992; Donnici and Serandrei-Barbero, 2002). Riverine discharge that is closely related to precipitation is higher during warm and wet interglacial periods (van der Laan et al., 2012). The eastern Mediterranean sapropels are remarkable examples of high productivity related to fresh water discharges. These organic-rich, dark layers are deposited during periods of northward penetration of the African monsoon along with wetter conditions and high insolation during boreal summer related to precession minima (Schenau et al., 1999; Pérez-Folgado et al., 2003; Larrasoaña et al., 2003; Gallego-Torres et al., 2007; Kotthoff et al., 2008; Liu et al., 2012). Under this conditions, river run-off increases and discharges huge amounts of terrestrial organic matter into the eastern Mediterranean (Rohling, 1994; Casford et al., 2002).

Paleoproductivity in the northeastern Atlantic during the Pliocene, Pleistocene and Holocene has been extensively studied (Lebreiro et al., 1997; Eberwein and Mackensen, 2008; Martinez et al., 1999; van der Laan et al., 2006, Naafs et al., 2010; Salgueiro et al., 2010: Zarriess and Mackensen, 2010). According to these studies, changes in global climate influence the humidity and wind systems controlling the intensity and seasonality of primary productivity. In contrast, information about productivity in the northeastern Atlantic during the Messinian is scarce (van der Laan et al., 2006, 2012). The interruption of the MOW at 6.18 Ma (Pérez-Asensio et al., 2012a) might have modified the paleoproductivity in the northeastern Atlantic because this event weakened the AMOC promoting cooling in the northern hemisphere (Pérez-Asensio et al., 2012a). As mentioned before, glacial conditions would produce stronger winds favoring high productivity related to upwelling currents. However, so far there is no detailed study on the productivity changes of the northeastern Atlantic during the Messinian and its relationship with global climate and oceanography to prove this hypothesis.

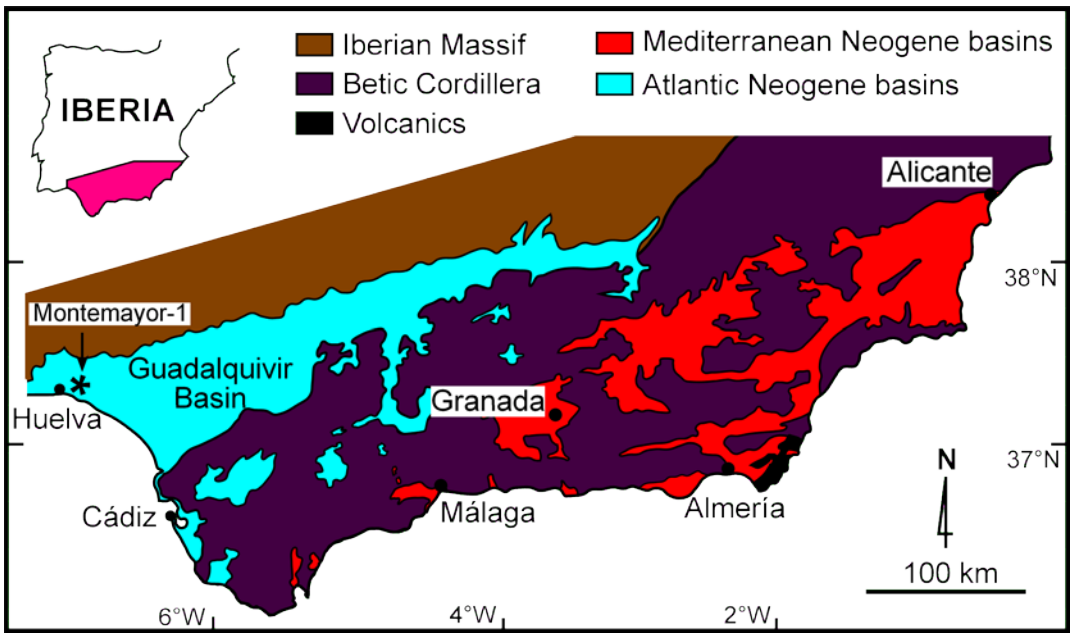

Figure 5.1. Geological setting of the lower Guadalquivir Basin. Asterisk points to the location of the Montemayor-1 core.

In this study, we analyse foraminiferal stable O and C isotope records and benthic foraminifera in the Montemayor-1 core (SW Spain) (Fig. 5.1). This core is located near the Guadalhorce Corridor, the last Betic Corridor to be closed (Martín et

al., 2001, 2009). The core includes a continuous Messinian record and was under the influence of the MOW before the closure of this Betic seaway (Pérez-Asensio et al., 2012a). Paleoceanographic changes produced by the MOW interruption affected the global oceanography and climate (Pérez-Asensio et al., 2012a). These changes could have controlled the productivity of the region during the Messinian since the MOW contributes to the AMOC (Bigg and Wadley, 2001; Bigg et al., 2003), which is a key controlling factor of the global oceanic circulation, carbon cycling and climate (Bethoux et al., 1999, Bigg et al., 2003; Murphy et al., 2009). Therefore, the location of this core is exceptional to investigate the productivity changes and organic carbon cycling in the eastern North Atlantic during the Messinian, to assess the effect of the cessation of the MOW on the productivity, and to decipher the relationship between productivity and global oceanography and climate. The aims of this study are: 1) to unravel the controlling mechanisms for the paleoproductivity changes in the northeastern Atlantic during the Messinian; 2) and to evaluate the impact of the MOW interruption on the Messinian paleoproductivity in the northeastern Atlantic.

5.2. Geographical and geological setting

The study area is located in the northwestern margin of the lower Guadalquivir Basin (SW Spain) (Fig. 5.1). This basin is an ENE-WSW elongated Atlantic foreland basin which is bounded to the N by the Iberian Massif, to the S by the Betic Cordillera, and to the W by the Atlantic Ocean (Sanz de Galdeano and Vera, 1992; Vera, 2000; Braga et al., 2002) (Fig. 5.1). The sedimentary filling of the basin consists of marine deposits ranging from the early Tortonian to the late Pliocene (Aguirre, 1992, 1995; Aguirre et al., 1993, 1995; Riaza and Martínez del Olmo, 1996; Sierro et al., 1996; Braga et al., 2002; González-Delgado et al., 2004; Martín et al., 2009).

In the study area, the Neogene deposits that filled the lower Guadalquivir Basin have been divided into four lithostratigraphic units formally described as formations. From bottom to top: 1) carbonate-siliciclastic mixed deposits of the Niebla Formation (Civis et al., 1987; Baceta and Pendón, 1999), 2) greenish-bluish clays of the Arcillas de Gibraleón Formation (Civis et al., 1987), 3) fossiliferous sands and silts of the Arenas de Huelva Formation (Civis et al., 1987), and 4) sands of the Arenas de Bonares Formation (Mayoral and Pendón, 1987).

The Guadalquivir Basin acted as a corridor, the so-called North Betic Strait, connecting the Atlantic and the Mediterranean during the latest Serravallian-earliest Tortonian (Aguirre et al., 2007; Martín et al., 2009; Braga et al., 2010). Other Betic seaways that connected the Atlantic and the Mediterranean through the Guadalquivir Basin after the closure of the North Betic Strait during the early Tortonian, were gradually closed during the late Miocene. The main late Tortonian Atlantic-Mediterranean gateways were the Dehesas de Guadix Corridor and the Granada Basin (Esteban et al., 1996; Braga et al., 2003; Betzler et al., 2006; Martín et al., 2009). The Guadalhorce Corridor was the last Betic Corridor and was closed in the early Messinian (Martín et al., 2001; Pérez-Asensio et al., 2012a). After its closure, the only Atlantic-Mediterranean connections were established through the Rifian Corridors, N Morocco (Esteban et al., 1996).

5.3. Material and methods

The studied material is the 260 m long continuous Montemayor-1 core which is located in the northwestern edge of the lower Guadalquivir Basin close to the village of Moguer (Huelva, SW Spain) (Figs. 5.1 and 5.2). This core includes sediments from the four aforementioned formations (Pérez-Asensio et al., 2012b) (Fig. 5.2). The age model of the core is based on magnetobiostratigraphy and O stable isotope data (Larrasoaña et al., 2008; Pérez-Asensio et al. 2012a, in prep. 2) (Fig. 5.2). In this work, we studied an interval of 140 m, from 240 to 100 m, which ranges from 6.67 to 5.38 Ma (Messinian). This interval includes marine sediments from the Arcillas de Gibraleón Formation (Fig. 5.2).

For faunal analysis, a total of 255 samples were collected with a sampling interval of 0.5 m. Samples were wet sieved over a 63 μm mesh and dried out in an oven at 40 ºC. Using a microsplitter samples were divided into sub-samples containing at least 300 benthic foraminifera. The sub-samples were dry sieved over a 125 μm mesh, and benthic foraminifera were identified and counted. Benthic foraminiferal counts were transformed into relative abundances. In order to assess the paleoproductivity changes we used the relative abundances of high-productivity target taxa including *Uvigerina peregrina* s.l. (*U. peregrina* + *U. pygmaea*), *Bulimina subulata*, *Brizalina spathulata*, and *Bulimina aculeata*.

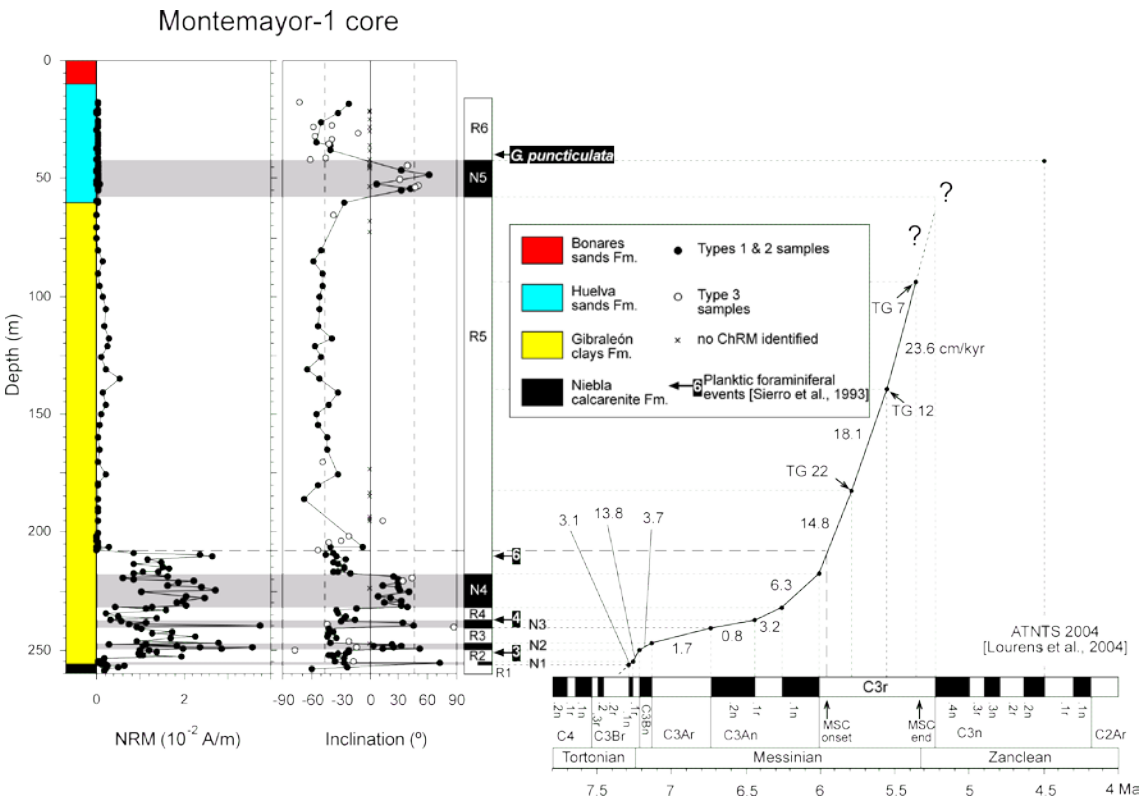

Figure 5.2. Lithology, age model, sedimentation rate (estimated in cm/kyr) and magnetobiostratigraphic framework for the Montemayor-1 core. Magnetostratigraphy was established according to the ATNTS2004 (Lourens et al., 2004). Type 1 samples have higher quality than types 2 & 3 samples (data from Larrasoaña et al., 2008). CrRM stands for characteristic remanent magnetization. Biostratigraphy is based on the planktonic foraminiferal events (PF events) of Sierro et al. (1993) and first occurrence of *Globorotalia puncticulata*. Position of glacial stages TG 22, 12 and 7 are shown. Question marks indicate uncertainties in the chronology and sedimentation rate.

For stable oxygen and carbon isotope analyses, a total of 160 samples were analysed. The sampling interval is 0.5 m from 240 to 170 m, and 2.5 m from 170 to 100 m. Approximately 10 tests of *Cibicidoides pachyderma* and 20 tests of *Globigerina bulloides* have been picked from the size fraction >125 μm. Prior to the analyses foraminifera were cleaned with ultrasonic bath and washed with distilled water. Stable isotope analyses were performed at the Leibniz-Laboratory for Radiometric Dating and Isotope Research, Kiel, Germany (see Pérez-Asensio et al., 2012a for details).

Additionally, Pearson correlation coefficients were calculated to assess the statistical correlation between O and C stable isotopes, relative abundance of target taxa and planktonic/benthonic (P/B) ratio, this last metric following Pérez-Asensio et al. (2012) (Table 5.1). Only coefficients with a p-value < 0.01 were considered significant.

	U. peregrina s.l.	*B. subulata*	*B. aculeata*	*B. spathulata*	P/B ratio	Benthic O	Benthic C	Planktic O	Planktic C
U. peregrina s.l.	1.000								
B. subulata		1.000							
B. aculeata			1.000						
B. spathulata	-0.301	-0.423	0.252	1.000					
P/B ratio	0.370			-0.460	1.000				
Benthic O		0.401		-0.211		1.000			
Benthic C	-0.218						1.000		
Planktic O		0.313				0.376		1.000	
Planktic C	-0.378			0.349	-0.551				1.000

Table 5.1. Pearson correlation coefficients at *p*-value < 0.01 of high productivity benthic foraminiferal species, the planktic and benthic O and C isotopes, and P/B ratio.

5.4. Results

5.4.1. High-productivity target taxa

The relative abundance of *Uvigerina peregrina* s.l. shows a fluctuating trend with its highest values from 6.67 to 5.87 Ma (Fig. 5.3). In this interval, it presents two minima at around 6.44 and 6.18 Ma and it gradually increases from 6.18 to 5.87 Ma (Fig. 5.3). This species sharply diminishes at 5.87 Ma. In the interval from 5.87 to 5.38 Ma, it has low average values around 10% (Fig. 5.3). *Bulimina subulata* is more abundant from 6.67 to 5.87 Ma where shows a local maximum at 6.44 Ma and a gradual increasing trend (Fig. 5.3). In the interval from 5.87 to 5.38 Ma, *B. subulata* experiences a gradual decrease. In contrast, *Brizalina spathulata* and *Bulimina aculeata* are more abundant between 5.87 and 5.38 Ma (Fig. 5.3). In this interval, both species progressively replace *B. subulata*.

5.4.2. Stable isotope data

The benthic O isotope record has stable average values of 1‰ before 6.35 Ma. Then, it reduces until a minimum of -0.93‰ at 6.18 Ma (Fig. 5.3). In the interval from 6.18 to 5.79 Ma, it gradually increases toward heavier values. Finally, $\delta^{18}O$ decreases from 5.79 to 5.72 Ma and remains with relatively low values (~0.4‰) from 5.72 to 5.38 Ma (Fig. 5.3). The planktic O isotope record shows a fluctuating trend with average

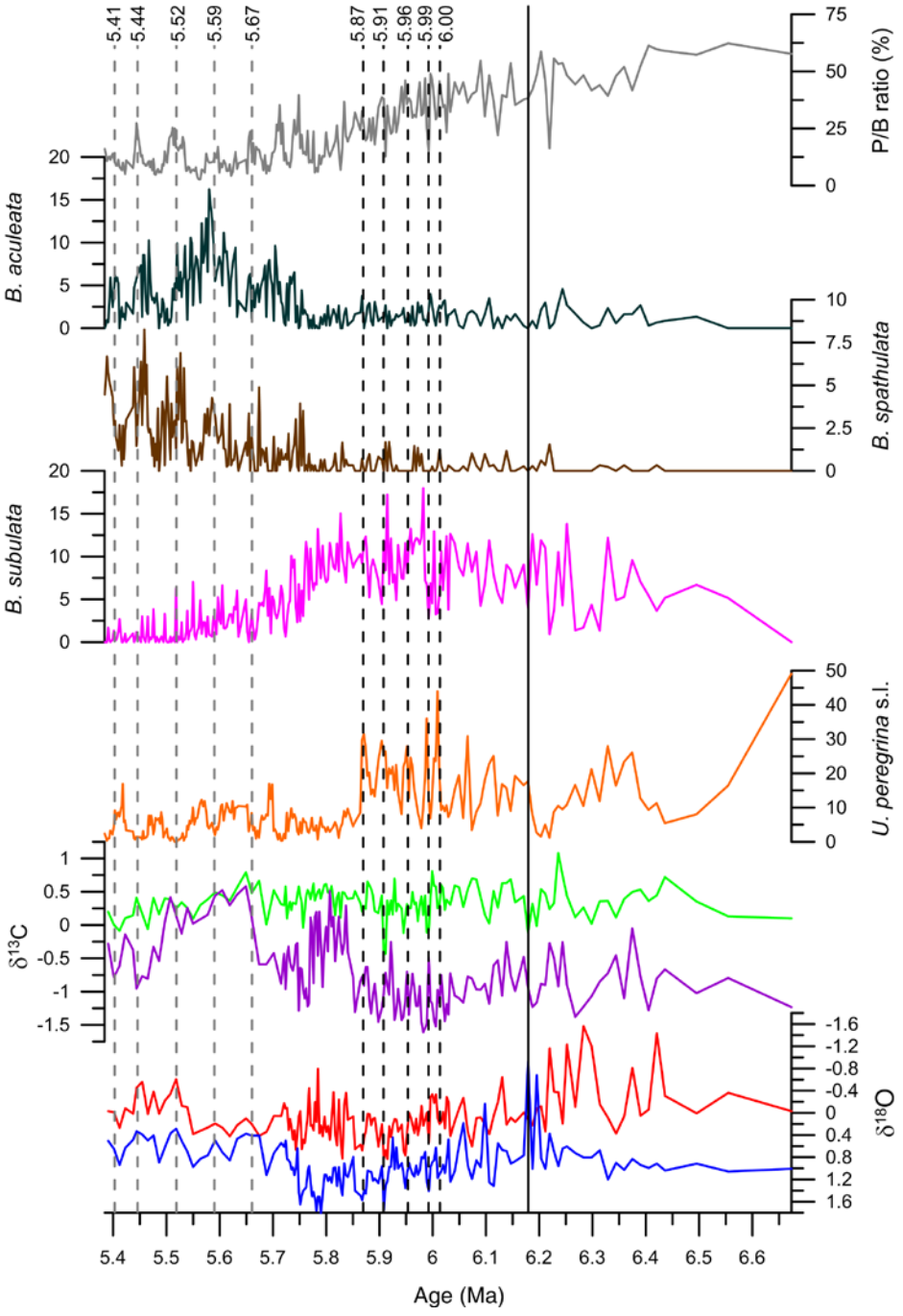

Figure 5 3. From top to bottom: P/B ratio (%) (Pérez-Asensio et al., 2012b); relative abundances (%) of high productivity foraminiferal species including *Bulimina aculeata*, *Brizalina spathulata*, *Bulimina subulata*, and *Uvigerina peregrina* s.l.; benthic (green) and planktic (purple) $\delta^{13}C$ records and benthic (dark blue) and planktic (red) $\delta^{18}O$ records in ‰ VPDB of the Montemayor-1 core. The vertical dashed lines indicate five events of high productivity related to upwelling currents in the upper slope (black) (6.00, 5.99, 5.96, 5.91 and 5.87 Ma), and five events of high productivity linked to riverine discharge in the outer shelf (grey) (5.67, 5.59, 5.52, 5.44, and 5.41 Ma). The vertical black solid line at 6.18 Ma marks the end of the Atlantic-Mediterranean Betic connection through the Guadalhorce Corridor.

values lower than 0‰ before 6.18 Ma (Fig. 5.3). In the interval from 6.18 to 5.79 Ma, the values progressively increase. After 5.79 Ma, the planktic O isotope record decreases at 5.75 and 5.52 Ma. The planktic and benthic O curves have a parallel trend as it is indicated by the positive correlation (Table 5.1).

The benthic C isotope record presents a fluctuating trend with average values of 0.4‰ before 6.18 Ma (Fig. 5.3). Then, $\delta^{13}C$ decreases from 6.18 to 5.9 Ma and it remains with values around 0.4‰ from 5.9 to 5.67 Ma. Finally, it gradually decreases from 5.67 to 5.38 Ma. The planktic C isotopic values show fluctuations around values of -0.8‰ before 6.18 Ma (Fig. 5.3). $\delta^{13}C$ diminishes reaching its lowest values from 6.05 to 5.85 Ma. At 5.85 Ma, the planktic C isotope record abruptly rises from -1‰ to 0‰ and it remains with high average values of 0‰ until 5.77 Ma. Then, it sharply decreases up to -1‰ and it increases until values of 0‰ at 5.67 Ma. Finally, it gradually diminishes from 5.67 to 5.38 Ma.

5.5. Discussion

5.5.1 Paleoproductivity changes and organic carbon cycling in the northeastern Atlantic during the Messinian

Paleoproductivity changes and organic carbon cycling in the northeastern Atlantic depends on the global glacioeustatic fluctuations that, in turn, affect the distribution of the high productivity benthic foraminiferal species. In the study site, glacial periods are characterized by high planktic and benthic O isotopic values (Fig. 5.3). This is supported by a positive statistical correlation between these proxies (Table 5.1). Furthermore, relatively low P/B ratios coincide with high $\delta^{18}O$ (Fig. 5.3) and cool and dry climate (Jiménez-Moreno et al. submitted) supporting a glacioeustatic origin for sea-level fluctuations.

Benthic foraminifer assemblages from the Montemayor-1 core suggest a shallowing upwards trend from upper slope to outer platform settings in the studied core interval (Pérez-Asensio et al., 2012b). Thus, effects of the local paleoenvironmental evolution of this region of the lower Guadalquivir Basin are superimposed to the global glacioeustatic variations. In the upper slope deposits of the study core (from 246.5 to 179 m core depth in Pérez-Asensio et al., 2012b), glacial periods coincide with low $\delta^{13}C$ values (Fig. 5.3).

Regarding the benthic C isotopes, Piotrowski et al. (2005) stated that the glacial decrease in the $\delta^{13}C$ is between 0.46 and 0.32‰ during glacial-to-interglacial fluctuations in the global C budget. In the Montemayor-1 core, however, fluctuations in the benthic $\delta^{13}C$ are around 1‰ (Fig. 5.3). Therefore, other factors should have contributed to the benthic $\delta^{13}C$ signature, such as influence of nutrient-rich waters. The observed ^{13}C-depleted values in the upper slope deposits could be related either with nutrient-rich upwelling currents (Eberwein and Mackensen, 2006, 2008) or with refractory organic matter reworked from exposed continental shelf sediments during sea-level lowstands (Vincent et al., 1980; Loutit and Keigwin, 1982; Kouwenhoven et al., 1999). In our study case, upper slope deposits are characterized by the abundance of the *Uvigerina peregrina* s.l. (Pérez-Asensio et al., 2012b). This is a mesotrophic benthic foraminiferal species (e.g. Schmiedl et al., 2000; Phipps et al., 2012) that dominates under the influence of fresh marine organic matter supplied by upwellings (Fontanier et al., 2003; Koho et al., 2008; Schmiedl et al., 2010). Therefore, high productivity can be likely attributed to upwelling currents, which is also consistent with the observed negative correlation between *U. peregrina* s.l. and benthic C isotopic values (Table 5.1). Further, these high productivity periods occurred during glacial periods as indicated above and coinciding with other authors' findings (Martins et al., 2006; Mendes et al., 2004; Mojtahid et al., 2006; Schmiedl et al., 1997). The driving mechanism for enhanced upwelling in the lower Guadalquivir Basin might be stronger winds promoting Ekman pumping during glacial periods as occurred in the Quaternary (Schmiedl and Mackensen, 1997; Lebreiro et al., 1997; Poli et al., 2010; Salgueiro et al., 2010).

The effect of upwelling currents is also confirmed by the negative correlation between planktic C isotopes and *U. peregrina* s. l. (Table 5.1). Planktic $\delta^{13}C$ values of the Montemayor-1 core are strikingly lower than the benthic ones. Commonly, surface waters have higher $\delta^{13}C$ signatures than deep waters because of the biological pump, i.e. removal of light ^{12}C from surface waters due to primary productivity and release of ^{12}C in the bottom waters (Rohling et al., 2004). The low planktic $\delta^{13}C$ values from the Montemayor-1 core are due to the fact that they have been measured in *Globigerina bulloides*, which inhabits waters from surface to intermediate depths (20-300 m) (Pujol and Vergnaud-Grazzini, 1995). Therefore, this species is likely reflecting the isotopic signature of nutrient-rich ^{13}C-depleted upwelling subsurface waters masses. In addition, low planktic $\delta^{13}C$ are concomitant with high $\delta^{18}O$ (Fig. 5.3) suggesting strong mixing

between cold nutrient-rich bottom waters and surface waters (Grunert et al., 2010). Furthermore, the $\delta^{13}C$ of *G. bulloides* decreases during upwelling events because of the fractionation of carbon isotopes due to vital effects (Lebreiro et al., 1997; Naidu and Niitsuma, 2004). During strong upwelling faster calcification rates due to high-nutrient availability requires higher respiration, which involves more respired CO_2 enriched with ^{12}C (Naidu and Niitsuma, 2004). These effects would explain the very low planktic $\delta^{13}C$ signatures along the Montemayor-1 core.

According with the benthic foraminiferal assemblages in the upper slope deposits (Pérez-Asensio et al., 2012b), peaks of relative abundance of *U. peregrina* s.l. during glacial periods alternate with high percentages of *Bulimina subulata* (Fig. 5.3). *Bulimina subulata,* like other species of the genus, feeds from more degraded organic matter (Schmiedl et al., 2000) than *Uvigerina peregrina* s.l., which feeds from fresh and labile organic matter (Fontanier et al., 2003; Koho et al., 2008; Schmiedl et al., 2010). This difference in trophic behaviour might account for the low abundances of *B. subulata* during glacial periods when fresh organic matter is available on the sea-floor. In contrast, more degraded organic matter is accumulated after upwelling events fostering increases of *B. subulata* during interglacial periods. *U. peregrina* s.l. and *B. subulata* abundances decrease in a different way after 5.87 Ma. At this age, *Uvigerina peregrina* s.l. virtually disappears while *B. subulata* diminishes gradually. The upper slope *U. peregrina* s.l. is replaced by epifaunal taxa, mainly *P. ariminensis*, inhabiting an oligotrophic shelf edge setting (Pérez-Asensio et al., 2012b). This sharp decrease of *U. peregrina* s.l. might be due to the absence of fresh organic matter related to upwelling currents that does not reach the shelf edge. Oligotrophic conditions in the shelf edge are also consistent with the relatively high planktic $\delta^{13}C$ values (Fig. 5.3). A bottom current along the platform margin preventing upwelling waters from reaching the shelf edge could account for these oligotrophic conditions during glacial conditions . In contrast, *B. subulata* diminishes gradually because it is able to feed from degraded organic matter that remains more time at the sea floor than fresh organic matter.

At 5.77 Ma, *Planulina ariminensis* disappears pointing to the transition from the shelf edge to the outer shelf (Pérez-Asensio et al., 2012b). This event is concomitant with a significant sea-level drop and is close to the glacial stage TG 20 (5.75 Ma) (Pérez-Asensio et al., 2012a, 2012b; in prep. 2). From 5.77 to 5.67 Ma, the planktic $\delta^{13}C$ increases significantly (Fig. 5.3) pointing to a decrease in the productivity most likely related to interglacial conditions as it is shown by the decrease in benthic and

planktic $\delta^{18}O$ (Fig. 3). After 5.67 Ma, the outer-shelf setting is characterised by high abundance of *Brizalina spathulata* and *Bulimina aculeata* (Fig. 5.3) (Pérez-Asensio et al, 2012b). It is well established that *B. spathulata* can thrive with continental degraded organic matter derived from river run-off (Donnici and Serandrei-Barbero, 2002; Duchemin et al., 2008; Schmiedl et al., 2010). In the Montemayor-1 core, the upwelling-related *U. peregrina* s.l. shows high abundance during glacial periods, whereas *B. spathulata* has relatively low values. This is supported by a negative correlation between both species (Table 5.1). Hence, *B. spathulata* does not seem to be controlled by the influence of fresh organic matter derived from upwelling currents, as previously interpreted (Pérez-Asensio et al., 2012b).

B. aculeata is able to feed from both fresh and degraded organic matter (Schmiedl and Leuschner, 2005). It has been also found in low-oxygen environments with supply of continental degraded organic matter under river run-off influence (Schmiedl et al., 2000, Pérez-Asensio and Aguirre, 2010). In the study site, it shows the highest percentages coinciding with high values of *B. spathulata* during interglacial periods (Fig. 5.3). Therefore, both *B. spathulata* and *B. aculeata* indicate supply of continental degraded organic matter related to riverine discharge during interglacial periods.

These periods are characterised by relatively high sea-level (Fig. 5.3), as well as warm and humid climate as it is indicated by palynological analyses (Jiménez-Moreno et al., submitted). Consequently, a higher humidity might have promoted higher river run-off and more supply of continental degraded organic matter during interglacial periods. This is consistent with the gradual increase of *B. spathulata* concomitant with a long-term decrease in $\delta^{13}C$ and low $\delta^{18}O$ (Fig. 5.3) and with the progressive shallowing upward trend in the core (Pérez-Asensio et al., 2012b) since continental organic matter reached areas closer to the coast. Very depleted planktic C isotopic values of *Globigerina bulloides* at 5.44, and 5.41 Ma might also reflect enhanced precipitation (Milker et al., 2012) (Fig. 5.3). Increased humidity could be related to the global warming linked to interglacial stage TG 11 that started before the Miocene-Pliocene boundary and persisted until the mid Pliocene (Vidal et al., 2002; Pérez-Asensio et al., in prep. 2).

5.5.2. Effect of the MOW interruption on the paleoproductivity in the northeastern Atlantic during the Messinian

The MOW promotes the NADW formation and therefore contributes to the AMOC increasing the North Atlantic density gradient and promoting the resumption of the AMOC after its collapse (Rogerson et al., 2012). A reduction or interruption of the MOW would result in a decrease or interruption of the NADW formation (Rahmstorf, 1998) and, consequently, would reduce the AMOC causing cooling and ice sheet growth in the northern hemisphere (Zahn et al., 1997; Clark et al., 2002). This glaciation would lead to high productivity conditions due to stronger winds that induce Ekman pumping stimulating upwellings (Lebreiro et al., 1997; Salgueiro et al., 2010).

The stable isotope records of the Montemayor-1 core indicates that MOW bathed the study area during the early Messinian up to 6.18 Ma (Pérez-Asensio et al., 2012a). Therefore, the global glacioeustatic control on the productivity at the study area might have a superimposed influence of the MOW before 6.18 Ma. Thus, the study area was alternatively affected by the MOW and the upwelling currents from the Atlantic (Atlantic Upwelled Waters, AUW) (Fig. 5.4A-B). At the present-day, during the Quaternary and the Plio-Pleistocene, the MOW has benthic $\delta^{13}C$ values higher than Atlantic waters indicating well-ventilated bottom waters (Vergnaud-Grazzini, 1983; Schönfeld and Zahn, 2000; Raddatz et al., 2011). Fluctuations in the upwelling-related *Uvigerina peregrina* s.l. and the benthic $\delta^{13}C$ could reflect the alternation between the MOW and the AUW before 6.18 Ma. Thus, low abundance of *U. peregrina* s.l. and high benthic $\delta^{13}C$ at 6.44 and 6.18 Ma (Fig. 5.3) indicates a well-ventilated bottom with low organic flux to the sea floor. This indicates that the MOW winnowed organic matter particles and increased the bottom-water oxygenation (Fig. 5.4A). Furthermore, high benthic $\delta^{13}C$ could also indicate well-ventilated bottom waters linked to a strong AMOC during interglacial periods (Fig. 5.4A). In contrast, high abundance of *U. peregrina* s.l. and low benthic $\delta^{13}C$ at 6.6 and 6.35 Ma (Fig. 5.3) point to the influence of low-oxygen AUW (Fig. 5.4B). In addition, low benthic $\delta^{13}C$ could also reflect low ventilation due to a reduced AMOC during glacial conditions (Zahn et al., 1997) (Fig. 5.4B-C). Hence, the AMOC was weaker during glacials than during interglacials as occurs in the Holocene and Pleistocene (Broecker et al., 1985).

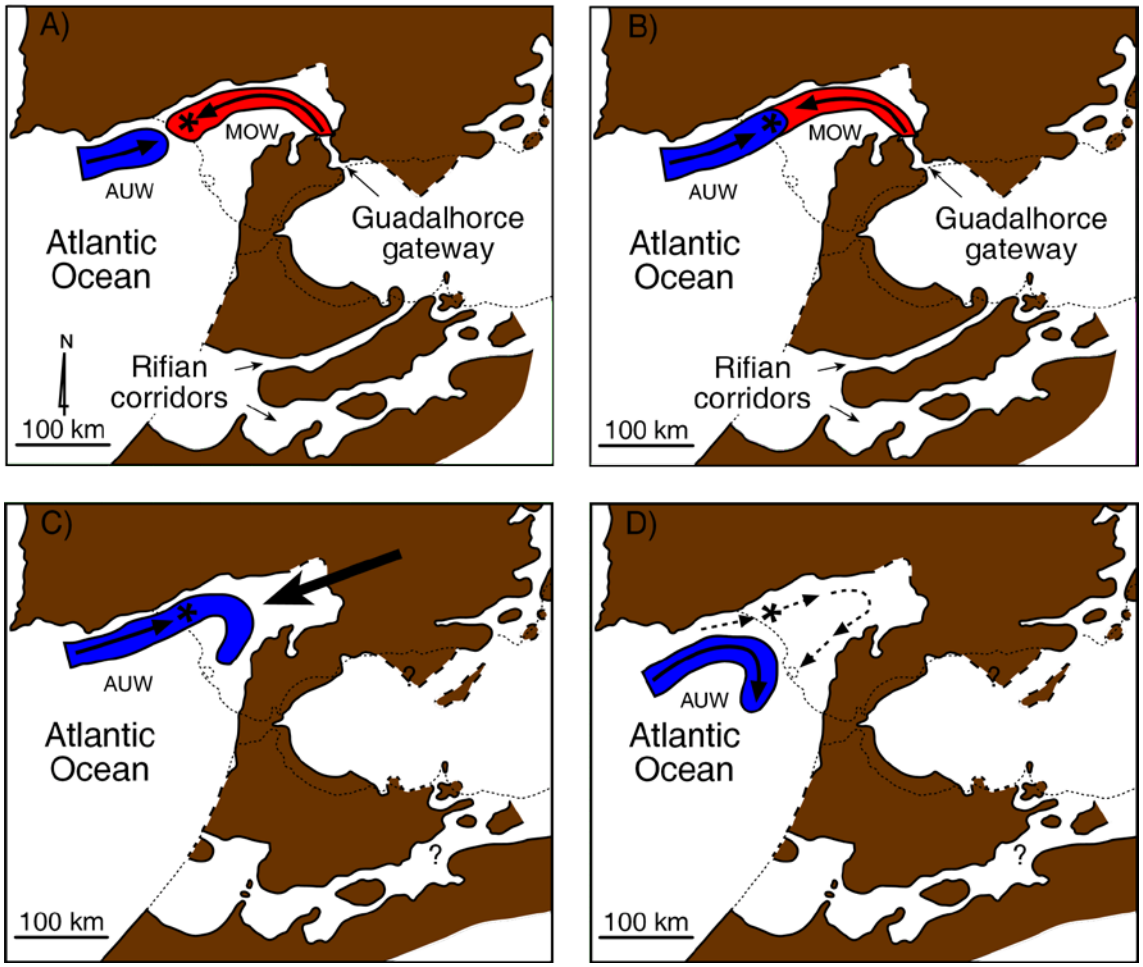

Figure 5.4. Paleogeographic and paleoceanographic evolution of the lower Guadalquivir Basin during the Messinian (based on Martín et al., 2009): A) Interglacial conditions before 6.18 Ma, when only the Mediterranean Outflow Water (MOW) reaches the studied core (asterisk); B) Glacial conditions before 6.18 Ma, when the Atlantic Upwelled Water (AUW) and the MOW reach the studied core; C) Glacial conditions after 6.18 Ma, when only AUW reaches the core because the MOW is interrupted. The black thick arrow marks the progradation of the main depositional systems along the axis of the Guadalquivir Basin; and D) Studied core (asterisk) influenced by a current along the shelf-break (dashed arrows) that prevented the AUW from reaching the study area between 5.87 to 5.77 Ma.

After the closure of the Guadalhorce Corridor at 6.18 Ma, there is a gradual decrease in the benthic $\delta^{13}C$ signature that could be due to the interruption of the MOW and the influence of oxygen-depleted AUW (Fig. 5.3). The planktic $\delta^{13}C$ shows a progressive decrease towards depleted values indicating also a higher influence of nutrient-rich AUW. Concomitantly, *U. peregrina* s.l., which thrives under upwelling conditions, gradually increases reaching its highest abundance (Fig. 5.3). Therefore, after the cessation of the MOW only AUW reached the study area promoting high

productivity related to upwelling currents (Fig. 5.4C-D). In addition, high productivity could have been favoured by the cessation of the MOW, which weaken the AMOC and promotes northern hemisphere cooling (Pérez-Asensio et al., 2012a). A reduced AMOC associated to high productivity has also been recorded in the SE Atlantic Ocean during the Messinian (Rommerskirchen et al., 2011).

5.6 Conclusions

Paleoproductivity changes and organic carbon cycling in the northeastern Atlantic during the Messinian are controlled by global glacioeustasy. Glacial periods (cold and dry climate) are characterized by high planktic and benthic $\delta^{18}O$, low planktic and benthic $\delta^{13}C$, low sea-level and high abundance of *U. peregrina* s.l. These proxies points to high productivity related to upwelling currents during glacial periods. These upwelling currents were produced by Ekman pumping due to intense winds. On the contrary, interglacial periods (warm and humid climate) show low planktic and benthic $\delta^{18}O$, high sea-level and high abundance of *B. subulata* in the upper slope, and *B. spathulata* and *B. aculeata* in the outer shelf. These indicators suggest presence of degraded organic matter after upwelling events in the upper slope and supply of degraded continental organic matter derived from river run off in the outer shelf.

Before the closure of the Guadalhorce Corridor, the study area was alternatively influenced by the well-ventilated MOW and the poor-ventilated AUW. Once this Betic seaway was closed at 6.18 Ma, the interruption of the MOW, that reduced the AMOC and promoted glacial conditions in the northern hemisphere, favoured high productivity conditions. The variability of the AMOC is recorded by fluctuations in the benthic $\delta^{13}C$. High benthic $\delta^{13}C$ indicates well-ventilated bottom waters due to strong AMOC during interglacial periods. In contrast, low benthic $\delta^{13}C$ reflect poor ventilation as a result of weak AMOC during glacial periods.

Acknowledgements

This work was funded by the Research Projects CGL2010-20857 and CGL2009-11539/BTE of the Ministerio de Ciencia e Innovación of Spain, and the Research Group RNM-190 of the Junta de Andalucía. JNPA was funded by a research F.P.U. grant (ref.

AP2007-00345) awarded by the Ministerio de Educación of Spain. We want to thank N. Andersen (Leibniz-Laboratory, Kiel, Germany) for stable isotope analysis.

CHAPTER 6

CHAPTER 6

GLACIOEUSTATIC CONTROL ON THE ORIGIN AND CESSATION OF THE MESSINIAN SALINITY CRISIS

José N. Pérez-Asensio, Julio Aguirre, Gonzalo Jiménez-Moreno, Gerhard Schmiedl, Jorge Civis

In preparation for submission

Abstract

The desiccation of the Mediterranean during the Messinian salinity crisis (MSC) is one of the most intriguing geological events of the recent Earth's history. However, timing and mechanisms triggering both its onset and end are still controversial. We present a novel approach by looking at the MSC from the Atlantic, but close to the Gibraltar Arc, analyzing a complete Messinian record; the Montemayor-1 core (Guadalquivir Basin, SW Spain). Our results support global cooling and associated glacioeustatic sea-level drop coinciding with the MSC onset (5.96 Ma). Backstripping analysis shows that tectonic uplifting in the Gibraltar Arc area was insufficient to promote the observed sea-level fall. The later flooding of the Mediterranean occurred during a stable tectonic period and a sea-level rise during global warming. We postulate a two-step flooding event: 1) Glacioeustatic sea-level rise during interglacial stage TG11 (5.52 Ma) led to subtropical Atlantic waters entered the west-central Mediterranean through pathways south of the Gibraltar Strait, probably the Rifian corridors. 2) Water overload favored intensification of regressive fluvial erosion in the Gibraltar threshold, generating the Gibraltar Strait and producing the complete Mediterranean refilling during the earliest Pliocene.

6.1. Introduction

The Messinian salinity crisis (MSC) in the Mediterranean has attracted the interest of Earth scientists ever since the publication by Hsü et al. (1973). The general consensus is that the Mediterranean was isolated from the Atlantic due to the closure of the Betic and the Rifian corridors with deposition of the Lower and Upper Evaporites. There are still crucial issues under heated debates, particularly concerning the ultimate mechanisms leading to the isolation of the Mediterranean. Global glacioeustatic sea level lowering, regional tectonic uplift in the Gibraltar area, or a combination of both processes have been invoked as trigger mechanisms (Weijermars, 1988; Kastens, 1992; Duggen et al., 2003; Hilgen et al., 2007). Additionally, there is no consensus on the timing and causes of the reestablishment of normal marine conditions in the Mediterranean after the MSC (Martín and Braga, 1994; Riding et al., 1998; Krijgsman et al., 1999b; Hilgen et al., 2007). These discrepancies can be attributed to the particular Messinian paleogeography of the Mediterranean associated with different local tectono-sedimentary regimes and problems of accurate correlation of deep-basin and marginal-basin deposits (e.g. Roveri and Manzi, 2006).

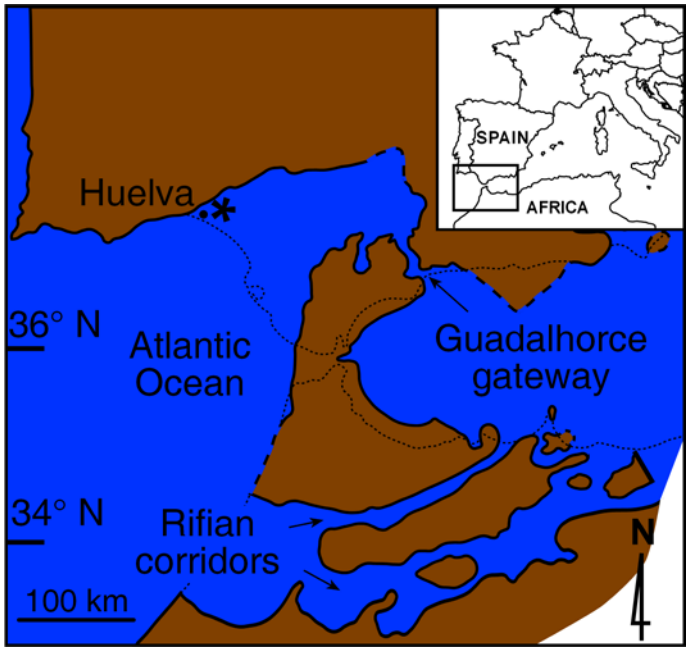

Figure 6.1. Paleogeographic map of the Gibraltar Arc area during the early Messinian (after Martín et al., 2009). The asterisk indicates the location of the studied core.

Here, we present data that, in combination with published ones, provide a solution for the MSC conundrum. We have studied the Montemayor-1 core (Guadalquivir Basin, SW Spain) (Fig. 6.1) that shows a continuous Messinian sedimentary record in the vicinity of the Gibraltar Arc. The core is accurately dated (Fig. 6.2) and provides an unbiased perspective of the MSC from the open Atlantic Ocean, offering the unique opportunity of linking global oceanic processes with regional Mediterranean events coetaneous with the desiccation. Our main goal is to provide a comprehensive model for understanding the desiccation and re-filling of the Mediterranean during the Messinian.

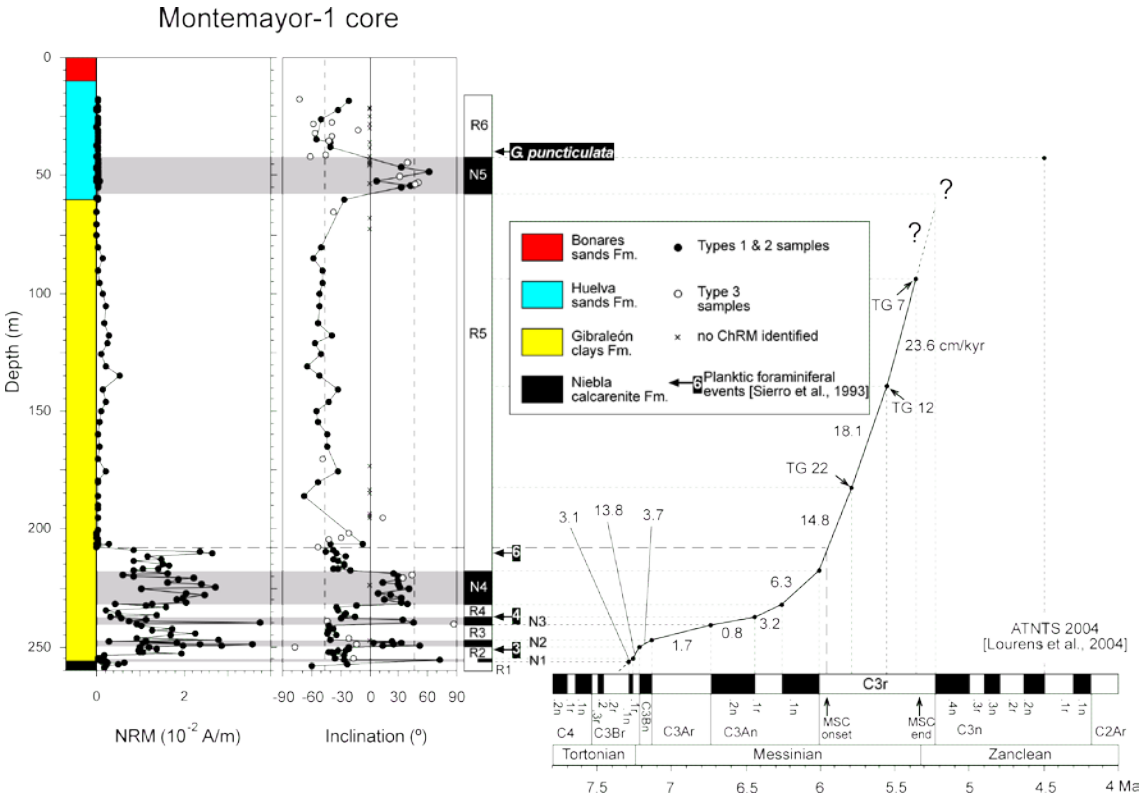

Figure 6.2. Age model and sedimentation rate (in cm/kyr) for the Montemayor-1 core. Position of stages TG22, TG12, and TG7 is indicated. Question marks show imprecision in the age model.

6.2. The Montemayor-1 core

The Montemayor-1 core is close to Huelva (SW Spain) (Fig. 6.1). It consists of latest Tortonian-early Pliocene marine deposits (Pérez-Asensio et al., 2012a). Here, we have studied the interval ranging from 6.17 to 5.19 Ma. We have analyzed $\delta^{18}O$ of

foraminifers as proxy of paleoclimatic changes and for establishing the age model of the core (Figs 6.2 and 6.3). We have also carried out a backstripping analysis, following the procedure of van Hinsbergen et al. (2005) to evaluate vertical movements of the basement before, during and after the MSC in the vicinity of the Gibraltar Strait (Fig. 6.4). We integrate these data with additional paleontological findings from the core (Pérez-Asensio et al., 2012a, 2012b; Jiménez-Moreno et al., submitted), and reconcile them with available information to propose a model for the onset and end of the MSC.

Chronology of the Montemayor-1 core is based on magnetobiostratigraphy (Larrasoaña et al., 2008) and O stable isotope data (Fig. 6.2). We have extended the age model of Pérez-Asensio et al. (2012b) by accurately identifying the glacial stages TG22, TG20, TG12 and TG4, as well as the interglacial stages TG11 and TG7 (Figs. DR1 and DR2).

6.3. MSC onset and end

6.3.1. Beginning of the MSC

The MSC started at 5.96 ± 0.02 Ma (Krijgsman et al., 1999b), coinciding with the Lower Evaporite deposition. Our results show a significant sea-level fall of 227 m at this time based on benthic foraminifera (Pérez-Asensio et al., 2012a) (Fig. 6.3). This is sufficient to disconnect the Mediterranean from the Atlantic since Betic and Rifian corridors were about 120 m and 100 m in depth, respectively (Martín et al., 2001; Krijgsman et al., 1999a). A dramatic reduction in the dinoflagellate/pollen ratio in the core (Fig. 6.3) at this time also indicates shallowing (Jiménez-Moreno et al., submitted). Relative abundance of *Quercus* pollen (Fig. 6.3), and other thermophilous plants, decreases substantially at this time pointing to cool and arid conditions concurrent with the beginning of the MSC (Jiménez-Moreno et al., submitted). This cooling and sea-level drop match with minima of the ETP, eccentricity and obliquity orbital curves, as well as with an increase in the benthic $\delta^{18}O$ in Montemayor-1 core (Fig. 6.3). The sea-level lowering is also documented in the benthic $\delta^{18}O$ of Atlantic and Pacific oceans (Shackleton et al., 1995, Vidal et al., 2002) (Fig. DR3). This cooling was probably associated with ice-sheet expansions on western Antarctica and the Arctic taking place during the late Miocene (Zachos et al., 2001).

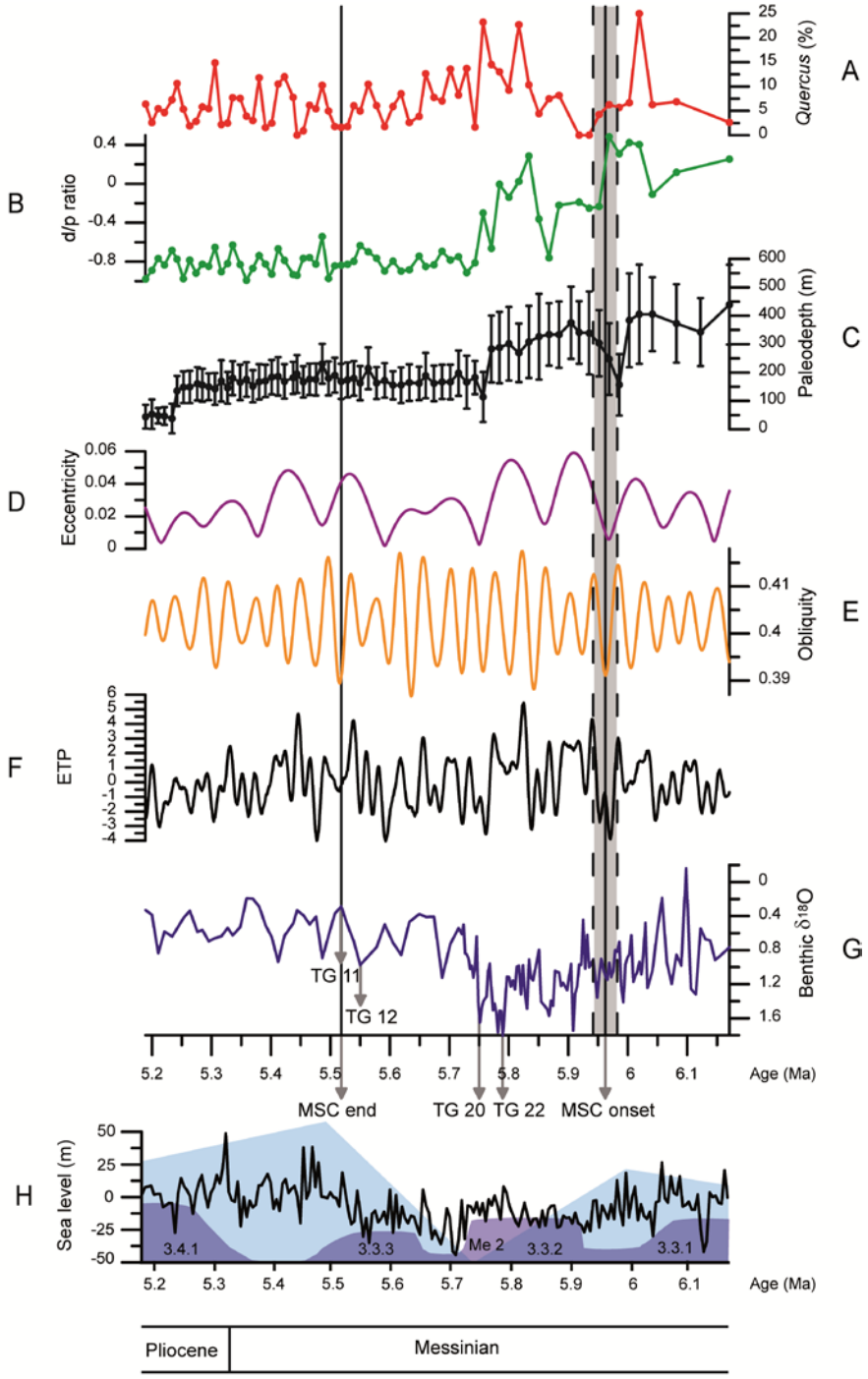

Figure 6.3. A: Relative abundance of *Quercus* pollen (Jiménez-Moreno et al., submitted). B: Dinocyst/pollen ratio (Jiménez-Moreno et al., submitted) C: Paleodepth estimate based on benthic foraminiferal assemblages (Pérez-Asensio et al., 2012a). D: Eccentricity curve from La2010 orbital solution (Laskar et al., 2011). E: Obliquity curve from La2004 orbital solution (Laskar et al., 2004). F: Eccentricity, tilt and precession (ETP) curve. G: Benthic $\delta^{18}O$ in Montemayor-1 core. H: Global sea-level curves of Hardenbol el al. (1998) (light blue) and Miller et al. (2005), as well as the 4th order eustatic cycles of Esteban et al. (1996) (purple). Age of the MSC onset (5.96 ± 0.02 Ma) and termination (5.52 Ma) indicated with vertical lines.

The sea-level drop lasted ~17 kyr in the Montemayor-1 core and occurred at an average rate of 13.4 mm/yr. Backstripping analysis shows that after a long-term tectonic stability during early Messinian, there is an uplifting trend from the MSC (5.99 Ma) to the TG20 glacial stage (5.75 Ma) (Fig. 6.4). This time interval is limited by two pulses of tectonic rising with average values of 25.5 mm/yr at the base and 17.2 mm/yr at the top. They are unlikely high and probably exaggerated due to the global sea-level changes used in the analysis (Miller et al., 2005), which indicate corresponding sea-level drops of 40 m and 16.8 m. However, our data show sea-level falls of 227 m and 169 m respectively (Pérez-Asensio et al., 2012a). Eliminating these two pulses, the resulting average uplifting rate is 0.5 mm/yr, close to the estimation of Braga et al. (2003), 0.2 mm/yr, for the Late Neogene uplift of the Betic Cordillera. The critical uplift rate that would cause the complete isolation of the Mediterranean is ca. 5 mm/yr (García-Castellanos and Villaseñor, 2011). Sedimentation rate in Montemayor-1 core at the time of the MSC onset is 14.8 cm/kyr (Fig. 6.2). Even considering the highest possible tectonic uplift (5 mm/yr) plus the sedimentation rate (0.148 mm/yr), summing up 5.2 mm/yr, the observed sea-level drop is still fast (13.4 mm/yr). Therefore, although tectonic uplift occurred, the combined effect of tectonism and sedimentation rate played subordinate roles in the MSC initiation.

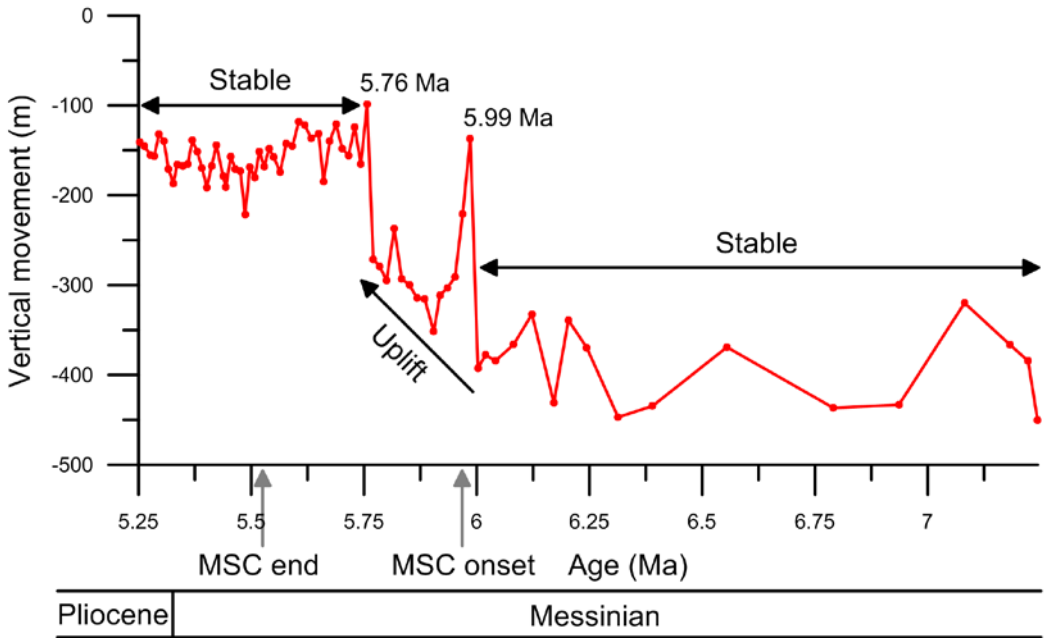

Figure 6.4. Estimation of the vertical movement of the basement in meters obtained by backstripping analysis.

6.3.2. Closing the MSC

It is conventionally alleged that the Upper Evaporites deposition took place from 5.50 Ma to 5.33 Ma (Miocene/Pliocene boundary) (Krijgsman et al., 1999b). These deposits have been assumed coetaneous with the brackish-freshwater Lago-Mare deposits, implying a complete disconnection of the Mediterranean (Krijgsman et al., 1999b). This hypothesis contrasts with the proposal that fully marine post-evaporitic sediments formed in marginal basins of SE Spain during the late Messinian (Riding et al., 1998; Braga et al., 2006). Geomorphologic features of late Messinian drainage systems in the western Mediterranean also point to a flooding before the Miocene/Pliocene boundary (Estrada et al., 2011; García et al., 2011).

Our results reveal a shift of 1‰ and 0.7‰ in $\delta^{18}O$ of planktonic and benthic foraminifera, respectively, from the glacial stage TG12 (5.55 Ma) to the interglacial TG11 (5.52 Ma) that correlate with a global sea level rise (Figs. 6.3 and DR3). Eccentricity and ETP curves increase (Fig. 6.3) supporting a glacioeustatic control of this isotopic shift. The same trend is recorded in the Atlantic and Pacific oceans (Shackleton et al., 1995; Vidal et al., 2002) (Fig. DR3), and is related to a period of global warming that persisted until the mid Pliocene (Vidal et al., 2002). Global sea level rise during the TG12-TG11 transition is ~75 m (Miller et al., 2005), close to our estimation of 68.3 m (Pérez-Asensio et al., 2012a) (Fig. 6.3). Backstripping analysis shows a tectonic stable period during the late Messinian (Fig. 6.4), suggesting that tectonism in the vicinity of the Gibraltar Arc was insignificant. Therefore, we propose that the glacioeustatic sea level rise at TG11 could have triggered the western Mediterranean flooding shortly before the Miocene/Pliocene boundary. This agrees with the idea that a small connection to the Atlantic was enough to a fast reinundation of the Mediterranean (Meijer and Krijgsman, 2005) and with the presence of upper Messinian marine deposits in western Mediterranean marginal basins (Riding et al., 1998; Braga et al., 2006).

It is assumed that Atlantic waters flooded into the Mediterranean through the Gibraltar Strait (Blanc, 2002; Meijer and Krijgsman, 2005; Estrada et al., 2011). In such a case, cold Atlantic waters would enter the Mediterranean (Martín et al., 2010). However, photozoan carbonates developed at the uppermost Messinian deposits in SE Spain (Braga et al., 2006). To accommodate this finding we postulate a two-step flooding process: 1) The west-central Mediterranean was inundated during the TG11

glacioeustatic sea level rise. Warm Atlantic waters entered the Mediterranean from more meridional latitudes than Gibraltar Strait, probably through Rifian Corridors, promoting the formation of coral reefs in SE Spain (Martín et al., 2010). Messinian canyons excavated at NW Morocco shelf might account for this first inundation (Loget and van den Driessche, 2006). 2) Water loading due to this initial flooding caused subsidence of the western Mediterranean basin. This accelerated regressive fluvial erosion in the Gibraltar isthmus (Blanc, 2002; Loget and van den Driessche, 2006) to attain its complete opening due to overflow of Atlantic waters during the early Zanclean. This second stage would lead to the catastrophic flow of more northern-derived and cooler Atlantic waters through the Gibraltar Strait (Martín et al., 2010) filling up the entire Mediterranean Basin.

6.4. Conclusions

Our results prove that glacioeustasy accounts for the initiation (5.96 Ma) and the end (5.52 Ma) of the MSC, with negligible contribution of tectonics in the Gibraltar Arc area. We postulate a two-steps flooding of the Mediterranean: 1) Atlantic waters entering western-central Mediterranean through Rifian Corridors during the stage TG11 (5.52 Ma). 2) Intensification of regressive fluvial erosion in the Gibraltar threshold during the earliest Pliocene led to the opening of the Gibraltar Strait and complete refilling of the Mediterranean.

Acknowledgments

This work is part of the projects CGL2010-20857 and CGL2009-11539, and the Research Group RNM-190. JNPA was funded by a F.P.U. grant (ref. AP2007-00345). We acknowledge Dr. Kotthoff for his comments on an early draft. We also thank N. Andersen (Leibniz-Laboratory, Kiel, Germany) for stable isotope analyses.

DATA REPOSITORY

Age model

The age model of the core is based on magnetobiostratigraphy and O stable isotope data. Magnetostratigraphy chronology is established using the ATNTS2004 (Lourens et al., 2004). Biostratigraphy is based on the planktonic foraminiferal events of Sierro et al., (1993) and first occurrence of *Globorotalia puncticulata*. In the lower part of the core, eight magnetic reversal boundaries, from chron C3Br.2r to chron C3An.1n, are used as tie points. Within the long reversal magnetic chron C3r, there are no biostratigraphic data to define the age model. Thus, this time interval has been calibrated using a combination of the $\delta^{18}O$ foraminifera record of the Montemayor-1 core (Fig. DR1) and the obliquity curve from the orbital solution (Fig. DR2). The correlation between these two datasets permits to accurately identify several glacial-interglacial TG stages, such as the glacial stages TG22, TG20, TG12 and TG4, as well as the interglacial stages TG11 and TG7, to constraint the time frame (Figs. DR1 and DR2).

Stages TG22 and TG20 are two distinctive maxima at the end of an increasing trend in the $\delta^{18}O$ benthic foraminifera record. The cycle TG12-TG11 represents an important $\delta^{18}O$ decrease that correlates with the major global warming and sea-level rise during the late Messinian. Both the TG22-TG20 couple and the TG12-TG11 isotopic shift have been globally observed, including the Pacific Ocean and the Atlantic Ocean (Fig. DR3). Finally, TG7 and TG4 can be confidently recognized by counting glacial-interglacial stages from TG12 onwards when comparing the TG stages, as named in the Rifian corridor by van der Laan et al. (2005, 2006) and the La2004 orbital solution curve (Fig. DR2).

We have used the astronomically calibrated ages of the TG22 (5.79 Ma), TG12 (5.55 Ma) (Krijgsman et al., 2004) and TG7 (5.36 Ma) (van der Laan et al., 2006) to tighten the age model (Fig. DR2).

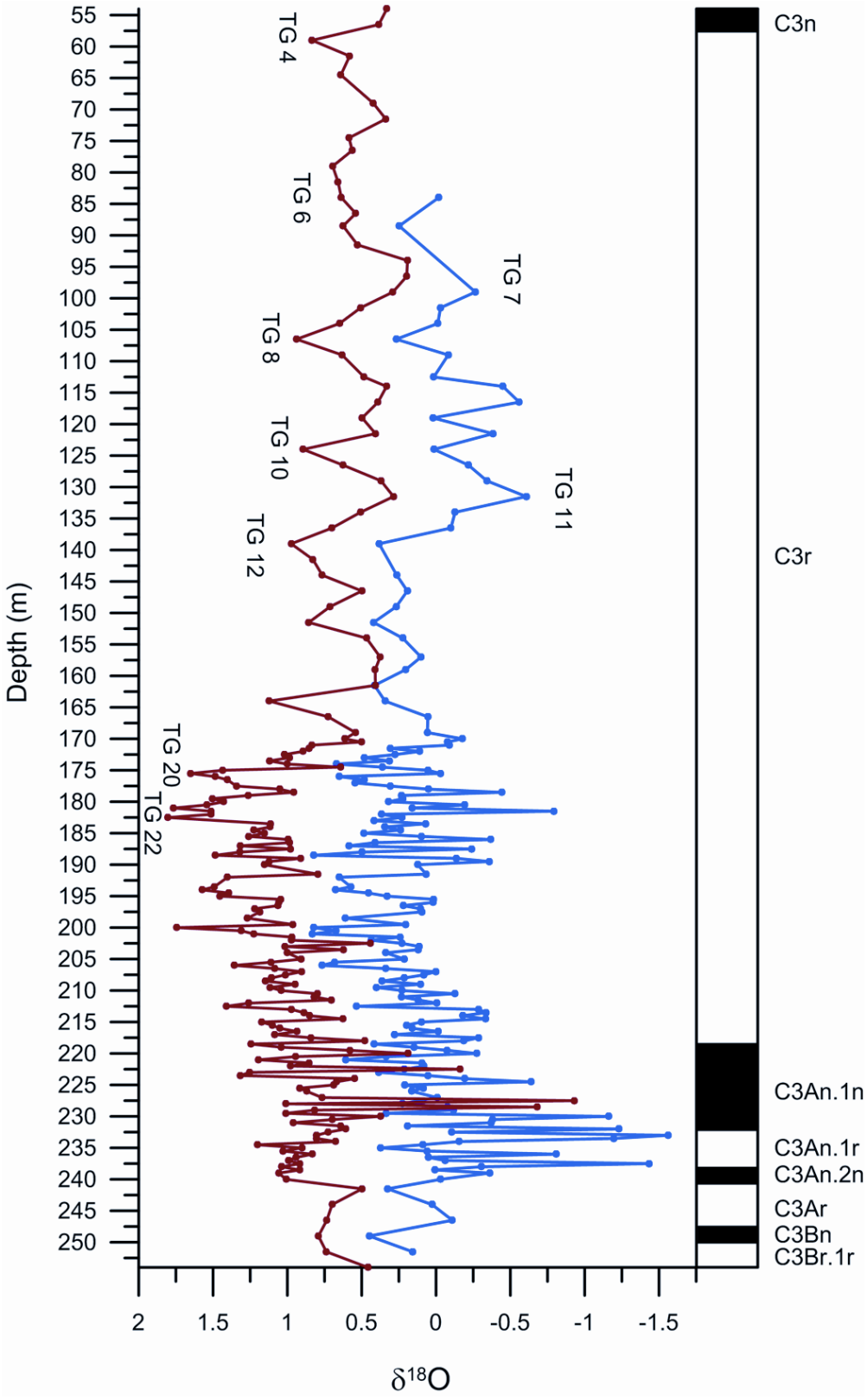

Figure DR1. Benthic (red) and planktonic (blue) foraminiferal oxygen isotope records and magnetostratigraphic reversal boundaries from the Montemayor-1 core *versus* core depth with indication of some of the TG stages used for time constraint.

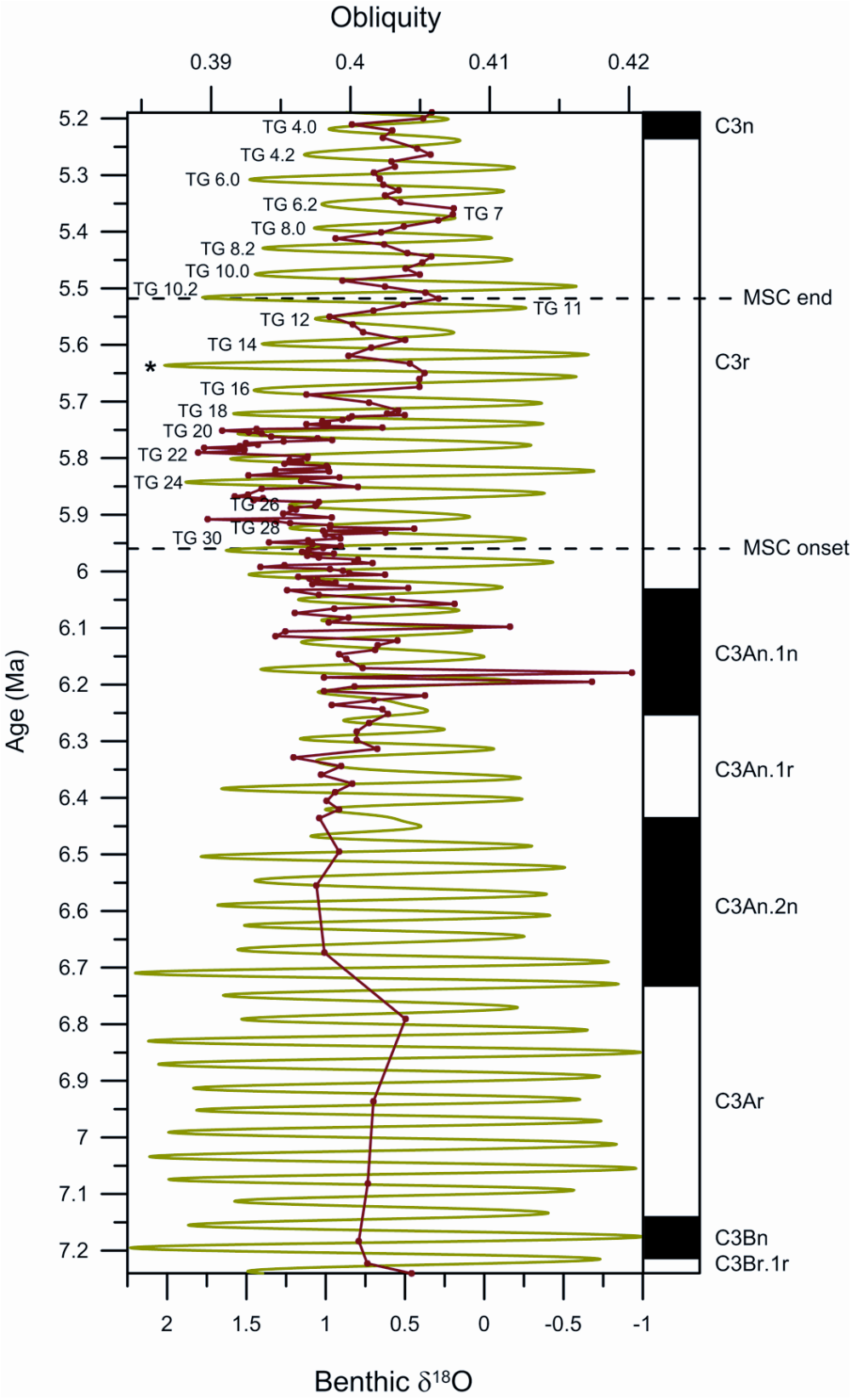

Figure DR2. Benthic oxygen isotope record (red) from the Montemayor-1 and obliquity (green) from La2004 orbital solution *versus* time. TG nomenclature follows Shackleton et al. (1995) and van der Laan et al. (2005, 2006). Horizontal dashed lines mark the ages of the beginning and the end of the MSC.

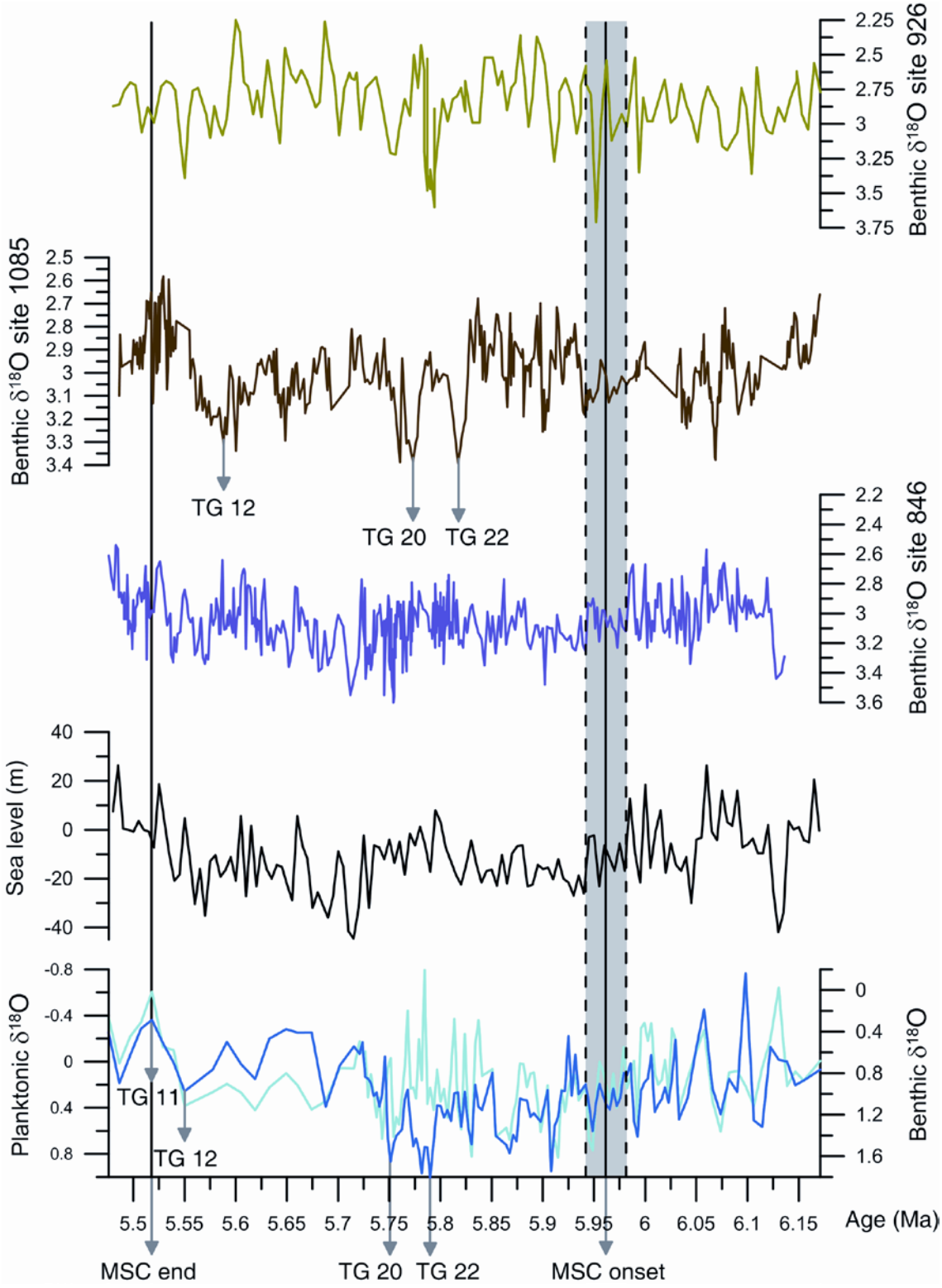

Figure DR3. Benthic (dark blue) and planktonic (light blue) foraminiferal O isotope records from the Montemayor-1 core (lowermost curves) compared with benthic $\delta^{18}O$ records from Site 846 in the Pacific Ocean, as well as Sites 1085 and 926 in the Atlantic Ocean, and global sea level curve (Miller et al., 2005). Age of the MSC onset and termination are indicated with the vertical lines.

CHAPTER 7

CHAPTER 7

MESSINIAN HISTORY OF THE LOWER GUADALQUIVIR BASIN

The Montemayor-1 core in the northwestern margin of the lower Guadalquivir Basin covers a marine sedimentary record that ranges from the latest Tortonian (C3Br.2r, ca. 7.4 Ma) to the lower Pliocene (Zanclean, C3n/C2Ar boundary, ca. 4.3-4.2 Ma) (Larrasoaña et al., 2008). The core was accurately dated using magnetostratigraphy, biostratigraphy and oxygen isotope stratigraphy. According to the age model established for the core, the entire Messinian is recorded. Consequently, it includes marine sediments that were deposited in the Atlantic Ocean before, during and after the Messinian salinity crisis (MSC). In addition, the sedimentation rate of the core is high during the Messinian presenting a very high resolution. Therefore, the Montemayor-1 core is exceptional to precisely analyse the MSC from an Atlantic perspective where there were neither desiccation nor evaporite deposition that could hamper the study of this crucial geological event of the recent history of the Earth.

7.1. Paleoenvironmental evolution

The late Miocene-early Pliocene paleoenvironmental evolution of the lower Guadalquivir Basin can be assessed based on benthic foraminiferal assemblages of the Montemayor-1 core (Pérez-Asensio et al., 2012a) (Fig. 7.1). The dominance of the *Nonion fabum* assemblage in the basal part of the Montemayor-1 core indicates an inner-middle shelf setting during the latest Tortonian. This assemblage presents a very low diversity and dominance of intermediate infaunal taxa, characteristics of eutrophic conditions with high supply of organic matter and low oxygenation. The most likely food source might be continental degraded organic matter supplied by river run-off.

During the latest Tortonian-earliest Messinian, the inner-middle shelf *Nonion fabum* assemblage is replaced by the *Cibicidoides pachyderma* assemblage and then by the *Uvigerina peregrina* s.l. and *Anomalinoides flinti* assemblages. This change in the benthic foraminiferal assemblages suggests a sharp sea-level rise from the inner-middle

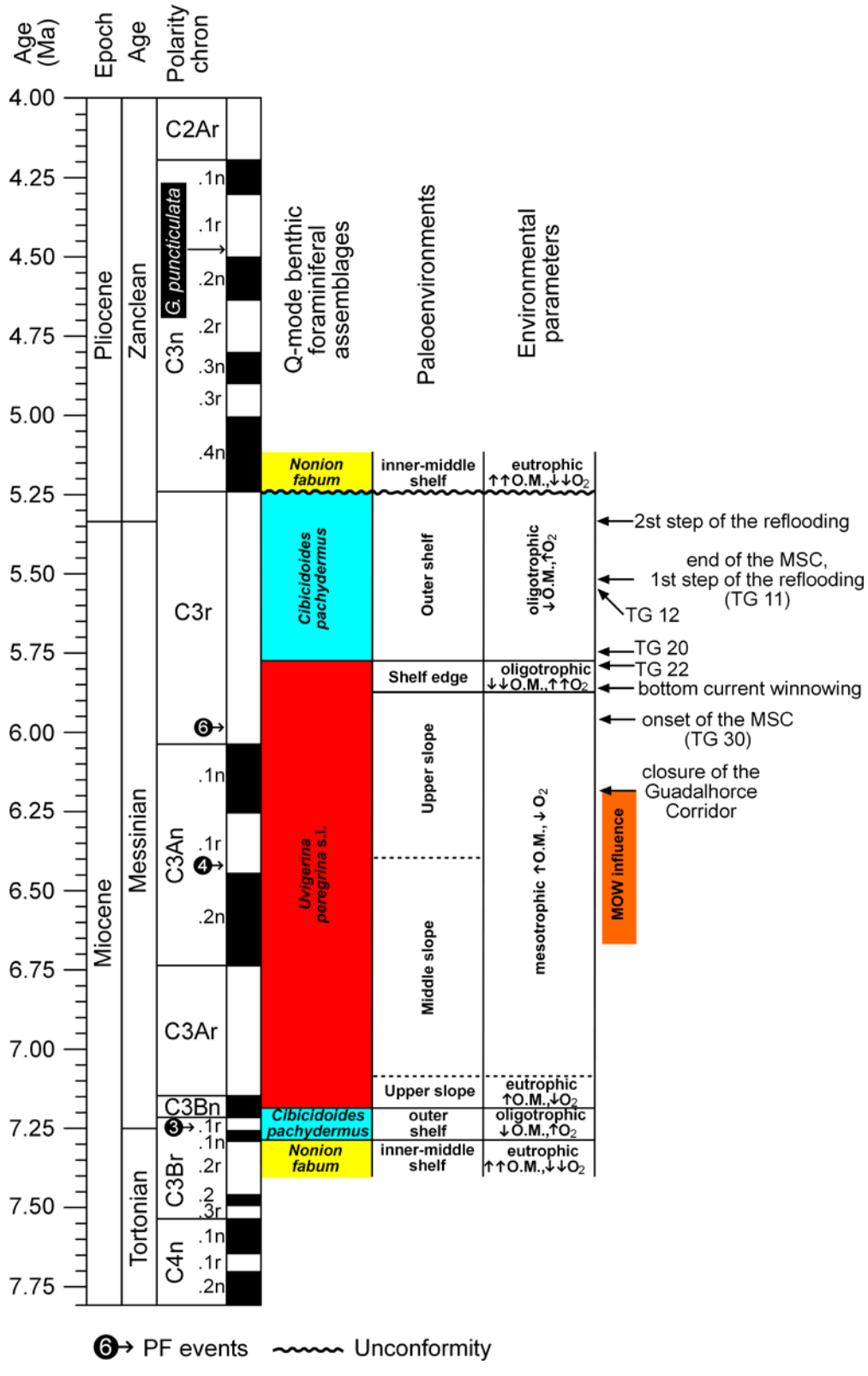

Figure 7.1. Chronology, magnetobiostratigraphic framework, Q-mode benthic foraminiferal assemblages, paleoenviroments, environmental parameters of the Montemayor-1 core. Significant glacial interglacial TG stages, onset and end of the MSC, MOW influence, closure of the Guadalhorce corridor and bottom water winnowing on the shelf edge are indicated as well. Dashed lines indicates uncertainities.

shelf to the upper-middle slope, which is inhabited by *Anomalinoides flinti*, *Siphonina reticulata*, and *Oridorsalis umbonatus*.

Later, the middle slope species disappeared suggesting a sea-level drop from the middle slope to the upper slope during the early Messinian. At this age, the upper slope was inhabited by the *Uvigerina peregrina* s.l. assemblage, which is highly diverse and dominated by shallow infaunal taxa. This paleoenvironment was under mesotrophic conditions with moderate oxygenation. Furthermore, the *Uvigerina peregrina* s.l. assemblage indicates influence of marine fresh organic matter related to upwelling currents. In the upper slope, glacioeustatic fluctuations controlled the productivity (Pérez-Asensio et al., in prep. 1). Glacial periods are characterised by high productivity related to upwelling currents. In the eastern South Atlantic Ocean and the western North Atlantic, increased abundance of *U. peregrina* s.l. indicating high productivity is also recorded during glacial periods in the Quaternary (Schmiedl and Mackensen, 1997; Poli et al., 2010). The presence of poor-ventilated nutrient-rich deep waters, i.e. upwelling currents, is supported by low benthic and planktic $\delta^{13}C$ (Pérez-Asensio et al., in prep. 1). The driving mechanism for intense upwelling in the study area might be strong winds during glacial conditions fostering Ekman pumping, as occurred in the Quaternary (Lebreiro et al., 1997; Salgueiro et al., 2010). In contrast, the productivity was lower during interglacial periods because of the low abundance of *U. peregrina* s.l. (Pérez-Asensio et al., in prep. 1). Nevertheless, there is some marine organic matter on the upper slope during interglacials as it is recorded by increased numbers of *Bulimina subulata*. This species feeds from degraded organic matter that is available on the seafloor after upwelling events (Pérez-Asensio et al., in prep. 1).

During the late Messinian, sea-level continued falling from the upper slope to the shelf edge and outer shelf. The shelf edge is characterised by the dominance of the low diverse *Cibicidoides pachyderma* assemblage, high abundance of epifaunal-shallow infaunal taxa and the highest abundance of epifaunal taxa. This suggests a particularly oligotrophic environment with very low input of organic matter and the highest oxygenation. Significantly high planktic $\delta^{13}C$ also support low productivity at the shelf edge. Paradoxically, oligotrophic conditions at the shelf edge coincide with a glacial period. A possible explanation might be the presence of a bottom current preventing the nutrient-rich upwelling waters from reaching the shelf edge (Pérez-Asensio et al., in prep. 1). In general, the outer shelf was an oligotrophic well-oxygenated setting dominated by the *Cibicidoides pachyderma* assemblage and epifaunal shallow infaunal

taxa. However, the outer shelf had some input of both marine and continental organic matter. Under glacial conditions, marine fresh organic matter was supplied by upwelling currents as it is indicated by the presence of *Uvigerina peregrina* s.l.. On the contrary, high abundance of *Brizalina spathulata* and *Bulimina aculeata* reveal high supply of continental degraded organic matter derived from river run-off during wet and warm interglacial periods. Low planktic and benthic $\delta^{13}C$ and $\delta^{18}O$ are consistent with presence of terrestrial degraded organic matter during interglacial periods (Pérez-Asensio et al., in prep. 1). This is particularly evident during the interglacial stage TG 11 when there was a long-term decrease in both $\delta^{13}C$ and $\delta^{18}O$ along with a gradual increase in *B. spathulata*.

Finally, sea-level fell abruptly from the outer shelf to the inner-middle shelf close to the Miocene-Pliocene boundary. As in the latest Tortonian, the inner-middle shelf was inhabited by the *N. fabum* assemblage pointing to an eutrophic environment with low oxygenation and high supply of terrestrial degraded organic matter provided by riverine discharge during the early Pliocene.

7.2. Paleoceanography

The Montemayor-1 core is located in front of the Guadalhorce Corridor, the last Betic corridor to be closed. According to the siphon model of Benson et al. (1991), the Mediterranean Outflow Water (MOW) entered the Atlantic through the Betic corridors during the Messinian. Therefore, the core is exceptionally well suited for detecting the MOW in the Atlantic Ocean, and recording paleoceanographic and paleoproductivity changes in the northeastern Atlantic before and after the MOW interruption. Middle-upper slope marine sediments of the Montemayor-1 core recorded influence of the MOW during the early Messinian when the Guadalhorce corridor was open (Pérez-Asensio et al., 2012b) (Fig. 7.1). At this age, the MOW maintained the North Atlantic Deep Water (NADW) promoting a strong Atlantic meridional overturning circulation (AMOC) (Reid, 1979; Rahmstorf, 1998; Bigg and Wadley, 2001; Bigg et al., 2003). The presence of the oligotrophic well-ventilated MOW is reflected by constant benthic $\delta^{18}O$ values that depart from the global O isotopic trend, high benthic $\delta^{13}C$ and low abundance of *U. peregrina* s.l. (Pérez-Asensio et al., 2012b, in prep. 1). Apart from the MOW, the Montemayor-1 core also recorded the influence of poorly ventilated nutrient-

rich Atlantic Upwelled Waters (AUW) as it is indicated by low benthic $\delta^{13}C$ and high abundance of *U. peregrina* s.l..

After the closure of the Guadalhorce Corridor at 6.18 Ma, the reduction and eventual interruption of the MOW when the Rifian Corridors were closed could have had a strong impact on the NADW, AMOC, global climate and paleoproductivity (Pérez-Asensio et al., 2012b, in prep. 1). The cessation of the MOW would reduce the AMOC as it is supported by the diminished NADW production in the South Atlantic between 6.0 and 5.5 Ma (Billups, 2002) and low benthic $\delta^{13}C$ in the Montemayor-1 core after 6.18 Ma (Pérez-Asensio et al., in prep. 1). This event would affect the global thermohaline circulation and global climate because a week AMOC due to the interruption of the MOW would lead to northern hemisphere cooling (Clark et al., 2002; Pérez-Asensio et al. 2012b). Concomitantly, ice sheets were developed in the northern hemisphere as a result of this cooling (Fronval and Jansen, 1996; Thiede et al., 1998). This glacial conditions produced by a weak AMOC would promote, in turn, stronger winds that induced upwelling (Lebreiro et al., 1997; Zahn et al., 1997; Clark et al., 2002; Salgueiro et al., 2010). The gradual decrease in benthic and planktic $\delta^{13}C$ and progressive increase of *U. peregrina* s.l. after 6.18 Ma reflect high productivity in the study area as a result of the glacial conditions favored by the MOW interruption (Pérez-Asensio et al., in prep. 1).

The closure of the Guadalhorce Corridor was a critical event for the onset of the MSC in the Mediterranean Sea. After this event, the Atlantic-Mediterranean water mass exchange was restricted to the Rifian corridors (Esteban et al., 1996). Consequently, the restriction of the Atlantic-Mediterranean exchange produced a blockage of deep-water outflow inducing water-mass stratification with sluggish deep water circulation, low oxygenation and rising salinities in the Mediterranean (Kouwenhoven et al., 1999, 2006; Kouwenhoven and van der Zwaan, 2006). These gradually stressing conditions due to the restriction of the Atlantic-Mediterranean exchange are recorded by benthic foraminifera from the Mediterranean (Kouwenhoven et al., 2006).

The Atlantic-Mediterranean exchange was restored after the opening of the Strait of Gibraltar increasing the NADW production around the Miocene-Pliocene boundary as it is recorded in the South Atlantic and the western equatorial Atlantic Ocean (King et al., 1997; Billups, 2002). A higher NADW production might have promoted a stronger AMOC as occur during interglacial periods in the Holocene and Pleistocene (Broecker et al., 1985).

7.3. Onset and cessation of the MSC

The remarkable data obtained from the continuous Montemayor-1 core has allowed to unravel the main Messinian events out of the complex stratigraphic framework of the Mediterranean because the Atlantic sedimentary record of the core was not affected by evaporite deposition (Pérez-Asensio et al., in prep. 2). Here, a comprehensive explanation for the causes that isolated the Mediterranean from the Atlantic triggering the evaporite deposition is provided. Results from the Montemayor-1 core allow for the first time to decipher the contribution of glacioeustatic sea-level fall and regional tectonic uplifting in the Gibraltar Arc area to the onset of the MSC. All proxies recorded at the time of the initiation of the MSC suggest that glacioeustatic sea level fall had a major contribution, while regional tectonic uplift in the Arc of Gibraltar was negligible.

The proposed causes and timing for the end of the MSC has also puzzled Earth Scientists for decades, and they are still controversial. Some authors suggest that the MSC ends with the reflooding of the Mediterranean at the base of the Pliocene (e.g. Krijgsman et al., 1999b; Hilgen et al., 2007), whereas others claim that the reflooding had already started in the latest Messinian (e.g. Martín and Braga, 1994; Riding et al., 1998). The new data obtained from the Montemayor-1 core clearly show that the marine re-filling of the Mediterranean already started in the latest Messinian coinciding with the interglacial stage TG 11 and a period of tectonic stability. Further, it is postulated that this process took place in two steps, one during the latest Messinian and the other during the lowermost Pliocene (Pérez-Asensio et al. in prep. 2) (Fig. 7.1). This is consistent with the presence of fully marine post-evaporitic sediments in the satellite basins of SE Spain and the central Mediterranean during the late Messinian (Martín and Braga, 1994; Riding et al., 1998; Aguirre and Sánchez-Almazo, Braga et al., 2006; Carnevale et al., 2006a, 2006 b, 2008). This pre-Pliocene flooding is also supported by the geomorphology of the late Messinian drainage systems in the western Mediterranean (Estrada et al., 2011; García et al., 2011). Furthermore, the presence of photozoan carbonates at the uppermost Messinian sediments in basin from SE Spain indicates the influence of warm waters (Braga et al., 2006; Martín et al., 2010). To explain theses findings, a novel two-step re-flooding process is proposed: 1) inflow of warm waters through the Rifian corridors during interglacial stage TG 11 (5.52 Ma), not through the Strait of Gibraltar as previously thought (Blanc, 2002; Meijer and

Krijgsman, 2005; Estrada et al., 2011; Bache et al., 2012). This first step fostered the development of coral reefs in SE Spain (Martín et al., 2010), and it is recorded in the canyons excavated at NW Morocco shelf (Loget and van den Driessche, 2006). 2) The first flooding would provoke water loading that might have increased the subsidence of the westernmost basin floor. This event would accelerate the regressive fluvial erosion in the Gibraltar Arc (Blanc, 2002; Loget et al., 2005; Loget and van den Driessche, 2006) until the Strait of Gibraltar was completely open during the early Zanclean. Then, cool waters from the northern Atlantic that entered through the Strait of Gibraltar would have re-filled the whole Mediterranean basin during the earliest Pliocene. This favored the deposition of heterozoan carbonates in the Mediterranean continental shelves during a period of rising global temperatures (Martín et al., 2010). An alternative model proposes that the entire Mediterranean was re-flooded trough the Strait of Gibraltar during TG 11 in two steps: step I (5.56?–5.46 Ma): a relatively moderate and slow sea-level rise as a result of the beginning of a progressively increasing erosion of the Gibraltar isthmus; and step II (5.46 Ma): a particularly sudden and dramatic flooding due to the collapse of Gibraltar channel (Bache et al., 2009, 2012). However, as mentioned before the presence of coral reefs in the western Mediterranean indicate that warm Atlantic waters would have entered into the Mediterranean from more southern paths, most likely through the Rifian Corridors. Therefore, timing and processes proposed by Bache et al. (2009, 2012) for the two-step re-filling of the Mediterranean are improbable since they do not fit the evidences.

CHAPTER 8

CHAPTER 8

CONCLUSIONS

1) The paleoenvironmental evolution and paleoceanographic changes during the late Miocene-early Pliocene of the lower Gualdalquivir Basin have been studied based on benthic foraminiferal assemblages and stable isotopes (O and C) from the Montemayor-1 core (SW Spain). Data show a complete upward transgressive-regressive sea-level cycle. Furthermore, the distribution, composition, diversity and microhabitat preferences of the benthic foraminiferal assemblages were controlled by the trophic conditions, specifically the quantity and quality of the organic-mater flux to the sea floor.

2) Deposits of the Montemayor-1 core were accurately dated based on magnetostratigraphy, biostratigraphy and stable oxygen isotope stratigraphy.

3) The studied core is close to the last Betic gateway to be closed, the Guadalhorce Corridor. According to the age model, this seaway was closed at 6.18 Ma. The presence of the Mediterranean outflow waters (MOW) before 6.18 Ma in the lower Guadalquivir area supports the siphon model of Benson et al. (1991) with Mediterranean outflow through the Betic Corridors and Atlantic influx through the Rifian Corridors.

4) The interruption of the MOW after the closure of the Guadalhorce Corridor might have decreased the North Atlantic deep waters (NADW) weakening the Atlantic meridional overturning circulation (AMOC) from 6.0 to 5.5 Ma. This would have promoted cooling in the northern hemisphere favouring a high primary productivity in the northeastern Atlantic.

5) Global glacioeustatic fluctuations controlled the paleoproductivity and organic carbon cycling in the northeastern Atlantic during the Messinian. High productivity due to intense upwelling currents that were induced by strong winds is recorded during glacial periods. Furthermore, poor bottom-water ventilation due to a week AMOC is evidenced by low benthic $\delta^{13}C$ during glacial conditions. In the interglacial periods, productivity was related to degraded organic matter after upwelling events in the upper slope and input of degraded continental organic matter from riverine

discharge in the outer shelf. In addition, high benthic $\delta^{13}C$ suggests well-ventilated bottom waters produced by a strong AMOC during interglacial periods.

6) A model for the onset and end of the MSC is established. The initiation of the MSC was principally produced by a glacioeustatic sea-level lowering with only a minor contribution of tectonic uplift. The reflooding of the Mediterranean took place in two steps during a period of tectonic stability, thus glacioeustacy forced the re-filling. Firstly, relatively warm Atlantic water flowed, at least into the western-central Mediterranean, most likely through the Rifian Corridors during the glacioeustatic sea-level rise associated to the interglacial stage TG 11 (5.52 Ma). Secondly, cold water refilled the entire Mediterranean through the Strait of Gibraltar during the earliest Pliocene.

CONCLUSIONES

1) La evolución paleoambiental y los cambios paleoceanográficos durante el Mioceno tardío-Plioceno temprano de la Cuenca del bajo Guadalquivir han sido estudiados a partir de las asociaciones de foraminíferos bentónicos y los isótopos estables (O y C) del testigo de Montemayor-1 (SO de España). Los datos muestran un ciclo de nivel del mar transgresivo-regresivo completo hacia techo. Además, la distribución, composición, diversidad y preferencias de microhábitats de las asociaciones de foraminíferos bentónicos estaban controladas por las condiciones tróficas, específicamente la cantidad y calidad del flujo de materia orgánica que alcanzaba el fondo del mar.

2) Los depósitos del testigo de Montemayor-1 han sido datados con precisión a partir de la magnetoestratigrafía, bioestratigrafía y estratigrafía de isótopos de oxígeno del testigo.

3) El testigo estudiado se sitúa cerca del último corredor Bético que se cerró, el Corredor del Guadalhorce. Según el modelo de edad, este corredor se cerró hace 6,18 millones de años. La presencia de la corriente de salida del Mediterráneo (MOW) antes de 6,18 millones de años en el área del bajo Guadalquivir apoya el modelo sifón de Benson et al., (1991) con corriente de salida del Mediterráneo a través de los Corredores Béticos y entrada de aguas del Atlántico a través de los Corredores Rifeños.

4) La interrupción de la MOW después del cierre del Corredor del Guadalhorce podría haber disminuido la formación de agua profunda del Atlántico Norte (NADW) debilitando la circulación termohalina meridional del Atlántico (AMOC) entre 6,0 y 5,5 millones de años. Esto habría fomentado el enfriamiento del hemisferio norte favoreciendo una alta productividad primaria en el Atlántico nororiental.

5) Las fluctuaciones glacioeustáticas controlaron la paleoproductividad en el Atlántico nororiental durante el Messiniense. Durante los periodos glaciales, se registra una alta productividad debida a corrientes de afloramiento intensas que fueron inducidas por vientos fuertes. Además, valores bajos del $\delta^{13}C$ medido en foraminíferos bentónicos durante periodos glaciales indica que el fondo del mar estaba poco ventilado. En los periodos interglaciales, la productividad estaba asociada a materia orgánica degradada después de eventos de corrientes de afloramiento en el talud superior y aporte de materia orgánica continental degradada proporcionada por la descarga fluvial en la plataforma externa. Además, valores altos del $\delta^{13}C$ medido en foraminíferos bentónicos

sugieren que había una buena ventilación del fondo marino producida por una AMOC fuerte durante los periodos interglaciales.

6) En esta tesis se establece un modelo para el comienzo y final de la crisis de salinidad del Messiniense en el Mediterráneo (CSM). El inicio de la CSM se produjo principalmente por una bajada del nivel del mar glacioeustática con sólo una contribución menor del levantamiento tectónico. La reinundación del mediterráneo tuvo lugar en dos pasos durante un periodo de estabilidad tectónica, por lo tanto el glacieustatismo forzó la reinundación. En primer lugar, aguas relativamente cálidas del Atlántico fluyeron, al menos en el Mediterráneo occidental-central, probablemente a través de los Corredores Rifeños durante una elevación del nivel de mar glacioeustática asociada al estadío interglacial TG 11 (5,52 millones de años). En segundo lugar, aguas frías del Atlántico rellenaron todo el Mediterráneo a través del Estrecho de Gibraltar durante la primera parte del Plioceno temprano.

CHAPTER 9

CHAPTER 9

FUTURE PERSPECTIVES

The results of this PhD thesis have improved our understanding about paleoenvironmental, paleoproductivity and paleoceanographic changes in the lower Guadalquivir Basin and the northeastern Atlantic during the Messinian, and its relationship with global climate. Furthermore, it has been clarified the contribution of global glacioeustatic processes and regional tectonic uplifting to the onset and end of the MSC in the Mediterranean. Some of the new findings of this PhD thesis will surely pushed future research on Messinian paleoceanography and paleoclimate. For example, the Messinian impact of the Mediterranean Outflow Water (MOW) on the eastern Atlantic circulation and global climate and paleoproductivity has been analysed for the first time. In the future, the knowledge about the spatial and temporal distribution of the MOW during the Messinian might be improved with a multidisciplinary approach including sedimentology, geochemistry and micropaleontology. Particularly, the use of paleothermometers such as the Mg/Ca ratio measured on foraminiferal shells and Nd isotopes could be critical to trace the MOW in the past. This technique has shown excellent results for studying the MOW during the Pliocene (Khélifi et al., 2009). The MOW has also been recorded in the Messinian using Pb and Nd isotopes (Abouchami et al., 1999). Sedimentary analyses are also very important to record the MOW and to assess its intensity. An extraordinary example is the study of contourites in the Gulf of Cádiz for the Pliocene-Quaternary (e.g. Hernández-Molina et al., 2006, 2011; Toucanne et al., 2007; Llavé et al., 2007, 2011). The same methodology for studying recent contourites could be applied to the Messinian records. A key issue to know better the spatial and temporal distribution of the MOW is to analysed different locations for the same time interval, and if it is possible locations with different paleobathymetries for the same time lapse. This will help to establish a reliable distribution pattern for the MOW in the lower Guadalquivir Basin as well as northeastern Atlantic during the Messinian.

Once temporal and spatial distribution of the MOW is studied in detail, the impact of the MOW on global climate, paleoceanography and paleoproductivity might

be tested comparing simulations made by modelling analyses and the Messinian oceanic records from the Atlantic. This would be essential to check the validity of modelling analyses. Moreover, the study of MOW during the Messinian both on the Betic and Rifian corridors might improve the lack of knowledge about the models of Atlantic-Mediterranean water mass exchange during the Messinian. For this purpose, complete Messinian records should be studied in the Atlantic and Mediterranean sides of the Betic and Rifian corridors.

In addition, it would be very interesting to perform cyclostratigraphic studies on high resolution, continuous, accurately dated Messinian sedimentary records from the Atlantic like the Montemayor-1 core. These studies might be useful to analyse global paleoclimatic changes and to separate global and local processes. Cyclostratigraphic analyses have been performed in Pliocene sediments from the northeastern Atlantic both on SW Spain and NW Morocco (Sierro et al., 2000; van der Laan et al., 2006). However, Messinian cyclostratigraphy of sediments from the northeastern Atlantic was only studied close to the Rifian corridors (van der Laan et al., 2005, 2012). Therefore, further research is needed to establish the cyclostratigraphy of the Atlantic side of the Betic corridors during the Messinian, and to compare these new results with those from the Rifian corridors.

Finally, the novel model for the initiation and end of the MSC proposed in this PhD thesis that try to separate the contribution of glacioeustatic fluctuations and tectonic activity needs to be tested in other locations. Future research on this topic could reinforce or refute this model.

References

Abouchami, W., Galer, S.J.G., Koschinsky, A., 1999. Pb and Nd isotopes in NE Atlantic Fe–Mn crusts: proxies for trace metal paleosources and paleocean circulation. Geochimica et Cosmochimica Acta 63, 1489–1505.

Abrantes, F. 1991.Variability of upwelling off NW Africa during the latest Quaternary: Diatom evidence. Paleoceanography 6, 431−460.

Abrantes, F., 2000. 200000 yr diatom records from Atlantic upwelling sites reveal maximum productivity during LGM and a shift in phytoplankton community structure at 185000 yr. Earth and Planetary Science Letters 176, 7–16.

Aguirre, J., 1992. Evolución de las asociaciones fósiles del Plioceno marino de Cabo Roche (Cádiz). Revista Española de Paleontología Extra, 3−10.

Aguirre, J., 1995. Implicaciones paleoambientales y paleogeográficas de dos discontinuidades estratigráficas en los depósitos pliocénicos de Cádiz (SW de España). Revista de la Sociedad Geológica de España 8, 161−174.

Aguirre, J., Braga, J.C., Martín, J.M., 1993. Algal nodules in the Upper Pliocene deposits at the coast of Cadiz (S Spain). Bollettino della Società Paleontologica Italiana Special Volume 1, 1−7.

Aguirre, J., Braga, J.C., Martín, J.M., 2007. El Mioceno marino del Prebético occidental (Cordillera Bética, SE de España): historia del cierre del Estrecho Norbético. In: Aguirre, J., Company, M., Rodríguez-Tovar, F.J. (Eds.), XIII Jornadas de la Sociedad Española de Paleontología: Guía de Excursiones. Instituto Geológico y Minero de España-Universidad de Granada, Granada, pp. 53–66.

Aguirre, J., Castillo, C., Férriz, F.J., Agustí, J., Oms, O., 1995. Marine continental magnetobiostratigraphic correlation of the Dolomys subzone (middle of Late Ruscinian): implications for the Late Ruscinian age. Palaeogeography, Palaeoclimatology, Palaeoecology 117, 139–152.

Aguirre, J., Sánchez-Almazo, I.M., 2004. The Messinian post-evaporitic deposits of the Gafares area (Almería-Níjar basin, SE Spain). A new view of the "Lago-Mare" facies. Sedimentary Geology 168, 71–95.

Armstrong, H.A., Brasier, M.D., 2005. Microfossils, second edition. Blackwell Publishing, Oxford.

Arnold, A.J., Parker, W.C., 1999. Biogeography of planktonic foraminifera. In: Sen Gupta, B.K. (Ed.), Modern Foraminifera. Kluwer Academic Publishers, Dordrecht, pp. 103–122.

Baceta, J.I., Pendón, J.G., 1999. Estratigrafía y arquitectura de facies de la Formación Niebla, Neógeno superior, sector occidental de la Cuenca del Guadalquivir. Revista de la Sociedad Geológica de España 12, 419–438.

Bache, F., Olivet, J.L., Gorini, C., Rabineau, M., Baztan, J., Aslanian, D., Suc, J.-P., 2009. Messinian erosional and salinity crises: view from the Provence Basin (Gulf of Lions, Western Mediterranean). Earth and Planetary Science Letters 286, 139–157.

Bache, F., Popescu, S.-M., Rabineau, M., Gorini, C., Suc, J.-P., Clauzon, G., Olivet, J.-L., Rubino, J.-L., Melinte-Dobrinescu, M.C., Estrada, F., Londeix, L., Armijo, R., Meyer, B., Jolivet, L., Jouannic, G., Leroux, E., Aslanian, D., Dos Reis, A.T., Mocochain, L., Dumurdžanov, N., Zagorchev, I., Lesić, V., Tomić, D., Çağatay, M.N., Brun, J.-P., Sokoutis, D., Csato, I., Ucarkus, G., Çakir, Z., 2012. A two-step process for the reflooding of the Mediterranean after the Messinian Salinity Crisis. Basin Research 24, 125–153.

Bakun, A., Field, D.B., Redondo-Rodriguez, A., Weeks, S.J., 2010. Greenhouse gas, upwelling-favorable winds, and the future of coastal ocean upwelling ecosystems. Global Change Biology 16, 1213–1228.

Báldi, K., Hohenegger, J., 2008. Paleoecology of benthic foraminífera of Baden-Sooss section (Badenian, Middle Miocene, Vienna Basin, Austria). Geologica Carpathica 59, 411–424.

Barbieri, R., 1998. Foraminiferal paleoecology at the Tortonian–Messinian boundary, Atlantic coast of northwestern Morocco. Journal of Foraminiferal Research 28, 102–123.

Barbieri, R., Ori, G.G., 2000. Neogene palaeoenvironmental evolution in the Atlantic side of the Rifian Corridor (Morocco). Palaeogeography, Palaeoclimatology, Palaeoecology 163, 1–31.

Barmawidjaja, D.M., Jorissen, F.J., Puskaric, S., van der Zwaan, G.J., 1992. Microhabitat selection by benthic foraminifera in the northern Adriatic Sea. Journal of Foraminiferal Research 22, 297–317.

Benson, R.H., 1986. Messinian salinity crisis. Encyclopedia of Earth System Science 3, 161–167.

Benson, R.H., Rakic-El Bied, K., Bonaduce, G., 1991. An important current reversal (influx) in the Rifian corridor (Morocco) at the Tortonian–Messinian Boundary: the end of Tethys ocean. Paleoceanography 6, 164–192.

Berggren, W.A., Haq, B.U., 1976. The Andalusian Stage (Late Miocene): biostratigraphy, biochronology and palaeoecology. Palaeogeography, Palaeoclimatology, Palaeoecology 20, 67–129.

Berggren, W.A., Benson, R.H., Haq, B.U., Riedel, W.R., Sanfilippo, A., Schrader, H.J., Tjalsma, R.C., 1976. The El Cuervo Section (Andalusia, Spain): micropaleontologic anatomy of an early Late Miocene lower bathyal deposit. Marine Micropaleontology 1, 195–247.

Bethoux, J.P., Gentili, B., Morin, P., Nicolas, E., Pierre, C., Ruiz-Pino, D., 1999. The Mediterranean Sea: a miniature ocean for climatic and environmental studies and a key for the climatic functioning of the North Atlantic. Progress in Oceanography 44, 131–146.

Betzler, C., Braga, J.C., Martín, J.M., Sánchez-Almazo, I.M., Lindhorst, S., 2006. Closure of a seaway: stratigraphic record and facies (Guadix basin, southern Spain). International Journal of Earth Sciences (Geologische Rundschau) 95, 903–910.

Bigg, G.R., Wadley, M.R., 2001. Millennial-scale variability in the oceans: an ocean modelling view. Journal of Quaternary Science 16, 309–319.

Bigg, G.R., Jickells, T.D., Liss, P.S., Osborn, T.J., 2003. The role of the oceans in climate. International Journal of Climatology 23, 1127–1159.

Billups, K., 2002. Late Miocene through early Pliocene deep water circulation and climate change viewed from the sub-Antarctic South Atlantic. Palaeogeography, Palaeoclimatology, Palaeoecology 185, 287−307.

Blanc, P.-L., 2002. The opening of the of the Plio-Quaternary Gibraltar Strait: assessing the size of a cataclysm. Geodynamica Acta 15, 303–317.

Boggs, S., 2009. Petrology of Sedimentary Rocks. Cambridge University Press, Cambridge.

Boltovskoy, E., Wright, R., 1976. Recent foraminifera. W. Junk, The Hague.

Borsetti, A.M., Curzi, P.V., Landuzzi, V., Mutti, M., Ricci Lucchi, F., Sartori, R., Tomadin, L., Zuffa, G.G., 1990. Messinian and pre-Messinian sediments from OPD Leg 107 sites 652 and 654 in the Tyrrhenian Sea: sedimentologic and petrographic study and possible comparisons with Italian sequences In: Kastens, K.A., Mascle, J., et al., (Eds.), Proceedings of the Ocean Drilling Program, Scientific Results, 107, pp. 169–186.

Braga, J.C., Martín, J.M., 1996. Geometries of reef advance in response to relative sea-level changes in a Messinian (uppermost Miocene) fringing reef (Cariatiz reef, Sorbas Basin, SE Spain). Sedimentary Geology 107, 61–81.

Braga, J.C., Martín, J.M., Aguirre, J., 2002. Tertiary. Southern Spain. In: Gibbons, W., Moreno, T. (Eds.), The Geology of Spain. The Geological Society, London, pp. 320–327.

Braga, J.C., Martín, J.M., Quesada, C., 2003. Patterns and average rates of late Neogene–Recent uplift of the Betic Cordillera, SE Spain. Geomorphology 50, 3–26.

Braga, J.C., Martín, J.M., Riding, R., Aguirre, J., Sánchez-Almazo, I.M., Dinarès-Turell, J., 2006. Testing models for the Messinian salinity crisis: the Messinian record in Almería, SE Spain. Sedimentary Geology 188–189, 131–154.

Braga, J.C., Vescogni, A., Bosellini, F.R., Aguirre, J., 2009. Coralline algae (Corallinales, Rhodophyta) in western and central Mediterranean Messinian reefs. Palaeogeography, Palaeoclimatology, Palaeoecology 275, 113–128.

Braga, J.C., Martín, J.M., Aguirre, J., Baird, C.D., Grunnaleite, I., Jensen, N.B., Puga- Bernabéu, A., Saelen, G., Talbot, M.R., 2010. Middle-Miocene (Serravallian) temperate carbonates in a seaway connecting the Atlantic Ocean and the Mediterranean Sea (North Betic Strait, S Spain). Sedimentary Geology 225, 19–33.

Broecker,W.S., Peteet, D.M., Rind, D., 1985. Does the ocean-atmosphere system have more than one stable mode of operation. Nature 315, 21–26.

Brown, J., Colling, A., Park, D., Phillips, J., Rothery, D., Wrigh, J., 1989. Ocean Circulation. The Open University, Pergamon Press, England.

Bryden, H.L., Stommel, H.M., 1984. Limiting processes that determine basic features of the circulation in the Mediterranean Sea. Oceanologica Acta 7, 289−296.

Butler, R.W.H., Lickorish, W.H., Grasso, M., Pedley, H.M., Ramberti, L., 1995. Tectonics and sequence stratigraphy in Messinian basins, Sicily: constraints on the initiation and termination of the Mediterranean salinity crisis. Geological Society of America Bulletin 107, 425–439.

Butzin, M., Lohmann, G., Bickert, T., 2011. Miocene ocean circulation inferred from marine carbon cycle modeling combined with benthic isotope records. Paleoceanography 26, PA1203, doi:10.1029/2009PA001901.

Cacho, I., Grimalt, J.O., Sierro, F.J., Shackleton, N., Canals, M., 2000. Evidence for enhanced Mediterranean thermohaline circulation during rapid climatic coolings. Earth and Planetary Science Letters 183, 417−429.

Carnevale, G., Caputo, D., Landini, W., 2006a. Late Miocene fish otoliths from the Colombacci Formation (Northern Apennines, Italy): implications for the Messinian 'Lago-mare' event. Geolical Journal 41, 537–555.

Carnevale, G., Landini, W., Sarti, G., 2006b. Mare versus Lago-mare: marine fishes and the Mediterranean environment at the end of the Messinian salinity crisis. Journal of the Geological Society of London 163, 75–80.

Carnevale, G., Longinelli, A., Caputo, D., Barbieri, M., Landini, W., 2008. Did the Mediterranean marine reflooding precede the Mio-Pliocene boundary?. Paleontological and geochemical evidence from upper Messinian sequences of Tuscany, Italy. Palaeogeography Palaeoclimatology Palaeoecology 257, 81–105.

Casford, J.S.L., Rohling, E.J., Abu-Zied, R., Cooke, S., Fontanier, C., Leng, M., Lykousis, V., 2002. Circulation changes and nutrient concentrations in the late Quaternary Aegean Sea: a nonsteady state concept for sapropel formation. Paleoceanography 17, 1024–1034.

Civis, J., Sierro F.J., 1987. Los foraminíferos bentónicos en la sección de Gibraleón (Formación <<Arcillas de Gibraleón>>, Huelva). In: Civis, J. (Ed.), Paleontología del Neógeno de Huelva. Ediciones Universidad de Salamanca, Salamanca, pp. 55–64.

Clark, P.U., Pisias, N.G., Stocker, T.F., Weaver, A.J., 2002. The role of thermohaline circulation in abrupt climate change. Nature 415, 863–869.

Clauzon, G., Suc, J.P., Gautier, F., Berger, A., Loutre, M.F., 1996. Alternative interpretation of the Messinian salinity crisis: controversy resolved? Geology 24, 363–366.

Clauzon, G., Suc, J.P., Popescu, S.M., Marunteanu, M., Rubino, J.L., Marinescu, F., Melinte, M.C., 2005. Influence of Mediterranean sea-level changes on the Dacic Basin (Eastern Paratethys) during the late Neogene: the Mediterranean Lago Mare facies deciphered. Basin Research 17, 437–462.

Corbí, H. (2010). Los foraminíferos de la cuenca neógena del Bajo Segura (sureste de España). Bioestratigrafía y cambios paleoambientales en relación con la Crisis de Salinidad del Mediterráneo. PhD thesis, University of Alicante, Spain.

Cosentino, D., Federici, I., Cipollari, P., Gliozzi, E., 2006. Environments and tectonic instability in central Italy (Garigliano Basin) during the late Messinian Lago-Mare episode: new data from the onshore Mondragone 1 well. Sedimentary Geology 188–189, 297–317.

Cosentino, D., Bertini, A., Cipollari, P., Florindo, F., Gliozzi, E., Grossi, F., Lo Mastro, S., Sprovieri, M., 2012. Orbitally forced paleoenvironmental and paleoclimate changes in the late postevaporitic Messinian of the central Mediterranean Basin. Geological Society of America Bulletin 124, 499–516.

Criado-Aldeanueva, F., García-Lafuente, J., Vargas, J.M., Del Río, J., Vázquez, A., Reul, A., Sánchez, A., 2006. Distribution and circulation of water masses in the Gulf of Cádiz from in situ observations. Deep-Sea Research II 53, 1144–1160.

De Rijk, S., Jorissen, F.J., Rohling, E.J., Troelstra, S.R., 2000. Organic flux control on bathymetric zonation of Mediterranean benthic foraminifera. Marine Micropaleontology 40, 151–166.

Di Stefano, A., Verducci, M., Lirer, F., Ferraro, L., Iaccarino, S.M., Hüsing, S.K., Hilgen, F.J., 2010. Paleoenvironmental conditions preceding the Messinian Salinity Crisis in the Central Mediterranean: Integrated data from the Upper Miocene Trave section (Italy). Palaeogeography, Palaeoclimatology, Palaeoecology 297, 37–53.

Diester-Haass, L., Schrader, H.-J., 1979. Neogene coastal upwelling history off northwest and southwest Africa Marine Geology, 29, 39–53.

Diz, P., Francés, G., 2008. Distribution of live benthic foraminifera in the Ría de Vigo (NW Spain). Marine Micropaleontology 66, 165–191.

Diz, P., Francés, G., Rosón, G., 2006. Effects of contrasting upwelling–downwelling on benthic foraminiferal distribution in the Ría de Vigo (NW Spain). Journal of Marine Systems 60, 1–18.

Donnici, S., Serandrei Barbero, R., 2002. The benthic foraminiferal communities of the northern Adriatic continental shelf. Marine Micropaleontology 44, 93–123.

Duchemin, G., Jorissen, F.J., Le Loc'h, F., Andrieux-Loyer, F., Hily, C., Thouzeau, G., 2008. Seasonal variability of living benthic foraminifera from the outer continental shelf of the Bay of Biscay. Journal of Sea Research 59, 297–319.

Duggen, S., Hoernle, K., van den Bogaard, P., Rüpke, L. Morgan, J.P., 2003. Deep roots of the Messinian salinity crisis. Nature 422, 602–606.

Eberwein, A., Mackensen, A., 2006. Live and dead benthic foraminifera and test δ13C record primary productivity off Morocco (NW-Africa). Deep-Sea Research Part I 53, 1379–1405.

Eberwein, A., Mackensen, A., 2008. Last Glacial Maximum paleoproductivity and water masses off NW-Africa: evidence from benthic foraminifera and stable isotopes. Marine Micropaleontology 67, 87–103.

Einsele, G., 1992. Sedimentary Basins, Evolution, Facies and Sediment Budget. Springer-Verlag, Berlin.

Esteban, M., Braga, J.C., Martín, J.M., Santisteban, C., 1996. Western Mediterranean reef complexes. In: Franseen, E.K., Esteban, M., Ward, W.C., Rouchy, J.M. (Eds.), Models for Carbonate Stratigraphy from Miocene Reef Complexes of Mediterranean Regions. : Concepts in Sedimentology and Paleontology, Vol. 5. Society of Economic Paleontologists and Mineralogists, Tulsa, Oklahoma, pp. 55–72.

Estrada, F., Ercilla, G., Gorini, C., Alonso, B., Vázquez, J.T-, García-Castellanos, D., Juan, C., Maldonado, A., Ammar, A., Elabbassi, M., 2011. Impact of pulsed Atlantic water inflow into the Alboran Basin at the time of the Zanclean flooding. Geo-Marine Letters 31, 361–376.

Fariduddin, M., Loubere, P., 1997. The surface ocean productivity response of deeper water benthic foraminifera in the Atlantic Ocean. Marine Micropaleontology 32, 289–310.

Flores, J.A., 1987. El nanoplancton calcáreo en la formación «Arcillas de Gibraleón»: síntesis bioestratigráfica y paleoecológica. In: Civis, J. (Ed.), Paleontología del Neógeno de Huelva. Ediciones Universidad de Salamanca, Salamanca, pp. 65–68.

Fontanier, C., Jorissen, F.J., Licari, L., Alexandre, A., Anschutz, P., Carbonel, P., 2002. Live benthic foraminiferal faunas from the Bay of Biscay: faunal density, composition, and microhabitats. Deep-Sea Research I 49, 751–785.

Fontanier, C., Jorissen, F.J., Chaillou, G., David, C., Anschutz, P., Lafon, V., 2003. Seasonal and interannual variability of benthic foraminiferal faunas at 550 m depth in the Bay of Biscay. Deep-Sea Research I 50, 457–494.

Fortuin, A.R., Krijgsman, W., 2003. The Messinian of the Nijar basin (SE Spain): sedimentation, depositional environments and paleogeographic evolution. Sedimentary Geology 160, 213–242.

Fronval, T., Jansen, E., 1996. Late Neogene paleoclimates and paleoceanography in the Iceland-Norwegian Sea: evidence from the Iceland and VØring Plateaus. Proceedings of the Ocean Drilling Program, Scientific Results 151, 455−468.

Galán, E., González, I., 1993. Contribución de la mineralogía de arcillas a la interpretación de la evolución paleogeográfica del sector occidental de la Cuenca del Guadalquivir. Estudios Geológicos 49, 261–275.

Galán, E., González, I., Mayoral, E., Vázquez, M.A., 1989. Caracterización y origen de la facies glauconítica de la Cuenca del Guadalquivir. Estudios geológicos 45, 169–175.

Gallego-Torres, D., Martínez-Ruiz, F., Paytan, A., Jiménez-Espejo, F.J., Ortega-Huertas, M., 2007. Pliocene–Holocene evolution of depositional conditions in the eastern Mediterranean: role of anoxia vs. productivity at time of sapropel deposition. Palaeogeography, Palaeoclimatology, Palaeoecology 246, 424–439.

Garcés, M., Krijgsman, W., Agustí, J., 1998. Chronology of the late Turolian deposits of the Fortuna basin (SE Spain): implications for the Messinian evolution of the eastern Betics. Earth and Planetary Science Letters 163, 69−81.

García-Castellanos, D., Villaseñor, A., 2011. Messinian salinity crisis regulated by competing tectonics and erosion at the Gibraltar arc. Nature 480, 359−363.

García, M., Maillard, A., Aslanian, D., Rabineau, M., Alonso, B., Gorini, C., Estrada, F., 2011. The Catalan margin during the Messinian Salinity Crisis: physiography, morphology and sedimentary record. Marine Geolology 284, 158–174.

Gautier, F., Clauzon, G., Suc, J.P., Cravatte, J., Violanti, D., 1994. Age et durée de la crise de la salinité messinienne. Comptes Rendus de la Academie de la Sciences de Paris 318, 1103–1109.

Gebhardt, H., 1993. Neogene foraminifera from the Eastern Rabat area (Morocco): stratigraphy, palaeobathymetry and palaeoecology. Journal of African Earth Sciences 16, 445–464.

Gebhardt, H., 1999. Middle to Upper Miocene benthonic foraminiferal palaeoecology of the Tap Marls (Alicante Province, SE Spain) and its palaeoceanographic implications. Palaeogeography, Palaeoclimatology, Palaeoecology 145, 141–156.

Gläser, I., Betzler, C., 2002. Facies partitioning and sequence stratigraphy of cool-water, mixed carbonate–siliciclastic sediments (Upper Miocene Guadalquivir Domain, southern Spain). International Journal of Earth Sciences (Geologische Rundschau) 91, 1041–1053.

Goineau, A., Fontanier, C., Jorissen, F.J., Lansard, B., Buscail, R., Mouret, A., Kerhervé, P., Zaragosi, S., Ernoult, E., Artéro, C., Anschutz, P., Metzger, E., Rabouille, C., 2011. Live (stained) benthic foraminifera from the Rhône prodelta (Gulf of Lion, NW Mediterranean): environmental controls on a river-dominated shelf. Journal of Sea Research 65, 58–75.

Gonzalez, R., Dias, J.M.A., Lobo, F., Mendes, I., 2004. Sedimentological and paleoenvironmental characterisation of transgressive sediments on the Guadiana Shelf (Northern Gulf of Cádiz, SW Iberia). Quaternary International 120, 133–144.

González-Delgado, J.A., Civis, J., Dabrio, C.J., Goy, J.L., Ledesma, S., Pais, J., Sierro, F.J., Zazo, C., 2004. Cuenca del Guadalquivir. In: Vera, J.A. (Ed.), Geología de España. SGE-IGME, Madrid, pp. 543–550.

González-Regalado, M.L., 1989. Estudio sistemático de los foraminíferos bentónicos de las arenas fosilíferas del Plioceno de Huelva: su significado paleoecológico. Estudios Geológicos 45, 101–119.

González-Regalado, M.L., Ruiz, F., 1990. Los ostrácodos del tramo inferior de la Formación “Arcillas de Gibraleón” (Gibraleón, provincia de Huelva, S.W. España). Revista de la Sociedad Geológica de España 3, 23–31.

González-Regalado, M.L., Ruiz, F., Tosquella, J., Baceta, J.I., Pendón, J.G., Abad, M., Hernández-Molina, F.J., Somoza, L., Díaz del Río, V., 2001. Foraminíferos bentónicos actuales de la plataforma continental del norte del Golfo de Cádiz. Geogaceta 29, 61–64.

González-Regalado, M.L., Ruiz, F., Abad, M., Pendón, J.G., Tosquella, J., 2005. Los foraminíferos bentónicos del horizonte glauconítico inferior de la <<Formación Arcillas de Gibraleón>> (Depresión del Guadalquivir, SO España). Geogaceta 38, 127–130.

González-Regalado, M.L., Ruiz, F., Abad, M., Civis, J., González-Delgado, J.A., Muñoz, J.M., García, E.X.M., Pendón, J.G., Toscano, A., 2009. Impact of storms on Pliocene benthic foraminiferal assemblages of southwestern Spain. Ameghiniana 46, 345–360.

Grunert, P., Soliman, A., Harzhauser, M., Müllegger, S., Piller, W.E., Rögl, F., 2010. Upwelling conditions in the Early Miocene Central Paratethys Sea. Geologica Carpathica 61, 129–145.

Gutiérrez-Mas, J.M., Hernández-Molina, F.J., López-Aguayo, F., 1996. Holocene Sedimentary dynamics on the Iberian continental shelf of the Gulf of Cádiz (SWSpain). Continental Shelf Research 16, 1635–1653.

Hammer, Ø., Harper, D.A.T., Ryan, P. D., 2001. PAST: Paleontological Statistics Software Package for Education and Data Analysis. Palaeontologia Electronica 4, 1−9.

Haq, B.U., Hardenbol, J., Vail, P.R., 1987. Chronology of fluctuating sea levels since the Triassic. Science 235, 1156–1167.

Hardenbol, J., Thierry, J., Farley, M.B., Jaquin, T., de Graciansky, P., Vail, P.R., 1998.Mesozoic and Cenozoic sequence chronostratigraphic framework of European basins - chart 2: Cenozoic sequence chronostratigraphy. In: de Graciansky, P., Hardenbol, J., Jaquin, T., Vail, P.R. (Eds.), Mesozoic and cenozoic sequence stratigraphy of european basins: SEPM Special Publication, 60.

Harris, L.C., Whiting, B.M., 2000. Sequence-stratigraphic significance of Miocene to Pliocene glauconite-rich layers, on- and offshore of the US Mid-Atlantic margin. Sedimentary Geology 134, 129–147.

Haunold, T.G., Baal, C., Piller, W.E., 1997. Benthic foraminiferal associations in the Northern Bay of Safaga, Red Sea, Egypt. Marine Micropaleontology 29, 185–210.

Hayek, L.A.C., Buzas, M.A., 1997. Surveying Natural Populations. Columbia University Press, New York.

Hayward, B.W., Grenfell, H.R., Sabaa, A., Hayward, J.J., 2003. Recent benthic foraminifera from offshore Taranaki, New Zealand. New Zealand Journal of Geology and Geophysics 46, 489–518.

Hernández-Molina, F.J., Llave, E., Stow, D.A.V., Garcia, M., Somoza, L., Vazquez, J.T., Lobo, F.J., Maestro, A., Diaz del Rio, V., Leon, R., 2006. The contourite depositional system of the Gulf of Cadiz: a sedimentary model related to the bottom current activity of the Mediterranean outflow water and its interaction with the continental margin. Deep-Sea Research Part II 53, 1420–1463.

Hernández-Molina F.J., Serra, N., Stow, D.A.V., Llave, E., Ercilla, G., Van Rooij, D., 2011. Along-slope oceanographic processes and sedimentary products around the Iberian margin. Geo-Marine Letters 31, 315–341.

Hilgen, F., Kuiper, K., Krijgsman, W., Snel, E., van der Laan, E., 2007. Astronomical tuning as the basis for high resolution chronostratigraphy: the intricate history of the Messinian Salinity Crisis. Stratigraphy 4, 231−238.

Hodell, D.A., Benson, R.H., Kennett, J.P., Rakic-El Bied, K., 1989. Stable isotope stratigraphy of latest Miocene sequences in northwest Morocco: the Bou Regreg section. Paleoceanography 4, 467–482.

Hodell, D.A., Benson, R.H., Kent, D.V., Boersma, A., Rakic-El Bied, K., 1994. Magnetostratigraphic, biostratigrahic, and stable isotope stratigraphy of an Upper Miocene drill core from the Salé Briqueterie (northwestern Morocco): a high-resolution chronology for the Messinian stage. Paleoceanography 9, 835–855.

Hodell, D.A., Curtis, J.H., Sierro, F.J., Raymo, M.E., 2001. Correlation of late Miocene to early Pliocene sequences between the Mediterranean and North Atlantic. Paleoceanography 16, 164−178.

Hohenegger, J., 2005. Estimation of environmental paleogradient values based on presence/absence data: a case study using benthic foraminifera for paleodepth estimation. Palaeogeography, Palaeoclimatology, Palaeoecology 217, 115–130.

Hohenegger, J., Andersen, N., Báldi, K., Ćorić, S., Pervesler, P., Rupp, C., Wagreich, M., 2008. Paleoenvironment of the Early Badenian (Middle Miocene) in the southern Vienna Basin (Austria) — multivariate analysis of the Baden-Sooss section. Geologica Carpathica 59, 461–487.

Hsü, K.J., Ryan, W.B.F., Cita, M.B., 1973. Late Miocene Desiccation of the Mediterranean. Nature 242, 240–244.

Hsü, J.K., Montadert, L., Bernoulli, D., Cita, M.B., Erickson, A., Garrison, R.E., Kidd, R.B., Mélières, F., Müller, C., Wright, R., 1977. History of the Mediterranean salinity crisis. Nature 267, 1053–1078.

Huang, T.C., Stanley, D.J., 1972. Western Alboran Sea: sediment dispersal, ponding and reversal of currents. In: Stanley, D.J. et al., (Eds), The Mediterranean Sea: a natural sedimentation laboratory. Dowden, Hutchinson & Ross, Stroudsburg, pp. 521–559.

Hüsing, S.K., Oms, O., Agustí, J., Garcés, M., Kouwenhovene, T.J., Krijgsman, W., Zachariasse, J., 2010. On the late Miocene closure of the Mediterranean- Atlantic gateway through the Guadix basin (southern Spain). Palaeogeography Palaeoclimatology Palaeoecology 291, 167–179.

Iaccarino, S.M., Bossio, A., 1999. Paleoenvironment of uppermost Messinian sequences in theWestern Mediterranean (sites 974, 975, and 978). In: Zahn, R., Comas, M.C., Klaus, A. (Eds.), Proceedings of the Ocean Drilling Program, Scientific Results, 161, pp. 529–541.

Iaccarino, S.M., Bertini, A., Di Stefano, A., Ferraro, L., Gennari, R., Grossi, F., Lirer, F., Manzi, V., Menichetti, E., Ricci Lucchi, M., Taviani, M., Sturiale, G., Angeletti, L., 2008, The Trave section (Monte dei Corvi, Ancona, Central Italy): an integrated paleontological study of the Messinian deposits. Stratigraphy, v. 5, 281-306.

Iles, A.C., Gouhier, T.C., Menge, B.A., Stewart, J.S., Haupt, A.J., Lynch, M.C., 2012. Climate-driven trends and ecological implications of event-scale upwelling in the California Current System. Global Change Biology 18, 783–796.

Iorga, M. C., Lozier, M. S., 1999. Signatures of the Mediterranean outflow from a North Atlantic climatology 1. Salinity and density fields. Journal of Geophysical ResearchOceans 104, 25985-26009.

James, R.H., Austin, W.E.N., 2008. Biogeochemical controls on palaeoceanographic environmental proxies: a review. In: Austin, W.E.N., James, R.H. (Eds), Biogeochemical Controls on Palaeoceanographic Environmental Proxies. Geological Society, London, pp. 3–32.

Jiménez-Moreno, G., Head, M.J., Harzhauser, M., 2006. Early and Middle Miocene dinoflagellate cyst stratigraphy of the Central Paratethys, Central Europe. Journal of Micropaleontology 25, 113-139.

Jiménez-Moreno, G., Pérez-Asensio, J.N., Larrasoaña, J.C., Aguirre, J., Civis, J., Rivas-Carballo, M.R., Valle-Hernández, M.F., González-Delgado, J.A., submitted. Vegetation, sea-level and climate changes during the Messinian salinity crisis. Geological Society of America Bulletin.

Jorissen, F.J., 1988. Benthic foraminifera from the Adriatic Sea; principles of phenotypic variation. Utrecht Micropaleontology Bulletin 37, 1–176.

Jorissen, F.J., Barmawidjaja, D.M., Puskaric, S., van der Zwaan, G.J., 1992. Vertical distribution of benthic foraminifera in the northern Adriatic Sea: the relation with the organic flux. Marine Micropaleontology 19, 131–146.

Jorissen, F.J., de Stigter, H.C., Widmark, J.G.V., 1995. A conceptual model explaining benthic foraminiferal microhabitats. Marine Micropaleontology 26, 3–15.

Jorissen, F.J., Fontanier, C., Ellen, T., 2007. Paleoceanographical proxies based on deep-sea benthic foraminiferal assemblage characteristics. In: Hillaire-Marcel, C., De Vernal, A. (Eds.), Developments in Marine Geology, Vol. 1. Elsevier, Amsterdam, pp. 263–325.

Kaiho, K., 1994. Benthic foraminiferal dissolved-oxygen index and dissolved-oxygen levels in the modern ocean. Geology 22, 719–722.

Kaiho, K., 1999. Effect of organic carbon flux and dissolved oxygen on the benthic foraminiferal oxygen index (BFOI). Marine Micropaleontology 37, 67–76.

Kastens, K.A., 1992. Did a glacio-eustatic sea level drop trigger the Messinian Salinity crisis? New evidence from Ocean Drilling Program site 654 in the Tyrrhenian Sea. Paleoceanography7, 333−356.

Keigwin, L.D., Aubry, M.P., Kent, D.V., 1987. North Atlantic late Miocene stable isotope stratigraphy, biostratigraphy, and magnetostratigraphy. Initial Reports of the Deep Sea Drilling Project 94, 935-963.

Khélifi, N., Sarnthein, M., Andersen, N., Blanz, T., Frank, M., Garbe-Schonberg, D., Haley, B.A., Stumpf, R., Weinelt, M., 2009. A major and long-term Pliocene intensification of the Mediterranean outflow, 3.5–3.3 Ma ago. Geology 37, 811–814.

King, T.A., Ellis Jr., W.G., Murray, D.W., Shackleton, N.J., Harris, S., 1997. Miocene evolution of carbonate sedimentation at the Ceara rise: a multivariate data/proxy approach. In: Shackleton, N.J., Curry, W.B., Richter, C., Bralower, T.J. (Eds.), Proceedings of the Ocean Drilling Program, Scientific Results. College Station, Texas, pp. 349–365.

Koho, K.A., García, R., de Stigter, H.C., Epping, E., Koning, E., Kouwenhoven, T.J., van der Zwaan, G.J., 2008. Sedimentary labile organic carbon and pore water redox control on species distribution of benthic foraminifera: a case study from Lisbon-Setúbal Canyon (southern Portugal). Progress in Oceanography 79, 55–82.

Kotthoff, U., Pross, J., Müller, U.C., Peyron, O., Schmiedl, G., Schulz, H., Bordon, A., 2008. Climate dynamics in the borderlands of the Aegean Sea during formation of sapropel S1 deduced from a marine pollen record. Quaternary Science Reviews 27, 832–845.

Koufos, G.D., Kostopoulos, D.S., Theodora, D., 2005. Neogene/Quaternary mammalian migrations in Eastern Mediterranean. Belgian Journal of Zoology 135, 181–190.

Kouwenhoven, T.J., van der Zwaan, G.J., 2006. A reconstruction of late Miocene Mediterranean circulation patterns using benthic foraminifera. Palaeogeography, Palaeoclimatology, Palaeoecology 238, 373–385.

Kouwenhoven, T.J., Seidenkrantz, M.-S., van der Zwaan, G.J., 1999. Deep-water changes: the near-synchronous disappearance of a group of benthic foraminifera from the Late Miocene Mediterranean. Palaeogeography, Palaeoclimatology, Palaeoecology 152, 259−281.

Kouwenhoven, T.J., Morigi, C., Negri, A., Giunta, S., Krijgsman, W., Rouchy, J.M., 2006. Palaeoenvironmental evolution of the eastern Mediterranean during the Messinian: constraints from integrated microfossil data of the Pissouri Basin (Cyprus). Marine Micropalaeontology 60, 17–44.

Krijgsman, W., Meijer, P.T., 2008. Depositional environments of the Mediterranean "Lower Evaporites" of the Messinian salinity crisis: constraints from quantative analyses. Marine Geology 253, 73–81.

Krijgsman, W., Langereis, C.G., Zachariasse, W.J., Boccaletti, M., Moratti, G., Gelati, R., Iaccarino, S., Papani, G., Villa, G., 1999a. Late Neogene evolution of the Taza-Guercif Basin (Rifian Corridor, Morocco) and implications for the Messinian salinity crisis. Marine Geology 153, 147–160.

Krijgsman, W., Hilgen, F.J., Raffi, I., Sierro, F.J., Wilson, D.S., 1999b. Chronology, causes and progression of the Messinian salinity crisis. Nature 400, 652–655.

Krijgsman, W., Fortuin, A.R., Hilgen, F.J., Sierro, F.J., 2001. Astrochronology for the Messinian Sorbas basin (SE Spain) and orbital (precession) forcing for evaporite cyclicity. Sedimentary Geology 140, 43–60.

Krijgsman, W. Gaboardi, S., Hilgen, F.J., Iaccarino, S., de Kaenel, E., van der Laan, E., 2004, Revised astrochronology for the Ain el Beida section (Atlantic Morocco): No glacio-eustatic control for the onset of the Messinian Salinity Crisis. Stratigraphy 1, 87−101.

Kucera, M., 2007. Planktonic foraminifera as tracers of past oceanic environments. In: Hillaire-Marcel, C., De Vernal, A. (Eds.), Developments in Marine Geology, Vol. 1. Elsevier, Amsterdam, pp. 213–262.

Lacombe, H., Tchernia, P., Gamberoni, L., 1985. Variable bottom water in the western Mediterranean basin. Progress in Oceanography 14, 319–338.

Larrasoaña, J.C., Roberts, A.P., Rohling, E.J., Winklhofer, M., Wehausen, R., 2003. Three million years of monsoon variability over the northern Sahara. Climate Dynamics 21, 689–698.

Larrasoaña, J.C., González-Delgado, J.A., Civis, J., Sierro, F.J., Alonso-Gavilán, G., Pais, J., 2008. Magnetobiostratigraphic dating and environmental magnetism of Late Neogene marine sediments recovered at the Huelva-1 and Montemayor-1 boreholes (lower Guadalquivir basin, Spain). Geo-Temas 10, 1175–1178.

Laskar, J., Robutel, P., Joutel, F., Gastineau, M., Correia, A.C.M., Levrard, B., 2004. A long-term numerical solution for the insolation quantities of the Earth. Astronomy & Astrophysics 428, 261–285.

Laskar, J., Fenga, A., Gastineau, M., Manche, H., 2011. La2010: a new orbital solution for the long-term motion of the Earth. Astronomy & Astrophysics 532, A89. doi: 10.1051/0004-6361/201116836.

Lebreiro, S.M., Moreno, J.C., Abrantes, F.F., Pflaumann, U., 1997. Productivity and paleoceanographic implications on the Tore Seamount (Iberian Margin) during the last 225 kyr: foraminiferal evidence. Paleoceanography 12, 718–727.

Leeder, M.R, 1982. Sedimentology, Processes and Products.Allen and Unwin, London.

Levin, L., Cage, J.D., 1998. Relationships between oxygen, organic matter and the diversity of bathyal macrofauna. Deep-Sea Research II 45, 129–163.

Liu, Q.S., Larrasoaña, J.C., Torrent, J., Roberts, A.P., Rohling, E.J., Liu, Z., Jiang, Z., 2012. New constraints on climate forcing and variability in the circum-Mediterranean region from magnetic and geochemical observations of sapropels S1, S5 and S6. Palaeogeography, Palaeoclimatology, Palaeoecology 333−334, 1−12.

Llave, E., Schönfeld, J., Hernández-Molina, F.J., Mulder, T., Somoza, L., Díaz del Río, V., Sánchez-Almazo, I., 2006. High-resolution stratigraphy of the Mediterranean outflow contourite system in the Gulf of Cadiz during the late Pleistocene: the impact of Heinrich events. Marine Geology 227, 241–262.

Llave, E., Hernández-Molina, F.J., Stow, D.A.V., Fernández-Puga, M.C., García, M., Vázquez, J.T., Maestro, A., Somoza, L., Díaz del Río, V., 2007. Reconstructions of the Mediterranean Outflow Water during the Quaternary since the study of changes in buried mounded drift stacking pattern in the Gulf of Cadiz. Marine Geophysical Research 28, 379–394.

Llave, E., Matias, H., Hernández-Molina, F.J., Ercilla, G., Stow, D.A.V., Medialdea, T., 2011. Pliocene–Quaternary contourites along the northern Gulf of Cadiz margin: sedimentary stacking pattern and regional distribution. Geo-Marine Letters 31, 377–390.

Loget, N., van den Driessche, J., 2006. On the origin of the Strait of Gibraltar: Sedimentary Geology 188-189, 341−356.

Loget, N., van den Driessche, J., Davy, P., 2005. How did the Messinian Salinity Crisis end?. Terra Nova 17, 414−419.

Loubere, P., 1987. Changes in mid-depth North Atlantic and Mediterranean circulation during the late Pliocene—Isotopic and sedimentological evidence. Marine Geology 77, 15−38.

Lourens, L.J., Hilgen, F.J., Shackleton, N.J., Laskar, J., Wilson, D.S., 2004. The Neogene Period. In: Gradstein, F.M., Ogg, J.G., Smith, A.G. (Eds.), A Geologic Time Scale 2004. Cambridge University Press, Cambridge, pp. 409–440.

Loutit, T.S., Keigwin, L.D., 1982. Stable isotopic evidence for latest Miocene sea-level fall in the Mediterranean region. Nature 300, 163−166.

Lutze, G.F., 1980. Depth distribution of benthic foraminifera on the continental margin off NW Africa. "Meteor" Forschungs-Ergebnisse, Part C 32, 31–80.

Lutze, G.F., Coulbourn, W.T., 1984. Recent benthic Foraminifera from the continental margin of northwest Africa: community structures and distribution. Marine Micropaleontology 8, 361–401.

Lutze, G.F., Thiel, H., 1989. Epibenthic foraminifera from elevated microhabitats: *Cibicidoides wuellerstorfi* and *Planulina ariminensis*. Journal of Foraminiferal Research 19, 153–158.

Mackensen, A., 2008. On the use of benthic foraminiferal δ13C in palaeoceanography: constraints from primary proxy relationships. In: Austin, W.E.N., James, R.H. (Eds), Biogeochemical Controls on Palaeoceanographic Environmental Proxies. Geological Society, London, pp. 121–133.

Maldonado, A., Nelson, C.H., 1999. Interaction of tectonic and depositional processes that control the evolution of the Iberian Gulf of Cadiz margin. Marine Geology 155, 217−242.

Maldonado, A., Somoza, L., Pallarés, L., 1999. The Betic orogen and the Iberian-African boundary in the Gulf of Cadiz: geological evolution (central North Atlantic). Marine Geology 155, 9–43.

Malmgren, B.A., Haq, B.U., 1982. Assessment of quantitative techniques in paleobiogeography. Marine Micropaleontology 7, 213–230.

Marshall, J., Schott, F., 1999. Open-ocean convection: Observations, theory, and models models. Reviews of Geophysics 37, 1–64.

Martín, J.M., Braga, J.C., 1994. Messinian events in the Sorbas basin in southeastern Spain and their implications in the recent history of the Mediterranean. Sedimentary Geology 90, 257–268.

Martín, J.M., Braga, J.C., Sánchez-Almazo, I.M., 1999. The Messinian record of the outcropping marginal Alboran basin deposits: significance and implications. In: Zahn R., Comas, M.C., Klaus, A. (Eds), Proceedings of the Ocean Drilling Program, Scientific Results, 161, pp. 543-551.

Martín, J.M., Braga, J.C., Betzler, C., 2001. The Messinian Guadalhorce corridor: the last northern, Atlantic–Mediterranean gateway. Terra Nova 13, 418–424.

Martín, J.M., Braga, J.C., Aguirre, J., Puga-Bernabéu, A., 2009. History and evolution of the North-Betic Strait (Prebetic Zone, Betic Cordillera): a narrow, early Tortonian, tidal-dominated, Atlantic–Mediterranean marine passage. Sedimentary Geology 216, 80–90.

Martín, J.M., Braga, J.C., Sánchez-Almazo, I.M., Aguirre, J., 2010. Temperate and tropical carbonate-sedimentation episodes in the Neogene Betic basins (S Spain) linked to climatic oscillations and changes in the Atlantic-Mediterranean connections. Constraints with isotopic data. In: Mutti, M., Piller, W., Betzler, C. (Eds.), Carbonate systems during the Oligocene–Miocene climatic transition. : International Association of Sedimentologists Special Publication, No. 42. Blackwell, Oxford, pp. 49–69.

Martinez, P., Bertrand, P., Shimmield, G.B., Cochrane, K., Jorissen, J., Foster, J.M., Dignan, M., 1999. Upwelling intensity and ocean productivity changes off Cape Blanc (Northwest Africa) during the last 70.000 years: geochemical and micropalaeontological evidence. Marine Geology 158, 57–74.

Martins, V., Jouanneau, J.-M., Weber, O., Rocha, F., 2006. Tracing the late Holocene evolution of the NW Iberian upwelling system. Marine Micropaleontology 59, 35–55.

Mayoral, E., Pendón, J.G., 1987. Icnofacies y sedimentación en zona costera. Plioceno superior (?), litoral de Huelva. Acta Geológica Hispánica 21–22, 507–513.

McKee, B.A., Aller, R.C., Allison, M.A., Bianchi, T.S., Kineke, G.C., 2004. Transport and transformation of dissolved and particulate materials on continental margins influenced by major rivers: benthic boundary layer and seabed processes. Continental and Shelf Research 24, 899–926.

MEDOC Group, 1970. Observation of formation of deep water in the Mediterranean Sea. Nature 227, 1037–1040.

Meijer, P.T., 2006. A box model of the blocked-outflow scenario for the Messinian Salinity Crisis. Earth and Planetary Science Letters 248, 486–494.

Meijer, P.Th., Krijgsman, W., 2005. A quantitative analysis of the desiccation and re-filling of the Mediterranean during the Messinian Salinity Crisis: Earth Planetary Science Letters 240, 510−520.

Meijer, P.Th., Slingerland, R., Wortel, M.J.R., 2004. Tectonic control on past circulation of the Mediterranean Sea: a model study of the Late Miocene. Paleoceanography 19, PA1026. doi:10.1029/2003PA000956.

Melki, T., Kallel, N., Jorissen, F.J., Guichard, F., Dennielou, B., Berné, S., Labeyrie, L., Fontugne, M., 2009. Abrupt climate change, sea surface salinity and paleoproductivity in the western Mediterranean Sea (Gulf of Lion) during the last 28 kyr. Palaeogeography, Palaeoclimatology, Palaeoecology 279, 96–113.

Mendes, I., Gonzalez, R., Dias, J.M.A., Lobo, F., Martins, V., 2004. Factors influencing recent benthic foraminifera distribution on the Guadiana shelf (Southwestern Iberia). Marine Micropaleontology 51, 171–192.

Milker, Y., 2010. Western Mediterranean shelf foraminifera: Recent distribution, Holocene sea-level reconstructions, and paleoceanographic implications. PhD thesis, University of Hamburg, Germany.

Milker, Y., Schmiedl, G., Betzler, C., Römer, M., Jaramillo-Vogel, D., Siccha, M., 2009. Distribution of recent benthic foraminifera in shelf carbonate environments of the Western Mediterranean Sea. Marine Micropaleontology 73, 207–225.

Milker, Y., Schmiedl, G., Betzler, C., Andersen, N., Theodor, M., 2012. Response of Mallorca shelf ecosystems to an early Holocene humid phase. Marine Micropaleontology 90–91, 1–12.

Miller, K.G., Kominz, M.A., Browning, J.V., Wright, J.D., Mountain, G.S., Katz, M.E., Sugarman, P.J., Cramer, B.S., Christie-Blick, N., Pekar, S.F., 2005. The Phanerozoic record of global sea-level change. Science 310, 1293−1298.

Millot, C., 1999. Circulation in the western Mediterranean Sea. Journal of Marine Systems 20, 423–442.

Mojtahid, M., Jorissen, F., Durrieu, J., Galgani, F., Howa, H., Redois, F., Camps, R., 2006. Benthic foraminifera as bio-indicators of drill cutting disposal in tropical east Atlantic outer shelf environments. Marine Micropaleontology 61, 58–75.

Mojtahid, M., Jorissen, F., Lansard, B., Fontanier, C., Bombled, B., Rabouille, C., 2009. Spatial distribution of live benthic foraminifera in the Rhône prodelta: faunal response to a continental-marine organic matter gradient. Marine Micropaleontology 70, 177–200.

Mojtahid, M., Griveaud, C., Fontanier, C., Anschutz, P., Jorissen, F.J., 2010a. Live benthic foraminiferal faunas along a bathymetrical transect (140–4800 m) in the Bay of Biscay (NE Atlantic). Revue de Micropaléontologie 53, 139–162.

Mojtahid, M., Jorissen, F., Lansard, B., Fontanier, C., 2010b. Microhabitat selection of benthic foraminifera in sediments off the Rhône river mouth (NW Mediterranean). Journal of Foraminiferal Research 40, 231–246.

Murphy, L.N., Kirk-Davidoff, D.B., Mahowald, N., Otto-Bliesner, B.L., 2009. A numerical study of the climate response to lowered Mediterranean Sea level during the Messinian Salinity Crisis. Palaeogeography, Palaeoclimatology, Palaeoecology 279, 636 41−59.

Murray, J.W., 1991. Ecology and Palaeoecology of Benthic Foraminifera. Longman Scientific & Technical, UK.

Murray, J.W., 2006. Ecology and Applications of Benthic Foraminifera. Cambridge University Press, Cambridge.

Naafs, B.D.A., Stein, R., Hefter, J., Khélifi, N., De Schepper, S., Haug, G.H., 2010. Late Pliocene changes in the North Atlantic Current. Earth and Planetary Science Letters 298, 434–442.

Naidu, P., Niitsuma, N., 2004. Atypical δ13C signature in Globigerina bulloides at the ODP Site 723An (Arabian Sea): implications of environmental changes caused by upwelling. Marine Micropaleontology 53, 1−10.

Nelson, C.H., 1990. Estimated post-Messinian sediment supply and sedimentation rates on the Ebro continental margin, Spain. Marine Geology 95, 395–418

Nelson, C.H., Baraza, J., Maldonado, A., 1993. Mediterranean undercurrent sandy contourites, Gulf of Cádiz, Spain. Sedimentary Geology 82, 103−131.

Nelson, C.H., Baraza, J., Maldonado, A., Rodero, J., Escutia, C., Barber Jr., J.H., 1999. Influence of the Atlantic inflow and Mediterranean outflow currents on Late Quaternary sedimentary facies of the Gulf of Cádiz continental margin. Marine Geology 155, 99–129.

Nisancioglu, K., Raymo, M. E., P. Stone, H., 2003. Reorganization of Miocene deep water circulation in response to the shoaling of the Central American Seaway. Paleoceanography, 18, 1006, doi: 10.102912002PA000767.

Odin, G.S., Matter, A., 1981. De glauconarium origine. Sedimentology 28, 611–641.

Özgökmen, T.M., Chassignet, E.P., Rooth, C.G.H., 2001. On the connection between the Mediterranean Outflow and the Azores current. Journal of Physical Oceanography 31, 461–480.

Parker, F.L., 1954. Distribution of the foraminifera in the northeastern Gulf of Mexico. Bulletin of the Museum of Comparative Zoology 111, 453–588.

Pascual, A., Martínez-García, B., Rodríguez-Lázaro, J., Martín-Rubio, M., 2008. Distribución de los foraminíferos bentónicos en la plataforma marina de Vizcaya y Este de Cantabria. Geogaceta 44, 131–134.

Perconig, E., 1973. El Andaluciense. XIII Coloquio Europeo de Micropaleontología. C. N. G. Enadimsa, Madrid, pp. 201–223.

Perconig, E., Granados, L.F., 1973. El estratotipo del Andaluciense. XIII Coloquio Europeo de Micropaleontología. C. N. G. Enadimsa, Madrid, pp. 225–251.

Pérez-Asensio, J.N., Aguirre, J., 2010. Benthic foraminiferal assemblages in temperate coral-bearing deposits from the Late Pliocene. Journal of Foraminiferal Research 40, 61–78.
Pérez-Asensio, J.N., Aguirre, J., Schmiedl, G., Civis, J., 2012a. Messinian paleoenvironmental evolution in the lower Guadalquivir Basin (SW Spain) based on benthic foraminifera. Palaeogeography, Palaeoclimatology, Palaeoecology 326−328, 135−151.
Pérez-Asensio, J.N., Aguirre, J., Schmiedl, G., Civis, J., 2012b. Impact of restriction of the Atlantic-Mediterranean gateway on the Mediterranean Outflow Water and eastern Atlantic circulation during the Messinian. Paleoceanography 27, PA3222, doi:10.1029/2012PA002309.
Pérez-Asensio, J.N., Aguirre, J., Schmiedl, G., Civis, J., in preparation 1. Messinian paleoproductivity changes and organic carbon cycling in the northeastern Atlantic.
Pérez-Asensio, J.N., Aguirre, J., Jiménez-Moreno, G., Schmiedl, G., Civis, J., in preparation 2. Glacioeustatic control on the Messinian salinity crisis.
Pérez-Folgado, M., Sierro, F.J., Bárcena, M.A., Flores, J.A., Vázquez, A., Utrilla, R., Hilgen, F.J., Krijgsman, W., Filippelli, G.M., 2003. Western versus eastern Mediterranean paleoceanographic response to astronomical forcing: a high-resolution microplankton study of precession-controlled sedimentary cycles during the Messinian. Palaeogeography, Palaeoclimatology, Palaeoecology 190, 317–334.
Phipps, M., Jorissen, F., Pusceddu, A., Bianchelli, S., de Stigter, H., 2012. Live benthic foraminiferal faunas along a bathymetrical transect (282-4987 m) on the Portuguese margin (NE Atlantic). Journal of Foraminiferal Research 42, 66−81.
Pinardi, N., Masetti, E., 2000. Variability of the large scale general circulation of the Mediterranean Sea from observations and modelling: a review. Palaeogeography Palaeoclimatology Palaeoecology 158, 153−173.
Piotrowski, A.M., Goldstein, S.L., Hemming, S.R., Fairbanks, R.G., 2005. Temporal relationships of carbon cycling and ocean circulation at glacial boundaries. Science 307, 1933–1938.
Poli, M.S., Meyers, P.A., Thunell, R.C., 2010. The western North Atlantic record of MIS 13 to 10: Changes in primary productivity, organic carbon accumulation and benthic foraminiferal assemblages in sediments from the Blake Outer Ridge (ODP Site 1058). Palaeogeography, Palaeoclimatology, Palaeoecology 295, 89−101.
Price, J. F., O'Neill-Baringer, M., 1994. Outflows and deep water production by marginal seas. Progress in Oceanography 33, 161–200.
Pujol, C., Vergnaud-Grazzini, C., 1995. Distribution patterns of live planktic foraminifers as related to regional hydrography and productive systems of the Mediterranean Sea. Marine Micropaleontology 25, 187−217.
Raddatz, J., Rüggeberg, A., Margreth, S., Dullo, W.-C., IODP Expedition 307 Scientific Party, 2011. Paleoenvironmental reconstruction of Challenger Mound initiation in the Porcupine Seabight, NE Atlantic. Marine Geology 282, 79−90.
Rahmstorf, S., 1998. Influence of Mediterranean Outflow on climate. Eos Transactions AGU 79, 281–282.
Ravelo, A.C., Hillaire-Marcel, C., 2007. The use of oxygen and carbon isotopes of foraminifera in paleoceanography. In: Hillaire-Marcel, C., De Vernal, A. (Eds.), Developments in Marine Geology, Vol. 1. Elsevier, Amsterdam, pp. 735–764.
Reid, J.L., 1979. On the contribution of the Mediterranean Sea outflow to the Norwegian-Greenland Sea. Deep-Sea Research 26, 1199−1223.
Retailleau, S., Howa, H., Schiebel, R., Lombard, F., Eynaud, F., Schmidt, S., Jorissen, F., Labeyrie, L., 2009. Planktic foraminiferal production along an offshore-onshore transect in the south-eastern Bay of Biscay. Continental Shelf Research 29, 1123–1135.
Rezqi, H., Oujidi, M., Boutakiout, M., Labraimi, M., 2000. Analyse quantitative des foraminifères benthiques actuels de la marge atlantique marocaine entre Cap Drâa et Cap Juby: reponses fauniques aux changements de I'environnement. Journal of African Earth Sciences 30, 375–400.
Riaza, C., Martínez del Olmo, W., 1996. Depositional model of the Guadalquivir-Gulf of Cádiz Tertiary basin. In: Friend, P., Dabrio, C.J. (Eds.), Tertiary basins of Spain. Cambridge University Press, Cambridge, pp. 330–338.
Riding, R., Martín, J.M., Braga, J.C., 1991. Coral–stromatolite reef framework, Upper Miocene, Almería, Spain. Sedimentology 38, 799–818.
Riding, R., Braga, J.C., Martín, J.M., Sánchez-Almazo, I.M., 1998. Mediterranean Messinian salinity crisis: constraints from a coeval marginal basin, Sorbas, southeastern Spain. Marine Geology 146, 1–20.
Riding, R., Braga, J.C., Martín, J.M., 1999. Late miocene Mediterranean desiccation: topography and significance of the 'Salinity Crisis' erosion surface on-land in southeast Spain. Sedimentary Geology 123, 1–7.
Riding, R., Braga, J.C., Martín, J.M., 2000. Late Miocene Mediterranean desiccation: topography and significance of the 'Salinity Crisis' erosion surface on-land in Southeast Spain: reply. Sedimentary Geology 133, 175–184.

Rogerson, M., Rohling, E.J., Weaver, P.P.E., Murray, J.W., 2005. Glacial to interglacial changes in the settling depth of the Mediterranean Outflow plume. Paleoceanography 20, PA3007, doi:10.1029/2004PA001106.

Rogerson, M., Rohling, E.J., Weaver, P.P.E., 2006. Promotion of meridional overturning by Mediterranean-derived salt during the last deglaciation. Paleoceanography, 21, PA4101, doi:10.1029/2006PA001306.

Rogerson, M., Colmenero-Hidalgo, E., Levine, R.C., Rohling, E.J., Voelker, A., Bigg, G., Schönfeld, J., Cacho, I., Sierro, F.J., Löwemark, L., Reguera, M.I., de Abreu, L., Garrik, K., 2010. Enhanced Mediterranean-Atlantic exchange during Atlantic freshening phases. Geochemistry, Geophysics, Geosystems 11, Q08013, doi:10.1029/ 2009GC002931.

Rogerson, M., Schönfeld, J., Leng, M.J., 2011. Qualitative and quantitative approaches in palaeohydrography: A case study from core-top parameters in the Gulf of Cadiz. Marine Geology 280, 150–167.

Rogerson, M., Rohling, E. J., Bigg, G. R., Ramirez, J., 2012. Paleoceanography of the Atlantic-Mediterranean exchange: Overview and first quantitative assessment of climatic forcing. Reviews of Geophysics 50, RG2003, doi:10.1029/2011RG000376.

Rohling, E.J., 1994. Review and new aspects concerning the formation of eastern Mediterranean sapropels. Marine Geology 122, 1–28.

Rohling, E.J., Cooke, S., 1999. Stable oxygen and carbon isotopes in foraminiferal carbonate shells. In: Sen Gupta, B.K. (Ed.), Modern Foraminifera. Kluwer Academic Publishers, Dordrecht, pp. 239–258.

Rohling, E.J., Sprovieri, M., Cane, T., Casford, J.S.L., Cooke, S., Bouloubassi, I., Emeis, K.C., Schiebel, R., Rogerson, M., Hayes, A., Jorissen, F.J., Kroon, D., 2004. Reconstructing past planktic foraminiferal habitats using stable isotope data: a case history for Mediterranean sapropel S5. Marine Micropaleontology 50, 89−123.

Roldán, F.J., 1995. Evolución neógena de la Cuenca del Guadalquivir. Ph.D. Thesis, University of Granada, Spain.

Rommerskirchen, F., Condon, T., Mollenhauer, G., Dupont, L., Schefuss, E., 2011. Miocene to Pliocene development of surface and subsurface temperatures in the Benguela Current system. Paleoceanography 26, PA3216. doi:10.1029/2010PA002074.

Rouchy, J.M., Caruso, A., 2006. The Messinian Salinity Crisis in the Mediterranean basin: a reassessment of data and an integrated scenario. Sedimentary Geology 188–189, 35–67.

Rouchy, J.-M., Orzag-Sperber, F., Blanc-Valleron, M.M., Pierre, C., Riviére, M., Comborieu-Nebout, N., Panayides, I., 2001. Paleoenvironmental changes at the Messinian–Pliocene boundary in the eastern Mediterranean (southern Cyprus basins): significance of the Messinian Lago-Mare. Sedimentary Geology 145, 93–117.

Rouchy, J.M., Caruso, A., Pierre, C., Blanc-Valleron, M.-M., Bassetti, M.A., 2007. The end of the Messinian salinity crisis: evidences from the Chelif Basin (Algeria). Palaeogeography, Palaeoclimatology, Palaeoecology 254, 386–417.

Roveri, M., Manzi, V., 2006. The Messinian salinity crisis: looking for a new paradigm?. Palaeogeography, Palaeoclimatology, Palaeoecology 238, 386–398.

Ryan, W.B.F., Cita, M.B., 1978. The nature and distribution of Messinian erosional surfaceindication of a several kilometer-deep Mediterranean in the Miocene. Marine Geology 27, 193–230

Salgueiro, E., Voelker, A.H.L., de Abreu, L., Abrantes, F., Meggers, H., Wefer, G., 2010. Temperature and productivity changes off the western Iberian margin during the last 150 ky. Quaternary Science Reviews 29, 680–695.

Sánchez-Almazo, I.M., Spiro, B., Braga, J.C., Martin, J.M., 2001. Constraints of stable isotope signatures on the depositional palaeoenvironments of upper Miocene reef and temperate carbonates in the Sorbas Basin, SE Spain. Palaeogeography, Palaeoclimatology, Palaeoecology 175, 153–172.

Sánchez-Almazo, I.M., Braga, J.C., Dinarès-Turell, J., Martín, J.M., Spiro, B., 2007. Palaeoceanographic controls on reef deposition: the Messinian Cariatiz reef (Sorbas Basin, Almería, SE Spain). Sedimentology 54, 637–660.

Sanz de Galdeano C., Rodríguez-Fernández, J. 1996. Neogene palaeogeography of the Betic Cordillera: an attempt at reconstruction. In: Friend, P. and Dabrio, C.J. (Eds), Tertiary basins of Spain. Cambridge University Press, Cambridge pp. 323−329.

Sanz de Galdeano, C., 1990. Geologic evolution of the Betic Cordilleras in the Western Mediterranean, Miocene to the present. Tectonophysics 172, 107–119.

Sanz de Galdeano, C., Vera, J.A., 1992. Stratigraphic record and palaeogeographical context of the Neogene basins in the Betic Cordillera, Spain. Basin Research 4, 21–36.

Sarnthein, M., Thiede, J., Pflaumann, U., Erlenkeuser, H., Fütterer, D., Koopmann, B., Lange, H., Seibold, E., 1982. Atmospheric and oceanic circulation patterns off northwest Africa during the past 25 million

years. In: Von Rad, U., Hinz, K., Sarnthein, M., Seibold, E. (Eds.), Geology of the Northwest Africa continental margin. Springer-Verlag, New York, pp. 545–604.
Schenau, S.J., Antonarakou, A., Hilgen, F.J., Lourens, L.J., Nijenhuis, I.A., van der Weijden, C.H., Zachariasse, W.J., 1999. Organic-rich layers in the Metochia section (Gavdos, Greece): evidence for a single mechanism of sapropel formation during the past 10 My. Marine Geology 153, 117–135.
Schmiedl, G., Mackensen, A., 1997. Late Quaternary paleoproductivity and deep water circulation in the eastern South Atlantic Ocean: Evidence from benthic foraminifera. Palaeogeography, Palaeoclimatology, Palaeoecology 130, 43−80.
Schmiedl, G., Mackensen, A., Müller, P.J., 1997. Recent benthic foraminifera from the eastern South Atlantic Ocean: dependence on food supply and water masses. Marine Micropaleontology 32, 249–287.
Schmiedl, G., de Bovée, F., Buscail, R., Charrière, B., Hemleben, C., Medernach, L., Picon, P., 2000. Trophic control of benthic foraminiferal abundance and microhabitat in the bathyal Gulf of Lions, western Mediterranean Sea. Marine Micropaleontology 40, 167–188.
Schmiedl, G., Mitschele, A., Beck, S., Emeis, K.-C., Hemleben, C., Schulz, H., Sperling, M., Weldeab, S., 2003. Benthic foraminiferal record of ecosystem variability in the eastern Mediterranean Sea during times of sapropel S5 and S6 deposition. Palaeogeography, Palaeoclimatology, Palaeoecology 190, 139–164.
Schmiedl, G., Leuschner, D.C., 2005. Oxygenation changes in the deep western Arabian Sea during the last 190,000 years: productivity versus deepwater circulation. Paleoceanography 20, PA2008. doi:10.1029/2004PA001044.
Schmiedl, G., Kuhnt, T., Ehrmann, W., Emeis, K.-C., Hamann, Y., Kotthoff, U., Dulski, P., Pross, J., 2010. Climatic forcing of eastern Mediterranean deep-water and benthic ecosystems during the past 22 000 years. Quaternary Science Reviews 29, 3006–3020.
Schönfeld, J., 1997. The impact of the Mediterranean Outflow Water (MOW) on benthic foraminiferal assemblages and surface sediments at the southern Portuguese continental margin. Marine Micropaleontology 29, 211−236.
Schönfeld, J., 2002. Recent benthic foraminiferal assemblages in deep high-energy environments from the Gulf of Cadiz (Spain). Marine Micropaleontology 44, 141–162.
Schönfeld, J., 2006. Taxonomy and distribution of the Uvigerina peregrina plexus in the tropical to northeastern Atlantic. Journal of Foraminiferal Research 36, 355–367.
Schönfeld, J., Zahn, R., 2000. Late Glacial to Holocene history of the Mediterranean Outflow. Evidence from benthic foraminiferal assemblages and stable isotopes at the Portuguese Margin. Palaeogeography Palaeoclimatology Palaeoecology 159, 85–111.
Schönfeld, J., Altenbach, A.V., 2005. Late Glacial to Recent distribution pattern of deepwater Uvigerina species in the northeastern Atlantic. Marine Micropaleontology 57, 1–24.
Schulz, M., Mudelsee, M., 2002, REDFIT: estimating red-noise spectra directly from unevenly spaced paleoclimatic time series. Computers & Geosciences 28, 421−426.
Seidenkrantz, M.-S., Kouwenhoven, T.J., Jorissen, F.J., Shackleton, N.J., van der Zwaan, G.J., 2000. Benthic foraminifera as indicators of changing Mediterranean–Atlantic water exchange in the late Miocene. Marine Geology 163, 387–407.
Sen Gupta, B.K., 1999. Introduction to modern foraminifera. In Sen Gupta, B.K. (Ed.), Modern Foraminifera. Kluwer Academic Publishers, Dordrecht, pp. 3–6.
Sgarrella, F.,Moncharmont Zei, M., 1993. Benthic foraminifera in the Gulf of Naples (Italy): systematics and autoecology. Bollettino della Società Paleontologica Italiana 32, 145–264.
Shackleton, N. J., Hall, M. A., 1997. The late Miocene stable isotope record, Site 926. Proceedings of the Ocean Drilling Program, Scientific Results 154, 367–374.
Shackleton, N.J., Hall, M.A., Pate, D., 1995. Pliocene stable isotope stratigraphy of site 846. Proceedings of the Ocean Drilling Program, Scientific Results 138, 337–355.
Sierro, F.J., 1985a. The replacement of the “Globorotalia menardii” group by the Globorotalia miotumida group: an aid to recognizing the Tortonian-Messinian boundary in the Mediterranean and adjacent Atlantic. Marine Micropaleontology 9, 525–535.
Sierro, F.J., 1985b. Estudio de los foraminíferos planctónicos, bioestratigrafía y cronoestratigrafía del Mio-Plioceno del borde occidental de la cuenca del Guadalquivir (S.O. de España). Stvdia Geologica Salmanticensia 21, 7–85.
Sierro, F.J., 1987. Foraminíferos planctónicos del Neógeno marino del sector occidental de la cuenca del Guadalquivir: síntesis y principales resultados. In: Civis, J. (Ed.), Paleontología del Neógeno de Huelva. Ediciones Universidad de Salamanca, Salamanca, pp. 23–54.
Sierro, F.J., Flores, J.A., 1992. Evolución de las fosas bética y rifeña y la comunicación Atlántico-Mediterráneo durante el Mioceno. Simposios del III Congreso Geológico de España y VIII Congreso Latinoamericano de Geología, 2, pp. 563–567.

Sierro, F.J., Flores, J.A., Civis, J., González-Delgado, J.A., Francés, G., 1993. Late Miocene globorotaliid event-stratigraphy and biogeography in the NE-Atlantic and Mediterranean. Marine Micropaleontology 21, 143–168.

Sierro, F.J., González-Delgado, J.A., Dabrio, C.J., Flores, J.A., Civis, J., 1996. Late Neogene depositional sequences in the foreland basin of Guadalquivir (SW Spain). In: Friend, P., Dabrio, C.J. (Eds.), Tertiary Basins of Spain. Cambridge University Press, Cambridge, pp. 339–345.

Sierro, F.J., Flores, J.A., Zamarreño, I., Vázquez, A., Utrilla, R., Francés, G., Hilgen, F.J., Krijgsman, W., 1999. Messinian pre-evaporite sapropels and precession-induced oscillations in western Mediterranean climate. Marine Geology 153, 137–146.

Sierro, F.J., Ledesma, S., Flores, J.A., Torrescusa, S., Martinez del Olmo,W., 2000. Sonic and gamma-ray astrochronology: cycle to cycle calibration of Atlantic climatic records to Mediterranean sapropels and astronomical oscillations. Geology 28, 695–698.

Sierro, F.J., Hilgen, F.J., Krijgsman, W., Flores, J.A., 2001. The Abad composite (SE Spain): a Messinian reference section for the Mediterranean and the APTS. Palaeogeography, Palaeoclimatology, Palaeoecology 168, 141–169.

Sierro, F.J., Hodell, D.A., Curtis, J.H., Flores, J.A., Reguera, I., Colmenero-Hidalgo, E., Bárcena, M.A., Grimalt, J.O., Cacho, I., Frigola, J., Canals, M., 2005. Impact of iceberg melting on Mediterranean thermohaline circulation during Heinrich events. Paleoceanography, 20, PA2019, doi:10.1029/2004PA001051.

Soria, J.M., Caracuel, J.E., Corbí, H., Dinarès-Turell, J., Lancis, C., Tent-Manclús, J.E., Viseras, C., Yébenes, A., 2008. The Messinian-early Pliocene stratigraphic record in the southern Bajo Segura Basin (Betic Cordillera, Spain). Implications for the Mediterranean salinity crisis. Sedimentary Geology 203, 267–288.

Soria, J.M., Fernández, J., Viseras, C., 1999. Late Miocene stratigraphy and palaeogeographic evolution of the intramontane Guadix Basin (central Betic Cordillera, Spain): implications for an Atlantic–Mediterranean connection. Palaeogeography, Palaeoclimatology, Palaeoecology 151, 255–266.

Spezzaferri, S., Tamburini, F., 2007. Paleodepth variations on the Eratosthenes Seamount (Eastern Mediterranean): sea-level changes or subsidence? eEarth Discussions 2, 115–132.

Stefanelli, S., 2004. Cyclic changes in oxygenation based on foraminiferal microhabitats: Early-Middle Pleistocene, Lucania Basin (southern Italy). Journal of Micropalaeontology 23, 81–95.

Stumpf, R., Frank, M., Schönfeld, J., Haley, B.A., 2010. Late Quaternary variability of Mediterranean outflow water from radiogenic Nd and Pb isotopes. Quaternary Science Reviews 29, 2462–2472.

Takata, H., Nomura, R., Khim, B.-K., 2010. Response of abyssal benthic foraminifera to mid-Oligocene glacial events in the eastern Equatorial Pacific Ocean (ODP Leg 199). Palaeogeography, Palaeoclimatology, Palaeoecology 292, 1–11.

Thiede, J., Winkler, A., Wolf-Welling, T., Eldholm, O., Myhre, A.M., Baumann, K.-H., Henrich, R., Stein, R., 1998. Late Cenozoic history of the polar North Atlantic: Results from ocean drilling. Quaternary Science Review 17, 185–208.

Toucanne, S., Mulder, T., Schönfeld, J., Hanquiez, V., Gonthier, E., Duprat, J., Cremer, M., Zaragosi, S., 2007. Contourites of the Gulf of Cadiz: A high-resolution record of the paleocirculation of the Mediterranean outflow water during the last 50,000 years. Palaeogeography, Palaeoclimatology, Palaeoecology 246, 354–366.

Van der Laan, E., Gaboardi, S., Hilgen, F.J, Lourens, L.J., 2005. Regional climate and glacial control on high-resolution oxygen isotope records from Ain El Beida (latest Miocene, NW Morocco): A cyclostratigraphic analysis in the depth and time domain. Paleoceanography 20, PA1001. doi: 10.1029/2003PA000995.

Van der Laan, E., Snel, E., de Kaenel, E., Hilgen, F.J., Krijgsman, W., 2006. No major deglaciation across the Miocene-Pliocene boundary: integrated stratigraphy and astronomical tuning of the Loulja sections (Bou Regreg area, NW Morocco). Paleoceanography 21, PA3011. doi:10.1029/2005PA001193.

Van der Laan, E., Hilgen, F.J.,. Lourens, L.J, de Kaenel, E., Gaboardi, S., Iaccarino, S., 2012. Astronomical forcing of Northwest African climate and glacial history during the late Messinian (6.5-5.5 Ma). Palaeogeography, Palaeoclimatology, Palaeoecology 313-314, 107–126.

Van der Zwaan, G.J., Jorissen, F.J., 1991. Biofacial patterns in river-induced shelf anoxia. In: Tyson, R.V., Pearson, T.H. (Eds.), Modern and Ancient Continental Shelf Anoxia: Geological Society, Special Publication, 58, pp. 65–82. London.

Van Hinsbergen, D.J.J., Kouwenhoven, T.J., van der Zwaan, G.J., 2005. Paleobathymetry in the backstripping procedure: correction for oxygenation effects on depth estimates. Palaeogeography, Palaeoclimatology, Palaeoecology 221, 245–265.

Van Marle, L.J., 1988. Bathymetric distribution of benthic foraminifera on the Australian-Irian Jaya continental margin, eastern Indonesia. Marine Micropaleontology 13, 97–152.

Van Morkhoven, F.P.C.M., Berggren, W.A., Edwards, A.S., 1986. Cenozoic cosmopolitan deep-water benthic foraminifera. Bulletin des Centres de Recherches Exploration- Production Elf-Aquitaine: Mémoire, 11. Pau.

Van Rooij, D., Iglesias, J., Hernandez-Molina, F.J., Ercilla, G., Gomez-Ballesteros, M., Casas, D., Llave, E., De Hauwere, A., Garcia-Gil, S., Acosta, J., Henrich, R., 2010. The Le Danois Contourite Depositional System: interactions between the Mediterranean Outflow Water and the upper Cantabrian slope (North Iberian Margin). Marine Geology 274, 1–20.

Vargas, J.M., García-Lafuente, J., Delgado, J., Criado, F., 2003. Seasonal and wind-induced variability of sea surface temperature patterns in the Gulf of Cádiz. Journal of Marine Systems 38, 205–219.

Vázquez, A., Utrilla, R., Zamarreno, I., Sierro, F.J., Flores, J.A., Francés, G., Bárcena, M.A., 2000. Precession-related sapropelites of the Messinian Sorbas Basin (South Spain): paleoenvironmental significance. Palaeogeography, Palaeoclimatology, Palaeoecology 158, 353–370.

Velde, B., 1996. Compaction trends of clay-rich deep sea sediments. Marine Geology 133, 193–201.

Vera, J.A., 2000. El Terciario de la Cordillera Bética: estado actual de conocimientos. Revista de la Sociedad Geológica de España 13, 345−373.

Vergnaud-Grazzini, C.,1983. Reconstruction of Mediterranean Late Cenozoic hydrography by means of carbon isotope analyses. Utrecht Micropaleontological Bulletins 30, 25−47.

Vidal, L., Bickert, T., Wefer, G., Röhl, U., 2002. Late Miocene stable isotope stratigraphy of SE Atlantic ODP Site 1085: Relation to Messinian events. Marine Geology 180, 71−85.

Viguier, C., 1974. Le Néogène de l'Andalousie Nord-occidentale (Espagne). Histoire Géologique du «Bassin du Bas Guadalquivir». Ph.D. Thesis, University of Bordeaux, France.

Villanueva-Guimerans, P., Canudo, I., 2008. Assemblages of recent benthic foraminifera from the northeastern Gulf of Cádiz. Geogaceta 44, 139–142.

Vincent, E., Killingley, J. S., Berger, W. H., 1980. The magnetic epoch-6 carbon shift: A change in the ocean's 13C/12C ratio 6.2 million years ago. Marine Micropaleontology 5, 185–203.

Voelker, A.H.L., Lebreiro, S.M., Schönfeld, J., Cacho, I., Erlenkeuser, H., Abrantes, F., 2006. Mediterranean outflow strengthening during northern hemisphere coolings: a salt source for the glacial Atlantic?. Earth and Planetary Science Letters 245, 39–55.

Walsh, J.J., 1991. Importance of continental margins in the marine biogeochemical cycling of carbon and nitrogen. Nature 350, 53–55.

Warny, S., Bart, P.J., Suc, J.-P., 2003. Timing and progression of climatic, tectonic and glacioeustatic influences on the Messinian Salinity Crisis. Palaeogeography, Palaeoclimatology, Palaeoecology 202, 59–66.

Weijermars, R., 1988. Neogene tectonics in the Western Mediterranean may have caused the Messinian Salinity Crisis and an associated glacial event. Tectonophysics 148, 211−219.

Wüst, G., 1961. On the vertical circulation of the Mediterranean Sea. Journal of Geophysical Research 66, 3261-3271.

Zachos, J.C., Pagani, M., Sloan, L., Thomas, E., Billups, K., 2001. Trends, Rhythms, and Aberrations in Global Climate 65 Ma to Present. Science 292, 686–693.

Zahn, R., Schönfeld, J., Kudrass, H.R., Park, M.H., Erlenkeuser, H., Grootes, P., 1997. Thermohaline instability in the North Atlantic during meltwater events: stable isotope and ice-rafted detritus records from core SO75-26KL, Portuguese margin. Paleoceanography 12, 696–710.

Zarriess, M, Mackensen, A., 2010. The tropical rainbelt and productivity changes off northwest Africa: A 31,000-year high-resolution record. Marine Micropaleontology 76, 76–91

Zhang, J., Scott, D.B., 1996. Integrated stratigraphy and paleoceanography of the Messinian (latest Miocene) across the North Atlantic Ocean. Marine Micropaleontology 29, 1−36.

Zonneveld, K.A.F., Versteegh, G.J.M., Kasten, S., Eglinton, T.I., Emeis, K.-C., Huguet, C., Koch, B.P., de Lange, G.J., de Leeuw, J.W., Middelburg, J.J., Mollenhauer, G., Prahl, F.G., Rethemeyer, J., Wakeham, S.G., 2010. Selective preservation of organic matter in marine environments; processes and impact on the sedimentary record. Biogeosciences 7, 483–511.

APPENDIX

The attached CD-ROM contains the following tables:

Table A.1. Census counts of benthic foraminifera of the Montemayor-1 core with total of benthic foraminifera and sample splits.

Table A.2. Benthic (*Cibicidoides pachyderma*) and planktonic (*Globigerina bulloides*) $\delta^{18}O$ and $\delta^{13}C$ in ‰ VPDB of the Montemayor-1 core.

Table A.1.

Core depth (m)	*Ammonia beccarii*	*Ammonia inflata*	*Ammonia tepida*	*Ammonia* sp.	*Amphicoryna scalaris*	*Amphicoryna semicostata*	*Amphicoryna sublineata*	*Amphicoryna* sp.	*Anomalinoides* cf. *ornatus*	*Anomalinoides flinti*	*Anomalinoides helicinus*	*Anomalinoides* sp.	*Asterigerinata mamilla*	*Asterigerinata planorbis*	*Asterigerinata* sp.	*Bigenerina nodosaria*	*Bolivina punctata*	*Bolivina reticulata*	*Bolivina* sp.	*Brizalina arta*	*Brizalina dilatata*	*Brizalina spathulata*	*Brizalina* sp.
256.50	52			23											1						2	3	
254.00								3		3		1										3	2
251.50				1						9		2									3	47	16
249.00										6								5			12	34	15
246.50				1			1	5									2					1	2
244.00	1						2			1	1	5						1			1	2	5
241.50	1									10		1									3	5	4
240.00										23		4											
239.00		1					3				2	1											
238.50										9	5	2											
238.00				1			1		1	14	2	2				1							
237.50	1						4			9	1	5		5		1					1	1	
237.00					1		1			7	5												
236.50							1			11	2	2											
236.00					1		2			2		1				1					4		
235.50					1		5			8	2	2										1	
235.00					1		4			6								1					
234.50					1			1		6	4	3										1	
234.00					1		3			9	3	4									1	1	
233.50					1		5		2	4		1				1							
233.00					1			1		4		1											
232.50				1							1					1							
232.00										1	1	3									5		
231.50																	1						
231.00										8		1					1						
230.50							4			2		2											
230.00	3	5		12																	1	5	
229.50							2					2									1	1	
229.00					1		8			2		1	1					2			1	2	
228.50		1		1			2			3		1				1							
228.00					2					5	3					1					2	1	
227.50							2			4		2									1		
227.00	2									7						1		1				1	
226.00							2																
225.50							4			3		5											
225.00							4			9		7									2	4	
224.50							1			9	3	1											
224.00	1	4		6			1			1		2					1						
223.50								2		1							1				6	1	3
223.00				2			2			1	1	5									2	1	
222.50							1	1		1								1			3	3	

222.00					1		2			4		4			1						2		
221.50					1			2		3							1				8	1	1
221.00							4			1											6	3	
220.50							1			3	1										1		
220.00							3			2		3									5	1	
219.5							1	2		7											1		1
219.00							2					4									2		
218.50							6	1		7		3									3	1	1
218.00		1					4			10		3				2					1	1	
217.50							2	2													2		1
217.00							3	2		3	1	1				1					1		
216.50					1		1	2		4		3											
216.00					1		1			4		2										1	
215.50							6	3		2	1					1					2	7	
215.00							3			2		1										1	
214.50							1			3													
214.00										5	2	2											
213.50							3			5		2									3	1	
213.00							2			3		2									1		
212.50										1											2		
212.00												1				1					4		
211.50							2																
211.00							3			1													
210.50		2					6					2									6	3	3
210.00							7	1		1	2	1									4	1	
209.50										2											3	4	2
209.00								3		1		2				1					1		
208.50				2			1	3		4		1									4	5	8
208.00										1		3									1		
207.50																							
207.00							2														1		
206.50								1															
206.00							5																
205.50							5	1													3		4
205.00							5									1							
204.00							1	4		1											1		
203.50							4	2														1	2
203.00							4			2						1							
202.50								1				2									3		
202.00							2														1	2	
201.50							2	5													2	6	2
201.00																							
200.50							5	8													3	5	4
200.00							2	3								1					8		
199.50																					3	2	
198.50							2	1													1	3	1
197.50							3	3		2		4											5
197.00								2															
196.50								1															3
196.00								3		5		3										3	

195.50							3	1				2									1	2	5
195.00								6													1		
194.50																							
194.00								1													13	3	
193.50				1																	3		
192.00										1											2		
191.50										1						1						1	3
190.00																					1	1	
189.50																					1	2	
189.00				1																	2	1	
188.50							2	1				1									2	5	
188.00																							
187.50		1																			9		1
187.00								1				1									1		
186.50								3									1				2	3	
186.00																					5	1	
185.00																2							1
184.50								2													3		
184.00								1				1											
183.50							3	3								1					2	2	
183.00				2				3		1											2		
182.50		1					1	7													4	2	1
182.00		2										1											1
181.50		4																					
181.00																							
180.50												1										1	
180.00								1		2													2
179.50				3				2		1											2	1	1
179.00				1				4															
178.50																						3	
178.00								5		1													
177.50							1	2			2	1									1	1	
177.00							2	5		1		2											
176.50		2		3			6	4		4							1				9	15	1
176.00				1			1	1		1		1									2	1	
175.50							1														9	13	9
175.00										5	2	2									2		
174.50				2				4		1											4	1	
174.00		1						1													2	9	5
173.50				4				2				2										5	1
173.00	3			3				4		1											4	4	
172.50				2				4		5												1	
172.00				1				1				1											
171.50				1				2		4												7	
171.00								4				1										2	
170.50	3			1																		3	
170.00	5			2				2													1	2	
169.50	3																				1	2	
169.00				4				2		1											2	4	
168.50					1		1	2		1												1	1

168.00																				2	4	1
167.50	3							1														
167.00	5			5						1												
166.50	2	4		2			3														7	
166.00	2			4				3		1												
165.50	2						2	1														
165.00	2			3			2	8														
164.50				8			1	9												2		
164.00				6				2													4	
163.50	2			10																	2	
163.00	5			5			1														4	
162.50	4			6				3		1										5	5	
162.00	2			7				4												1	1	
161.50				6								1					2			3	16	1
161.00	2			2						1												
160.50	1			8			1	3												1		
160.00	5			7			2	2												1		
159.50	2			6			1	5													3	1
159.00	1	1		9				2			1						2				7	5
158.50				1			1	4												2		1
158.00	11			6			4														10	
157.50	1			5				3				1									3	
157.00	3	2		17								2								5	5	2
154.50	9			13			3	3														1
154.00	6			3				2									1				3	2
153.50	6			10				1				1								1	6	
153.00	4			12																2	2	
152.50	3			16				2												3	2	
152.00	3			4				5													1	
151.50	7	2		5																2	12	
151.00	4			10																	1	
150.50	11			11				5												3	1	1
150.00	4			10				3													4	
149.50	5			13				3												6	4	
149.00	8	2		7																	10	1
148.50	9			14				2				1								4	8	
148.00	4			20			1													1	6	
147.50				4			1	4												3	5	
147.00	4			16			1	4												5	8	
146.50	5			8			1													3	10	
146.00	10			6				5												4	11	
145.50	5			11				4												7	13	5
144.50				11				3												1	7	2
144.00	5			5				3												6	11	7
143.50	5			14			2	8												4	7	
143.00	2			7				8												1	10	2
142.50				9				7												4	5	1
142.00				8			1	8												3	2	
141.50	2			11																	6	
141.00	2			17			1	6												6	3	2

140.50	3			13			1	2													2	2
140.00	4			7				5												1	1	2
139.50				7			1	10												3	3	1
139.00	1	1		2			2	4													5	
138.50				2			1	7													6	6
138.00	1			5				2												2		1
137.50	4			5			2	1												1	4	3
137.00	6			4			1	3												3	1	
136.50	2	2		7			2	1													5	4
136.00	6			4			2	1												1	10	
135.50	3			6			1	10												2	9	
135.00	1			6				7												2	18	2
134.50	2			8			2	4												6	6	
134.00				6			3													2	5	1
133.50	3			9			6	4												3	21	9
133.00	7			5			4									1				6	17	3
132.50	3			6			2	5												1	9	3
132.00	2			4			2	6												6	19	2
131.50	2	1		3			4	2									4				4	2
131.00	2			4				4												3	9	2
130.50	3			4			1	6												1	9	
130.00	6			10			5	3												4	6	
129.50	6			7				6												5	12	2
129.00	8	1		8			3													3	2	
128.50	1			5				5													7	
128.00	3			7				1												2	11	1
127.50	5			6			1	3												1	17	
127.00	3	2		11				2													14	
126.50	4			3		1	2										3				1	3
126.00	2	3		10	1			1										1		1	11	
125.50	5	3		2				2												5	13	
125.00	8			3				5													7	3
124.50	9			6				4												1	2	
124.00	10			5				3												1		
123.50	6	3		5			1	2												10	11	
123.00	7			9				7												7	2	1
122.50	10			19				6												4	5	3
122.00	6			18				2												7	1	
121.50	6	2		9			3										5				7	2
121.00	8	2		10				7												12	3	4
120.50	2			3				6												5	6	4
120.00	6			7			1	2									1			6	9	2
119.50	6			4			1	2												12	7	5
119.00	8			12			3									1				11	8	
118.50	7			5				2				1							1	4	19	1
118.00	4			6			3	1												5	14	
117.50	3			6				4												5	27	5
117.00	7			4			2	3												6	17	7
116.50	5	1		7			2										3			3	8	6
116.00	12			8			3													2	20	5

114.00	8			8			3													3	5	
113.50	3			5			1	1												6	14	2
113.00	2			7		1	1	3								1				2	18	4
112.50	14	1		7																5	11	
109.50	7			10			1													1	9	
109.00	4			10			1										1			2	7	
108.50	13			7			1	2												2	2	4
108.00	6			6				8								1			1	7	8	
107.50	5			9				1												4	1	4
106.50	5			7													3				8	1
106.00	5			4			2	10								1			1	4	5	3
105.50	17			4				4								1				14	8	6
105.00	11			5				4									1			21	8	3
104.50	9			2				2								2				9	9	
104.00	12			2														3		12	8	
103.50	8			2			1	4												15	14	5
102.50	6			5				3												9	15	9
102.00	3			3			3	1												7	16	13
101.50	3			4			6										4			5	17	10
101.00	2			6			2	2												5	21	10
100.00	6			2			1	5								3				3	15	12
99.00	6	1		2			1													3	4	2
96.50	1	2		8			2									1				1	7	8
94.00	7			7				5												3	8	1
91.50	6			8			1													1	3	
88.50	15	1		5				5												2	1	
86.50	12			17		1														2	5	
84.00	20			9				2				1								1	4	
81.50	5			9			3													10	10	
79.00	8			8				2												1	12	1
76.50	13			9			6													2	11	1
74.50	13			7				1												3	13	1
71.50	4			6				1					1								39	4
69.00	9	2		1																	77	
66.50	4			8				5							1	1				1	5	21	
64.50	28			33																	34	1
61.50	21	4		29																	11	
59.00	12	1		18				8												1	17	
56.50	9			11																	6	
54.00	21			14																4	19	
51.50	10			6																	4	3
49.00	28			13				1												9	57	
46.50	2			6																		1
44.00	21			5			2	1													12	3
41.50	18	1		12																	7	
39.00	111			12	5														5		9	
36.50	100	6	6	36											2						3	1

Bulimina aculeata	*Bulimina alazanensis*	*Bulimina costata*	*Bulimina elongata*	*Bulimina mexicana*	*Bulimina subulata*	*Bulimina* sp.	*Burseolina calabra*	*Cancris auriculus*	*Cancris* sp.	*Cassidulina carinata*	*Cassidulina crassa*	*Cassidulina laevigata*	*Cassidulina* sp. 1	*Cassidulina* sp. 2	*Cassidulinoides bradyi*	*Ceratobulimina* sp.	*Chrysalogonium* sp.	*Cibicides lobatulus*	*Cibicides refulgens*	*Cibicides wuellerstorfi*	*Cibicides* sp.	*Cibicidoides dutemplei*	*Cibicidoides floridanus*	*Cibicidoides incrassatus*
9			5		5			1	4			1						3	1		8	5	5	
8		6		1	14	4	14						6								4	9	5	
		1					3				2										9	12	10	5
1				1			4				2	1									7		5	2
19				7	56	7			1		1										5	2	1	
6				6	10	3	2		1		1									1	3		3	2
2		3		5	2		7				14									2	10	2	2	2
	1	4									3								1					
	1	8	1	7	16		3		1									1			6		2	1
4		2	3	4	20		4				1										8	1	1	2
3		4	2	10	18		1														10		2	
2		4		9	11						2		1					1	2		7		7	2
1		7	3	4	18				1		1										9		5	1
8		1	1	4	21																5		7	2
5		7	1	10	29																7		5	
5		6	3	10	16						1							1			6	1	5	3
2		2	2	4	17																7		8	
10				5	52				4		1										5			2
1		7		4	4		5		1				5								3		5	3
		9		6	15								2						1				5	
2		7		11	5		3		1		10										5	1	12	2
5		16		12	4						6				2						2		3	
8		4	2	4	41						5						1				3	2	5	1
15		8		11	14						4		2					2			3	1	3	5
8		5	2	3	31				1		5								1		6		13	2
2		14		10	12		6				2							1			2		18	
		11	1	6	3							2									6	7	10	
9		1	1	8	33		1		2		7		1								4	2	14	
7		3		8	39		4		1		5										4		7	1
		2		2	20		2		2		5							1			3	1	20	3
3		9		3	44				1		8											3	6	2
		3		4	12		2				4										5	1	11	2
1		7		5	34														1		2	1	14	1
5		7	2	4	19		5		1		5										3	1	14	3
3		6		7	27		2				5												3	
5		4		1	31		3				4										2		6	1
		4	2	3	15		4		2		5							1					14	
4		8	1	7	18		4														6	5	14	1
		1	5	4	23	6	4		2		1								1		2		2	
13		5	1		44	5			3		12										5		8	1
5		2	3	14	21	4	8		3		11										4		1	1

1		3		8	14		4		3		9							1			2		4	
5			1	8	33	3	3		2		3										13		2	2
6		9	3	5	24	1	1		1		2										1	2	1	
5		4		8	34																	1	4	1
		8	1	6	29		1				1										9	5	9	
1		1	3	3	27	10	2											1			4		5	
8		2		4	42	4	7				1										5	6	4	
7		1	7	6	54	9	2				3										8	1	3	3
5		2		12	12	4	7														4	1	2	2
1		14	2	26	36	1	1				1										2		3	
11		1	2	2	31		1				2										1		10	3
9		5	1	9	18	4	10														5	2	4	
7		10		7	32	5	8														8		1	1
15	1	11		4	32	8	1														17	1	10	1
6		3		2	11	1	1														2		2	1
1		1	5	3	11	6	10														1	1	4	
5		5		7	52																2		2	6
10		3	1	2	17	4	8		1						2						3	2	6	1
14				5	24				2									1			5		3	
8			2	3	10	3																	1	
1		1	2	4	21														1		6		2	
3		2	1	11	22	7							2								2		5	
3		2	1	7	55	4			1						1						1			3
8		5		8	37	5															2	5	2	
6		2			38	3			2													5	4	3
9		5	5	5	36	11	1		1												4	1	2	
2		1	4	5	38						1										2	1	4	2
1			5	9	40	4					1				2						3		2	
10		3	5		40	4									1						2	1	5	1
1		1			42				1												3		1	
5		1	2		34	6															7	2		2
3		1	4		24	8	1														5		2	1
2		1	1	3	35	9															1		1	1
7		13		6	22	3												1			8		2	
5				2	23	1															11	1	5	
4		5		3	34	7															5	1	1	
5		4	2	5	15	8					1		1								4		3	2
3		2	2	3	24								2								1	2		2
3		3	1		21	5							1								7		1	1
1		1	2	2	45	2			2								1				4	1	5	6
7		1	2	7	24	11			2												5		1	
		1			56				2												16	1	11	1
8			4	1	25	5	1		1												2		5	
4		4	3	1	41	6			1												6		5	
4		2	1	3	14																6		5	6
3		1	2	2	26	2															9	1	5	2
10			3		29	6																	3	4
1			2		29	3															2		5	5
3		1	2		31	3			1												4	1	3	2
9		3		1	16	4					1							2			7		5	1

8		3	3	1	28	4															6	1	5	2
3		4	1	2	37	6					1										4		1	
		2		3	38						1							1			7		9	
16		12	5	6	39	11					1							1			6		7	
6		5	2	13	34	5												1			4		5	
7		6	1	16	39	4															7		3	
3		2	2	3	27	2															2			1
1		3	2	2	35	3					1										6	1	1	
7		4	2	4	21	7								1									3	3
6		1	2		34	6						7		3							4	1	5	2
		7	8	5	30	5															2	4	1	
		2	1		40		1		1			1									5		3	
9		4	2	8	28	7			1												7	3	5	6
2		6	5	7	34	6			1												3	1	3	2
5		2	5	2	25	5			1												2	3	7	1
7		4	2	1	28	6															12	3	2	1
1		4	2	5	36	7															3		5	2
8		3	4	5	22	7															6	4	4	
1		3	1	9	22	8			1												1	1	1	3
5		1	2	1	24	3															5	4	6	
2		3		1	50	7															6	2	6	1
4		6	3	4	23	3															4		5	
			4	6	31	2	3														3		1	
		3	1		39		8							1					1		3	2	4	
1		2	1	6	21	3	6														5	2	2	1
		4		2	21	3	1														4	3	3	
5		1	4	2	20	12															18	2	3	1
		2	1	4	22	11															5	3	10	1
3		3	2	4	33	2			1												6	5	2	
		3	2	4	15	3															7	10	9	
5		1	6	8	34	4	15					2									4	3	4	2
5	1	3	2	8	35	4	3		1												5	2	7	
7		1	4	3	27	4			1												8	1	1	
7		2	4	12	13	5			1												3	9	5	
14		1	2	5	19		2											1			12	13	5	
1		6		3	8	5	4														6	5	4	
		15		27	47		64														26	18	26	
9				17	8	1	32								2			1			6	6	19	
2		5	1	14	12	1	12		2												5	3	8	
21	1	2	3	5	31		12														7	2	10	
20		7		6	29	2			3						1						5	4	4	
16		5		6	31		1		1							1					4	3	6	
20		4	1	3	16	3	1								1	1					9	3	9	
3		1		4	14	7			1												11	5	12	
16	1	2		1	8	1															8	11	7	
1		2		5	2																4	13	18	
2		1		5	5		1					1									6	13	16	
8		1		6	17	12															8	12	11	
10		4	5	4	21	7	1							1							5	6	3	
16	1			5	13	4	15		1						1						7	15	13	

12				5	10	5	38							1							3	14	13	
25	1	3	5	14	10	1	45								2						10	11	8	
29	1		1	11	10	4	22														7	15	17	
3		4	5	11	17	10	19														8	10	8	
15		7		13	16	6	5															3	14	
17		8	1	14	3	3	1		2												4	9	9	
24		6	1	8	19	8			1						1						5	7	6	
24		2	2	9	10	4	1														7	6	18	
4		5	5	8	25	6	5		1												4	5	7	
28		7	1	14	23	7	5														5	9	10	
21		9	1	16	15	3	9														4	9	12	
21		11	2	13	18		13					1									6	22	12	
14		10	2	5	13	7	8					1									8	4	9	
10		6	5	9	15	6	24								1						4	5	11	
16	3	2		5	8	7	16														11	3	14	
14		5	3	1	3	4	29														7	10	12	
8		6		17	1	1	20														9	5	13	
15		11	2	6	5		11														5	5	7	
4		5	1	16	12	4	1		1												9	5	14	
19		3	1	12	5	2						1									11	6	9	
18		3		9		1			1						1						11	4	14	
14		5	1	7	4	6															2	10	15	
6		11	4	4	15	3															6	4	8	
10		3		2	2	4															19	5	13	
4		10	5	5	18	4						1							4		16	10	16	
32	2	4	6	6	13	8															7	8	21	
27		9	3	4	13	8															1	2	16	
23		6	2	2	7	3			1												1	5	16	
18		11	2	3	10	4															7	4	25	
8		6	3	4	10	9															5	1	26	
20		7			8	4															15	9	16	
35		16	2	10	7	4								1							6	10	13	
28		10		4	5	3								1							7	5	18	
34		10	1	4	5										1						6	7	10	
15		5	6	5	20	6		1													1	5	21	
28		13		6	8	1															11	4	21	
26		14	4		8	3															4	6	14	
22		13	6	1	16	4															15	8	15	
21		18	5	2	3										1						9	12	16	
17		3	6	15	7	4															2	1	16	
30		12	1	2	9																5	3	16	
39	1	18	3	12	2																4	2	9	
55		16	10	10	3																11	5	23	
20		11	3	5	9	5			1		2										5	3	8	
41		9	1	8	2	2															8	7	10	
27		5		2	7	1															13	4	11	
23		5		3	7	2															9	4	11	
38		9	1	1	3	1															10	6	5	
11		9		7	18	5					1										7	14	14	
18		6	1	7	5				1												9	8	7	

24		9	5	3	4	1															8	8	10	
27		8	1	9	1				1												8	22	9	
22		22	1	7	3	2									1						15	17	20	
8		12	6	6	21	2															8	6	17	
34		17	1	5	6																3	7	12	
32		19			4	1															15	15	7	
19		11	1	3	4																8	18	17	
17		8	1	1	1																9	13	11	
3		10	2	4	11	3															7	9	17	
16		10	1	2	4																11	8	8	
30	3	20		1	1	1															5	6	7	
18		13	1	4	1	1						1									4	19	5	
18		10	1	8		1															6	15	12	
11		9	6	16	7	1									1						3	4	11	
20		13	2	6	1	1			1												6	5	10	
15	1	7		6	1																13	11	9	
14		7	1	4	2																10	15	16	
31		6	3	5																	4	5	9	
10		5	3	9	19						2								1		7	3	7	
16		8	2	2																	2	7	6	
11	1	5	2	4	2	1			1			1									9	2	13	
14		6	4	7	1	2			1			4									2	2	8	
4		9		17								1			1						9	9	9	
2		4		15	2							1									3	9	19	
3	2	9		10																	9	11	21	
1	1	5	2	5								1			1						5	8	22	
7	1	12		10								1							2		13	8	7	
5		8	1	15	2														1		9	20	15	
2		3	3	6	10						1	3									2	3	6	
9		5		9																	6	10	6	
11		5	4	9	1																2	7	15	
4		7	1	13	2				2												4	6	8	
5		2		10	1				1												8	14	10	
		2		4																	1	7	6	
7		7	1	7	1				1												5	7	8	
13		7	1	4	2																7	8	9	
11		2	1	4																	3	10	7	
11		3	1	5	2																1	9	18	
13		5	1	8	14						1	2	2				1				5	6	18	
11		7		5	2								4								1	6	9	
12		4	1	9	1										1						5	10	14	
24		15	1	3	2								3								7	9	7	
32		3	1	11																	5		3	
5		4	1	6	9																2	12	8	
6		3		3	3																2	6	7	
13		3	2	6																	4	17	13	
28		2		6	1																4	5	14	
27			1	4	2														1		1	8	11	
4		5		3	9							1									2	7	16	
23	1		4	8								7			1						5	5	11	

20	1	2		7	4	4															3	5	13	
16	1	2	1	6	1																8	6	12	
14		8	2	6																	6	5	9	
5		3	1	2	3							2						1				5	14	
9		3	3	4																	6	8	10	
3		3	3	9	3				1		1								1		4	12	19	
5		8	3	8	1				1												8	16	14	
4	2	4	3	18								1									4	6	6	
8	4	10	2	4																	8	6	3	
	1	5		10	8																3	2	12	
22		7		17	5						1										3	8	1	
31		13		8	3										1						12	11	6	
23		13	3	7	1																11	5	4	
19		11		8	1																7	1	3	
12	1	9	4	10	4																3	4	5	
8	2	11	1	3	1							1									11	6	13	
18		5	1	9								1									13	6	3	
9		12		5	1							9									14	5	3	
2		9	1	4	5	2						17		1					1		3	4	6	
3		8	3	12							1	10									12	7	9	
		3		4					1			5									19	6	16	
11	1	2		9	2									2							2	10	16	
2		4	1	5	12						2	7									5	9	25	
7		6	3	19	9							1			1						10	7	16	
2		7		15	4				1												4	5	20	
20	1	7	6	7	2							1									3	4	8	
7		5	4	2	17	2			1			1									4	4	8	
17		7	1		7				1		1	3			5						1	6	25	
10		4		9	5	4		2		3	3	3									3		14	
15		7	7	4	2							4									2	4	24	
19	1	1	4	9	11	1			1		2	1		1								3	9	
13		7	9	4	1	3							6	1							5	5	6	
10		1	2	2	9				1			2						1			5	5	48	
10		5	4	5	1	1						5									5	12	55	
1		3	4	1	7						2		4								2	3	21	
		11	14	1		6						8									2	8		
10		3	8	6	2	1						11		1								15		
16		2	41	3		2						9										7		
4		1	14	4	5				1													7		
9			45			1						7									1	10		
2		12	11		1				1		1	13												
2			10	1																		3		
4			16			3						18												
8			4									42						2				5		
6		14	21	3								21									1			
9		5	5			5									1							3		
8			10			1			1									1	1			4		

Cibicidoides kullenbergi	*Cibicidoides pachydermus*	*Cibicidoides ungerianus*	*Cibicidoides* sp.	*Cymbaloporetta squammosa*	*Dentalina aciculata*	*Dentalina inflexa*	*Dentalina leguminiformis*	*Dentalina* sp.	*Dimorphina* sp.	*Discorbis* sp.	*Dorothia gibbosa*	*Eggerella bradyi*	*Elphidium advenum*	*Elphidium complanatum*	*Elphidium macellum*	*Elphidium crispum*	*Elphidium* sp.	*Eponides* sp.	*Fissurina* sp.	*Florilus* sp.	*Fursenkoina schreibersiana*	*Glandulina* sp.	*Globobulimina affinis*	*Globobulimina ovula*
			4										1	3	3		18							1
	38	1	18				1	2																
	55	1	28				1																	
8	34		34															1		1				
	33		32					9		1										2				
	36	1	22					1																
11	83		24																	1				
	54		47					1										3						
	54		31				3	2																
	67		31																					
	94		31					1																
	64		19					3								1	3		2			1		
	77		19				1												1					
	59		25				2	1																
	47		14																3					
	45		21				1					1							1					
	65		10			1	1												1	1				
	53		24					3											1					
	80		23									1							1	1				
	86		11				1	1											4					
	62		14																2					
	51		22					1											1					
	41	1	19					4											1					
	68		21				1	2											1					
	57	2	17																1	1				
	75		15					1											1					
	119		30														1		1					
	44		14					3									1		1					
	88		19					1											2			1		
	86		17					1											1			1		
	42		14					1											1	1				
	43		17					1											2	1				
	67		37				1												1					
	61		14																3					
	52		12			2		1											1					
	44		16																					
	51		10					1									1		2			1		
	76		28					1															5	
	56	1	11					1											1					
	41		17					1												1			3	
	35	1	18					2																

	48	1	17																2					
	51	1	13					1											1					
	56		21					1				1							2	1			5	
	43		27																1					
	91		30				1	1																
	62		21					2																
	72	1	27																					
	82	2	23					3												1				
	84		24																1					
	61		17	1				1															1	
	48		18					1																
	71	1	25					1											1					
	52		15																			1	1	
	90		22	1			1	2											1					
	56		17																					
	88	1	18																					
	68		20					1		1														
	83	1	29																1					
	101		19					1																
	24		10																					
	34		9									1												
	63		17				1																	
	47		26																	1				
	81		23																					
	92		23					1												1				
	86		28					1											1			1		
	85		18					2											1	1		1		
	77		22							2														
	91		21					2																
	42		24																1					
	64		19																				2	
	42		24																1					
	40		15																	1				
	37	1	11					1		1														
	78		23					1											1					
	66		18					2																
	65	3	30																					
	99		22																					
	74		36					1											1					
	64		29				1	1											2			1	1	
	83	2	33					2											1					
	59		34									3							1					
	42	1	28				1	3																
	53	2	18						1															
	71	1	29					2																
	96		25		1			1											1					
	85		20																2	2				
	98	2	33																1					
	105	2	36																			1		
	73		28					2																

	65	2	38																	2				
	51		17				1																	
	57		30									2												
	45		16																1	1				
	89		28																	1				
	116		28					2												1		1		
	102		27																					
	98	1	20																					
	107	2	38																	1		1		
	121	3	44																1					
	95	4	30																	1				
	68		57																					
	89	6	41					1											1					
	102	1	21																	1		1		
	80		22				1	1															1	1
	108	1	31																1					
	104		44					2																
	97	1	41					1																
	115		34																					
	102	2	42					3																
	162	7	39																					
	78	1	24																					1
	111		30				1																	
	74		53									1												
	113		45																1					
	111	1	44																					
	105		30																			1		
	85	6	36																					
	93		38																					
	115	7	38					1																
	98	3	33					1																
	55	4	32					1																
	64		26					1											1					
	71	1	31																2	1			4	
	87	2	35																1	1				
	99	3	38					1																
	264		87																2					
	103		44		1			1											1					
	82	1	38					4											1				2	
	74		21					3												1				
	97		31																1					
	79		23					1											2					
	96	1	40																1					
	109	1	34															4						
	93	1	40					6																
	149	2	39																					
	131	3	36																					
	124		37																			3		
	137	4	40																					
	92		32					1			2													

	106		33					2																
	98		25					1														2		
	87		21		1																			
	117	1	40					1												1				
	72		22																1			3		
	69		16					3											1			2		
	51		19																			1		
	85		29																					
	89	2	25					1										3	1			1	1	
	74	1	18					1									2					2		
	93		29					1											1			1	2	
	101		16					3									1							
	78		16																					
	67	4	31					1										2					2	
	100		32	1																				
	136		23																					
	117		47																					
	94		34	1				2																
	108	5	38																				1	
	111		28					1											1					
	70		24																			2		
	127		30					1																
	51	6	32															5					1	
	100		27					1																
	80	5	31															1		1				
	54		21																					
	65		24																			1		
	75		21		1																			
	93		23																					
	68	5	33															3					1	
	82		29																					
	79		23					1																
	74		18					2														1		
	50	1	25					1														1		
	42		35					2										4						
	68		26					3																
	87		23																					
	70		23																					
	94		23					1																
	92	1	31				1											1					2	
	92	1	27																					
	63		13																					
	85		14																					
	78	1	28																					
	86	1	12																					
	79	1	19																			2		
	108		37																			1		
	98		23					1																
	112	1	55					1												1				
	114		28																					

	92	2	27	1																				
	97		32																					
	81	1	17																					
	87		17														1							
	75		19					2																
	89	2	23																					
	100	1	26																		1			
	97	4	34	1				1																
	99	7	39					3																
	163	1	31					3																
	109		25																					
	100		24					2																
	119	2	13																					
	102		28									1						1				1		
	104		23																					
	128	3	27																					
	98		23																					
	109	1	28	1																				
	95	4	24				2										2							
	106	3	20																1					
	144		27					1																
	83	1	21																		3			
	85		18																					
	120		28																					
	100		27					1													1			
	88		25																		3			
	88	2	21	1																				
	124	5	29				1														1			
	99		37					1									1							
	117	1	33																					
	119		25					2										1	1		3			
	96	2	26																		1			
	94	1	28	2				2													1			
	120	1	26				1																	
	81		23																1					
	105		18					1													1			
	107	1	25																					
	146		32		1			2																
	107	3	34					1									1					1	1	
	108		18																					
	96		17																		1			
	95	1	13					2										1						
	98		13					2										1			1			
	76		14																					
	105		10																					
	82		19				1																	
	99		22																					
	112		21					1										1						
	96	4	31					1									1		1					
	78	1	13					3																

	128		18	1																		3	
	88	2	13					2															
	107	2	19				1	1															
	88		28														1				1	1	2	
	93	1	23																				
	85		31																				
	92	2	21					1														3	
	59	1	20					1														1	
	77	3	19																				
	73	3	46					2										1	1				
	136		26																	1			
	181	1	38					1															
	143	1	18	2				1															
	79		20	1				1											1				
	90	2	13																			1	1
	75	3	19					1															
	85	3	8																	1			
	88	5	16	1																			
	61	3	22					1															
	104		14																				
	98		10					1															
	99	1	13					1														1	
	72		21					1										1					
	107		21				1	2															
	71		40																				
	77		25																2				
	86		35					1														1	
	76		20					1															
	56		31				3															2	
	61		17														1					1	
	55		29					2															1
	87		18					2									1		1				
	34	1	32																				
	38		29					3															
	34	1	36																				
	43	1	10					4													2		
	19	2	12				1	1															
	14	2	15														2				8		1	
	3		11				1	1													6		1	
			5																		8		1	
		1	1					2													8			
		2	13								2										18			
																					26			
	1	2	7								1								1		8		3	
		3									1										6		1	
		1	9								4						9				4			
							1				1						11				4			

Globobulimina sp.	*Globocassidulina oblonga*	*Globocassidulina subglobosa*	*Globulina* sp.	*Gyroidinoides laevigatus*	*Gyroidinoides soldanii* s.l.	*Gyroidinoides umbonatus*	*Gyroidinoides* sp.	*Hanzawaia boueana*	*Hanzawaia* sp.	*Heterolepa bellincionii*	*Hoeglundina elegans*	*Lagena costata*	*Lagena striata*	*Lagena* sp.	*Laticarinina pauperata*	*Lenticulina calcar*	*Lenticulina cultrata*	*Lenticulina curvisepta*	*Lenticulina echinata*	*Lenticulina inornata*	*Lenticulina rotulata*	*Lenticulina spinulosa*	*Lenticulina vortex*	*Lenticulina* sp.
								8						1										
1		17	1		8		2	3						1			1	2						20
		21			2		3	1																4
		27			2		5	1										1						3
		4		1			1																	3
		10		4	4		1	1			2													5
		43			3			1																3
		3		1	2			3										6						1
		9		1	11								1	4										9
		11		2	9				1															3
		9		1	1		1							2			1							9
		13		1	6			2	3					1				1						11
		31					1	3						3										1
		11	1					5	1															2
		2			4			7			3			1				3						6
		3		1	10			1			1													6
					18			4			7			1				1	1					14
		2		2	3			2			1			4				2						6
		1			8			4			7			3						1				9
		1			28			4			2			1				4						14
		2			2				2		4													8
		1		2	6			6	2		3	1		1				1					1	6
		2		2	1			1			1			1				1		1				4
		12		3	1			3			1			1										10
		1		1				3			1							1						2
		15			2			5						2				3						9
		19			5	1		6			3			1										5
		18		5	4			2			2	1						1						8
		4		1			1	2	1		4													7
		13			1			10			2							3						9
		2		3	2			8			5							1	1					6
		3		3	1						1			1										6
		13			4			6						1										5
		8		2	3			9			2			1										6
		10		2	3			7			2							5						2
		3		3	10			6						1										1
	2	6			13			3			2							1						7
1		8		1	2	3		2			2			1		1								8
		7	1	7	8	1		4	3		3													7
		1		1	3			6			6			1										3
		9			1			5						1										8

		18			1			3			1			1										8
		23			2			6			1													5
		17			4			5										2						9
		4			3			2			1													2
		15			2			1			1											1		5
		16		1	1						2													6
		20			1			3						1						1				3
		4		2			2	5			1			1	1			2						9
		25			3			5										1						3
		8					1	7	3		3		1	1	1			2					1	8
		10		3	1			3			2													7
		6					1	1						2										5
		6		6				3			1													6
		2			2		2	11			1													7
		2		1	2																			7
		13		3	1			2			2							4						9
		6		1	1			3	1					1				2						4
		3			6			2										3						6
		1			1			2																8
								3			4													7
		1																						2
		7			1			7			4												1	8
		9									1			1										11
		4			4		1	9						1										9
		3			3			1			9			1										12
		1					2	5			6			4										6
		9						2										2					1	4
		14						12			1													7
		16			1			5			3							1						8
		10						1									1			1				
		20			1			3			1						1	2						11
		8			1		1				2							1						8
		9			5			3			2			1										9
		7			5			5			5													7
		25						2						2										8
		15			2			2			3			2										8
		20			1		1	2			4													4
		16									5							2					1	8
		2			3		4	3			2			1				2						8
				1	4						9			1										6
		1			2			1			2													6
			1		2									1								1		6
		7			2													1				1		6
		10			1						2			2										9
		2			4			2			3			2				2						8
		3			2			3			3							2	1					10
		2			2		1	3			2			1										12
		1			3			1						2				1						4
		1			1			3			1													11
		2						4			2			2										10

							1	4			2			2				1						7
		3			2			1			2			1										11
		1			4			1						2						1				4
		1			3			2			7			1										5
1		1			3			4			2			1				1						10
		7			3	1		5			1							1						13
		15			4			11			1			1				1						6
		12			5			3			1			1										7
		12			1	2		1	1		2													2
		4			1		1	7			2			2				1						9
		4			1		2	5																18
		5			2			1						2										
		5						9																5
		14					1	3			3			1										6
		15			5			11			1			3										4
		6						8			2			1										7
		9			3			5			1							1						11
		8						7			2			1				2						8
		8			1		2	3			1			1										10
		4			2			5			4			1			1	2						10
		4						9			26			1										7
		10			2			7								1								10
		7			1			3						1										9
		5			3			5						1						1				3
		6			1			3			2													6
		8			2			11																14
		3			2			1			3			1										5
		3			2		1	3																6
		2		2	1			3																8
		6						6			2							2						8
		8			1		2	3																8
		9			1			8			2							1						9
1		12				1		4			5							1						14
		9	1		2		1	10			2			1				2						9
		5					2	3			2							2						8
		3					3	4						1										5
		11				2		5			3	5					2							15
		11			1			3			1							1						8
2		8			2			11			2													2
		5			9			8			2													16
		6			5			5			1			2										6
		22					2	6			2													6
1		19			3			5						1										16
		16			1		3	21										2						12
		7			1			7			2													6
		4						2			1							2			1			8
		7						6			2													10
1		6					1	1																7
2		5						4			3													3
		11						4			2			2		1								10

1		9						7								1								6
		14			1			2			2													9
		4						2						2				1						8
		3						10										2						6
		1					3	11			1													11
2		3			2		1	18			1			3										16
		9			3		3	7			1			1							1			12
2		9			3		2	9			3			1							2			16
		1			3			11									1	2						12
1		10					1	9			2													9
		8						5						1			1	2						12
		6			5	1		8																10
		10			3			6																14
		4			4			4			2							2						10
		3			3		2	7			1													8
		4			1		2	3			1			1										10
1		2						4			2												1	10
3		4					2	2			3			1										16
		7			2			5			5							1						13
		5			2			4			3													14
3		8			4			5						2		2		1						19
		3			1			3			1			4		1								19
		5					1	5			4			1										8
		9					1	4			4			1										17
		2			4			8			2							1						9
		1					4	7									1				1			18
1		1					3	3			3					1		1						18
4							2	2			1													9
		9					4	5			3													11
		2						9			1													11
1		2					1	1			1					1								12
		2						6			2													20
1		2					3	8			2			2		1								14
3		10					5	3			11													17
1		1				1	1	5			3							1					1	11
5		8			7		3				4													17
					1			1																15
					7			1			2													19
		3			2						2													18
								1			3			1										14
		5					2	1			1													14
		2					2	3			2													16
		4			2																			7
		5			3			12			3													9
		6					1	2			3													13
		6			2		1	2			12													14
				2				2			1													11
		1					3	3			4													7
		2					4	2																14
		3				2		3			2													9

		3					4	6			2													9
1							1	8			2													11
2					2		2	10			2							1						15
		2			2			4			4													12
2		6			2		1	8			2							4						19
2		3			1		3	5			2													19
2		4				2	2	7			6							1						12
5		2					2	6			5					1								18
		2	1		3			3			4													12
1		2			1			7			3													11
1		4						4			2													12
1		2						5			1					1								9
1	1	6			1		6	3			2													11
		12			1			3			3							2						9
1		9			1		3	4																9
		7			2		2	8																9
	1	11			5		1	1										1						10
	1	10					4																1	4
		1			9			8										1						6
		8			2		5	3								2								14
		4			3	1	3	1			1													12
		5			4	1	1	6																9
		7			1	1	6	2								1								11
		6			13			2										1						11
		8			3	1	3	4			3													8
1		13			4	2	5	3			1					1								13
		12			1		4	5																17
	1	18			6		7	6			6							3						16
		20			10		1	9			1					1								9
		6		1	5		3	5			5					1								13
		5			1	1	3	6			3													15
		7			1			3			2							1						11
		8			2	2	1	3			4													15
		7			3			3			4			1				1						24
		8			1		1	4																33
		5			2		1	5			3													16
1					2		1	8			2													21
		3			3		1	9			3													12
		3			3	6	1	7								1					1			13
		10			1		1	7			1					1		1						24
1		12			3	2	3	11			2												1	15
4		22			6		1	11			1					1								17
1		6			1		1	19			4					1								5
		16			5	2		8			2													21
2	1	24			7		3	2			3							1						12
1		14			2	1		8			2													19
		13			3		3	7			4			1			1							9
1		12			3	1	3	7			1							1						6
		8			3	5		7			6													5
		12			7	6	6	5			1							2						8

		20			10	1		4			3			11										
		19			2	1	8	8			1												1	13
		8			8		7	5			1					2								5
		13			7	1		4			2					3								9
		12			5	5	5	8			2													11
		8	1		2	1		8			2													18
		9			1	1	4	4																9
		6			2		4	15			2			1										5
2		4			6	1	4	5			1			2									1	19
		4			7			11																10
4		8			3	1	5	10						1										26
1		6			3		4	24			3					1								14
3		5			3	1	1	19			6													12
1		2			2		1	12			4			1		1								16
		7			6	2		8			5													6
3		8			5	2	2	9			1			1										12
3		8			4		3	8			1			1										7
1		5			2	1	4	12			1			2				1				1		4
		9			4	1		13			1							1						8
		12			1	2	2	7																4
		10				12	7	13																5
		20			3	2		10						1		1								3
		5			4	2		20			1					1	1	2						9
		8			7	2		8			3					1								7
		14	1		7			15			1			1										16
		3			1	2		4								1		1						10
		2			3			21			3			1			1							15
		4			4	2		3			1													15
		4			7	5		21			4			3										15
		18			4	1	1	6			1			1										18
		3			4			17			1			1		2								15
		4			1	1		10			1													14
					3	2		9		12	3													4
		5			7	2		14			1							1						10
		9	1			5		19		1	7													17
					2	3		16																4
						3		7			5			2		3								9
		1				3		1						1		1								6
		1				1					2			1		3								8
							2	1								1								2
																2								9
						1																		3
																								1
5				3	4									1										2
						2								3		3								1
1				2	4	1		5						6		2	1							2
		1				3								2										

Marginulina costata	*Marginulina glabra*	*Marginulina hirsuta*	*Marginulina* sp.	*Martinottiella communis*	*Melonis barleeanum*	*Melonis soldanii*	*Melonis* sp.	*Neoeponides* sp.	*Nodosarella* sp.	*Nodosaria pentecostata*	*Nodosaria* sp.	*Nonion fabum*	*Nonion* sp.	*Nonionella turgida*	*Nonionella* sp.	*Oridorsalis umbonatus*	*Orthomorphina tenuicostata*	*Orthomorphina* sp.	*Pandaglandulina dinapolii*	*Planularia* sp.	*Planulina ariminensis*	*Planulina* sp.	*Plectofrondicularia* sp.	*Pleurostomella* sp.
											1	114		3			1		1					
			3	3	1						1					1	1				15	3		
				8	2		1									2					19	6		
	1		1	3	5		4			2						13					6	3		1
1			4	6	5		8			4	5				1	1					2			
1			3	10	6		10				3					8					1	1		1
				7	9											7						1		
1				1	8											4					20	1		1
1			1	2			3				3					8					12	4		
				1			2				1					8					22	3		
2			4	5	7		8				1					8					12	5		
				2	2		1	2			1					2	1				18	7		
			1	3	8		1	1			1					1					32	5		
				3	3		2	2								18					14	6		
3			3		3		1			1						7					15			
2					1		2				1					2					22	7		
			1	4	5						1					5					25	3		
			3	12	5		2	1			4					9					14	2		
1			1	2	4			1			2					3					22	8		
1			1		1											6					15	1		
		1	3	4	3		2			1	2					20	1				9	2		1
				2			2				1					21					22	3		
				3			2				2					28					16	3		
2			2	12	2					1						6					28	6		
				6			1	1								24					26	4		
			1	7	6		1									20					24	4		1
1			1	1	13		2	1			1					1				1	0			
1			1	5	4											18	1				25	3		
1		1	2	1	2		4	1			4					5					22	4		
3				4	1			1		1	1					2					37	2		
1			1	8			1	1		1						64	1				21	6		
		1	1	6	3		3				1					32					14	1		
1			1	1	7											23	1				19	3		
1				5						1	2					11					19	1		
	1		2	4	3		1				3					46	1				27	4		
	1			5	2		4			1						19				1	33	1		
1			1	4	6		1			1						24	1				35	2		
2				1	9			1			1					6	1				7	6		
				1			3									7				2	10	2		
				4	6		1			1	2					17					17			
1				2	4		12				1					18					6	6		

			1	6	6	1	5						1			37					16	6		
			1	4	3		6				2					14	1				14	5		
			1	2	5		1				2					9					34	3		
1			1		3	2		2			2					6		1			14	2		
			1	5	7											30					28	5		
				3	1		3				1					10					17	4		
				2	11		6	1			1					7					24	4		
1				4	1		3	1			3					5					20	8		
			1	2	2		3	1								7		1			24	9		
2				3							3		1			9					17	3		
2				6	2	1	2									12					13	2		
			1	3	1		3	1								15					10	5		
1			2	5	4		2	2			1					11	2				19			
1				3	10	2		5			1					37					22	4		
1				2	2		1									10					8	1		
1			2	2	3		3				1					8					17	1		
					8		1									6					44	7		
			2	7	5		2									4					16	4		
			1	7	3						1					9					23	4		
			2			1	1				2					3					4	1		
			1	1				1								8					14			
			1	1	1		1						1			2					8	1		
										2	1					16		1			18	2		
				5	2						6					6					6	6		
2			1	4												17					19	2		
				3	2		1				4					3					18	4		
1				7	1		3									18					18			
				6							3					7				1	13	3		
				2			4									9	1				17	5		
1	1			2	2		1	1			1					8		1			12	3		
1			2	4			4	1								5	1			1	20	2		
1	1			3	2		3				3					13					17	2		
2				7	1	3	1				4					6					13	5		
2				2	2		6				1		1			5					19			
1	1			4	1		3			1	2					3					33	7		
				4	1											5				2	21	3		
			2	1	2		3									3					22	4		
1	1		1	6	1			1								4		1			25	7		
				1			4				3					5					14	4		
			2	6	1		3				5					15					27	5		1
			1	2	1	1	5				1					6				1	22	2		
2	1		1	2	3	2	1				1					7					30	1		
1			1	2	2	2				1	6					10					7	5		
			4	7	1		3				1					5					17	6		
1	1			4			2									5					12	3		
	1						1				3					18					19	7		
				4	4	1	1				4					14					31	5		
1			2	2		1	6									12	2				6	2		
2				6	2		1			2	1					22					32	1		
1			1	4												7					17	4		

	1		1	4		1					1					8					19			
			1	5		5	7				2					10					9	5		
1			2	1	1	2	1		2							19					9	2		
			1	2	7	6										18					23	6		
			1	2	1	2	2				2					9					39	6		
				2	1		2				1					35					44	7		
			1	4	1		2				3					8					26	13		
				2	2											9					24	5		
			1	4							2					1					24	4		
					1		3									13					38	6		
3			1	4	4		9									8					14			
4						1	2	1								6					34	5		
2				2	2		8	1								6					35	9		
2			2	3			1	1			1					3					27	5		
1			2	5	1	2	5				4					7				4	22	4		
2				2	2		10				3					6		1			29	5		
			1	3			7				4					3					22	2		
				6	4		6				2	1				1					19	3		
4				1			12				4					6					21	9		
2			2	1	1		5				2					5					25			
			3	3			7									5					48	7		
				5	4		9			2	4					5					23	3		
1			1	2	7		15				1					8					27	6		
5							6		1		1					2					44	1		
6				3			14				1					2					30	5		
			3	2	1		10				1					4					24	3		
5			1	4	5		7				2					2					47	3		
1				3	4	1	17									2					27	3		
			1	1	4		10									3					32	10		
1				5	1		3				2					6					16	2		
			1	3	1		3	1								7					25	7		
				2	6		15				3					4					21	4		
			3	4	4	2	10				3					11					22	1		
				4	2		3				1					6					0			
			2	3	1	1	3				4					8					0	2		
2				4	1		2				2					3					0			
2			2	2		7					2					4					0			
2			1	2	2		3				1					2					0			
1				2	3	1	2			1	1					5					0			
2				12			7				2		1								1	1		
1				4	3	2	6									7					0			
1			1	2	13			1			1					6					1	1		
4				1	12		9				8					4					0			
			2	3	8	3	3									4	1				0	2		
2				3	3	3	8				5					1					0			
2				1	4		4	1								1					0			
			1	2	3		10				2					1					0			
					5	2	12	2								2					0		1	
3				1	4		6									1					1			
3			2	1	1	1	6	1					1		1	3					0			

			1		3		4				1		1			3					0			
3				3	8		9				5					4					0			
				2	7		9				2					3					0			
2					9	1	8									5				1	0	1		
3				4		2	3				2					2					0			
2			1	6	2	4	3			3	1					3					0			
4				3	3	3	9				2										0			
1				2	4	1	2				1					7					0			
2				1	6	2	4				1	2				3					0			
2			1	7	3	3	7				2					13					0			
3			2	4	2	3	7				1					10					0			
			1	3	3	3	8									10					0			
1			1	2		2	14									4					0			
2				4	5	5	11									3					0			
2					2	1	6									7					0			
1				3	3		5				1					3					0			
3				1			4	2								6					0	1		
5				5	1		3				2					1					0			
6				2	5		2				3					2					0			
			1	3	5						1					6					0			
6					2	1	2	1							2	4					0			
2			1	1	1		5				1										0			
2			1	1	7	1	5									1	1				0			
4				1	1		1				3					2					0			
				1			3	1			1					2					0			
2			1	2	9	2	8				1										0			
				6	3	8	10									1					0			
3				5	6	1	6				1					7					0			
1				2			4				1					1					0			
				5	3	3	6	1			5					2					0			
3					3	3	3									3					0			
4			1	6	2	6	6			1	4					2					0			
3			1	5	2	1	6				5					3	1				0			
1			1	2	5	3	3			1	4	1				2	1				0			
3			1		2	3	3			1	1						1				0			
2				1	6		6				1					1	1				0			
2				1	4	2	10			1	1						1				0			
3				2	3	5	9									1					0			
2				1	1	1	9	1			3		1								0			
2			1	4	4	2	13														0			
2				3	3	2	10	2									1				0			
3				1	4	2	7	2			1					1					0			
1					5	2	11				3									1	0		1	
1				4	6	1	4														0			
3				1	1	1	8				3										0			
			1				3				4										0			
					1	1	2									3					0			
3				8	1		5			1	3										0			
1			2	6	1	2										1					0			
1				2			1				1										0			

1				1	6	1	5			1	4									0			
3			1	3	1		2			1	3	1					1			0			
4			1	4	3	6	9			1						2	1			0			
4				3		1	1					1				1				0			
5			1	7	3	6	5				3					1	1			0			
1			1	1	2		2				1					1	2			0			
			1	2	1	3	2				1	3				2				0			
				1	3	4	1	1			2	1				1	1			0			
3						3	5				2									0			
1					2	3	3			1	1						1			0			
1			1	1	3	1	6				3					1				0			
3			1	1	3	5	4										1	3		0			
2				3	6	5	2													0			
				2	5	3											3			0			
				3		3	1				1						1			0			
			1	6	4	3	3	1			1						1			0			
2				4	1	5	6						1			1				0			
			1	2	6	2	2				3									0			
1				5	10	3					1		1							0			
1				6	8	3	6	1			1						2			0			
2			1	2	9	3	4				7					2	1			0			
1				3	16	3	2				3	1				3				0			
1				1	12	2	8				3					1				0			
1				5	9	1		1		1							3			0			
1				7	8	5	2				2									0			
1				2	4	2	2			1	2									0			
3				2	4		6				1									0			
3			1	8	8	6					3	1					1			0			
1				2	6		7				3				1		1			0			
2			1	1	5	4	3	1			1					1				0			
				2	2						6						1			0			
1			1	11	3	1	2				3	1								0			
2				8	6	3					4									0			
4				12	4	1	3	1			5									0			
1			2	10	2	3	3				2					1	1			0		1	
4				10		4	7	1			4						2			0			
			3	3	4	6	4	1			1						1			0			
2				4	3	7	9				10	1								0			
				4	14	5	3	6		1	3	1	1			2	3			0			
			1	1	2	3	2	1			10	1				1	1			0			
					3	2	1				1	1				1	1			0			
			1	3	5	7	4	1			10						4			0			
				3	5	5	2	1			1					2	1			0			
5				2	8	3	5				3	1					4			0			
				4	7	4	9	1			4	1				2				0			
3				3	12	5	4			3	1	1				1				0			
1					4	3	5			3	2									0			
					5		2				2									0			
					13	1	4	1												0			
1				2	7	3	9				2									0			

				2	8			1			4						1				0			
2				1	4	8	4			1	2					1					0			
			1		1	1	5	2			2	1				1					0			
					4			2			2	1					6				0			
1				3	1	2	3				7										0			
5				1	2						7		1			1	4				0			
1				3	3	2	2	2			3					1					0			
2				2	3	4	4	1			2					1					0			
			2	5	4	6	6				4					5					0			
				8	5	3	1	1			2		1				3				0			
				7	1	2	4	1			14					2					0			
				6	7	3	2	3			3	1				3					0			
				2	3	3	3	3			1					1	1				0			
				4	2	7	2	2			2	1					2				0			
2				2	10			2			3						1				0			
				3	7	7	7				1					1	2				0			
1				3	7		4	1			1						1				0			
				2	9	4	7	1		1	1										0			
2			1	4	21	3	5	1					1								0			
				3	6	8	5	1			1										0			
1			1	4	6	18	8				2										0			
				1	9	6		1				6												
				5	4	2	1			1	2					1	4							
			1	4	10	1				2	6		2			1								
				7	6	4	4				2	1												
2			1	1	7	6		1			8					3			1	1		1		
1			2	2	12	1	7				7	2					5							
2					5	1	3				3						3							
					11		7	2			7	3												
1					9	2	1	1		1	4	3				2								
				3	16	5	3										2							
				4	4	1		2									1							
			1	1	5	2		1			1	1				3	1		1					
2				1	11						1	6				5	2							
			1	1	6	3	3	1				5				3	1							
1				3	4			1			1	23				2		5						
50					2		2				3	53												
9							1				5	63					6							
14				4	4							146												
1											2	128												
6												215							1					
4			1				3					112												
					4						1	319					2							
					19		4				7	1					9							
6					21						7	10	2	1			16							
					24						6	10			3		3							
2			1		4						2	22		4										

Praeglobobulimina ovata	*Pullenia bulloides*	*Pullenia quinqueloba*	*Pullenia salisburyi*	*Quinqueloculina* sp.	*Rectuvigerina* sp.	*Reussella spinulosa*	*Rosalina* sp.	*Siphonina reticulata*	*Siphotextularia concava*	*Sphaeroidina bulloides*	*Spiroloculina* sp.	*Spiroplectammina* sp.	*Spiroplectinella* sp.	*Stilostomella monilis*	*Stilostomella vertebralis*	*Stilostomella* sp. 1	*Stilostomella* sp. 2	*Stilostomella* sp. 3	*Textularia agglutinans*	*Textularia calva*	*Textularia pala*	*Textularia pseudorugosa*	*Textularia* sp.	*Trifarina angulosa*
						5							2											1
	6							2					1											
	1		1					8																
			3					25					1											
	4		2					7		4			2	1				21						1
	4							30					1	3				4						
	12		1					4		2			1											
	12		4					18		6	1					1								
	18	1	1					8		2				3				3						
	18		2					9		2			1	1				1						
	10							35		1	1													
	20	1						5		4			1	2										
		1						11		3														1
	3		2					6		4														
	4		1					3		3	1			1										
	3							4		2								1						
	25									5			6											
	12		1					7		3				1										
	15							1		13			1											
	26							2		4														
	19							1		13			2											
	12	1						1		10		1	3											
	8	1						6		6		1		1										
	17							1		9					1									
	4		1					1		2			1	1										
	13							6		3			1	3				1						
	20									11			2					3						
	18	2	1					2		4			2					1						
	5		1							4			1					1						
	13	1	2							5			5					2						
1	14	1						1		7								1						
	14							13		3			3					1						1
	18							5		6			1				1	1						
	7							2		3			2					2						
	12									2			2					2						
	17							12		2				1										
	13							5																
	8	1						1		4			2											
	8	2						1		1				1										
	9	2	2					1																
	11							4		1			2	2										

	21		2					3		1			2	1									1
	7		1				1	5		1				2									
	10									6													2
	7							1		1													
	14							2		1				1									1
	3							5		3													
	5		1					1		2								1					1
1	4		3					11		1				2									1
	14							2		2													2
1	5									2				3									3
	8							6		1													1
	7		3																				
	10		1							4													1
	13		1					9		5				2									
	10												2	1									
	15									1				1									1
	12																						
	4												1										
	8	1								3			1	3									
	1													1									
	7							1		2				4									
	2									5				1									
1	5							2		2				1									
	5							2		2													3
	2									7													
	3									2													
	4									4													2
	2									6				3									
	9							2		7			1	2									
	16							3		2								1					
	20							6															
	8							12		8			1										2
	6							5		2													
	17							4		1			1										1
	20							9		4													
	8							23		2													
	5							4		1			1										3
	2							4		1													
	11							2		5			1										3
	35							4		3													1
	16							11					1	2									
	18							4		2				3									
	10													2									2
	12												4	2				3					
	4							16		1			1										
	6		1					12										2					
	3							6		3			1	1									
	14							4		2				2									
	9							7		1			3	1									
	9							7					2	1				1					

	10							2		1			1											
	15									1								3						
2	18									3				1										
	22									4			3											
	14							1		1				4										
	25							10		3				1										
	15							3		4				1										
	22									1			1											
	11							11		1														1
	10							15																1
	9									1				1										
	3							1																
	8							9					1	7										
	7									4														
	2									2			3	4										1
1	3							1		2				2										1
	3									2				5										
	4												1											
1	14							3		2				1										
	3							3		1														
	4							1					1											
	4									4			5	11										1
1	2									2								2						
	2									3														
1	6												3	1										
	4												1	3										
	9									1			2	2										
	3												4											1
	8									1				3										
	8									1			1											2
	10							3		5			2											1
	8												7	3										1
	11									8			2	10				1						
	4									3			6	8				1						
1	11									3			2	1										
	4									6			6											
3	21							2		10														
1	15			1				4		6			8	2										
	10	1						1		5			5					2						1
	5									7			6	7										
	12			1						13			8	3										
	2			1						2			11	4										
	3									2			9	3										
										3			3	3										
	3									5			9	1										
	13									1			2	1										
	5												7											
	9									2			1	1										
1	17							1		1			2	1										2
	9									1			5	2				2						

1	11												3	1										
1	13									6			3	5										
	4												7					1						1
	5												1	3										
	4									1			5	5										
	3									5			7	6										
	2									4			5	6				2						
	3									4			3	5				1						
	9									7				2										1
	6									8			14	13				4						
	7									1			9	1				5						
	6									6			4	2										
	3									6			10	8										
	9									1			9	1										
	7									1			8	2										
	5									3			5											
	5									1			4											
	8									4			10	1										
	10									1			2	2										
	11									2			7											
1	7									7			9	3										
	3												5											
	5									1			4	5										
	1		1										8					1						
	3												2					1						
	11									7			6	3								1		
	17									5			9											
	14									4				4										1
	5									2			4	1										2
	3									4			7											
	4									6			11									1		
	5									5			8	5										
	2		1							7			4	3				1						
	4									5			5											
	10									5			6											
	8									5			11											
	5									5			7											
	6									6			6											
	4									5			6					1						
	11									8			5											
	1									5			4											
	11			1						5			8											
	11			1						9			8											
	3									10			7					1						
	3									4			5	1										
	6									2			7	1										
	4									2			4	1										
	6									1			4	2										
	4									3			9											
	3									3			4					1						

	5									4			8	4										
	7			1						2			11	4										
	6									7			5	2										
	9									2			5	2										
	8									3			4	1										
	8									2			4											
	12												4					1						
	10									2			8											1
	5									2														
	10									2			4											
	7									6			6	1										
1	10									2			7											
	5									7			10					1						
	11									6			11								3	3	1	
	7									3			7											
	5									8			9	3										1
1	8			1						6			12											
	13									6			10											
	19									4			8											
	15									11			15											
	13									3			6	2										1
	16									8			15											
	16			1						8			10	1										
	6									4			8											
	14									7			8											
	16			2						11			12	2										
	11			1						8			10	2										
	12			1						5			21	1								2		
	11									7			6											
	4			1						4			6	1				1				4		
	9									4			7									3		
	9									4			6					3				4		
	10									4			8	3								8		
	11									4			11	1					1					
	7									2			4									3		
	5									3			4	2								6		
	7									3			3					1						
	4									6			7	1								2		
	9									6			9	1										
	8									5			2	1								4		
	5									6			4	1								1	1	
	14									5			3					1				3		
	7			1						2			3					1				4	1	
	8			2						6			14						2		1			
	14									4			5									5		
	10									8			2	1								6		
1	11									9			4									2		
	6									4			4					1				4		
	9									4			6					3						
1	10									3			3									5		

	24									1			6					1						
	11									6			5										6	
	16									2			5										3	
2	15			1						13			8	3				1						
1	10									11			5										8	
	7									3			8	1	1									
	11			1						3			6					1					4	
	8									6			4	5									9	1
	17									8			9										7	
	17									7			3					2						
	17									7			7										1	
	13									18			4					1					2	
	6									19			3					1					9	
	10		1							6			1										8	
	14			2						11			9											
	13									13			5										3	
1	9		1							9			8										5	
	6									6			6										2	
	14									4			6											
1	12									7			5										2	
	10									11			5										3	
	13									11			10	1										
	17									10			8											
	17									5			8											
	15									3			12											
	34			1						8			3					1						
	17									3			3											
	25									9			13					1						
	15												7											
	21									9			12											
	19									7			11											
	22									20			3											
	17									11			5					2						1
1	24									15			8											
	7			1						6			22											2
	13												23											
	9												4											
	4				2					2			29											5
	2					1			6				20											
	6					1							10											1
	1					2			3	1			9											
					8								10						2					3
				1	2	3							78						11		3		4	5
	4								37				44							3		3	3	2
						6							68						8		4		4	2
				4		2	1		4				28						5	5	1		6	9

Trifarina bradyi	*Uvigerina canariensis*	*Uvigerina peregrina* s.l.	*Uvigerina rutila*	*Uvigerina striatissima*	*Vaginulina* sp.	*Vaginulinopsis* sp.	*Valvulineria complanata*	*Valvulineria spp.*	**Total**	**Split**
		2		4				2	303	7/256
	6	13		50					305	1/4
	13			4					301	1/16
1	14	13		5					313	5/64
		21		6					303	13/16
2	2	53		22					309	5/32
1		41		12					342	1/8
1		264		41					541	1/4
3	3	51	5	4					315	1/2
1		24	4	11					301	1/8
	6	19	1	4					351	1/4
2	2	34		6					320	3/16
	32	31	1	2					336	3/16
1	6	38	1	21					302	1/4
4		79		14					308	3/16
7	1	71	2	12					307	1/4
	1	57	7	17					341	3/8
3		119	8	28					432	1/4
1		36	3	1					314	1/2
		73		12					351	7/8
2		31	1	23					303	1/4
1		49	3	12					302	3/8
3		32	2	20					300	1/4
2		31		18					331	3/8
		31		22					299	1/4
2		29	1	9					335	1/8
4		4		1					330	3/8
2		15		8					306	1/2
7		5	1	29					329	5/8
1		8	1	3					307	3/4
2		28		15					355	1/2
2		53		21					305	1/2
1		62		16					380	3/8
4		58		9					307	1/2
1		29		21					325	1/4
7		54		17					344	3/16
		55	1	21					335	3/8
1	6	24		10					314	3/8
1	1	73		11					300	5/16
5		84	1	27					374	3/16
5		55	1	12					310	1/4

8	1	37	1	19					339	3/8
8		27		19					317	1/4
6		10	4	11					300	5/16
		91		19					299	1/4
5		26	4	14					375	3/16
3		60		15					308	3/16
		55	3	23					368	3/16
2	19	36		42	1				433	1/8
1		23	2	8					323	1/2
2		31		5					301	1/2
2	54	30	3	26					340	1/8
3	5	31		18					298	1/8
17	3	28	1	13					306	3/16
62	1	113		17					573	1/8
10	2	142	2	8					323	1/8
11		80		6					341	1/4
10	2	98	2	17					404	1/4
63	7	48		9					380	1/4
66		24	2	1					352	1/16
7	214	49							364	1/4
66	2	112	2	2					314	1/8
59	1	56		3					309	3/16
49		30	3						311	5/8
21		12		4					306	3/8
19		22	2	12					335	3/4
3		26	1						302	5/16
18	2	38	6	3					319	3/16
14	1	53	1	6					349	3/16
15		85	1	3					388	3/8
60		78				1			323	1/4
8		38	3						302	3/16
4		83							301	1/4
15	15	71	1	3					304	1/4
18		65							300	3/16
2		25		1					311	3/16
2		44	2						302	3/16
2		69			1				312	1/4
	1	46	6						309	3/16
		66	1						306	1/4
		74	1						380	5/8
		76							358	3/16
		51	7						332	3/8
		79		2					301	3/8
	15	88							351	5/8
		93							315	3/16
	1	85							365	1/4
	4	43							329	3/8
	2	46	3						302	7/16
		49	1						356	5/16
		62	5						307	1/4

		59	1	1					309	7/16
		83		2					303	7/16
		102		1					330	1/4
		126	4	1					426	3/8
		28							332	3/16
		24	1	1					422	3/8
		14							311	3/16
		29							300	1/4
		22							307	5/16
		35	1		1				395	3/8
		16		1					304	11/16
		11	11						268	1
		4							342	1/4
		13	4						300	1/2
		17	2	1					301	5/8
		14							321	3/8
		9	4						313	7/8
4	2	13							302	3/8
		9	2						317	7/8
		13	2						305	3/4
2		19	3						444	5/8
3	1	22	1						309	3/8
4		13	3						312	5/16
		2	19						298	1
		15	1			1			316	9/16
3		10							303	1/2
4		11	2		1				332	7/8
2		21	1						301	7/8
2	1	13	1						303	5/8
6		8	1						304	1/4
1		10	1						332	5/16
3		17		1					301	1/4
20	1	19	1	1					331	3/4
112		29		2	1				435	1/4
38		8		1					319	1/4
48		19		2					330	3/8
		15							700	1/2
		11							349	1/8
3		21		1	1				305	1/4
		26							324	1/2
1		23							338	1/4
1		30					7		314	3/16
		23					1		336	1/4
2		10							322	3/16
7		26					5		306	3/16
2		3					11		306	1/4
5		7					2		302	5/16
		1					7		306	1/4
3		1							323	3/8
3		7							304	5/16

1		2							305	3/16
1		9					1		364	3/16
2		11							303	3/16
10		11			1				352	1/4
8		50						1	304	1/4
5		37							301	1/4
3		51							306	1/4
3		25					1		327	1/4
2		24							306	1/8
21		26					7		390	3/16
11		23					5		364	3/16
8		30					14		392	3/16
11		16					2		303	3/16
17		4			1				330	3/16
16		10							309	1/4
10		3					2		327	3/16
7		14					1		330	5/32
2		10					2		301	1/4
9		30							359	5/16
3		14							300	1/4
17		9			1		2		307	5/8
11		36							333	3/8
21		31							302	1/4
8		33					1		316	3/16
4		30							302	3/16
14		34							340	3/8
14		21							318	3/8
11		37					6		313	3/8
11		26					4		309	3/16
10		27							309	5/32
14		31							306	3/16
21		44					2		391	3/8
14		28					2		319	1/4
13		19					2		308	3/16
12		33							302	1/4
15		39			1		8		376	3/8
11		18					5		311	3/8
12		11					3		306	3/8
8		14					5		330	3/8
8		6							309	3/16
1		11					1		303	9/32
9		17							308	9/32
7		13							342	5/16
6		14							305	3/16
8		29							319	1/4
6		36							304	3/16
1		31							302	3/32
2		38							310	1/8
1		42							369	3/16
		28							304	3/16

		21							302	3/16
2		22					1		324	5/32
2		17					1		339	3/16
10	1	30							300	3/16
14		21					11		341	3/16
7		16					2		303	1/8
5		20					7		329	5/32
6		11					3		311	5/64
7		14							303	1/8
1		5							341	1/8
6		4					3		312	5/32
12		1					2		304	5/32
1		8					3		317	7/32
8		4					2		311	3/16
3		3							306	3/16
6		2							346	5/32
5		2							304	3/16
7									315	5/32
12									304	5/32
3							4		307	3/16
3		2					1		335	3/16
11		4					3		308	3/16
7		4					3		307	5/32
4		1					2		307	1/4
2		3					5		306	5/32
8		4					1		305	5/32
2		12					3		310	3/16
15		13							432	1/8
8		7							305	1/8
3		4							312	3/32
3		20							326	5/64
9		26							307	1/8
1		16							309	1/8
1		21							310	7/32
8		20							304	1/4
7		20							320	1/4
5		22					1		318	7/64
6		14					2		374	1/8
5	1	8							375	3/16
3		21					10		340	3/32
2		23			1		3		304	3/64
9		18					5		373	1/8
9		24					1		318	3/32
2		6					3		309	1/16
2		4					4		310	7/64
7		4					2		313	1/4
6		3					2		328	3/32
7		10					1		317	3/32
11		2							304	3/32
7		4					1		315	5/64

6		5					3		347	1/8
7		2					2		305	3/32
2		3					1		301	5/64
3		9							304	3/32
4		10							302	1/16
5		19							305	5/64
2		17							304	3/32
2		51							307	5/64
6		34							326	7/64
6		22							304	5/64
2		36					2		423	1/16
6		43					1		532	1/8
2		27					4		423	1/16
2		28					11		314	1/16
2		13					6		307	3/32
4		7					5		325	3/32
4		10					7		307	5/64
1		3					9		306	3/32
7		3						3	303	1/8
5		1							316	7/64
5		8					1		340	3/32
1		13					2		303	5/64
4		4							305	3/32
3		2					1		340	5/32
3		6						2	308	5/128
3		5					5		306	7/32
2		5							330	5/32
		5							307	3/16
6		4							310	1
4		1							302	1/8
		1						3	305	3/32
4		3					2		304	3/32
3		4						3	304	1/8
							5		383	1/16
4		10						2	302	1/16
1		1					2		311	3/32
		2							311	7/16
					1		1		320	3/16
		5						2	305	1/16
		1					1		302	1/16
		1							326	1/8
		1					1		308	1/16
		1							404	1/8
		1					12		303	3/16
							20		303	9/64
							7		367	3/32
							3		306	3/32

Table A.2.

Core depth (m)	Benthic $\delta^{18}O$ (‰ VPDB)	Planktonic $\delta^{18}O$ (‰ VPDB)
254.00	0.46	
251.50	0.74	0.16
249.00	0.79	0.45
246.50	0.74	-0.11
244.00	0.70	0.03
241.50	0.50	0.33
240.00	1.01	-0.03
239.00	1.06	-0.36
238.50	0.92	0.01
238.00	1.04	-0.31
237.50	0.92	-1.43
237.00	0.99	-0.06
236.50	0.94	0.05
236.00	0.83	-0.81
235.50	1.03	0.06
235.00	0.90	0.37
234.50	1.20	0.09
234.00	0.68	-0.16
233.50	0.80	-1.20
233.00	0.80	-1.56
232.50	0.72	-0.11
232.00	0.61	-1.23
231.50	0.64	0.19
231.00	0.96	-0.37
230.50	0.70	-0.38
230.00	0.37	-1.16
229.50	1.01	0.33
229.00	0.82	-0.12
228.50	-0.68	-0.08
228.00	1.01	0.22
227.50	-0.93	0.12
227.00	0.77	-0.01
226.00	0.87	0.16
225.50	0.92	0.09
225.00	0.69	0.21
224.50	0.67	-0.64
224.00	0.55	-0.19
223.50	1.32	0.05
223.00	1.25	0.38
222.50	-0.16	0.21
222.00	0.98	0.08
221.50	0.86	0.09
221.00	1.19	0.61
220.50	0.94	0.34
220.00	0.19	-0.27

219.50	0.58	-0.08
219.00	1.04	0.15
218.50	1.24	0.42
218.00	0.48	-0.19
217.50	0.84	-0.29
217.00	1.08	0.28
216.50	0.94	-0.01
216.00	1.05	0.16
215.50	1.10	0.20
215.00	1.17	0.10
214.50	0.63	-0.33
214.00	0.85	-0.18
213.50	0.89	-0.34
213.00	0.97	-0.29
212.50	1.41	0.54
212.00	1.26	-0.01
211.50	0.70	0.12
211.00	0.82	0.23
210.50	0.80	-0.13
210.00	1.04	0.23
209.50	1.12	0.40
209.00	0.95	0.10
208.50	1.15	0.36
208.00	1.11	0.21
207.50	1.01	0.08
207.00	0.90	0.00
206.50	1.08	0.34
206.00	1.36	0.77
205.50	1.11	0.68
205.00	0.91	0.21
204.00	1.00	0.34
203.50	0.62	0.12
203.00	1.02	0.11
202.50	0.44	0.23
202.00	0.97	0.44
201.50	0.97	0.24
201.00	1.23	0.83
200.50	1.31	0.67
200.00	1.74	0.82
199.50	0.96	0.21
198.50	1.27	0.61
197.50	1.19	0.09
197.00	1.22	0.11
196.50	1.06	0.22
196.00	1.06	0.02
195.50	1.04	0.02
195.00	1.45	0.33
194.50	1.39	0.46
194.00	1.57	0.68
193.50	1.49	0.57

192.00	1.40	0.65
191.50	0.80	0.07
190.00	1.15	0.12
189.50	1.12	-0.36
189.00	0.91	-0.14
188.50	1.49	0.82
188.00	1.32	0.50
187.50	0.98	-0.24
187.00	1.32	0.59
186.50	0.98	0.41
186.00	0.99	-0.37
185.50	1.26	0.10
185.00	1.16	0.49
184.50	1.23	0.24
184.00	1.12	0.35
183.50	1.11	0.07
183.00		0.42
182.50	1.80	0.23
182.00	1.51	0.37
181.50	1.51	-0.79
181.00	1.77	0.16
180.50	1.54	-0.19
180.00	1.43	0.32
179.50	1.50	0.22
179.00	1.26	0.23
178.50	0.96	-0.44
178.00	1.05	0.05
177.50	1.34	0.31
177.00		0.55
176.50	1.40	0.48
176.00	1.49	0.65
175.50	1.65	-0.03
175.00	1.44	0.06
174.50	0.64	0.36
174.00	1.00	0.67
173.50	1.12	0.31
173.00	0.99	0.48
172.50	1.02	0.28
172.00	0.89	0.11
171.50	0.85	0.31
171.00	0.84	-0.09
170.50	0.50	-0.08
170.00	0.61	-0.18
169.00	0.54	0.06
166.50	0.73	0.06
164.00	1.12	0.34
161.50	0.41	0.41
159.00	0.41	0.20
157.00	0.38	0.10
154.00	0.47	0.22

151.50	0.86	0.42
149.00	0.71	0.27
146.50	0.50	0.19
144.00	0.77	0.26
141.50	0.83	
139.00	0.97	0.38
136.50	0.70	-0.10
134.00	0.51	-0.13
131.50	0.29	-0.61
129.00	0.37	-0.34
126.50	0.63	-0.22
124.00	0.89	0.01
121.50	0.41	-0.38
119.00	0.50	0.02
116.50	0.39	-0.56
114.00	0.33	-0.45
112.50	0.48	0.02
109.00	0.63	-0.08
106.50	0.94	0.27
104.00	0.65	-0.01
101.50	0.51	-0.03
99.00	0.29	-0.27
96.50	0.20	
94.00	0.19	
91.50	0.53	
88.50	0.63	0.25
86.50	0.54	
84.00	0.64	-0.02
81.50	0.66	
79.00	0.70	
76.50	0.56	
74.50	0.59	
71.50	0.34	
69.00	0.42	
66.50		
64.50	0.64	
61.50	0.58	
59.00	0.83	
56.50	0.39	
54.00	0.33	

Benthic $\delta^{13}C$ (‰ VPDB)	Planktonic $\delta^{13}C$ (‰ VPDB)
1.14	
1.08	0.06
0.64	-0.35
0.61	-0.07
0.53	-1.08
0.47	0.02
0.10	-1.23
0.13	-0.80
0.35	-1.02
0.72	-0.67
0.44	-0.80
0.36	-1.28
0.53	-0.77
0.50	-0.05
0.39	-1.10
0.11	-0.46
0.36	-0.73
0.36	-0.85
0.02	-1.07
0.26	-1.23
0.12	-1.38
0.44	-0.89
0.75	-0.26
1.08	-0.92
0.33	-0.49
0.24	-0.27
0.47	-0.90
0.54	-0.88
-0.02	-1.17
0.32	-1.23
-0.11	-0.94
0.43	-0.48
0.34	-0.99
0.69	-0.76
0.63	-0.25
0.63	-1.06
0.26	-0.53
0.51	-0.61
0.02	-1.18
0.16	-0.88
0.42	-0.97
0.69	-0.97
0.70	-0.80
0.53	-0.77
0.27	-1.17

0.57	-1.10
0.59	-1.06
0.30	-0.73
0.34	-1.34
0.38	-1.19
0.23	-1.44
0.55	-1.11
0.60	-0.75
0.30	-1.17
0.25	-0.98
0.58	-1.52
0.59	-1.43
0.81	-1.19
0.39	-1.14
-0.10	-0.49
-0.11	-1.48
0.44	-1.55
0.15	-1.61
0.43	-1.45
0.29	-0.92
0.06	-1.22
0.34	-1.22
0.31	-0.95
0.50	-0.73
0.25	-1.02
0.25	-1.35
0.31	-0.70
0.12	-1.14
-0.12	-1.38
0.25	-1.43
0.32	-0.96
0.21	-1.29
0.70	-1.43
0.16	-0.74
0.37	-0.25
0.16	-1.05
0.37	-0.91
-0.43	-0.72
-0.42	-1.03
0.45	-1.24
0.18	-1.46
0.21	-0.88
0.44	-1.06
0.54	-1.33
0.60	-1.11
0.65	-0.63
0.24	-0.63
0.28	-0.91
0.20	-0.78
0.33	-0.84

0.51	-1.31
0.40	-0.79
0.39	-0.40
0.44	0.29
0.49	-0.27
0.49	-0.44
0.11	-0.23
0.49	0.13
0.41	-0.20
0.15	-0.55
0.36	0.12
0.59	-0.02
0.48	0.51
0.49	-0.40
0.62	-0.02
0.61	-0.29
	-0.93
0.40	-0.24
0.53	0.20
0.50	-0.46
0.44	0.20
0.37	0.13
0.62	-0.87
0.50	-0.04
0.39	0.11
0.49	-1.17
0.53	-1.22
0.42	-0.95
	-1.10
-0.04	-0.97
0.34	-0.66
0.44	-0.64
0.58	-1.29
0.45	-0.27
0.31	-0.30
0.33	-0.56
0.34	-0.69
0.22	-0.64
0.35	-0.55
0.27	-0.32
0.10	-0.47
0.58	-0.96
0.30	-0.43
0.31	-0.88
0.52	-0.42
0.01	-0.59
0.67	-0.59
0.48	0.12
0.79	0.58
0.56	0.46

0.37	0.30
0.45	0.52
0.49	0.44
0.39	0.15
0.30	
0.10	0.02
0.26	0.26
0.34	-0.13
0.24	0.15
0.39	0.42
0.40	0.04
0.16	-0.54
0.41	-0.33
-0.06	-0.81
0.17	-0.77
0.41	-0.95
0.15	-0.37
0.10	-0.14
-0.09	-0.62
0.01	-0.78
0.20	-0.28
0.21	-0.44
0.24	
0.18	
0.16	
0.06	-0.03
0.37	
0.25	-0.93
-0.08	
0.08	
-0.05	
-0.31	
-0.10	
0.09	
-0.16	
-0.31	
-0.32	
-0.27	
-0.44	